

ACCEPTED MANUSCRIPT • OPEN ACCESS

## Roadmap on Energy Harvesting Materials

To cite this article before publication: Vincenzo Pecunia *et al* 2023 *J. Phys. Mater.* in press <https://doi.org/10.1088/2515-7639/acc550>

### Manuscript version: Accepted Manuscript

Accepted Manuscript is “the version of the article accepted for publication including all changes made as a result of the peer review process, and which may also include the addition to the article by IOP Publishing of a header, an article ID, a cover sheet and/or an ‘Accepted Manuscript’ watermark, but excluding any other editing, typesetting or other changes made by IOP Publishing and/or its licensors”

This Accepted Manuscript is © 2023 The Author(s). Published by IOP Publishing Ltd.



As the Version of Record of this article is going to be / has been published on a gold open access basis under a CC BY 4.0 licence, this Accepted Manuscript is available for reuse under a CC BY 4.0 licence immediately.

Everyone is permitted to use all or part of the original content in this article, provided that they adhere to all the terms of the licence <https://creativecommons.org/licenses/by/4.0>

Although reasonable endeavours have been taken to obtain all necessary permissions from third parties to include their copyrighted content within this article, their full citation and copyright line may not be present in this Accepted Manuscript version. Before using any content from this article, please refer to the Version of Record on IOPscience once published for full citation and copyright details, as permissions may be required. All third party content is fully copyright protected and is not published on a gold open access basis under a CC BY licence, unless that is specifically stated in the figure caption in the Version of Record.

View the [article online](#) for updates and enhancements.

# Roadmap on Energy Harvesting Materials

Vincenzo Pecunia<sup>1\*</sup>, S. Ravi P. Silva<sup>2\*</sup>, Jamie D. Phillips<sup>3</sup>, Elisa Artegiani<sup>4</sup>, Alessandro Romeo<sup>4</sup>, Hongjae Shim<sup>5</sup>, Jongsung Park<sup>6</sup>, Jin Hyeok Kim<sup>7</sup>, Jae Sung Yun<sup>8</sup>, Gregory C. Welch<sup>9</sup>, Bryon W. Larson<sup>10</sup>, Myles Creran<sup>11</sup>, Audrey Laventure<sup>11</sup>, Kezia Sasitharan<sup>12</sup>, Natalie Flores-Diaz<sup>12</sup>, Marina Freitag<sup>12</sup>, Jie Xu<sup>13</sup>, Thomas M. Brown<sup>13</sup>, Benxuan Li<sup>14</sup>, Yiwen Wang<sup>15</sup>, Zhe Li<sup>16</sup>, Bo Hou<sup>17</sup>, Behrang H. Hamadani<sup>18</sup>, Emmanuel Defay<sup>20</sup>, Veronika Kovacova<sup>20</sup>, Sebastjan Glinsek<sup>20</sup>, Sohini Kar-Narayan<sup>21\*</sup>, Yang Bai<sup>22</sup>, Da Bin Kim<sup>23</sup>, Yong Soo Cho<sup>23</sup>, Agnė Žukauskaitė<sup>24</sup>, Stephan Barth<sup>24</sup>, Feng Ru Fan<sup>25</sup>, Wenzhuo Wu<sup>26</sup>, Pedro Costa<sup>27, 28</sup>, Javier del Campo<sup>29,30</sup>, Senentxu Lanceros-Mendez<sup>(27-30)</sup>, Hamideh Khanbareh<sup>31</sup>, Zhong Lin Wang<sup>32</sup>, Xiong Pu<sup>33</sup>, Caofeng Pan<sup>33</sup>, Renyun Zhang<sup>34</sup>, Jing Xu<sup>35</sup>, Xun Zhao<sup>35</sup>, Yihao Zhou<sup>35</sup>, Guorui Chen<sup>35</sup>, Trinny Tat<sup>35</sup>, Il Woo Ock<sup>35</sup>, Jun Chen<sup>35</sup>, Sontyana Adonijah Graham<sup>36</sup>, Jae Su Yu<sup>36</sup>, Ling-Zhi Huang<sup>37</sup>, Dan-Dan Li<sup>37</sup>, Ming-Guo Ma<sup>37</sup>, JiKui Luo<sup>38</sup>, Feng Jiang<sup>39</sup>, Pool See Lee<sup>39</sup>, Bhaskar Dudem<sup>2</sup>, Venkateswaran Vivekananthan<sup>2</sup>, Mercouri G. Kanatzidis<sup>40</sup>, Hongyao Xie<sup>40</sup>, Xiao-Lei Shi<sup>41</sup>, Zhi-Gang Chen<sup>41</sup>, Alexander Riss<sup>42</sup>, Michael Parzer<sup>42</sup>, Fabian Garmroudi<sup>42</sup>, Ernst Bauer<sup>42</sup>, Duncan Zavanelli<sup>43</sup>, Madison K. Brod<sup>43</sup>, Muath Al Malki<sup>43</sup>, G. Jeffrey Snyder<sup>43</sup>, Kirill Kovnir<sup>44,45</sup>, Susan M. Kauzlarich<sup>46</sup>, Ctirad Uher<sup>47</sup>, Jinle Lan<sup>48</sup>, Yuan-Hua Lin<sup>49</sup>, Luis Fonseca<sup>50</sup>, Alex Morata<sup>51</sup>, Marisol Martin-Gonzalez<sup>52</sup>, Giovanni Pennelli<sup>53</sup>, David Berthebaud<sup>54</sup>, Takao Mori<sup>55,56</sup>, Robert J. Quinn<sup>57</sup>, Jan-Willem G. Bos<sup>57</sup>, Christophe Candolfi<sup>58</sup>, Patrick Gougeon<sup>59</sup>, Philippe Gall<sup>59</sup>, Bertrand Lenoir<sup>58</sup>, Deepak Venkateshvaran<sup>60</sup>, Bernd Kaestner<sup>61</sup>, Yunshan Zhao<sup>62</sup>, Gang Zhang<sup>63</sup>, Yoshiyuki Nonoguchi<sup>64</sup>, Bob C. Schroeder<sup>65</sup>, Emiliano Bilotti<sup>66</sup>, Akanksha K. Menon<sup>67</sup>, Jeffrey J. Urban<sup>68</sup>, Oliver Fenwick<sup>66</sup>, Ceyla Asker<sup>66</sup>, A. Alec Talin<sup>69</sup>, Thomas D. Anthopoulos<sup>70</sup>, Tommaso Losi<sup>71</sup>, Fabrizio Viola<sup>71</sup>, Mario Caironi<sup>71</sup>, Dimitra G. Georgiadou<sup>72</sup>, Li Ding<sup>73</sup>, Lian-Mao Peng<sup>73</sup>, Zhenxing Wang<sup>74</sup>, Muh-Dey Wei<sup>75</sup>, Renato Negra<sup>75</sup>, Max C. Lemme<sup>74,76</sup>, Mahmoud Wagih<sup>72,77</sup>, Steve Beeby<sup>72</sup>, Taofeeq Ibn-Mohammed<sup>78</sup>, K.B. Mustapha<sup>79</sup> and A.P. Joshi<sup>78</sup>

<sup>1</sup> School of Sustainable Energy Engineering, Simon Fraser University, Surrey V3T 0N1, BC, Canada

<sup>2</sup> Advanced Technology Institute, Department of Electrical and Electronic Engineering, University of Surrey, Guildford, Surrey GU2 7XH, United Kingdom

<sup>3</sup> Department of Electrical and Computer Engineering, University of Delaware, Newark, Delaware, USA

<sup>4</sup> LAPS- Laboratory for Photovoltaics and Solid-State Physics, Department of Computer Science, University of Verona, Ca' Vignal 1, Strada Le Grazie 15, 37134, Verona, Italy

<sup>5</sup> Australian Centre for Advanced Photovoltaics (ACAP), School of Photovoltaic and Renewable Energy Engineering, University of New South Wales, Sydney, NSW 2052, Australia

<sup>6</sup> Department of Energy Engineering, Future Convergence Technology Research Institute, Gyeongsang National University, Jinju, Gyeongnam 52828, Republic of Korea

<sup>7</sup> Optoelectronics Convergence Research Center, and Department of Materials Science and Engineering, Chonnam National University, Gwangju 61186, Republic of Korea

<sup>8</sup> Department of Electrical and Electronic Engineering, Advanced Technology Institute (ATI), University of Surrey, Guildford, Surrey GU2 7XH, United Kingdom

<sup>9</sup> Department of Chemistry, University of Calgary, Calgary, AB, Canada. T2N 4K9

<sup>10</sup> National Renewable Energy Laboratory, Golden, CO 80401, USA

<sup>11</sup> Département de chimie, Université de Montréal, Montréal, QC, Canada. H2V 0B3

<sup>12</sup> School of Natural and Environmental Sciences, Bedson Building, Newcastle University, NE1 7RU Newcastle upon Tyne, UK

<sup>13</sup> CHOSE (Centre for Hybrid and Organic Solar Energy), Department of Electronic Engineering, University of Rome Tor Vergata, Via del Politecnico 1, 00133 Rome, Italy

- 1  
2  
3  
4  
5  
6  
7  
8  
9  
10  
11  
12  
13  
14  
15  
16  
17  
18  
19  
20  
21  
22  
23  
24  
25  
26  
27  
28  
29  
30  
31  
32  
33  
34  
35  
36  
37  
38  
39  
40  
41  
42  
43  
44  
45  
46  
47  
48  
49  
50  
51  
52  
53  
54  
55  
56  
57  
58  
59  
60
- <sup>14</sup> International Collaborative Laboratory of 2D Materials for Optoelectronics Science and Technology of Ministry of Education, Institute of Microscale Optoelectronics, Shenzhen University, Shenzhen 518060, China
- <sup>15</sup> Electrical Engineering Division, Engineering Department, University of Cambridge, 9 JJ Thomson Avenue, Cambridge CB3 0FA, UK
- <sup>16</sup> School of Engineering and Materials Science, Queen Mary University of London, London E1 4NS, UK
- <sup>17</sup> Department of Physics and Astronomy, Cardiff University, Cardiff CF24 3AA, UK
- <sup>18</sup> National Institute of Standards and Technology, USA
- <sup>20</sup> Materials Research and Technology Department, Luxembourg Institute of Science and Technology (LIST), 41 Rue du Brill, Belvaux, L-4422 Luxembourg
- <sup>21</sup> Department of Materials Science and Metallurgy, University of Cambridge, 27 Charles Babbage Road, Cambridge CB3 0FS, United Kingdom
- <sup>22</sup> Microelectronics Research Unit, Faculty of Information Technology and Electrical Engineering, University of Oulu, Oulu, Finland
- <sup>23</sup> Department of Materials Science and Engineering, Yonsei University, Seoul 03722, Republic of Korea
- <sup>24</sup> Fraunhofer Institute for Organic Electronics, Electron Beam and Plasma Technology FEP
- <sup>25</sup> State Key Laboratory of Physical Chemistry of Solid Surfaces, College of Chemistry and Chemical Engineering, Innovation Laboratory for Sciences and Technologies of Energy Materials of Fujian Province (IKKEM), Xiamen University, Xiamen 361005, PR China
- <sup>26</sup> School of Industrial Engineering, Purdue University, West Lafayette, IN, 47907 USA
- <sup>27</sup> Physics Centre of Minho and Porto Universities (CF-UM-UP), University of Minho 4710-053 Braga, Portugal
- <sup>28</sup> Laboratory of Physics for Materials and Emergent Technologies, LapMET
- <sup>29</sup> BCMaterials, Basque Center for Materials, Applications and Nanostructures, UPV/EHU Science Park, 48940 Leioa, Spain;
- <sup>30</sup> OIKERBASQUE, Basque Foundation for Science, 48009 Bilbao, Spain
- <sup>31</sup> Department of Mechanical Engineering, University of Bath, Claverton Down, Bath BA2 7AY, UK
- <sup>32</sup> School of Materials Science and Engineering, Georgia Institute of Technology, Atlanta, GA, 30332-0245, USA
- <sup>33</sup> CAS Center for Excellence in Nanoscience, Beijing Key Laboratory of Micro-nano Energy and Sensor, Beijing Institute of Nanoenergy and Nanosystems, Chinese Academy of Sciences, Beijing, 101400 P. R. China
- <sup>34</sup> Department of Natural Sciences, Mid Sweden University, Holmgatan 10, SE 851 70 Sundsvall, Sweden
- <sup>35</sup> Department of Bioengineering, University of California, Los Angeles, Los Angeles, CA 90095, USA
- <sup>36</sup> Department of Electronics and Information Convergence Engineering, Kyung Hee University, 1732 Deogyong-daero, Giheung-gu, Yongin-Si, Gyeonggi-do 17104, Republic of Korea
- <sup>37</sup> Research Center of Biomass Clean Utilization, College of Materials Science and Technology, Beijing Forestry University, Beijing 100083, PR China
- <sup>38</sup> College of Information Science and Electronic Engineering, Zhejiang University, Hangzhou, 310027, China
- <sup>39</sup> School of Materials Science and Engineering, Nanyang Technological University, 50 Nanyang Avenue, Singapore 639798, Singapore
- <sup>40</sup> Department of Chemistry, Northwestern University, Evanston, IL, USA
- <sup>41</sup> School of Chemistry and Physics, Queensland University of Technology, Brisbane, QLD 4000, Australia
- <sup>42</sup> Institute of Solid-State Physics, TU Wien, A-1040 Wien, Austria
- <sup>43</sup> Department of Materials Science and Engineering, Northwestern University, Evanston, IL, USA
- <sup>44</sup> Department of Chemistry, Iowa State University, Ames, IA 50011, USA
- <sup>45</sup> US DOE Ames Laboratory, Ames, IA 50011, USA

- 1  
2  
3  
4  
5  
6  
7  
8  
9  
10  
11  
12  
13  
14  
15  
16  
17  
18  
19  
20  
21  
22  
23  
24  
25  
26  
27  
28  
29  
30  
31  
32  
33  
34  
35  
36  
37  
38  
39  
40  
41  
42  
43  
44  
45  
46  
47  
48  
49  
50  
51  
52  
53  
54  
55  
56  
57  
58  
59  
60
- <sup>46</sup> Department of Chemistry, University of California Davis, Davis, CA 95616, USA
- <sup>47</sup> Department of Physics, University of Michigan, Ann Arbor, Michigan 48109, United States
- <sup>48</sup> State Key Laboratory of Organic-Inorganic Composites, College of Materials Science and Engineering, Beijing University of Chemical Technology, North Third Ring Road 15, Chaoyang District, Beijing 100029, P. R. China
- <sup>49</sup> State Key Laboratory of New Ceramics and Fine Processing, School of Materials Science and Engineering, Tsinghua University, Shuangqing Road 30, Haidian District, Beijing 100084, P. R. China
- <sup>50</sup> Instituto de Microelectrónica de Barcelona (IMB-CNM, CSIC), C/Til·lers s/n (Campus UAB), Bellaterra, Barcelona, Spain
- <sup>51</sup> Catalonia Institute for Energy Research (IREC), Jardins de Les Dones de Negre 1, 08930, Sant Adrià de Besòs, Barcelona, Spain
- <sup>52</sup> Instituto de Micro y Nanotecnología (IMN-CNM-CSIC), C/ Isaac Newton 8, PTM, E-28760 Tres Cantos, Spain
- <sup>53</sup> Dipartimento di Ingegneria della Informazione, Università di Pisa, Via G.Caruso, I-56122, Pisa, Italy
- <sup>54</sup> CNRS-Saint Gobain-NIMS, IRL 3629, LINK, National Institute for Materials Science (NIMS), 1-1 Namiki, Tsukuba, 305-0044 Japan
- <sup>55</sup> National Institute for Materials Science (NIMS), WPI International Center for Materials Nanoarchitectonics (WPI-MANA), 1-1 Namiki, Tsukuba, 305-0044 Japan
- <sup>56</sup> Graduate School of Pure and Applied Sciences, University of Tsukuba, Tennoudai 1-1-1, Tsukuba, 305-8671, Japan
- <sup>57</sup> Institute of Chemical Sciences and Centre for Advanced Energy Storage and Recovery, School of Engineering and Physical Sciences, Heriot-Watt University, Edinburgh, EH14 4AS, UK
- <sup>58</sup> Institut Jean Lamour, UMR 7198 CNRS – Université de Lorraine, 2 allée André Guinier-Campus ARTEM, BP 50840, 54011 Nancy Cedex, France
- <sup>59</sup> Institut des Sciences Chimiques de Rennes, UMR 6226 CNRS – Université de Rennes 1 - INSA de Rennes, 11 allée de Beaulieu, CS 50837, F-35708 Rennes Cedex, France
- <sup>60</sup> Cavendish Laboratory, University of Cambridge, JJ Thomson Avenue, Cambridge, CB3 0HE, United Kingdom
- <sup>61</sup> Technische Bundesanstalt (PTB), Berlin, Germany, Abbestrasse 2-12, 10587, Berlin, Germany
- <sup>62</sup> NNU-SULI Thermal Energy Research Center (NSTER) and Center for Quantum Transport and Thermal Energy Science (CQTES), School of Physics and Technology, Nanjing Normal University, Nanjing 210023, China
- <sup>63</sup> Institute of High Performance Computing, A\*STAR, Singapore
- <sup>64</sup> Faculty of Materials Science and Engineering, Kyoto Institute of Technology, Kyoto 606-8585, Japan
- <sup>65</sup> Department of Chemistry, University College London, 20 Gordon Street, London WC1H 0AJ, UK
- <sup>66</sup> School of Engineering and Materials Science, Queen Mary University of London, Mile End Road, London E1 4NS, UK
- <sup>67</sup> George W. Woodruff School of Mechanical Engineering, Georgia Institute of Technology, Atlanta, GA 30332, USA
- <sup>68</sup> The Molecular Foundry, Lawrence Berkeley National Laboratory, Berkeley, CA 94720, USA
- <sup>69</sup> Sandia National Laboratories, Livermore, CA 94551, USA
- <sup>70</sup> King Abdullah University of Science and Technology (KAUST), KAUST Solar Center (KSC), Thuwal 23955-6900, Saudi Arabia
- <sup>71</sup> Center for Nano Science and Technology@PoliMi, Istituto Italiano di Tecnologia, Via Pascoli, 70/3, 20133 Milano
- <sup>72</sup> Electronics and Computer Science, University of Southampton, Highfield Campus, Southampton SO17 1BJ, United Kingdom
- <sup>73</sup> Key Laboratory for the Physics and Chemistry of Nanodevices, Peking University, Beijing 100871, China



<sup>74</sup> AMO GmbH, Otto-Blumenthal-Str. 25, 52074 Aachen, Germany

<sup>75</sup> Chair of High Frequency Electronics, RWTH Aachen University, Kopernikusstr. 16, 52074 Aachen, Germany

<sup>76</sup> Chair of Electronic Devices, RWTH Aachen University, Otto-Blumenthal-Str. 2, 52074 Aachen, Germany

<sup>77</sup> James Watt School of Engineering, University of Glasgow, Glasgow G12 8QQ, UK

<sup>78</sup> Warwick Manufacturing Group (WMG), The University of Warwick, Coventry, CV4 7AL, UK

<sup>79</sup> Departments of Mechanical, Materials and Manufacturing Engineering, University of Nottingham (Malaysia Campus), Semenyih 43500, Selangor, Malaysia

\*Author to whom any correspondence should be addressed.

E-mail: [vincenzo\\_pecunia@sfu.ca](mailto:vincenzo_pecunia@sfu.ca), [sk568@cam.ac.uk](mailto:sk568@cam.ac.uk), [s.silva@surrey.ac.uk](mailto:s.silva@surrey.ac.uk)

## Abstract

Ambient energy harvesting has great potential to contribute to sustainable development and address growing environmental challenges. Converting waste energy from energy-intensive processes and systems (e.g., combustion engines and furnaces) is crucial to reducing their environmental impact and achieving net-zero emissions. Compact energy harvesters will also be key to powering the exponentially growing smart devices ecosystem that is part of the Internet of Things, thus enabling futuristic applications that can improve our quality of life (e.g., smart homes, smart cities, smart manufacturing, and smart healthcare). To achieve these goals, innovative materials are needed to efficiently convert ambient energy into electricity through various physical mechanisms, such as the photovoltaic effect, thermoelectricity, piezoelectricity, triboelectricity, and electromagnetic power transfer. By bringing together the perspectives of experts in various types of energy harvesting materials, this Roadmap provides extensive insights into recent advances and present challenges in the field. Additionally, the Roadmap analyzes the key performance metrics of these technologies in relation to their ultimate energy conversion limits. Building on these insights, the Roadmap outlines promising directions for future research to fully harness the potential of energy harvesting materials for green energy anytime, anywhere.

**Keywords:** energy harvesting materials, photovoltaics, thermoelectric energy harvesting, piezoelectric energy harvesting, triboelectric energy harvesting, electromagnetic energy harvesting, sustainability

---

## 1. Introduction - Vincenzo Pecunia and S. Ravi P. Silva

## 2. Materials for Indoor Photovoltaics

2.1 Introduction to indoor photovoltaics - Vincenzo Pecunia and S. Ravi P. Silva

2.2 III-V compound semiconductors for indoor photovoltaics - Jamie D. Phillips

2.3 CdTe solar cells for indoor applications - Elisa Artegiani and Alessandro Romeo

2.4 Kesterites for indoor photovoltaics - Hongjae Shim, Jongsung Park, Jin Hyeok Kim and Jae Sung Yun

2.5 Organic photovoltaics for indoor light to electricity conversion - Gregory C. Welch, Bryon W. Larson, Myles Creran, Audrey Laventure

2.6 Dye-sensitized photovoltaics for indoor applications - Kezia Sasitharan, Natalie Flores-Diaz and Marina Freitag

2.7 Lead-halide perovskites for indoor photovoltaics - Jie Xu and Thomas M. Brown

2.8 Lead-Free Halide Perovskites and Derivatives for Indoor Photovoltaics - Vincenzo Pecunia

2.9 Quantum-dot absorbers for indoor photovoltaics - Benxuan Li, Yiwen Wang, Zhe Li and Bo Hou

2.10 Accurate characterization of indoor photovoltaic performance - Behrang H. Hamadani

### 3. Materials for Piezoelectric Energy Harvesting

3.1 Introduction to Piezoelectric Energy Harvesting – Lead-based oxide perovskites - Emmanuel Defay, Veronika Kovacova and Sebastjan Glinsek

3.2 Lead-free oxide perovskites for Piezoelectric Energy Harvesting - Yang Bai

3.3 Nanostructured Inorganics for Piezoelectric Energy Harvesting - Da Bin Kim and Yong Soo Cho

3.4 Nitrides for Piezoelectric Energy Harvesting - Agnė Žukauskaitė and Stephan Barth

3.5 2D Materials for Piezoelectric Energy Harvesting - Feng Ru Fan and Wenzhuo Wu

3.6 Organics for Piezoelectric Energy Harvesting - Pedro Costa, Javier del Campo and Senentxu Lanceros-Mendez

3.7 Bio-inspired materials for Piezoelectric Energy Harvesting - Hamideh Khanbareh

### 4. Materials for Triboelectric Energy Harvesting

4.1 Introduction to materials for triboelectric energy harvesting - Zhong Lin Wang

4.2 Synthetic polymers for triboelectric energy harvesting - Xiong Pu and Caofeng Pan

4.3 Nanocomposites for triboelectric energy harvesting - Renyun Zhang

4.4 Nanoparticles, Surface texturing and functionalization for triboelectric energy harvesting - Jing Xu, Xun Zhao, Yihao Zhou, Guorui Chen, Trinny Tat, Il Woo Ock and Jun Chen

4.5 Nature-inspired materials for triboelectric energy harvesting - Sontyana Adonijah Graham and Jae Su Yu

4.6 MXenes materials for triboelectric energy harvesting - Ling-Zhi Huang, Dan-Dan Li and Ming-Guo Ma

4.7 Perovskite-based triboelectric nanogenerators - JiKui Luo

4.8 Towards self-powered woven wearables via triboelectric nanogenerators - Feng Jiang and Pooi See Lee

4.9 Theoretical Investigations towards the Materials Optimization for Triboelectric Nanogenerators - Bhaskar Dudem, Venkateswaran Vivekananthan and S. Ravi P. Silva

### 5. Materials for Thermoelectric Energy Harvesting

5.1 Introduction on Materials for Thermoelectric Energy Harvesting - Mercuri G. Kanatzidis and Hongyao Xie

5.2 Chalcogenides for thermoelectric energy harvesting - Xiao-Lei Shi and Zhi-Gang Chen

5.3 Full-Heuslers for thermoelectric energy harvesting - Alexander Riss, Michael Parzer, Fabian Garmroudi and Ernst Bauer

5.4 Half Heuslers for Thermoelectric Energy Harvesting - Duncan Zavanelli, Madison K. Brod, Muath Al Malki, G. Jeffrey Snyder

5.5 Clathrates for thermoelectric energy harvesting - Kirill Kovnir and Susan M. Kauzlarich

5.6 Skutterudites for thermoelectric energy harvesting - Ctirad Uher

5.7 Oxides for thermoelectric energy harvesting - Jinle Lan and Yuan-Hua Lin

- 1  
2  
3 5.8 SiGe for thermoelectric energy harvesting - Luis Fonseca, Alex Morata, Marisol Martin-Gonzalez and  
4 Giovanni Pennelli  
5 5.9 Mg<sub>2</sub>IV (IV = Si, Ge and Sn)-based systems for thermoelectric energy harvesting - David Berthebaud  
6 and Takao Mori  
7 5.10 Zintl phases for thermoelectric energy harvesting - Robert J. Quinn and Jan-Willem G. Bos  
8 5.11 Molybdenum-based cluster chalcogenides as high-temperature thermoelectric materials -  
9 Christophe Candolfi, Patrick Gougeon, Philippe Gall, Bertrand Lenoir  
10 5.12 Organic Thermoelectrics - Deepak Venkateshvaran and Bernd Kaestner  
11 5.13 Two-dimensional (2D) materials for thermoelectric applications - Yunshan Zhao and Gang Zhang  
12 5.14 Carbon nanotubes for thermoelectric energy harvesting - Yoshiyuki Nonoguchi  
13 5.15 Polymer-carbon composites for thermoelectric energy harvesting - Bob C. Schroeder and Emiliano  
14 5.16 Hybrid organic-inorganic thermoelectrics - Akanksha K. Menon and Jeffrey J. Urban  
15 5.17 Halide perovskites for thermoelectric energy harvesting - Oliver Fenwick and Ceyla Asker  
16 5.18 Metal organic frameworks for thermoelectric energy conversion applications - A. Alec Talin  
17  
18  
19  
20

## 21 **6. Materials for Radiofrequency Energy Harvesting**

- 22 6.1 Introduction to materials for radiofrequency energy harvesting - Thomas D. Anthopoulos  
23 6.2 Organic semiconductors for radiofrequency rectifying devices - Tommaso Losi, Fabrizio Viola and  
24 Mario Caironi  
25 6.3 Metal-oxide semiconductors for radiofrequency rectifying devices - Dimitra G. Georgiadou  
26 6.4 Carbon nanotubes for radiofrequency rectifying devices - Li Ding and Lian-Mao Peng  
27 6.5 2D Materials for radiofrequency rectifying devices - Zhenxing Wang, Muh-Dey Wei, Renato Negra,  
28 Max C. Lemme  
29 6.6 Materials for Rectennas and radiofrequency energy harvesters - Mahmoud Wagih and Steve Beeby  
30  
31  
32

## 33 **7. Sustainability Considerations in Energy Harvesting Materials Research** - Ibn-Mohammed, T. 34 Mustapha, K.B. and Joshi, A.P 35 36 37 38 39 40 41 42 43 44 45 46 47 48 49 50 51 52 53 54 55 56 57 58 59 60

## 1 - Introduction

Vincenzo Pecunia<sup>1</sup> and S. Ravi P. Silva<sup>2</sup>

<sup>1</sup> School of Sustainable Energy Engineering, Simon Fraser University, Surrey V3T 0N1, BC, Canada

<sup>2</sup> Advanced Technology Institute, Department of Electrical and Electronic Engineering, University of Surrey, Guildford, Surrey GU2 7XH, United Kingdom

In the face of the rising global energy demand and the existential challenge posed by climate change, it is more urgent than ever to generate green energy in order to preserve our planet and sustain human development. Alongside the need for renewable energy technologies for the conversion of primary green energy into electricity in large-scale installations (e.g., solar, wind, and wave farms), reducing our carbon footprint also requires harnessing the vast energy reservoir all around us in the form of ambient light, mechanical vibrations, thermal gradients, and radiofrequency electromagnetic waves [1]. Harvesting this energy via compact harvesters paves the way not only for more efficient use of our energy sources (for instance, consider the recycling of waste heat from an oven or industrial machinery) but also for sustainably powering technologies with considerable potential to enhance our quality of life without increasing our carbon footprint [2], [3]. Prominently, compact energy harvesters are key to enabling the Internet of Things (IoT), which aims to make our everyday objects and environments ‘smart’ via its ecosystem of interconnected smart sensors, thereby allowing for better functionality of technology and its optimum use (for instance, leading to smart homes, smart cities, smart manufacturing, precision agriculture, smart logistics, and smart healthcare) [4]. Importantly, the IoT device ecosystem will comprise several trillions of sensors in the near future [5]. This would make it unfeasible and unsustainable to exclusively rely on batteries as their power source—due to their environmental impacts as well as the challenge and cost of replacing hundreds of millions of batteries globally every day. However, compact energy harvesters could overcome this challenge by allowing IoT devices to operate continuously and in an eco-friendly manner throughout their lifetime [6], [7]. The burgeoning of wearable electronics, with its vast potential for health and wellness applications [8], is another related domain that would greatly benefit from compact energy harvesters—given that, in addition to being surrounded by ambient energy, the human body itself is a source of waste energy in the form of body heat and motion.

Energy harvesting is critically dependent on the availability of suitable materials (and devices thereof) to convert ambient energy into usable electric energy. Therefore, research in materials and devices for energy harvesting is key to providing energy harvesting technologies that can meet the needs of real-world applications. Such research requires a broad, cross-cutting effort, ranging from the discovery of new materials to the study of their energy harvesting properties, the engineering of their compositions, microstructure, and processing, and their integration into devices and systems. Given the diverse forms of ambient energy, materials are being developed to convert such energy through various physical mechanisms, the most prominent of which are the photovoltaic effect, piezoelectricity, triboelectricity, thermoelectricity, and radiofrequency power transfer (**Figure 1**). The rapid rise in the number of publications in this field (**Figure 2**) demonstrates its growing importance and the breadth of the community that has joined this research effort.

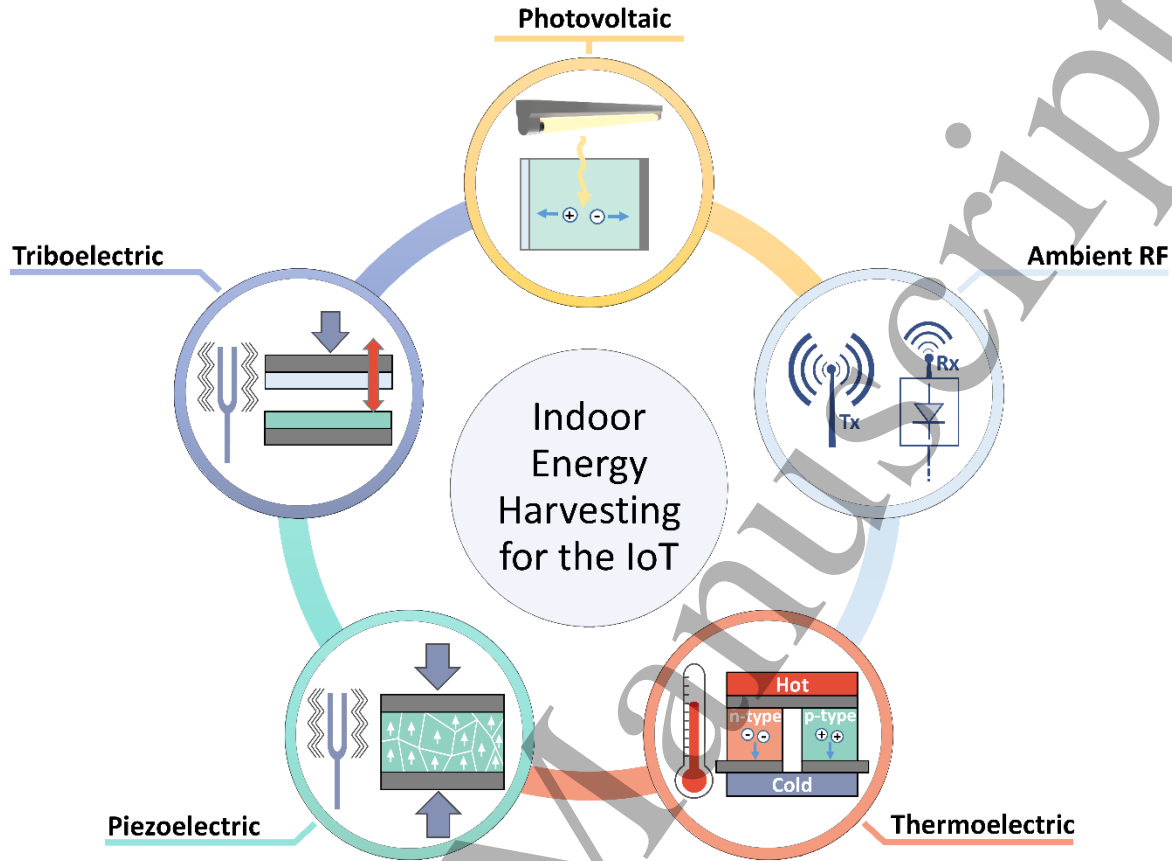


**Figure 1.** Prominent energy harvesting technologies covered in this Roadmap. Reproduced from Ref. [7] under the terms of a [CC BY 4.0 open-access license](https://creativecommons.org/licenses/by/4.0/).

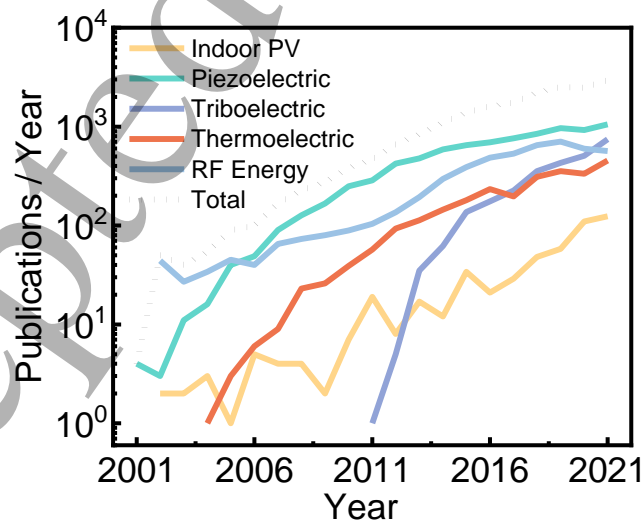


**Figure 2.** Publications per year for the various energy harvesting technologies covered in this Roadmap. This data was obtained from the Web of Science by searching the phrases 'indoor photovoltaics', 'piezoelectric harvesting', 'triboelectric harvesting', 'thermoelectric harvesting', and 'RF harvesting'.

1  
2  
3 While the vision of ‘green energy anytime, anywhere’ may still be some way into the future, energy  
4 harvesting technologies already offer numerous opportunities. For instance, photovoltaic harvesters have  
5 already been commercialized to power various smart sensors, while triboelectric, thermoelectric,  
6 piezoelectric, and RF energy harvesters have already been demonstrated to be capable of powering  
7 wearable devices [9]–[12].  
8

9 Although the various energy harvesting technologies rely on considerably different classes of materials  
10 and devices, they all share the same overarching goals and challenges—which will continue to drive future  
11 research pursuits in this area—as discussed below.  
12

13 *Efficiency.* A major challenge faced by all energy harvesting technologies is the limited power density  
14 available from ambient energy sources, which makes it essential to develop energy harvesting materials  
15 and devices that can efficiently convert such energy. Current energy harvesting technologies typically  
16 deliver electric power densities well below the  $\text{mW cm}^{-2}$  when harvesting ambient energy. This can be  
17 limiting for energy-intensive applications that do not allow aggressive duty cycling (i.e., a system operation  
18 pattern with long intervals in sleep mode, during which the harvested energy can be stored, alternating  
19 with short intervals in active mode, during which the stored energy is consumed) [2], [7]. Additionally,  
20 many emerging applications require compact energy harvesters with feature sizes in the millimetre-to-  
21 centimetre range. Therefore, boosting power conversion efficiencies is a vital goal of energy harvesting  
22 research. The success of this endeavour critically depends not only on characterizing and gaining insight  
23 into the fundamental properties of energy harvesting materials, but also on the discovery of new materials  
24 and the engineering of their device architectures to reduce loss mechanisms.  
25  
26

27 *Manufacturability.* Real-world applications critically require the development of energy harvesting  
28 technologies that can be manufactured at scale. Therefore, a priority is to develop energy harvesting  
29 materials that can be produced with simple methods, involving low capital cost and low material and  
30 energy consumption.  
31  
32

33 *Environmental Sustainability.* While energy harvesters inherently have no carbon emissions during  
34 operation, they will fully realize their purpose of providing green energy if they have minimal  
35 environmental impacts throughout their lifecycle. Therefore, a priority is to develop energy harvesting  
36 technologies that rely on Earth-abundant, non-toxic source materials and can be processed with low  
37 energy consumption. Additionally, it is important to consider the fate of these materials and devices at  
38 their end of life. Therefore, a key priority is to pursue energy harvesting materials and devices that lend  
39 themselves to be easily recycled from cradle to grave [13]. Moreover, for applications that involve a short  
40 life cycle, energy harvesters that are biodegradable would be highly desirable.  
41

42 *Cost.* For any energy harvesting technology to have a practical impact, it is necessary that its cost is  
43 sufficiently low to enable widespread deployment. In contrast to large-scale installations for the  
44 conversion of primary green energy into electricity (e.g., solar and wind farms), the crucial cost-related  
45 objective for ambient energy harvesters is not necessarily to minimize the cost per Watt. Indeed, the  
46 paramount aim is to ensure that ambient energy harvesters have a cost that is a manageable fraction of  
47 the system cost, while also being capable of supplying an energy output adequate for the application at  
48 hand. Cost is obviously a challenging metric to evaluate at the early stage of a technology, given that  
49 learning curves typically result in substantial cost reductions over time. Nonetheless, it is important to  
50 keep cost considerations in context as energy harvesting technologies are being developed, prioritizing  
51 solutions that rely on Earth-abundant materials and low-energy manufacturing processes.  
52  
53

54 *Form Factors.* For energy harvesters to be deployed ubiquitously, it is essential to develop them in flexible  
55 form factors so as to seamlessly place them on all kinds of objects and surfaces. Therefore, a research  
56  
57  
58  
59  
60



direction of paramount importance is to develop energy harvesting materials and devices capable of high power conversion efficiencies while being mechanically flexible or stretchable and optimized for small areas. The ubiquity and functionality of this novel system will act as an overlay to future wearables.

This Roadmap provides extensive insights into the status and prospects of the various energy harvesting technologies being researched to address the aforementioned challenges. It does so by covering the various classes of materials being developed for photovoltaic (Section 2), piezoelectric (Section 3), triboelectric (Section 4), thermoelectric (Section 5), and radiofrequency (Section 6) energy harvesting. In particular, this Roadmap highlights the key trends in materials properties and device performance underlying these prominent energy harvesting technologies, also discussing the open challenges and the potential strategies to overcome them. Finally, a perspective is presented on the key sustainability challenges that need to be tackled in energy harvesting materials research (Section 7). Based on these insights, it is envisaged that this Roadmap will catalyse further advances in energy harvesting materials and devices, bringing us closer to realizing the vision of ‘green energy anywhere, anytime’.

## References

- [1] L. B. Kong, T. Li, H. H. Hng, F. Boey, T. Zhang, and S. Li, “Introduction,” in *Waste Energy Harvesting*, Heidelberg, Germany: Springer, 2014, pp. 1–18. doi: 10.1007/978-3-642-54634-1\_1.
- [2] L. Portilla *et al.*, “Wirelessly powered large-area electronics for the Internet of Things,” *Nat Electron*, vol. 6, no. 1, Dec. 2022, doi: 10.1038/s41928-022-00898-5.
- [3] V. Pecunia, M. Fattori, S. Abdinia, H. Siringhaus, and E. Cantatore, *Organic and Amorphous-Metal-Oxide Flexible Analogue Electronics*. Cambridge University Press, 2018. doi: 10.1017/9781108559034.
- [4] Q. Hassan, Ed., *Internet of Things A to Z*. Hoboken, NJ, USA: John Wiley & Sons, Inc., 2018. doi: 10.1002/9781119456735.
- [5] J. Bryzek, “Roadmap for the Trillion Sensor Universe”, iNEMI Spring Member Meeting and Webinar, Berkeley, CA, 2013.
- [6] P. Harrop, “Battery Elimination in Electronics and Electrical Engineering 2018–2028,” Cambridge, UK, 2018.
- [7] V. Pecunia, L. G. Occhipinti, and R. L. Z. Hoye, “Emerging Indoor Photovoltaic Technologies for Sustainable Internet of Things,” *Adv Energy Mater*, vol. 11, no. 29, p. 2100698, Aug. 2021, doi: 10.1002/aenm.202100698.
- [8] G. Wang, C. Hou, and H. Wang, Eds., *Flexible and Wearable Electronics for Smart Clothing*. Weinheim, Germany: Wiley, 2020. doi: 10.1002/9783527818556.
- [9] S. Bose, B. Shen, and M. L. Johnston, “A Batteryless Motion-Adaptive Heartbeat Detection System-on-Chip Powered by Human Body Heat,” *IEEE J Solid-State Circuits*, vol. 55, no. 11, pp. 2902–2913, Nov. 2020, doi: 10.1109/JSSC.2020.3013789.
- [10] Y. Song *et al.*, “Wireless battery-free wearable sweat sensor powered by human motion,” *Sci Adv*, vol. 6, no. 40, Oct. 2020, doi: 10.1126/sciadv.aay9842.
- [11] A. J. Bandodkar *et al.*, “Battery-free, skin-interfaced microfluidic/electronic systems for simultaneous electrochemical, colorimetric, and volumetric analysis of sweat,” *Sci Adv*, vol. 5, no. 1, Jan. 2019, doi: 10.1126/sciadv.aav3294.
- [12] I. Mathews, S. N. Kantareddy, T. Buonassisi, and I. M. Peters, “Technology and Market Perspective for Indoor Photovoltaic Cells,” *Joule*, vol. 3, no. 6, pp. 1415–1426, Jun. 2019, doi: 10.1016/j.joule.2019.03.026.
- [13] S. Nandy, E. Fortunato, and R. Martins, “Green economy and waste management: An inevitable plan for materials science,” *Progress in Natural Science: Materials International*, vol. 32, no. 1, pp. 1–9, Feb. 2022, doi: 10.1016/j.pnsc.2022.01.001.

## 2. Materials for Indoor Photovoltaics

### 2.1 Introduction to indoor photovoltaics

Vincenzo Pecunia<sup>1</sup> and S. Ravi P. Silva<sup>2</sup>

<sup>1</sup> School of Sustainable Energy Engineering, Simon Fraser University, Surrey V3T 0N1, BC, Canada

<sup>2</sup> Advanced Technology Institute, Department of Electrical and Electronic Engineering, University of Surrey, Guildford, Surrey GU2 7XH, United Kingdom

Photovoltaic devices enable the direct conversion of light into electricity: the energy harvested from the light impinging on the photoactive material of choice (*absorber*) excites the charges within the material; the resultant mobile charges are transported to and collected at two opposite electrodes, thereby delivering an electric current and voltage (Figure 1a) that can be used for doing work. The ubiquity of light makes photovoltaics a highly attractive energy harvesting technology due to their wide deployability [1]. Moreover, the wave nature of light—with its very short wavelength in comparison to the thickness of the material layers typically found in photovoltaic devices—ensures that much energy density can be transported even in the case of non-line-of-sight situations without a physical medium being present. Additionally, based on typical ambient illumination levels, the power density that photovoltaics can supply is at the high end of all the energy harvesting technologies (Section 1), with the intermittency of its underlying energy transmission being generally manageable due to the predictability of its temporal patterns. By virtue of all these factors, photovoltaics occupies a prominent role both in indoor energy harvesting and for large-scale outdoor deployment, with its significance and impact being expected to grow dramatically in the future as the current materials challenges are addressed [2].

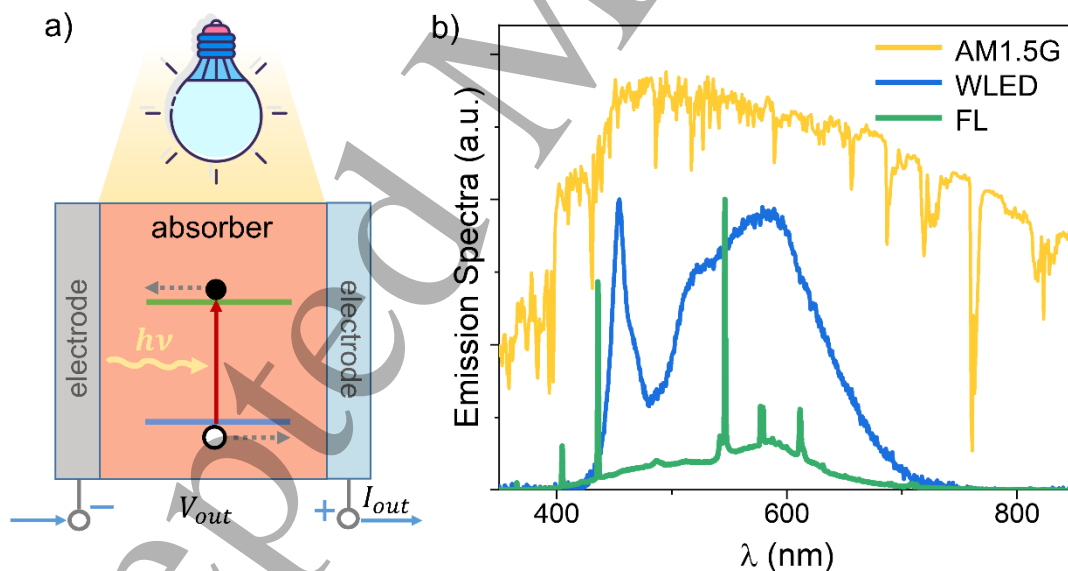


**Figure 1.** a) Sketch of the operation of a photovoltaic device: photons (each having an energy equal to  $h\nu$ ) are dissipated in the absorber and are thus converted into mobile charges, i.e., electrons (denoted by a solid black circle) and holes (denoted by an empty circle), whose transport to and collection at the electrodes result in an electric current and voltage. The icon representing the LED bulb is re-used with permission from Flaticon.com. b) Normalized emission spectra of the Sun (AM1.5G) and fluorescent (FL) and white LED (WLED) lamps.

The use of photovoltaics for the conversion of terrestrial outdoor solar light into electricity—through arrays of solar panels deployed on rooftops or in large-scale solar farms (*outdoor solar photovoltaics*)—is undoubtedly dominant and justifiably so due to the high energy density (in the range of 10–100 mW cm<sup>-2</sup>)



2) of outdoor terrestrial solar illumination. Harvesting outdoor solar light also applies to building-integrated photovoltaics, which involves solar panels embedded into the building envelope (e.g., as part of façades, roofs, and windows). Alongside solar photovoltaics, recent years have witnessed the rapid rise of indoor photovoltaics, which involves the conversion of ambient *indoor* light into electricity. This trend parallels the strong demand for energy technologies that could sustainably power the exponentially growing ecosystem of IoT smart sensors—expected to grow to several trillion units in the near future—that are an essential constituent of the Internet of Things (IoT). Indeed, most IoT applications rely on smart devices placed indoors (e.g., for smart homes, smart buildings, and smart manufacturing). From an energy harvesting perspective, indoor photovoltaics presents a more stringent scenario, given the considerably lower power density found in the ambient indoor light (in the range of 70–350  $\mu\text{W cm}^{-2}$ ) supplied by fluorescent (FL) and white light-emitting diode (WLED) lighting. Therefore, developing photovoltaic technologies that can function at such low illumination levels is critical to sustainably powering the vast IoT smart sensor ecosystem. The significance and potential of indoor photovoltaics are also confirmed by the growth of its market size, which is projected to reach 1 billion dollars within the next few years, meanwhile having a compound annual growth rate (CAGR) of 70 % and hence being the fastest-growing segment within the entire photovoltaic market (cf., solar photovoltaics and building-integrated photovoltaics are growing with a CAGR of 7.4 % and 16 %, respectively) [3].

The performance of an indoor photovoltaic cell can be quantified in terms of its indoor power conversion efficiency (PCE(i)), which expresses the ratio between the maximum electric power generated by the cell,  $P_{el,max}$ , and the light intensity reaching the cell from the indoor light source,  $P_{opt,S_n(\lambda)}$ , where  $S_n(\lambda)$  is the spectral irradiance at the surface of the photovoltaic cell:

$$PCE(i)_{S_n(\lambda)} = P_{el,max} / P_{opt,S_n(\lambda)} \quad (1)$$

Note that, due to the current lack of a standard spectrum for the assessment of PCE(i), a given indoor photovoltaic cell may present differing PCE(i) values depending on the light source considered—with the relative efficiency variations depending on the level of spectral match between the absorber and the illuminant as well as the irradiance of the latter. Additionally, note that the acronym PCE(i) is adopted herein to refer to the power conversion efficiency of indoor photovoltaic cells to prevent confusion with the power conversion efficiency of outdoor terrestrial solar cells (commonly indicated as PCE). Indeed, while conceptually analogous, the two metrics are not directly comparable due to the different luminous sources relevant to the two scenarios.

In addition to their much lower irradiance levels compared to outdoor terrestrial solar light, typical artificial indoor light sources (i.e., FL and WLED lighting) are characterized by a rather distinct spectral content, as their emission spectra exclusively cover the visible range (cf. approximately half of the terrestrial solar light falls in the near-infrared spectral region) (Figure 1b). This aspect is particularly consequential because it impacts the conditions that an absorber should meet to deliver optimum photovoltaic efficiency. As shown in Figure 2a, in the radiative limit and for typical indoor light sources (i.e., FL and WLED lighting), the optimum bandgap for an absorber to deliver high-efficiency indoor photovoltaics amounts to 1.8–2.0 eV (cf. outdoor terrestrial solar photovoltaics requires a bandgap of  $\cong 1.2$ –1.4 eV for optimum performance) [1]. Moreover, the narrower spectral range of indoor light sources compared to the solar spectrum (Figure 1b) enables maximum theoretical efficiencies (in the radiative limit) of up to  $\cong 60$  % for single-junction devices (cf. the corresponding limit for outdoor terrestrial solar photovoltaics amounts to 33.7%) [1]. This implies that indoor photovoltaics could theoretically deliver power densities of up to  $\cong 40$ –200  $\mu\text{W cm}^{-2}$  (for typical indoor illumination levels of 70–350  $\mu\text{W cm}^{-2}$ ).

While crystalline silicon (c-Si) is the dominant semiconductor technology for terrestrial solar photovoltaics, the PCE(i) values of commercial c-Si solar cells are rather low (up to  $\cong 12\%$ ) because of their low shunt resistance and comparatively narrow bandgap of c-Si (1.12 eV) [4]. In fact, hydrogenated amorphous silicon (a-Si:H) cells have long been the commercially dominant technology for indoor photovoltaics [5]: not only do they deliver PCE(i) values of 4–9% [4] in commercial devices due to the wider bandgap of a-Si:H ( $\cong 1.6$ –1.8 eV), but they also allow simpler manufacturing and mechanical flexibility, thereby enabling significant cost reductions and the facile integration of indoor photovoltaics in a wide range of objects and environments. Notwithstanding the commercial dominance of a-Si:H in the indoor photovoltaics arena, commercial a-Si:H cells are characterized by a particularly large efficiency deficit with respect to the ultimate efficiency potential of indoor photovoltaics (i.e., the radiative-limit efficiency  $PCE(i)_{RL}$ ), which can be traced to a significant extent to the inherent optoelectronic and materials properties of a-Si:H. Consequently, a grand challenge in indoor photovoltaics research is to develop absorbers and device architectures that are capable not only of reliably surpassing the commercial state of the art (essentially, the 10% PCE(i) threshold) but that can also approach the ultimate PCE(i) limit of 60%. This endeavor is all the more worthwhile because its success would enhance the reach and impact of indoor photovoltaics as a leading energy harvesting technology: it would enable indoor photovoltaics to extend the operational lifetime of battery-less smart devices, enhance their miniaturization, and deliver sufficient power for smart devices capable of more complex, multifunctional, and energy-intensive computing.

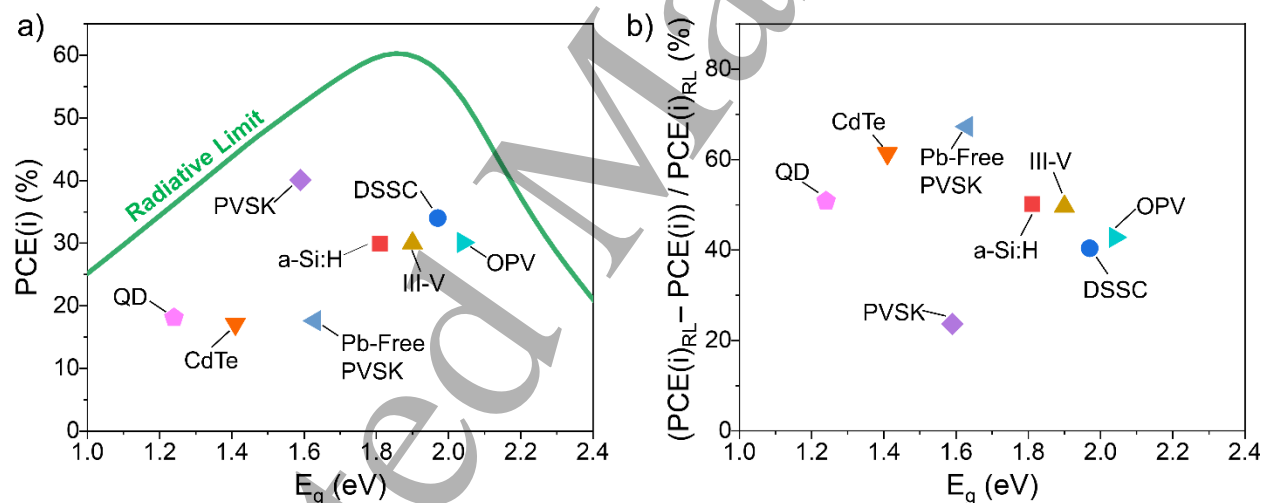


**Figure 2.** a) PCE(i) of the champion devices of various indoor photovoltaic technologies for an illuminance of or close to 1000 lx. We calculated the radiative limit (denoted by the green trace) for single-layer device structures based on the WLED spectrum shown in Figure 1b, while the data points are derived from Refs. [6]–[13]. b) Relative PCE(i) deficit with respect to the PCE(i) in the radiative limit,  $PCE(i)_{RL}$ , for the various technologies presented in a). PVSK: halide perovskites; Pb-Free PVSK: lead-free halide perovskites; DSSC: dye-sensitized solar cells; OPV: organic photovoltaics; QD: quantum dots.

The ambition to realize indoor photovoltaics with efficiencies approaching the radiative limit has prompted the exploration of new materials and new device architectures, as well as the revisitation of conventional photovoltaic technologies in the context of indoor light harvesting. In regard to emerging technologies, remarkable progress has been achieved with organic (Section 2.5), dye-sensitized (Section 2.6), and perovskite (Section 2.7) cells, all delivering PCE(i) values in the range of 30–40% in champion devices (Figure 2a). Meanwhile, alternative families of absorbers—e.g., kesterites (Section 2.4), lead-free perovskite derivatives (Section 2.8), and non-toxic quantum dot semiconductors (Section 2.9)—have been pursued to address the toxicity or material scarcity issues faced by some of the emerging technologies.

Moreover, the re-energized exploration of silicon-based absorbers and the optimization of III-V technologies (Section 2.2) for indoor photovoltaics have delivered significant progress, with efficiencies in the 30–40 % being achieved in some cases (Figure 2a). Concurrently, CdTe has also shown promising indoor photovoltaic performance (Sections 2.3) (Figure 2a).

Despite these considerable research achievements, the ultimate radiative efficiency limit of 60 % is far from being reached, as also revealed by the plot in Figure 2b, which presents the relative PCE(i) deficit of the various photovoltaic technologies with respect to the PCE(i) in the radiative limit,  $PCE(i)_{RL}$ . This plot highlights a particularly large relative efficiency deficit of 40–70 % for nearly all technologies, which therefore prompts the pursuit of new materials and device architectures to advance the state of the art—e.g., compositional engineering and defect passivation strategies to reduce recombination losses, as well as device engineering to enhance the shunt resistance. Additionally, even when a smaller deficit is achieved (as in the perovskite case), Figure 2a highlights that bandgap optimization remains crucial for the 60% efficiency limit to be approached, which points to the need to focus on materials technologies that allow bandgap tuning toward the 1.9 eV optimum.

Furthermore, the lack of a standard indoor light spectrum (e.g., see Figure 1b) has made the characterization of the efficiency of indoor photovoltaics prone to ambiguities (see Equation 1), thereby giving rise to the need to establish solid characterization protocols for the field to advance further, as discussed in Section 2.10.

Apart from performance considerations, the future progress of indoor photovoltaics will also considerably depend on the use of technologies that are based on eco-friendly, Earth-abundant materials and straightforward manufacturing processes. Toxicity issues are particularly significant because indoor photovoltaics are intended to be deployed in everyday objects and environments. Hence, it is crucial to avoid that the end-users could be exposed to toxic materials accidentally released from indoor photovoltaic cell. Therefore, materials engineering and materials discovery toward eco-friendly, Earth-abundant, and easy-to-make indoor photovoltaics are key to ensuring its sustainability [1].

The following contributions (Sections 2.2–2.10) discuss the specifics of these grand challenges in the context of various indoor photovoltaic technologies, also identifying potential avenues to overcome these challenges. By presenting a comprehensive roadmap of indoor photovoltaic materials, we envisage that the insights provided herein and in the rest of this section could catalyze further advances in the field toward the realization of the full potential of indoor photovoltaics as a green energy harvesting technology.

## References

- [1] V. Pecunia, L. G. Occhipinti, and R. L. Z. Hoyer, "Emerging Indoor Photovoltaic Technologies for Sustainable Internet of Things," *Advanced Energy Materials*, vol. 11, no. 29, p. 2100698, Aug. 2021, doi: 10.1002/aenm.202100698.
- [2] S. R. P. Silva, "EDITORIAL: Now is the Time for Energy Materials Research to Save the Planet," *ENERGY & ENVIRONMENTAL MATERIALS*, vol. 4, no. 4, pp. 497–499, Oct. 2021, doi: 10.1002/eem2.12233.
- [3] "BCC Research (2018). Global Markets, Technologies and Devices for Energy Harvesting: EGY097C," Wellesley, MA, USA, 2018. Accessed: Jun. 19, 2022. [Online]. Available: <https://www.bccresearch.com/market-research/energy-and-resources/global-markets-technologies-and-devices-for-energy-harvesting.html>

- [4] M. Freunek, M. Freunek, and L. M. Reindl, "Maximum efficiencies of indoor photovoltaic devices," *IEEE Journal of Photovoltaics*, vol. 3, no. 1, pp. 59–64, Jan. 2013, doi: 10.1109/JPHOTOV.2012.2225023.
- [5] I. Mathews, S. N. Kantareddy, T. Buonassisi, and I. M. Peters, "Technology and Market Perspective for Indoor Photovoltaic Cells," *Joule*, vol. 3, no. 6, pp. 1415–1426, Jun. 2019, doi: 10.1016/j.joule.2019.03.026.
- [6] B. Hou *et al.*, "Multiphoton Absorption Stimulated Metal Chalcogenide Quantum Dot Solar Cells under Ambient and Concentrated Irradiance," *Advanced Functional Materials*, vol. 30, no. 39, p. 2004563, Sep. 2020, doi: 10.1002/adfm.202004563.
- [7] J.-J. Cao *et al.*, "Multifunctional potassium thiocyanate interlayer for eco-friendly tin perovskite indoor and outdoor photovoltaics," *Chemical Engineering Journal*, vol. 433, p. 133832, Apr. 2022, doi: 10.1016/j.cej.2021.133832.
- [8] L.-K. Ma *et al.*, "High-Efficiency Indoor Organic Photovoltaics with a Band-Aligned Interlayer," *Joule*, vol. 4, no. 7, pp. 1486–1500, Jul. 2020, doi: 10.1016/j.joule.2020.05.010.
- [9] Y. Dai, H. Kum, M. A. Slocum, G. T. Nelson, and S. M. Hubbard, "High efficiency single-junction InGaP photovoltaic devices under low intensity light illumination," in *2017 IEEE 44th Photovoltaic Specialist Conference (PVSC)*, Jun. 2017, pp. 222–225. doi: 10.1109/PVSC.2017.8366547.
- [10] I. Mathews *et al.*, "Analysis of CdTe photovoltaic cells for ambient light energy harvesting," *Journal of Physics D: Applied Physics*, vol. 53, no. 40, p. 405501, Sep. 2020, doi: 10.1088/1361-6463/ab94e6.
- [11] X. He *et al.*, "40.1% Record Low-Light Solar-Cell Efficiency by Holistic Trap-Passivation using Micrometer-Thick Perovskite Film," *Advanced Materials*, vol. 33, no. 27, p. 2100770, Jul. 2021, doi: 10.1002/adma.202100770.
- [12] H. Michaels *et al.*, "Dye-sensitized solar cells under ambient light powering machine learning: towards autonomous smart sensors for the internet of things," *Chemical Science*, vol. 11, no. 11, pp. 2895–2906, 2020, doi: 10.1039/C9SC06145B.
- [13] G. Kim, J. W. Lim, J. Kim, S. J. Yun, and M. A. Park, "Transparent Thin-Film Silicon Solar Cells for Indoor Light Harvesting with Conversion Efficiencies of 36% without Photodegradation," *ACS Applied Materials & Interfaces*, vol. 12, no. 24, pp. 27122–27130, Jun. 2020, doi: 10.1021/acsami.0c04517.

## 2.2 III-V compound semiconductors for indoor photovoltaics

Jamie D. Phillips

Department of Electrical and Computer Engineering, University of Delaware, Newark, Delaware, USA

### Status

Photovoltaic energy harvesting from indoor lighting sources presents unique challenges and constraints in comparison to conventional solar photovoltaics, where the differing cost and performance tradeoffs lend themselves to consider III-V compound semiconductor devices. The narrowband spectrum of indoor lighting sources, irradiance levels that are orders of magnitude lower than typical sunlight conditions, and desire for direct integration of power systems on devices place emphasis on high cell performance and integration capabilities. Compound semiconductors based on III-V materials provide a range of available bandgap energies that span the desired window in the visible spectrum for indoor lighting, while also demonstrating very high optical absorption coefficients and carrier transport properties that can achieve high power conversion efficiency at low irradiance conditions. The optimal bandgap energy of approximately 2 eV for photovoltaics operating under high-efficiency indoor lighting are well matched to mature III-V materials including AlGaAs and InGaP, with a theoretical power conversion efficiency of

around 50 % and higher <sup>[1]</sup> at typical indoor irradiance conditions (500 lux). Experimentally, power conversion efficiencies of >20 % have been reported for AlGaAs<sup>[2]</sup> and >30 % for InGaP<sup>[3]</sup>, dramatically outperforming prior commercial indoor photovoltaic devices based on amorphous silicon (<10%). The high performance of III-V devices, and opportunities for further improvements in efficiency, are linked to the outstanding fundamental electronic and optical material properties and the ability to “bandgap engineer” sophisticated device structures. The superior power conversion efficiency offered by III-V photovoltaics provides unique opportunities for miniaturized self-powered systems, where unlike solar photovoltaics, power density is more important than cost per unit area. Indoor photovoltaics based on III-V compounds are likely to play a major role in self-powered devices for the internet of things (IoT) through continued advances to improve power conversion efficiency and to develop architectures for direct system integration.

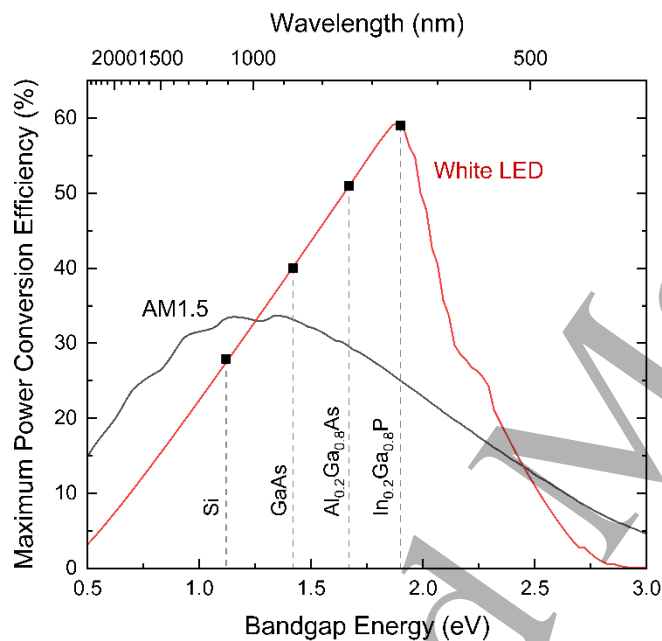


**Figure 1.** Calculated maximum power conversion efficiency versus bandgap energy for photovoltaic cells under AM1.5 and White LED illumination. Select semiconductor materials are shown, illustrating the high potential efficiency for III-V compound semiconductors.

### Current and Future Challenges

Primary research challenges for realizing the potential of III-V indoor photovoltaics can be categorized as issues related to cell performance, cost feasibility, and system integration. While high power conversion efficiency has already been realized for AlGaAs and InGaP devices, performance is still only about half of the theoretical limit for indoor lighting conditions. Continued optimization of device structures for the indoor lighting spectrum and irradiance levels would be expected to result in substantial gains in efficiency. Device structure optimization parameters to pursue include epitaxial structure thickness, bandgap, and doping concentration of emitter, base, window, and barrier layers<sup>[4]</sup>. Reduction of dark current is a primary limitation for low irradiance conditions, which is dominated in III-V devices by non-radiative surface/sidewall perimeter recombination<sup>[5]</sup>. Further reductions in dark current will require approaches to passivate recombination centers or to isolate minority carriers from these interfaces. Cost feasibility is a pervasive challenge for III-V devices due to the higher cost of substrate materials and epitaxial growth processes in comparison to silicon microelectronics. However, the high performance

1  
2  
3 offered by III-V photovoltaics make them preferable for applications where power density is at a premium  
4 provided that the cost of the energy harvesting device is a manageable fraction of the overall system cost.  
5 Cost-effective approaches to realize III-V photovoltaics are a current research challenge, which includes  
6 strategies for large scale production to leverage economies of scale. The adoption of III-V photovoltaics  
7 will depend on the ability for direct system integration to provide an effective power unit. Target  
8 applications will likely be miniaturized self-powered systems where the overall efficiency of the power  
9 unit require optimization and co-design of the photovoltaic device, power management circuitry, and any  
10 energy storage devices. At the photovoltaic device level, there are research challenges to consider the  
11 development of appropriate multi-junction devices and series-connected modules on a chip for efficient  
12 voltage up-conversion<sup>[6]</sup>.  
13  
14

### 15 **Advances in Science and Technology to Meet Challenges**

16 A primary thrust for improving the efficiency of III-V indoor photovoltaics should explore means of  
17 reducing non-radiative surface/sidewall recombination. Example techniques may include continued  
18 exploration of chemical surface treatments and surface passivation layers. High-quality epitaxial regrowth  
19 of wide-bandgap III-V materials on exposed interfaces may offer dramatic improvements in interface  
20 quality. There have been several techniques that have been proposed to develop cost-effective III-V  
21 photovoltaics (primarily for solar energy conversion) including epitaxial liftoff<sup>[7]</sup>, hydride vapor phase  
22 epitaxy (HVPE)<sup>[8]</sup>, and roll-to-roll printing<sup>[9]</sup>. The epitaxial liftoff approach offers a method for substrate  
23 reuse, eliminating the major cost of substrates as a part of the overall cell cost. Techniques such as HVPE  
24 can reduce the cost of epitaxial growth through efficient use of precursor materials. Large scale  
25 production such as roll-to-roll printing offer a means to achieve low cost at high volume. Technology  
26 advances will be needed to enable III-V device integration with systems ranging from the macroscale to  
27 the microscale. Larger scale devices and systems (approximately 1 cm and larger) will require  
28 development of suitable packaging technologies to interface with systems. An attractive advantage of III-  
29 V devices is the ability to use thin device layers via wafer liftoff, where mechanically flexible photovoltaic  
30 devices<sup>[7]</sup> may be used to accommodate a wide range of system form factors. Smaller scale systems at the  
31 millimeter size and below will rely on continued advances in heterogeneous integration with silicon  
32 microelectronics. This is a technology area that is rich for development, where there is a desire to leverage  
33 both the high-performance of III-V materials and sophistication of silicon microelectronics for applications  
34 including photonic integrated circuits, microelectromechanical systems, high-frequency electronics, and  
35 energy conversion systems such as described in this work. Heterogeneous integration strategies include  
36 epitaxial liftoff and cold welding, direct wafer bonding, micro-transfer printing, and selective epitaxy of  
37 III-V materials on silicon.  
38  
39  
40  
41

### 42 **Concluding Remarks**

43 The outstanding optical and electronic properties of III-V compound semiconductors offer the highest  
44 power conversion efficiency for indoor photovoltaics, with continued room for performance  
45 improvement through optimization of device structures and material interfaces. The adoption of III-V  
46 photovoltaics will depend on the cost practicality of these devices for a given system application. The most  
47 likely applications to incorporate III-V indoor photovoltaics will be systems where size, weight, and power  
48 are at a premium. Furthermore, the continued trajectory of advanced self-powered microscale systems  
49 may be enabled by the high power density provided by III-V photovoltaics.  
50  
51

### 52 **References**

53 [1] M. Freunek, M. Freunek and L. M. Reindl, "Maximum efficiencies of indoor photovoltaic devices," *IEEE Journal of Photovoltaics*,  
54 vol. 3, no. 1, pp. 59-64, Jan. 2013, doi: 10.1109/JPHOTOV.2012.2225023.  
55  
56  
57  
58  
59  
60



- [2] A. S. Teran, J. Wong, W. Lim, G. Kim, Y. Lee, D. Blaauw, and J. D. Phillips, "AlGaAs Photovoltaics for Indoor Energy Harvesting in mm-Scale Wireless Sensor Nodes," *IEEE Transactions on Electron Devices*, vol. 62, no. 7, pp. 2170-2175, July 2015, doi: 10.1109/TED.2015.2434336.
- [3] Y. Dai, H. Kum, M. A. Slocum, G. T. Nelson and S. M. Hubbard, "High efficiency single-junction InGaP photovoltaic devices under low intensity light illumination," 2017 IEEE 44th Photovoltaic Specialist Conference (PVSC), 2017, pp. 222-225, doi: 10.1109/PVSC.2017.8366547.
- [4] J. Phillips, E. Moon, and A. Teran, "Indoor Photovoltaics Based on AlGaAs", *Indoor Photovoltaics*, M. Freunek Müller (Ed.). doi: 10.1002/9781119605768.ch9
- [5] A. S. Teran, E. Moon, W. Lim, G. Kim, I. Lee, D. Blaauw, J. D. Phillips., "Energy Harvesting for GaAs Photovoltaics Under Low-Flux Indoor Lighting Conditions," *IEEE Transactions on Electron Devices*, vol. 63, no. 7, pp. 2820-2825, July 2016, doi: 10.1109/TED.2016.2569079.
- [6] E. Moon, M. Barrow, J. Lim, D. Blaauw and J. D. Phillips, "Dual-Junction GaAs Photovoltaics for Low Irradiance Wireless Power Transfer in Submillimeter-Scale Sensor Nodes," in *IEEE Journal of Photovoltaics*, vol. 10, no. 6, pp. 1721-1726, Nov. 2020, doi: 10.1109/JPHOTOV.2020.3025450.
- [7] K. Lee, J. D. Zimmerman, T. W. Hughes, and S. R. Forrest, "Non-Destructive Wafer Recycling for Low-Cost Thin-Film Flexible Optoelectronics", *Adv. Funct. Mater.*, 24: 4284-4291 (2014). doi: 10.1002/adfm.201400453
- [8] K. A. W. Horowitz, T. Remo, B. Smith and A. Ptak, "A Techno-Economic Analysis and Cost Reduction Roadmap for III-V Solar Cells", National Renewable Energy Laboratory Technical Report NREL/TP-6A20-72103, (2018).
- [9] D. Khatiwada, C. A. Favela, S. Sun, C. Zhang, S. Sharma, M. Rathi, P. Dutta, E. Galstyan, A. Belianinov, A. V. Ievlev, S. Pouladi, A. Fedorenko, J. H. Ryou, S. Hubbard, and V. Selvamanickam, "High-efficiency single-junction p-i-n GaAs solar cell on roll-to-roll epi-ready flexible metal foils for low-cost photovoltaics", *Prog Photovolt Res Appl.*, 28: 1107– 1119 (2020). doi: 10.1002/pip.3308

### 2.3 CdTe solar cells for indoor applications

Elisa Artegiani<sup>1</sup> and Alessandro Romeo<sup>1</sup>.

<sup>1</sup>LAPS- Laboratory for Photovoltaics and Solid-State Physics, Department of Computer Science, University of Verona, Ca' Vignal 1, Strada Le Grazie 15, 37134, Verona, Italy

#### Status

CdTe thin film based solar cell technology has achieved, so far, the largest deployment on large scale manufacturing among thin film technologies. These have a very good advantage for PIPV (product integrated photovoltaics) that is the capability to be deposited on every type of substrate, from glass to metal and they can become extremely lightweight and flexible when deposited on flexible substrates [1].

In year 2021 almost 80 % of the thin film solar cell market was CdTe based with an overall production of 6.1 GWp [2]. CdTe photovoltaic devices have achieved an efficiency of 22.1 % on a small area for outdoor solar photovoltaics [3] but most important, unlike other technologies, the efficiency of the solar modules in production is not far from the record values: 18.7 %. The main reason for this achievement is due to the intrinsic properties of the CdTe absorber, which has a very simple phase diagram. The required stoichiometry (tendentially 50-50 for Cd and Te) is easily obtained also at relatively low temperatures (below 400 °C) and with no issues of unexpected and uncontrolled secondary phases [3].

CdTe is a direct band gap semiconductor with a value of 1.45 eV which is very near to the Shockley-Queisser optimum for outdoor solar photovoltaics, it also has a high absorption coefficient that allows to collect the photons with thicknesses down to 2 micrometers [3]. Furthermore, CdTe can be successfully

deposited with a large variety of different deposition methods, the most important are : thermal evaporation [4], close space sublimation [5], electrodeposition [6], vapour transport deposition [7].

In low light conditions, the spectrum changes with a wavelength shift towards the blue region, so the light power is concentrated in the 300 – 500 nm range. In this case, CdTe, which is mainly operating in the visible part of the spectrum, is much better performing, as also shown by different independent analysis. The highest efficiency indoor obtained from CdTe devices to date is 17.1 % under white LED.

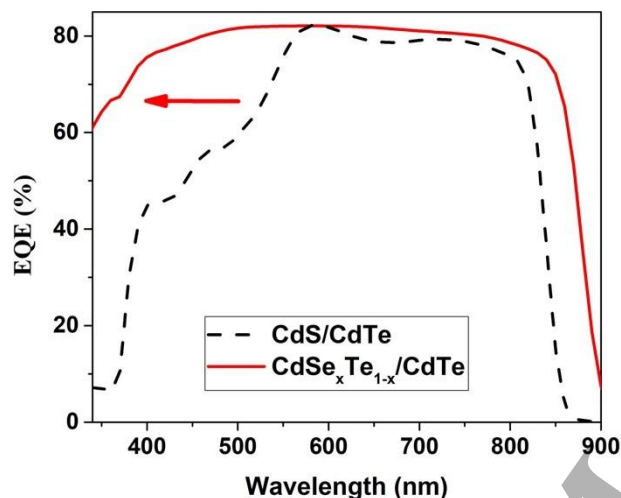


Fig. 1. External quantum efficiency: CdS/CdTe vs CdSe<sub>x</sub>Te<sub>1-x</sub>/CdTe

### Current and Future Challenges

CdTe thin film solar cells are typically fabricated in superstrate configuration, on a transparent conductive oxide coated soda lime glass.

Historically the cell is based on a CdS buffer layer for the separation of the charges. CdS is a semiconductor with a band gap of 2.4 eV and needs to be very thin in order to reduce the parasitic absorption in the 400 nm range. However, in recent times the structure of the solar cell has been radically changed with the introduction of a graded band gap. In this case CdTe compound forms a junction with a CdSe<sub>x</sub>Te<sub>1-x</sub> mixed compound (with a band gap of 1.4 eV). In this configuration CdS is no longer necessary and a high resistance layer (HRT) is interposed between the CdSe<sub>x</sub>Te<sub>1-x</sub> film and the front contact.

This is particularly important for indoor application because it increases the spectral response in the spectral region of indoor lights, as shown in figure 1.

CdTe solar cells are most successfully fabricated by physical vapor deposition processes, such as vapor transport deposition/ close space sublimation that are based on the sublimation of the CdTe in an inert gas atmosphere at a substrate temperature of about 500 °C, as well as thermal evaporation where CdTe is deposited in vacuum at a substrate temperature in the range of 300-350 °C.

The device made in our laboratories consists of a commercial SnO<sub>2</sub>/SnO<sub>2</sub>:F (TO/FTO) coated soda lime glass (TEC12), so in our case the HRT layer is TO, while also Mg<sub>x</sub>Zn<sub>1-x</sub>O can be used [8]. CdSe and CdTe are deposited by thermal evaporation, the typical standard CdCl<sub>2</sub> treatment for CdTe recrystallization, CdSe-CdTe mixing and CdSe<sub>x</sub>Te<sub>1-x</sub>/CdTe junction promotion is provided by drop casting of methanol solution.



1  
2  
3 With a similar process, CdS was used as buffer layer, we have previously demonstrated flexible CdTe  
4 devices on either polyimide or ultra-thin glass [1]. This is a very important feature for consumer electronics  
5 and so for indoor applications since it allows to adapt to different products, and it does not increase the  
6 weight of the final device.

7 CdTe solar cells have a demonstrated superior performance under low light irradiance where the  
8 reduction of open circuit voltage is restrained. With a very simple 1-diode model the ideality factor  
9 reduces towards one suggesting a change in transport mechanism corresponding to a more ideal junction  
10 [9]. This effect has been registered also in our samples.  
11  
12  
13  
14

### 15 **Advances in Science and Technology to Meet Challenges**

16 In figure 2 we compare the efficiencies of the cells measured under halogen and LED illumination, with  
17 different light irradiances. These values are normalized to the efficiency measured in standard conditions  
18 (AM 1.5 - 1 sun).  
19

20 Under low light irradiance, the efficiency is only slightly reduced in the case of halogen lamp, while it even  
21 increases when illuminated by LED. In both cases, this is due to a modest reduction in open circuit voltage  
22 along with an improvement in fill factor.  
23

24 The increase of efficiency for the LED case is due to the irradiation spectrum of this light which is exactly  
25 concentrated in the same range of the CdTe response (see fig. 1). This, considering the transition to LED  
26 lighting, further favours CdTe technology for indoor applications.  
27

28 One very important limitation for CdTe technology to indoor application is the national and international  
29 regulations that consumer electronics are subjected to. These set a maximum concentration of chemical  
30 elements that are considered dangerous to humans. Despite that CdTe is not registered as carcinogenic  
31 due to its impressive stability (1-decomposition occurs with temperatures above 1100 °C; 2-solubility in  
32 water does not occur), it is subjected to ROHS (Restriction of Hazardous Substances Directive directive)  
33 in EU (similar directives are extended to other countries). For ROHS regulation the maximum permitted  
34 concentrations in non-exempt products are 0.1 % or 1000 ppm (except for cadmium, which is limited to  
35 0.01 % or 100 ppm) by weight. The restrictions are attributed to a so-called *homogeneous* material in  
36 the product, this applies to each part that can be separated mechanically. In the latest design of CdTe  
37 solar cells where CdS is removed, cadmium, which is a heavy metal, is present only in the absorber.  
38 Considering the different densities of CdTe (5.85 g/cm<sup>3</sup>) and of soda lime glass (2.8 g/cm<sup>3</sup>) as well as  
39 considering the thickness of the two encapsulating glasses ( $\geq 3$  mm) we can roughly estimate a required  
40 CdTe thickness of less than 0.8  $\mu\text{m}$ . Our standard CdTe thickness is about 4.5  $\mu\text{m}$ , about 5 times above  
41 the limit. However, we have demonstrated that is possible to fabricate CdTe devices with 0.7  $\mu\text{m}$  with  
42 still an overall conversion efficiency of 8 % [10].  
43  
44  
45  
46  
47  
48  
49  
50  
51  
52  
53  
54  
55  
56  
57  
58  
59  
60

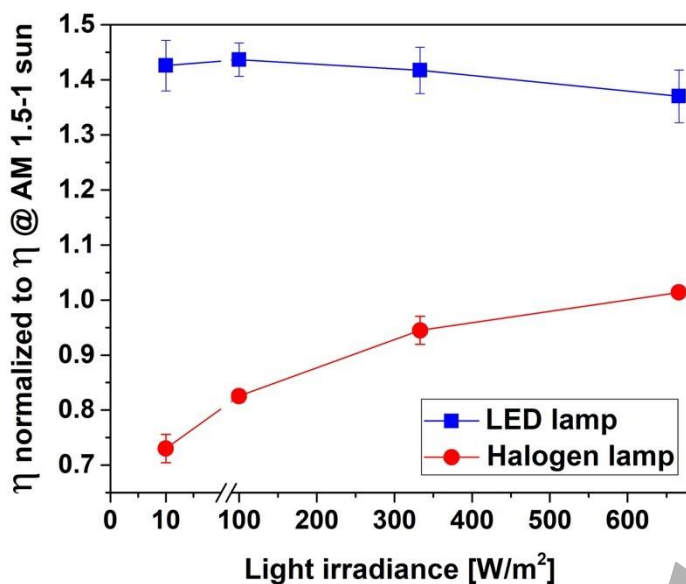


Fig.2. Efficiency of CdTe solar cells in respect to irradiation power and spectrum.

### Concluding Remarks

CdTe has shown to be a very good candidate for product integrated photovoltaics due to its robustness, reliability, high efficiency, and its suitability to be deposited on flexible devices.

Moreover, it has shown a remarkable behaviour for low light irradiation as demonstrated by different reports and papers also mentioned in this section. Furthermore, we have proved that with the new CdSe<sub>x</sub>Te<sub>1-x</sub>/CdTe configuration the device is very well performing under low light, and it is particularly suitable for LED indoor irradiation.

The main limitation to its application on devices is the ROHS directive which allows only 0.01 % of Cd weight compared to the complete PV device. This however can be overcome if the solar cell is made with ultra-thin CdTe, below 0.8 μm. This configuration has been already demonstrated also at our laboratory. Efficiencies could become quite interesting if a back reflecting mirror would be applied on the back contact.

### Acknowledgements

We would like to acknowledge Matteo Bertoncello, Matteo Meneghini and Gaudenzio Meneghesso from the Department of Information Engineering, University of Padua, for the EQE measurements. This work was partially made in the framework of BIntegra (Building Integrated Solar Energy Generation and Agrivoltaics) project funded by FSE-REACT-EU PON- CUP B39J21025850001.

### References

- [1] A. Salavei *et al.*, "Comparison of high efficiency flexible CdTe solar cells on different substrates at low temperature deposition," *Sol. Energy*, vol. 139, pp. 13–18, 2016.
- [2] Fraunhofer Institute for Solar Energy Systems and PSE Projects GmbH, "Photovoltaics Report - 2022- Fraunhofer ISE," no. February, p. <https://www.ise.fraunhofer.de/conte%0Ant/dam/ise/d,2022>.

- [3] A. Romeo and E. Arregiani, "CdTe-based thin film solar cells: Past, present and future," *Energies*, vol. 14, no. 6, 2021.
- [4] E. Arregiani *et al.*, "Analysis of a novel CuCl<sub>2</sub> back contact process for improved stability in CdTe solar cells," *Prog. Photovoltaics Res. Appl.*, vol. 27, no. 8, pp. 706–715, 2019.
- [5] A. Bosio, A. Romeo, D. Menossi, S. Mazzamuto, and N. Romeo, "Review: The second-generation of CdTe and CuInGaSe<sub>2</sub> thin filmPV modules," *Cryst. Res. Technol.*, vol. 46, pp. 857–864, 2011.
- [6] A. A. Ojo and I. M. Dharmadasa, "15.3% efficient graded bandgap solar cells fabricated using electroplated CdS and CdTe thin films," *Sol. Energy*, vol. 136, pp. 10–14, 2016.
- [7] B. E. McCandless, W. a Buchanan, and R. W. Birkmire, "High Throuput Processing of CdTe / CdS Solar Cells," in *Conference Record of the 33rd IEEE Photovoltaic Specialists Conference*, 2008, pp. 1–6.
- [8] I. Mathews *et al.*, "Analysis of CdTe photovoltaic cells for ambient light energy harvesting," *J. Phys. D. Appl. Phys.*, vol. 53, no. 40, 2020.
- [9] D. L. Bätzner, A. Romeo, H. Zogg, and A. N. Tiwari, "CdTe/CdS Solar Cell Performance under Low Irradiance," in *Proceedings of 17th European Photovoltaic Solar Energy Conference and Exhibition*, 2002, vol. 1, no. October, pp. 1180–1183.
- [10] A. Salavei, I. Rimmaudo, F. Piccinelli, and A. Romeo, "Influence of CdTe thickness on structural and electrical properties of CdTe/CdS solar cells," *Thin Solid Films*, vol. 535, pp. 257–260, May 2013.

## 2.4 Kesterites for indoor photovoltaics

Hongjae Shim<sup>1</sup>, Jongsung Park<sup>2</sup>, Jin Hyeok Kim<sup>3</sup> and Jae Sung Yun<sup>4</sup>

<sup>1</sup>Australian Centre for Advanced Photovoltaics (ACAP), School of Photovoltaic and Renewable Energy Engineering, University of New South Wales, Sydney, NSW 2052, Australia

<sup>2</sup>Department of Energy Engineering, Future Convergence Technology Research Institute, Gyeongsang National University, Jinju, Gyeongnam 52828, Republic of Korea

<sup>3</sup>Optoelectronics Convergence Research Center, and Department of Materials Science and Engineering, Chonnam National University, Gwangju 61186, Republic of Korea

<sup>4</sup>Department of Electrical and Electronic Engineering, Advanced Technology Institute (ATI), University of Surrey, Guildford, Surrey GU2 7XH, United Kingdom

### Status

Kesterite Cu<sub>2</sub>ZnSn(S,Se)<sub>4</sub> (CZTSSe) absorbers have incontrovertible advantages for indoor photovoltaics (PV) due to their non-toxicity, high stability, high absorption coefficient (10<sup>4</sup> cm<sup>-1</sup>), and direct bandgap. Their bandgap tuneability (from 1.0 to 1.94 eV) by adjusting the [S]/[S+Se] ratio and substituting their constituents (Cu and Sn with Ag and Ge, respectively) allows the deposition of kesterites with optimum bandgap for indoor PV (1.9–2.0 eV) [1]. Furthermore, the possibility of depositing kesterite absorbers on flexible substrates facilitates their integration into diverse shapes and dimensions, as needed for IoT devices. In fact, related Cu(In,Ga)(S,Se)<sub>2</sub> (CIGS) chalcopyrite absorbers also have the same advantages; however, their rare constituents (In, Ga) may hinder the mass production of indoor energy harvesters. Therefore, kesterite absorbers can be a promising solution for indoor applications. However, their indoor PV performance requires further improvement, given that their highest reported efficiency to date is 8.8% under visible LED light illumination with an irradiance of 18.5 mW/cm<sup>2</sup> [2]–[4].

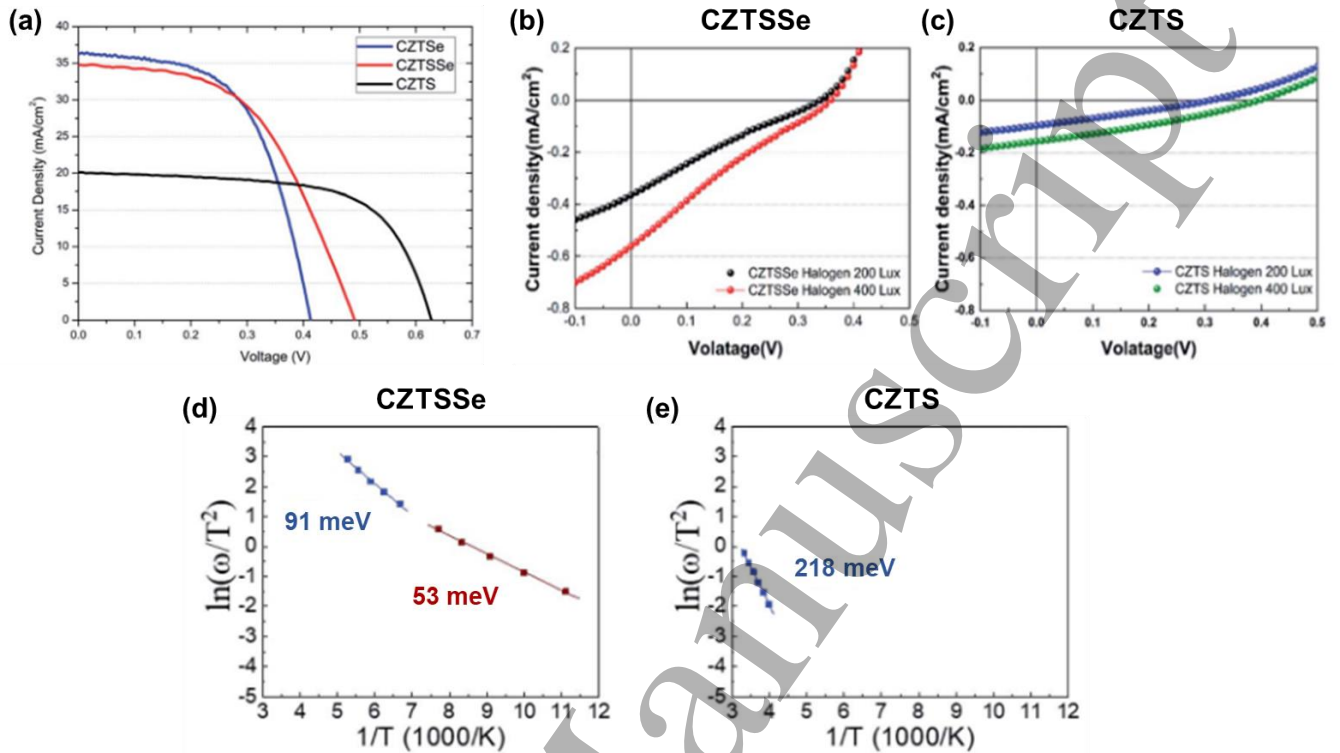


Figure 1. J-V curves of CZTS, CZTSe, and CZTSSe devices under 1 sun illumination (a). Low light intensity J-V curves of CZTSSe (b) and CZTS (c) devices under 200 lux and 400 lux (halogen lamp). Arrhenius plots of CZTSSe (d) and CZTS (e) were derived from temperature-dependent capacitance spectra measured by admittance spectroscopy (AS). [3]

### Current and Future Challenges

The advantages of kesterites have expanded their potential for both outdoor and indoor applications. However, these assets may only be exploited if the efficiencies reach levels attractive for commercialisation (15%). In this regard, enormous works, including optimisation of their elemental compositions, interface engineering, heterojunction optimisation and treatment, and defect engineering have been conducted. Despite the diverse approaches to improving device performance, the evolution of their outdoor efficiency has stagnated at around 13% for a decade. The considerably high density of intrinsic defects (e.g.,  $\text{Cu}_{\text{Zn}}$  and  $\text{Zn}_{\text{Cu}}$  antisites) and defect clusters (e.g.  $[\text{Cu}_{\text{Zn}} + \text{Zn}_{\text{Cu}}]$ ), originating from compatible ionic radii of Cu and Zn, have been widely reported [4]. The charged point defects and defect clusters in bulk and near the interface of the p-type absorber layer and n-type buffer layer have been suspected to reduce  $V_{\text{oc}}$ , thus limiting the device performance. Considering the vulnerability of indoor PV devices caused by charge carrier traps under weak light, the role of defects and defect clusters that can induce trap levels would become more significant. Furthermore, CZTSSe-based devices with a high composition of Se possess the highest outdoor performance whilst increasing S incorporation generally deteriorates the device performance by forming Sn-related defects. A higher Se composition results in the reduction of bandgap around 1.1 eV, which is far away from the optimum bandgap of indoor PV device (1.9 eV to 2.0 eV); hence, it is not preferable for the performance of indoor kesterites. J. Park et al. [3] compared the indoor device performance of CZTS-, CZTSe-, and CZTSSe-based solar cells (Figure 1b-c), whose outdoor performances were compatible (Figure 1a). This study demonstrated reduced efficiency in the CZTS devices due to a severe  $V_{\text{oc}}$  drop under weak light (Figure 1c). The deeper defect level at 218 meV in the CZTS device compared to those (at 53 and 91 meV) in the CZTSSe counterpart was regarded

1  
2  
3 as responsible for the lower device performance (Figure 1e). A higher sulphur ratio is needed to widen  
4 the bandgap of CZTS absorbers for indoor PV. Hence, investigating the role of defects in kesterite films  
5 and developing proper defect engineering methods seem to be the key priorities for kesterite indoor PV.  
6

### 7 **Advances in Science and Technology to Meet Challenges**

8 One powerful approach to alleviate the dysfunctionalities of the antisite defects and defect clusters in  
9 kesterites for indoor applications is substituting Cu ions with cations such as Ag and Ge. J. Park et al. [1]  
10 demonstrated that the antisite defects related to Cu, Zn, and Sn were effectively suppressed by the  
11 cations, achieving enhanced device performance at low light illuminations. Under 1 sun illumination, the  
12 performance enhancement by incorporation of both Ag and Ge was comparable (from 7.5 to 9.04 and  
13 9.05 %, respectively). Nevertheless, at low-intensity light conditions, the CZTSSe device with Ag  
14 incorporation exhibited higher performance than that with Ge incorporation. While the Ag device had a  
15 higher defect density ( $\sim 2 \times 10^{17} \text{ cm}^{-3} \text{ eV}^{-1}$ ) than the Ge device, its lower defect energy level (86 meV) was  
16 found to be beneficial under low light illumination. Therefore, the superior performance of the Ag device  
17 in weak light despite high defect density can be interpreted based on its lower defect energy level. This  
18 work gives an insight into the necessity of different approaches to defect engineering for indoor PV  
19 devices compared to the outdoor PV counterpart, opening possibilities for high-performance indoor PV  
20 based on kesterites with wider bandgap. Also, improved efficiency in CZTS solar cells was achieved by  
21 inserting a passivation layer ( $\text{Al}_2\text{O}_3$ ) between the kesterite absorber and Cd-free buffer layer was reported  
22 by X. Cui et al. [5]. The passivation reduced the local potential fluctuation of band edges and resulted in  
23 the widening of bandgap and enhancement of  $V_{oc}$  (see Figure 2a). For further efficient absorption of  
24 indoor light entering from all directions for more homogenous intensities, dedicated device engineering  
25 efforts are also required. For instance, H. Deng et al. [2] designed robust bifacial CZTSSe-based PV with  
26 outdoor efficiency of over 9% and indoor efficiency of 8.8%, which could harvest energy from light  
27 absorbed via both the front and back surfaces, using flexible Mo-foil substrates (see Figure 2b).  
28  
29  
30  
31  
32  
33  
34  
35  
36  
37  
38  
39  
40  
41  
42  
43  
44  
45  
46  
47  
48  
49  
50  
51  
52  
53  
54  
55  
56  
57  
58  
59  
60

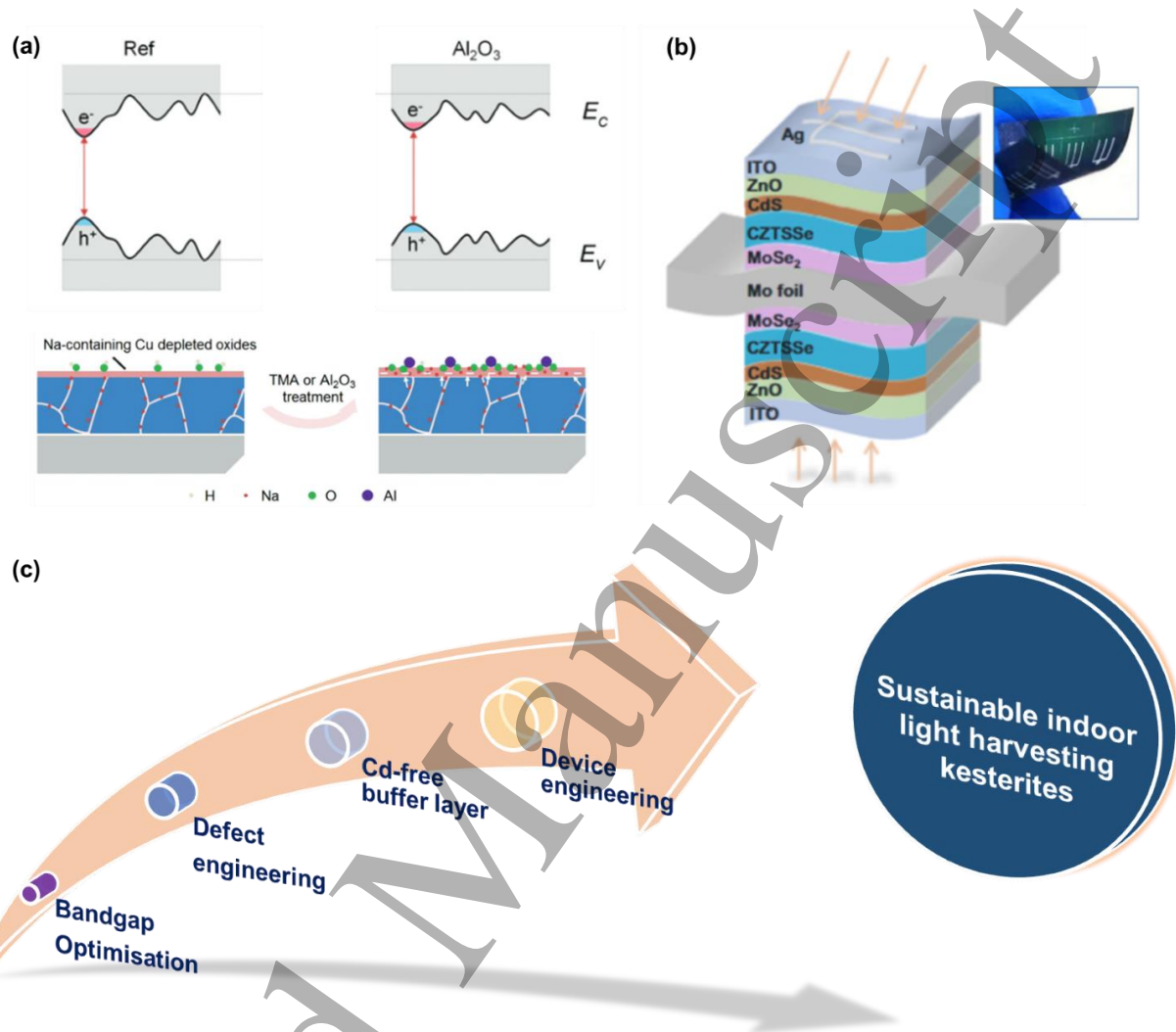


Figure 2. (a) (Top) Diagram illustrating the band gap fluctuation in CZTS with and without Al<sub>2</sub>O<sub>3</sub> treatment and (bottom) surface modification mechanism in CZTS subjected to ALD-Al<sub>2</sub>O<sub>3</sub> treatment [5]. (b) Device structure of bifacial CZTSSe photovoltaic cells on a flexible substrate [2]. Roadmap for efficient and eco-friendly kesterite PV for indoor applications.

### Concluding Remarks

Among various candidates for indoor PV materials, kesterites can be promising due to their non-toxicity, high stability, high absorption coefficient, and direct and tuneable bandgap. In Figure 2c, we illustrate a schematic of the roadmap for efficient and eco-friendly kesterites for indoor applications. Firstly, the right bandgap composition has to be set with appropriate defect engineering to mitigate the defect density as well as the defect level positions. Also, the Cd buffer layer must be replaced with other materials to realize fully eco-friendly PV. Finally, novel device engineering (for instance, a device architecture with kesterite absorbers coated on both sides of a flexible substrate) will lead kesterites to be competitive in the future indoor PV market.



## Acknowledgements

This work was supported by Priority Research Centers Program through the National Research Foundation of Korea(NRF) funded by the Ministry of Education, Science and Technology(2018R1A6A1A03024334), by the National Research Foundation of Korea(NRF) grant funded by the Korea government(MSIT) (No.2022R1A2C2007219), and by Basic Science Research Program through the National Research Foundation of Korea(NRF) fund by the Ministry of Education (NRF-2022R111A3069502)

## References

- [1] J. Park *et al.*, "Suppression of Defects Through Cation Substitution: A Strategic Approach to Improve the Performance of Kesterite  $\text{Cu}_2\text{ZnSn}(\text{S},\text{Se})_4$  Solar Cells Under Indoor Light Conditions," *Solar RRL*, vol. 5, no. 4, Apr. 2021, doi: 10.1002/solr.202100020.
- [2] H. Deng *et al.*, "Novel symmetrical bifacial flexible CZTSSe thin film solar cells for indoor photovoltaic applications," *Nature Communications*, vol. 12, no. 1, Dec. 2021, doi: 10.1038/s41467-021-23343-1.
- [3] J. Park *et al.*, "Investigation of low intensity light performances of kesterite CZTSe, CZTSSe, and CZTS thin film solar cells for indoor applications," *Journal of Materials Chemistry A*, vol. 8, no. 29, pp. 14538–14544, Aug. 2020, doi: 10.1039/d0ta04863a.
- [4] P. D. Antunez, D. M. Bishop, Y. Luo, and R. Haight, "Efficient kesterite solar cells with high open-circuit voltage for applications in powering distributed devices," *Nature Energy*, vol. 2, no. 11, pp. 884–890, Nov. 2017, doi: 10.1038/s41560-017-0028-5.
- [5] X. Cui *et al.*, "Cd-Free  $\text{Cu}_2\text{ZnSnS}_4$  solar cell with an efficiency greater than 10% enabled by  $\text{Al}_2\text{O}_3$  passivation layers," *Energy and Environmental Science*, vol. 12, no. 9, pp. 2751–2764, Sep. 2019, doi: 10.1039/c9ee01726g.

## 2.5 Organic photovoltaics for indoor light to electricity conversion

Gregory C. Welch<sup>1</sup>, Bryon W. Larson<sup>2</sup>, Myles Creran<sup>3</sup>, Audrey Laventure<sup>3</sup>

<sup>1</sup>Department of Chemistry, University of Calgary, Calgary, AB, T2N 4K9, Canada

<sup>2</sup>National Renewable Energy Laboratory, Golden, CO 80401, USA

<sup>3</sup>Département de chimie, Université de Montréal, Montréal, QC, H2V 0B3, Canada

### Status

Organic photovoltaics (OPV) are a widely investigated clean energy (light to electricity) conversion technology in academia.<sup>1–3</sup> Recently, the technology has been commercialized with various products available to the general public. Key advantages compared to traditional silicon-based photovoltaics include solution processability of the photoactive layer and charge transport interlayers components, which enables ultra-low-cost manufacturing *via* coating and printing techniques, a high degree of OPV module flexibility/conformability and form factors (i.e. shapes and sizes), and tunable light harvesting properties. Limitations include the power conversion efficiency (PCE) and operational lifetimes, both inhibiting widespread utilization.

Owing to the high molar absorptivity of organic molecules in the visible region of the electromagnetic spectrum (i.e. white light) and the exciton-based processes involved in organic photovoltaics, they have been predicted to be capable of converting indoor light into useable electricity.<sup>4–6</sup> Indeed, the global indoor light harvesting market is expected to grow from \$140M in 2017 to >\$1B (USD) by 2023, with a projected demand for such devices by then exceeding 60 million per year. While the output power is by default low (microwatts per  $\text{cm}^2$ ) such devices are suitable for low-power, wireless electronic sensors for

the Internet of Things (IoT). Potential application has been recently demonstrated with an OPV device reaching 25% efficiency under 1000 lux (i.e. a standard LED light bulb).<sup>7</sup>

The organic semiconductors (p- and n-types,  $\pi$ -conjugated compounds) that comprise the photoactive layers of OPVs are ideally suited for utility in harvesting light from artificial sources including LEDs and incandescent bulbs. Fine control of the chemical structure of these compounds allows for tailoring of optoelectronic properties. Design rules related to the p- and n-type organic semiconductors are now well established and optical absorption of photoactive blends can be matched to specific light emission and energy levels optimized to minimize energy loss and maximize operating voltages.<sup>8</sup> In addition, such materials can be (1) prepared *via* atom-economical synthetic procedures rendering them low-cost and accessible and (2) be processed into photoactive films from halogen-free solvents using roll-to-roll compatible coating methods facilitating a transition from laboratory-to-fabrication, as shown in Figure 1B.<sup>9</sup>

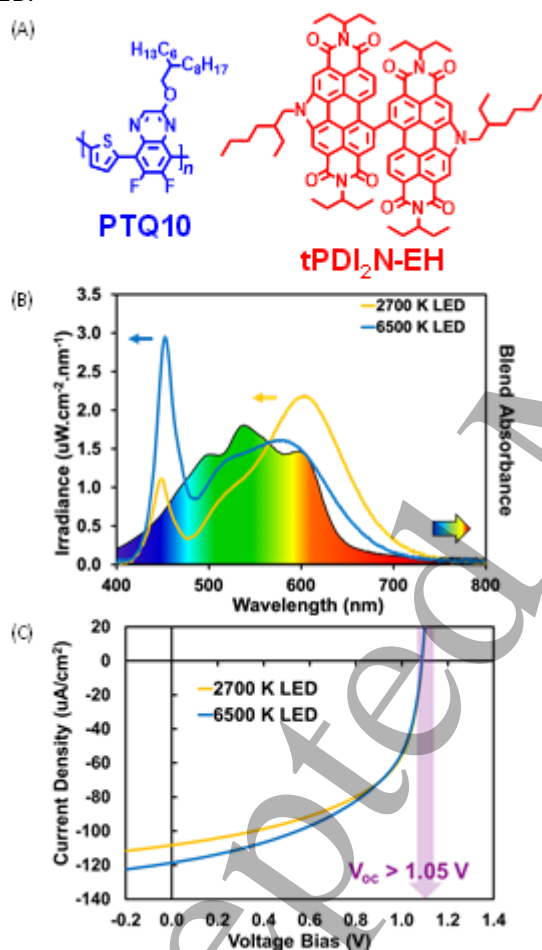


Figure 1. (A) Chemical structures of reported organic semiconductors with demonstrated utility as effective LED light harvesters. PTQ10 is a donor polymer (p-type) and tPDI<sub>2</sub>N-EH is a non-fullerene acceptor (n-type). Both materials can be made on scale and are processible from halogen-free solvents. (B) Optical absorption spectrum of a PTQ10:tPDI<sub>2</sub>N-EH bulk-heterojunction film (rainbow) overlapping with the irradiance of warm and cool LED emission. (C) Current-voltage curves of an OPV device with a PTQ10:tPDI<sub>2</sub>N-EH bulk-heterojunction exhibiting a high open-circuit voltage, a result of tailored electronic energy levels. Reproduced from Ref. 9 with permission from the Royal Society of Chemistry.



### Current and Future Challenges

*Materials Design.* Most reports on iOPVs have simply used known materials developed for outdoor (1 sun, i.e., 100 mW/cm<sup>2</sup>) environments. Thus, there is a great opportunity to develop new custom-made photoactive materials with matched optical absorption to the emission from specific light sources (approximately 400-700 nm). In the design of such organic semiconductor materials, minimizing energy loss and maximizing operating voltages is far more important than reaching higher and higher PCEs as the intended use is to run low-power devices. Materials should adopt a facile synthesis and be processible from halogen-free solvents, and thus be compatible with large area roll-to-roll coating. In this case, classic organic semiconductors that have fallen out of favor such as P3HT and PCDTBT may find new life owing to a low-cost synthesis and strong absorption of indoor lighting.

*Accurate Photovoltaic Measurements.* Standardization of OPV characterization is easier when the reference spectrum is always our Sun (outdoor PV). The task of standardizing non-solar light conversion is a challenge that must be overcome so that reliable power output specifications to design IoT or sensors around are known. Translational equations are used by institutions like NREL, EST-JRC, and AIST to interpret device output under a given reference condition.<sup>10</sup> When the reference condition is not the sun (the case for the majority of iOPV intended uses), existing translational equations are invalid. Since new translational methodologies don't exist yet for indoor PV standards, substantial uncertainty exists in reported indoor PCEs to date, especially when lux meters, as opposed to spectral radiometric equipment, are used to establish incident power. One major current challenge is that the traceable reference cells that are used to measure indoor light power, were calibrated against 1 sun when certified, and therefore don't apply to the indoor spectrum.

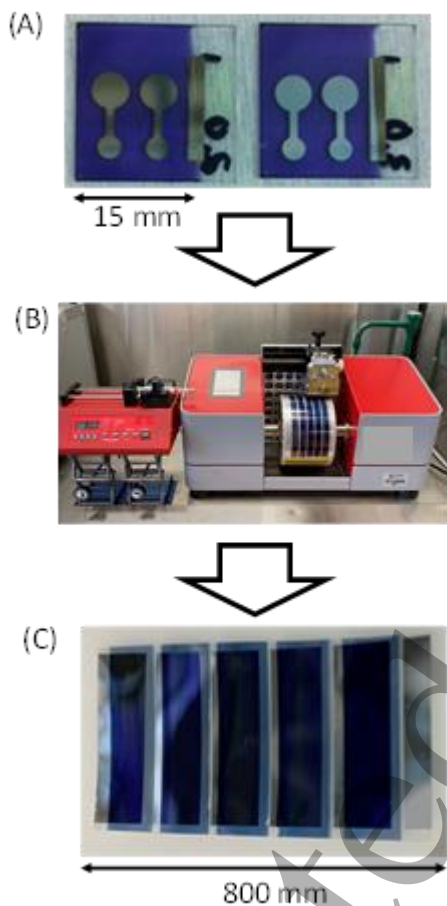
*Device Engineering.* Given the different environmental operating constraints of indoor vs. outdoor light harvesting, iOPV requires new design criteria (in many ways relaxed relative to outdoor OPV) for device stack materials that are tailored specifically for indoor conditions. Indeed, metal oxide UV-soaking does not happen inside, reinforcing the need to use different charge transport layer materials.

### Advances in Science and Technology to Meet Challenges

Matching the indoor light emission wavelength range to the absorbance spectrum of the photoactive layer of the iOPV device can be achieved by a rational design and/or blending of the p- and n-type organic  $\pi$ -conjugated compounds. To meet this challenge faster, the conventional experimental trial-and-error approach would benefit from pairing up with computational simulations and predictions. Feedback loops could also be developed where the results of molecular design and/or processing conditions act as inputs, while output designs and conditions are suggested via artificial intelligence tools. Once the formulation of the photoactive layer is selected, another major challenge lies in its processing, especially since processing can dramatically affect the resulting microstructure of the film, and thus, its absorption profile. It needs to be compatible with industrially relevant coating techniques, such as blade- and slot-die coating (c.f. Figure 2) and be conducted in ambient conditions (no spin-coating nor glove-box processing). Photoactive layer formulations that present a performance that is thickness independent also need to be targeted.

A way to ensure a proper comparison of device performance is to move away from PCE and instead compare W/m<sup>2</sup> values produced directly against appropriate reference incident total irradiance spectra. The latter will require the most effort to produce, since many indoor reference spectra, in W/m<sup>2</sup>, will need to be collected, but afterwards new reference cells can be certified against these spectra and then the traditional translational equation methodologies can be applied.

1  
2  
3 Alternatives to charge transport layers requiring post-processing high temperature annealing and UV  
4 activation or soaking are required for iOPV prepared on flexible (mostly polymer-based) substrates and  
5 operating with indoor light. Such charge extracting interfaces design is a paramount to ensure iOPV  
6 operational lifetime in a context where the absence of UV light, humidity and temperatures swings in  
7 indoor conditions impact far less the photoactive layers than under 1 sun conditions. Formulations that  
8 can be coated using roll-to-roll compatible techniques without requiring a high temperature annealing,  
9 like SnO<sub>2</sub> nanoparticles, need to be further developed. Module fabrication (different form factors) and  
10 circuit integration would greatly benefit from electrical engineering inputs, where connection of devices  
11 (series or parallel) can tune the module power delivery.  
12



43 Figure 2. Required transition for OPV application in indoor light recycling. (A) Common lab-scale OPV  
44 devices made via spin-coating. (B) Affordable roll-coaters for research and development. (C) OPV module  
45 (5 cell) made via roll-coating using halogen free solvents with current photoactive and interlayer materials.  
46 Photos original from Welch lab.  
47

#### 48 Concluding Remarks

49 Overall, the organic photovoltaic for indoor light conversion to electricity presents several challenges for  
50 the scientific community that are yet to be tackled. Seizing this opportunity to develop the next generation  
51 of iOPV calls for interdisciplinary research efforts, leading to advances within the materials chemistry,  
52 device engineering and metrology landscapes. Moreover, three key concepts need to be kept in mind  
53 during this endeavor towards a lab-to-fab transition for iOPV devices: scalability, sustainability, and  
54 standardization. The scalability and the sustainability of the photoactive layer and charge transport  
55  
56  
57  
58  
59  
60

interlayer compounds synthesis and of their thin film coating processes, and the standardization of the device performance evaluation. These key concepts stand as *sine qua non* conditions to ensure a perennial technology transfer from research and development to a widespread adoption of iOPV as power sources for wireless, low-voltage devices.

### Acknowledgements

M.C. thanks the Centre Québécois sur les Matériaux Fonctionnels (CQMF, a Fonds de recherche du Québec – Nature et Technologies strategic network) and A.L. thanks the Canada Research Chairs program for financial support. G.C.W thanks the University of Calgary. This work was authored in part by the National Renewable Energy Laboratory, operated by Alliance for Sustainable Energy, LLC, for the U.S. Department of Energy (DOE) under Contract No. DE-AC36-08GO28308 with writing support for BWL by ARPA-E DIFFERENTIATE program under grant no. DE-AR0001215. The views expressed in the article do not necessarily represent the views of the DOE or the U.S. Government.

### References

- (1) Zhang, J.; Tan, H. S.; Guo, X.; Facchetti, A.; Yan, H. Material Insights and Challenges for Non-Fullerene Organic Solar Cells Based on Small Molecular Acceptors. *Nat. Energy* **2018**, *3*, 720–731.
- (2) Cheng, P.; Li, G.; Zhan, X.; Yang, Y. Next-Generation Organic Photovoltaics Based on Non-Fullerene Acceptors. *Nat. Photonics* **2018**, *12* (3), 131–142.
- (3) Hou, J.; Inganäs, O.; Friend, R. H.; Gao, F. Organic Solar Cells Based on Non-Fullerene Acceptors. *Nat. Mater.* **2018**, *17* (2), 119
- (4) Mathews, I.; Kantareddy, S. N.; Buonassisi, T.; Peters, I. M. Technology and Market Perspective for Indoor Photovoltaic Cells. *Joule* **2019**, *3* (6), 1415–1426.
- (5) You, Y.-J.; Song, C. E.; Hoang, Q. V.; Kang, Y.; Goo, J. S.; Ko, D.-H.; Lee, J.-J.; Shin, W. S.; Shim, J. W. Highly Efficient Indoor Organic Photovoltaics with Spectrally Matched Fluorinated Phenylene-Alkoxybenzothiadiazole-Based Wide Bandgap Polymers. *Adv. Funct. Mater.* **2019**, *29* (27), 1901171.
- (6) Shin, S.-C.; Koh, C. W.; Vincent, P.; Goo, J. S.; Bae, J.-H.; Lee, J.-J.; Shin, C.; Kim, H.; Woo, H. Y.; Shim, J. W. Ultra-Thick Semi-Crystalline Photoactive Donor Polymer for Efficient Indoor Organic Photovoltaics. *Nano Energy* **2019**, *58*, 466–475.
- (7) Cui, Y.; Wang, Y.; Bergqvist, J.; Yao, H.; Xu, Y.; Gao, B.; Yang, C.; Zhang, S.; Inganäs, O.; Gao, F.; et al. Wide-Gap Non-Fullerene Acceptor Enabling High-Performance Organic Photovoltaic Cells for Indoor Applications. *Nat. Energy* **2019**, 1–8.
- (8) Dayneko, S. D.; Pahlevani, M.; Welch, G. C. Indoor Photovoltaics: Photoactive Material Selection, Greener Ink Formulations, and Slot-Die Coated Active Layers. *ACS Applied Materials and Interfaces*. **2019**. *11*, 49, 46017-46025.
- (9) Tintori, F.; Laventure, A.; Koenig, J. B. D.; Welch, G. C. High Open-Circuit Voltage Roll-to-Roll Compatible Processed Organic Photovoltaics. *Journal of Materials Chemistry C*. **2020**. *8*, 13430-13438.
- (10) Osterwald, C.R. Translation of device performance measurements to reference conditions. *Solar Cells*. **1986**. *18*, 269-279.

## 2.6 Dye-sensitized photovoltaics for indoor applications

Kezia Sasitharan<sup>1</sup>, Natalie Flores-Diaz<sup>1</sup> and Marina Freitag<sup>1</sup>

<sup>1</sup>School of Natural and Environmental Sciences, Bedson Building, Newcastle University, NE1 7RU Newcastle upon Tyne, UK

### Status

Dye-sensitized solar cells (DSCs) comprise of a mesoporous semiconducting layer (usually  $\text{TiO}_2$ ) functioning as a working electrode (WE), to which sensitizer molecules are adsorbed. The counter electrode (CE) faces the sensitizer, with a redox mediator between CE and the WE. Upon light absorption, photo-induced electron transfer occurs from the sensitizer to the  $\text{TiO}_2$ . The redox mediator enables regeneration of the dye, facilitating the transfer of positive charges from the WE to the CE, as demonstrated in Figure 1. DSCs primarily absorb in the visible region (from 400 to 650 nm) and outperform GaAs solar cells under diffuse light conditions, while also being inexpensive and environment friendly.[3]

Even under ambient light illumination, DSCs can maintain a high photovoltage. This is attributed to the tuneable energy levels in Cu(II/I) electrolyte systems and reduced recombination along with fast charge separation processes in organic dyes. Molecular engineering of the dyes, and their combination (co-sensitizers) for improved matching of their absorbance with the emission of the artificial light sources (as shown in Figure 2) has significantly pushed the efficiency of DSCs for indoor photovoltaics (IPVs). A PCE of 28.9% was observed under 1000 lux fluorescent light tube using  $[\text{Cu}(\text{tmby})_2]^{2+/1+}$  redox coupled with  $\text{TiO}_2$  films co-sensitized with the dye D35 and XY1. [4] The continued development of panchromatic rigid-structure dyes, alternative hole transport materials and design flexibility has enabled improved PCEs, currently reaching 13% under AM1.5G conditions and 34% under indoor light.[5]

In recent years, DSCs have shown remarkable progress in harvesting energy from artificial light sources, making them a suitable option for various low power devices used indoors. In 2020, DSCs were successfully tested to power battery-free IoT devices capable of machine learning under ambient light conditions.[6]

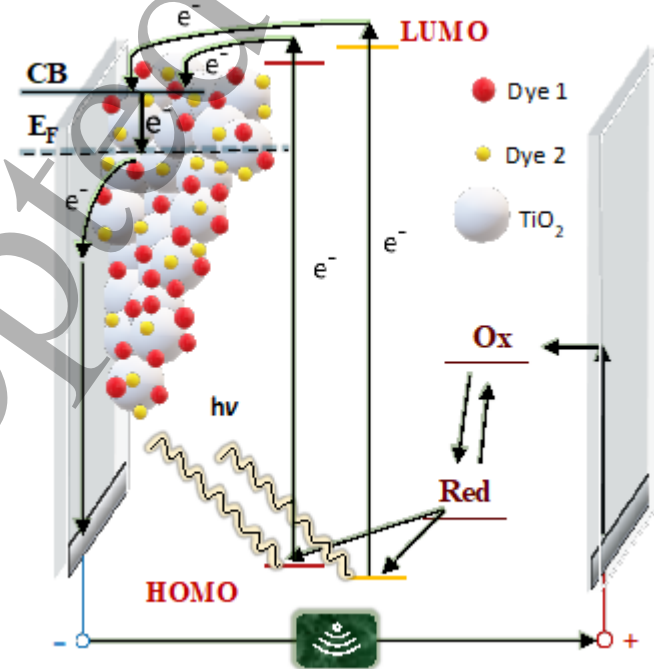


Figure 1. Working principles of DSCs with a co-sensitized system and a redox mediator Ox/Red.

### Current and Future Challenges

The conversion of ambient light into usable energy paves the way for the widespread implementation of self-powered wireless devices.[7] To attain their full potential as IPVs, DSCs must achieve PCEs closer to the maximum theoretical value of 52%. [8] Their integration as a sustainable power source for sensors and wireless electronics will lead to self-powered monitoring systems, data collection, and wireless communication, thereby saving energy in buildings, industries, and households. [9] Indoor DSCs with co-sensitized systems can achieve high PCEs employing dyes absorbing at 550–600 nm and a co-sensitizer absorbing in the blue region of the visible spectra, offering an excellent match to the ambient light spectra. This approach also reduces electron recombination rates from the conduction band of the  $\text{TiO}_2$  to the redox mediator. Interfacial engineering and redox mediators with high redox potentials are required to further reduce electron recombination and maintain high photovoltage. The commercialization of DSCs is hindered by the inability to develop solid-state devices on a large scale. Solid-amorphous copper-based HTMs showed significant power densities at 1000 lux (approximately  $110 \text{ mW/cm}^2$ ), and scalable deposition methods are being developed. [10]

### Advances in Science and Technology to Meet Challenges

To advance the field of DSCs for ambient applications, it will be necessary to simultaneously improve DSCs and IoT devices with innovative hardware and software, combining chemistry, engineering, and computer science. By developing new materials, it is possible to increase the  $V_{oc}$  above 1.0 V at 1000 lux. For instance, novel preparation methods and surface treatments for semiconductors with higher conduction band energies than  $\text{TiO}_2$  (such as  $\text{Zn}_2\text{SnO}_4$ ,  $\text{SrTiO}_3$ , and  $\text{BaTiO}_3$ ) should be investigated to increase dye loading and decrease interfacial electron recombination.

Since recombination processes cause most DSC performance losses, research should focus on developing a fundamental understanding of the interaction between dyes and charge transport materials and their impact on photovoltaic processes. This will enable the development of alternative charge carrier materials with improved charge transport, reduced recombination losses, and enhanced long-term stability. Furthermore, liquid electrolytes should be replaced with solid-state charge transport materials to reduce leakage, solvent evaporation, dye photodegradation, dye desorption, and counter electrode corrosion. Novel architecture designs are needed to allow backside illumination and incorporate carbon-based composites at the counter electrodes, enabling solid-state monolithic devices. [8]

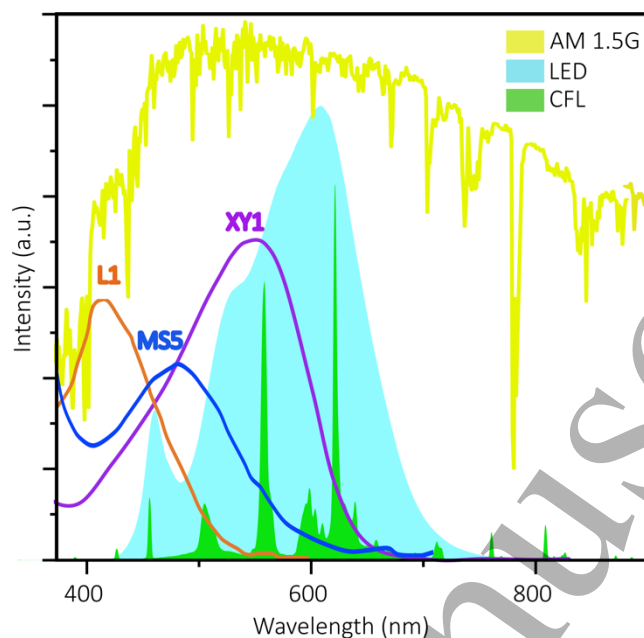


Figure 2. Normalized emission spectra of warm white CFL and LED bulbs, and of the AM1.5G spectrum with absorption overlay of prominent indoor dyes: L1, XY1 and MS5.

Future research will focus on efficient converters with low power fluctuations and energy buffers to maintain a constant voltage throughout the operation/sleep cycles of indoor electronic devices. Due to the scarcity of battery recycling facilities and materials, supercapacitor research must be addressed. Coupling supercapacitors or novel energy storage devices to DSCs will enable constant power delivery when the indoor light is unavailable.[9]

### Concluding Remarks

Self-powered and 'smart' IoT devices and networks can now be powered by ambient light harvesters, a previously untapped energy source. Indoor dye-sensitized photovoltaics with nontoxic materials and high efficiency will play an important role in IoT sustainability.

Considering that indoor environments are more stable in terms of temperature, humidity, and light, designing materials with higher performance properties is plausible. New electronic configurations custom designed for various IoT applications must be developed to provide constant voltage and power. With these further developments in both material design and device architecture, the PCEs of DSCs under indoor light can be pushed closer to the theoretical limit to generate a new era of autonomous, smart and self-powered devices.

The progress of these systems can depend on the following factors:

- Upscaling DSCs to minimodules delivering 3-5 V to fulfil IoT requirements.
- Advances in the stability and efficiency of commercially available IPVs
- Novel energy storage devices, particularly non-conventional storage approaches.
- New methods to improve the energy of CPUs/MCUs, wireless communication devices and sensors.
- Computing algorithms and topologies enabling self-powered IoT devices with environmental- and self-awareness.

Highly efficient ambient DSCs are ultimately intended to assist us in maximising the benefits of interconnected IoTs and wireless device innovations while reducing their own environmental and energy impacts. [10]

### Acknowledgements

M.F. acknowledges the support by the Royal Society through the University Research Fellowship (URF\R1\191286), Research Grant 2021 (RGS\R1\211321), and EPSRC New Investigator Award (EP/V035819/1). N.F-D. acknowledges the support by the EU Horizon 2020 MSCA-IF funding, project 101028536.

### References

- [3] I. Mathews, S. N. Kantareddy, T. Buonassisi, and I. M. Peters, "Technology and Market Perspective for Indoor Photovoltaic Cells," *Joule*, vol. 3, no. 6, pp. 1415–1426, 2019.
- [4] M. Freitag, J. Teuscher, Y. Saygili, X. Zhang, F. Giordano, P. Liska, J. Hua, S. M. Zakeeruddin, J. E. Moser, M. Graetzel, and A. Hagfeldt, "Dye-sensitized solar cells for efficient power generation under ambient lighting," *Nature Photonics*, vol. 11, no. 6, pp. 372-378, 2017.
- [5] H. Michaels, M. Rinderle, R. Freitag, I. Benesperi, T. Edvinsson, R. Socher, A. Gagliardi, and M. Freitag, "Dye-sensitized solar cells under ambient light powering machine learning: towards autonomous smart sensors for the internet of things," *Chemical Science*, vol. 11, no. 11, pp. 2895–2906, 2020.
- [6] M. Li, F. Igbari, Z. K. Wang, and L. S. Liao, "Indoor Thin-Film Photovoltaics: Progress and Challenges," *Advanced Energy Materials*, vol. 10, no. 28, pp. 1–25, 2020.
- [7] C. Zheng, Q. Wu, S. Guo, W. Huang, Q. Xiao, and W. Xiao, "The correlation between limiting efficiency of indoor photovoltaics and spectral characteristics of multi-color white LED sources," *Journal of Physics D: Applied Physics*, vol. 54, no. 31, p. 315503, aug 2021.
- [8] B. Li, B. Hou, and G. A. J. Amaratunga, "Indoor photovoltaics, The Next Big Trend in solution-processed solar cells", *InfoMat*, vol. 3, no. 5, pp. 445–459, 2021.
- [9] H. Michaels, I. Benesperi, and M. Freitag, "Challenges and prospects of ambient hybrid solar cell applications," *Chemical Science*, vol. 12, no. 14, pp. 5002–5015, 2021.
- [10] E. Hittinger and P. Jaramillo, "Internet of things: Energy boon or bane?" *Science*, vol. 364, no. 6438, pp. 326–328, 2019.

## 2.7 Lead-halide perovskites for indoor photovoltaics

Jie Xu and Thomas M. Brown

CHOSE (Centre for Hybrid and Organic Solar Energy), Department of Electronic Engineering, University of Rome Tor Vergata, Via del Politecnico 1, 00133 Rome, Italy

ORCID: 0000-0003-2141-3587 (T. M. Brown); ORCID: 0000-0003-0416-5200 (J. Xu)

### Status

Recent and ever-increasing published literature has shown that perovskite solar cells (PSCs) are clearly one of the best candidates for indoor photovoltaics (IPV) owing to their exceptional power-conversion-efficiency (PCE) under low light conditions in the visible range, i.e. those emitted by white light sources such as LEDs and compact fluorescent lamps used for indoor illumination. The earliest demonstrations of IPV performance of PSCs can be traced down to Chen et al. for the PEDOT:PSS/PCBM p-i-n architecture in 2015 [1], and Di Giacomo et al. [2] for the classical TiO<sub>2</sub> and Spiro-OMeTAD architecture. In both these works, PCEs as high as 24% at 200 lx and 27% at 1000 lx were obtained, which are substantially higher



than those ever achieved at standard test conditions (see figure 1(a)). In 2017 Lucarelli et al. reported the first flexible PSCs fabricated on PET substrates delivering a PCE of 11-12% in the 200 - 400 lx range under LED white light [3]. After only a few years, efficiencies of indoor perovskite solar cells (i-PSCs) have continued to soar, reaching current records in rigid cells of 34.8% at 200 lx, the most common range found in homes [4], and 40.2% at the higher 1000 lx found less often, in environments like supermarkets [5], and 30.7% (212 lx), 31.9% (1062 lx) in flexible PEN cells [6], and 20.6% (200 lx) in ultrathin flexible glass [7]. Notably, these record efficiencies of i-PSCs have surpassed their competitors, both commercial such as a-Si as well as new generation PV such as DSSCs and OPV as shown in figure 1(b) [4]. The continuing improvement in efficiency, together with corresponding step forwards in module performance and stability that is required in the future, as well as overcoming environmental/toxicity concerns of perovskite semiconductors, can open up huge markets for this technology. In fact, the low-power (20-50  $\mu\text{W}$  average power consumption) Internet of Things (IoT) and wireless sensor networks fields are becoming more and more prevalent in our daily lives, with more than tens of billions of IoT devices predicted to be deployed by 2025. IPV can become a key enabling technology to power these indoor microelectronic devices (for example, sensors, watches, and calculators) [8].

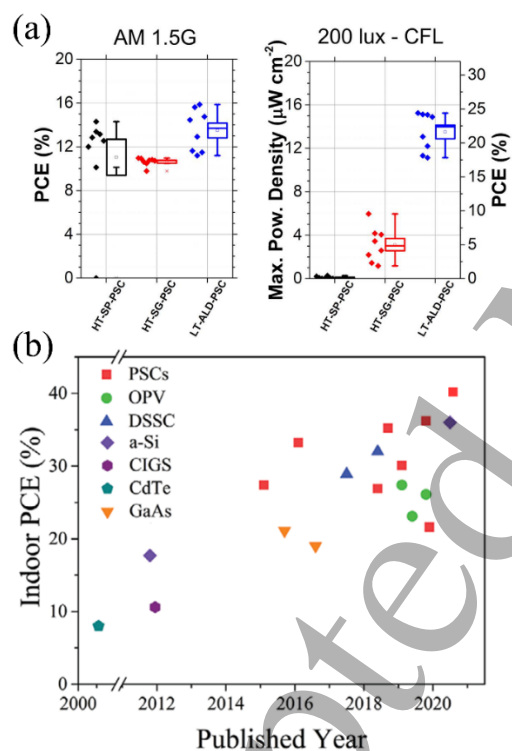


**Figure 1.** a) Left, distribution of power conversion efficiencies (PCE) of the first n-i-p perovskite solar cells developed for indoor light harvesting with different electron transport layers (ETLs) deposited either with atomic layer deposition (ALD, black), spray pyrolysis (red), or double ETL of ALD deposited c-TiO<sub>2</sub> together with a meso-TiO<sub>2</sub> ETL in a TCO/c-TiO<sub>2</sub>/meso-TiO<sub>2</sub>/CH<sub>3</sub>NH<sub>3</sub>PbI<sub>3</sub>/Spiro-O-MeTAD/Au architecture (blue) under AM1.5 G, 1000 W m<sup>-2</sup> standard test conditions (STC). Right, distribution of maximum power density (MPD) and estimated PCE produced by the same devices measured under a CFL lamp at an illuminance of 200 lx; The efficiencies depend greatly on the quality of the ETL, much more than at STC, and the maximum efficiencies reached are significantly higher than those at STC; Reproduced with permission from [2]. b) Summary of power-conversion-efficiency reached of representative works for indoor perovskite solar cells



(PSCs, red squares) and competitors such as a-Si (purple rhombus), DSSC (blue triangle) and OPV (green circle), with PCEs reaching 34.8% at 200lx and 40.2% at 1000 lux; Adapted with permission from [4].

## **Current and Future Challenges**

### Stability

PSCs have achieved impressive efficiencies in a short period of time. Indoor stability remains an aspect of concern, although they operate in a milder environment compared to outdoors. Many of IoT devices need to last only a few years rather than more than 25-years under the much more taxing conditions under the sun, outdoors. Thus, systematic studies of degradation under indoor illumination as well as developing device and encapsulation materials that can match commercial lifetime requirements should be carried out.

### Large-area fabrication

Scaling up the manufacturing processes is key for commercialization. Previous studies have shown that i-PSCs are more sensitive to trap-state density and recombination currents [2, 3], due to the lower incident optical power of indoor lights compared to sunlight, resulting in a higher ratio of recombining electrons to photo-generated electrons. Preparation of high-quality transport and perovskite films (Figure 1a) over large areas as well as maintaining high shunt resistances in contacting series-connected cells in monolithic modules is crucial for device performance. Ideal geometries for modules will also differ depending on illumination conditions.

### Manufacturing Costs

Reducing manufacturing costs is an important factor for successful commercialization. Achieving comparable market price with its competitors, currently a-Si PV, as well as by other means such as conventional batteries, is required as well as reducing as much as possible the cost of its integration with the product.

### Possible Toxicity Concerns

The operating environment of indoor PV consists in most places of spaces where there is human activity, such as the living room, office, and shops. Therefore, the possible toxicity of lead-halide perovskite inevitably becomes an important question to answer even if the quantity of lead is minuscule in such devices. On the one hand this is a regulatory issue, on the other a technical one which can be tackled with formulation of new materials (e.g. lead-free alternatives) or proper encapsulation and sealing.

### Standardization protocols

As an emerging technology, IPV does not yet have a generally accepted standard measurement protocol similar to established PV technologies for power generation outdoors. Moreover, there is only one standard light source outdoors (i.e. the sun), while artificial light sources are continuously updated in pursuit of higher efficiency and longer lifetimes. Establishment of measurement protocols will greatly help the field.

## **Advances in Science and Technology to Meet Challenges**

Continuing to improve efficiency towards its theoretical limit of 56% under LED light [9], can be achieved by band gap (the optimal one is around 1.9 eV, higher than that at STC) and defect-passivation engineering [4, 8, 10] both in the perovskite layer as well as the transport layers and its interfaces [2, 3, 5]. Stability needs to be tackled by new material and device architectures (intrinsic) as well as encapsulation (extrinsic) to avoid permeation of moisture and oxygen. For the former, reducing defect formation through grain boundary and interface passivation and the amount of small molecular ions with inorganic ones can

increase stability as well as synthesizing perovskite absorbers with more stable 2D/3D structures. Cheng et al. tailored a  $\text{CH}_3\text{NH}_3\text{PbI}_{2-x}\text{BrCl}_x$  perovskite absorber with bandgap of 1.8 eV for indoor light harvesting, achieving a PCE of 36.2% on  $0.1 \text{ cm}^2$  and 30.6% on an appreciable active area of  $2.25 \text{ cm}^2$  under fluorescent light at 1000 lux (see figure 2(a)). Furthermore, halide segregation suppressed by chloride introduction led to excellent long-term stability, sustaining over 95% of original efficiency for  $0.1 \text{ cm}^2$  encapsulated cells under 2000 h of continuous light soaking [11]. However, this work does not report performance in the more common 200-500lx range found in home and offices. All-inorganic i-PSCs have recently attracted much attention due to improved thermal stability. Guo et al. recently reported a  $\text{CsPbI}_2\text{Br}$  all-inorganic i-PSC with a PCE of 34.2% and a  $V_{\text{oc}}$  of 1.14 V under LED at 200 lx and superior thermal stability (see figure 2(b)) [12]. Commonly used approaches for encapsulation include curable adhesive and glass-glass laminated encapsulation using a variety of different adhesives [13]. Glass is an excellent permeation barrier, thus should also be considered as a possible substrate together with plastic ones even for flexible devices [7]. Encapsulation can become a solution also for the possible toxicity issue via lead sequestration engineering. Researchers have initially explored materials including epoxy resin, hydroxyapatite, and sulfonic acid-based resins to suppress leakage of internal lead [14]. Research on lead free perovskites for i-PSCs is described in section 2.9. To reduce manufacturing costs, it is necessary to develop new cost-effective constituent materials and fabrication technologies that enable very uniform films over large areas as well as low costs, such as slot-die coating.

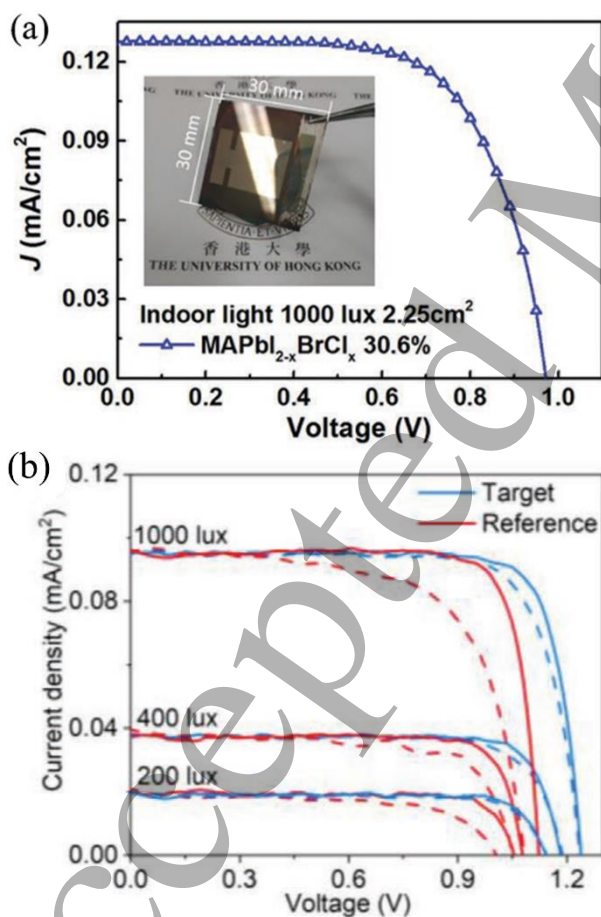


**Figure 2.** (a) 30.6% for indoor perovskite solar cells (i-PSCs) with area  $>1 \text{ cm}^2$  (i.e.  $2.25 \text{ cm}^2$ ) with a tailored triple-anion  $\text{MAPbI}_{2-x}\text{BrCl}_x$  Perovskite material under fluorescent light at 1000 lux, Reproduced with

1  
2  
3 permission from [11]. (b) All-inorganic CsPbI<sub>2</sub>Br i-PSCs with a record-high efficiency of 34.2% with V<sub>oc</sub> of  
4 1.14 V under LED illumination at 200 lux, Reproduced from [12].  
5  
6

### 7 **Concluding Remarks**

8 The huge market for IoT devices worth tens of billions in the future brings unprecedented opportunities  
9 for IPV. Perovskite solar cells have numerous advantages for integration with indoor IoT electronic  
10 devices, such as being mechanical flexible, light weight, and low cost. Simultaneously, i-PSCs have  
11 surpassed their counterparts and achieved outstanding indoor efficiency of over 34% at 200lx and 40% at  
12 1000 lx, becoming one of the prominent leaders for potential commercialization. However, the above-  
13 mentioned achievements were obtained under laboratory conditions. Many challenges such as stability,  
14 maintaining performance over large sizes, possible toxicity, reducing manufacturing and integration costs  
15 must be addressed in the future to promote the commercialization of i-PSCs. The path to  
16 commercialization for indoor products compared to outdoor installations may be more evident not only  
17 because of the outstanding performance but also of the more lenient environment for stability. This  
18 review has aimed to propose some guidelines and ideas to overcome these challenges. Furthermore, the  
19 outstanding performance under low intensity light can be appealing not only for photovoltaics but also  
20 for imaging/vision devices of the future.  
21  
22  
23

### 24 **Acknowledgements**

25 JX gratefully acknowledges financial support from the China Scholarship Council (CSC, No.202004910288).  
26 The project has received funding from Italian Ministry of University and Research (MIUR) through the  
27 PRIN2017 BOOSTER (project n.2017YXX8AZ) grant. TMB gratefully acknowledges funding by the Air Force  
28 Office of Scientific Research's Biophysics program through award number FA9550-20-1-0157.  
29  
30  
31

### 32 **References**

- 33 [1] Chen C, Chang J, Chiang K, Lin H, Hsiao S, and Lin H 2015 Perovskite photovoltaics for dim-light  
34 applications Adv. Energy Mater. **25** 7064-70  
35 [2] Di Giacomo F, Zardetto V, Lucarelli G, Cinà L, Carlo A Di, Creatore M, and Brown T M 2016 Mesoporous  
36 perovskite solar cells and the role of nanoscale compact layers for remarkable all-round high efficiency  
37 under both indoor and outdoor illumination Nano Energy **30** 460-9  
38 [3] Lucarelli G, Giacomo F D, Zardetto V, Creatore M, and Brown T M 2017 Efficient light harvesting from  
39 flexible perovskite solar cells under indoor white light-emitting diode illumination Nano Res. **10** 2130-45  
40 [4] He X, Chen J, Ren X, Zhang L, Liu Y, Feng J, Fang J, Zhao K, and Liu S 2021 40.1% Record Low-light solar-  
41 cell efficiency by holistic trap-passivation using micrometer-thick perovskite film Adv. Mater. **33** 2100770  
42 [5] Dong C, Li X, Ma C, Yang W, Cao J, Igbari F, Wang Z, and Liao L 2021 Lycopene-Based Bionic Membrane  
43 for Stable Perovskite Photovoltaics Adv. Funct. Mater. **31** 2011242  
44 [6] Chen C et al 2022 Full-Dimensional Grain Boundary Stress Release for Flexible Perovskite Indoor  
45 Photovoltaics Adv. Mater. **34** 2200320  
46 [7] Castro-Hermosa S, Lucarelli G, Top M, Fahland M, Fahlteich J, and Brown T M 2020 Perovskite  
47 photovoltaics on roll-to-roll coated ultra-thin glass as flexible high-efficiency indoor power generators Cell  
48 Reports Phys. Sci. **1** 100045  
49 [8] Lee M et al 2021 Enhanced Hole-Carrier Selectivity in Wide Bandgap Halide Perovskite Photovoltaic  
50 Devices for Indoor Internet of Things Applications Adv. Funct. Mater. **31** 2008908  
51 [9] Wu M, Kuo C, Jhuang L, Chen P, Lai Y, and Chen F 2019 Bandgap engineering enhances the performance  
52 of mixed-cation perovskite materials for indoor photovoltaic applications Adv. Energy Mater. **9** 1901863  
53  
54  
55  
56  
57  
58  
59  
60

- [10] Mathews I, Kantareddy S N R, Sun S, Layurova M, Thapa J, Correa-Baena J P, Bhattacharyya R, Buonassisi T, Sarma S, and Peters I M 2019 Self-Powered Sensors Enabled by Wide-Bandgap Perovskite Indoor Photovoltaic Cells *Adv. Funct. Mater.* **29** 1904072
- [11] Cheng R, Chung C, Zhang H, Liu F, Wang W, Zhou Z, Wang S, Djurišić A B, and Feng S 2019 Tailoring triple-anion perovskite material for indoor light harvesting with restrained halide segregation and record high efficiency beyond 36% *Adv. Energy Mater.* **9** 1901980
- [12] Guo Z, Jena A K, Takei I, Ikegami M, Ishii A, Numata Y, Naoyuki S. and Miyasaka T 2021 Dopant-Free Polymer HTM-Based CsPbI<sub>2</sub>Br Solar Cells with Efficiency Over 17% in Sunlight and 34% in Indoor Light *Adv. Funct. Mater.* **31** 2103614
- [13] Ma S, Yuan G, Zhang Y, Yang N, Li Y and Chen Q 2022 Development of encapsulation strategies towards the commercialization of perovskite solar cells *Energy Environ. Sci.* **15** 13-55
- [14] Muhammad B T, Kar S, Stephen M, and Leong W L 2022 Halide perovskite-based indoor photovoltaics: recent development and challenges *Mater. Today Energy* **23** 100907

## 2.8 Lead-free halide perovskites and derivatives for indoor photovoltaics

Vincenzo Pecunia

School of Sustainable Energy Engineering, Simon Fraser University, Surrey V3T 0N1, BC, Canada

### Status

Lead-free halide perovskites and derivatives (*lead-free perovskites* for short in the following) are a broad class of metal-halide-based compounds (**Figure 1**) [1]. They may present the ABX<sub>3</sub> perovskite structure (with A<sup>+</sup> being a monovalent cation, B<sup>2+</sup> a divalent metal/metalloid anion, and X<sup>-</sup> a halide anion) featuring a three-dimensional network of corner-sharing [BX<sub>6</sub>]<sup>4-</sup> octahedra. Derivatives of this structure may involve metal-halide octahedra arranged in different corner-sharing or edge-sharing structural motifs, which can be either three-dimensional (e.g., as in compounds with a formula B(I)<sub>m</sub>B(III)<sub>n</sub>X<sub>m+3n</sub>, where B<sup>+</sup> and B<sup>3+</sup> are monovalent and trivalent metals, respectively, and X<sup>-</sup> is a halide anion) or lower-dimensional (e.g., as in zero- and two-dimensional A<sub>3</sub>B<sub>2</sub>X<sub>9</sub> compounds, with A<sup>+</sup> being a monovalent cation, B<sup>3+</sup> a trivalent metal, and X<sup>-</sup> a halide anion) (**Figure 1**). A common feature of all of these compounds is their being based on metals/metalloids alternative to lead—for instance, tin, germanium, antimony, bismuth, and silver.

The development of lead-free perovskites, which has taken place primarily during the past 5 years, has been driven by the strong interest in realizing eco-friendly alternatives to lead-based halide perovskites, which manifest highly favourable optoelectronic properties but are burdened by the severe toxicity of lead. Originally, aiming to replicate the promising performance of lead-halide perovskites in solar photovoltaics, the development of lead-free perovskites exclusively targeted their use in solar cells [1]. Departing from this narrow view, the Author and his team began investigating in early 2019 the indoor photovoltaics (IPV) performance of two-dimensional lead-free perovskites comprising planes of corner-sharing metal-halide octahedra [2], which deliver superior optoelectronic properties compared to their zero-dimensional counterparts [3] (**Figure 1a**). Alongside the understanding that the typical placement of IPV in proximity to the end-users makes it beneficial to resort to lead-free, eco-friendly materials [4], this investigation was motivated by the realization that the wide bandgaps of many such compounds would lead to a favourable spectral match with indoor light sources (**Figure 2a**). This effort resulted in the first-ever demonstration of the capabilities and potential of lead-free-perovskite IPV [5]. Despite this being the first attempt, indoor PCEs (PCE(i)s) approaching 5% (i.e., within the same range of mainstream, commercial a-Si:H IPV) were already obtained with Cs<sub>3</sub>Sb<sub>2</sub>Cl<sub>x</sub>I<sub>9-x</sub>, which also delivered device stability of



more than 5 months [5]. Building on this breakthrough, a subsequent study adopted a triple-cation variant of  $\text{Cs}_3\text{Sb}_2\text{Cl}_9$  (by mixing  $\text{Cs}^+$  with methylammonium and formamidinium cations; see **Figure 1c**) to achieve a PCE(i) of 6.37 % [6].

Alongside the discovery of the IPV capabilities of lead-free perovskites, the Author and his team also demonstrated, for the first time, mm-scale lead-free-perovskite IPV powering printed-transistor electronics, pointing to the opportunity of realizing solution-processed, wirelessly powered smart devices [5], [7]. Additionally, the analysis of the ultimate IPV performance of a wide range of lead-free perovskites pointed to other compounds with considerable IPV potential [5] (e.g., Ag-Bi-I compounds [8] and  $\text{Rb}_3\text{Sb}_2\text{I}_9$  [9]). Fulfilling this prediction,  $\text{AgBiI}_4$ -based IPV with an efficiency of up to 5.2 % was subsequently demonstrated [10]. Most recently, emerging Cu-Ag-Bi-I-based absorbers with near optimum bandgap for IPV have been shown to deliver PCE(i) values up to 9.53 % [11]–[13], thereby highlighting the considerable IPV potential of copper-silver pnictohalides [8]. Furthermore, a hybrid absorber combining  $\text{Cs}_3\text{Sb}_2\text{I}_9$  and an organic molecule, ITIC, was reported to deliver PCE(i) values of up to 9.2% [14]. However, note that this result does not strictly fall within the lead-free-perovskite IPV domain, given that the resultant PCE(i) crucially builds on the optoelectronic properties of ITIC. In fact, ITIC has already delivered PCE(i) values of  $\cong 18\%$  in organic IPV devices [15]; hence, the use of ITIC- $\text{Cs}_3\text{Sb}_2\text{I}_9$  essentially taps from the capabilities of organic IPV without impacting the intrinsic capabilities of lead-free-perovskite IPV, while delivering a considerable efficiency drop compared to fully organic ITIC-based IPV [15]. Finally, the investigation of tin-based-perovskite IPV has resulted in considerably higher PCE(i) values (up to 17.6% with  $\text{FA}_{0.75}\text{MA}_{0.25}\text{SnBr}_2$ ), given their higher photovoltaic capabilities already demonstrated in solar photovoltaics research, although burdened by considerable instability (e.g., undergoing a 40% efficiency drop after 400 min) [16], [17].

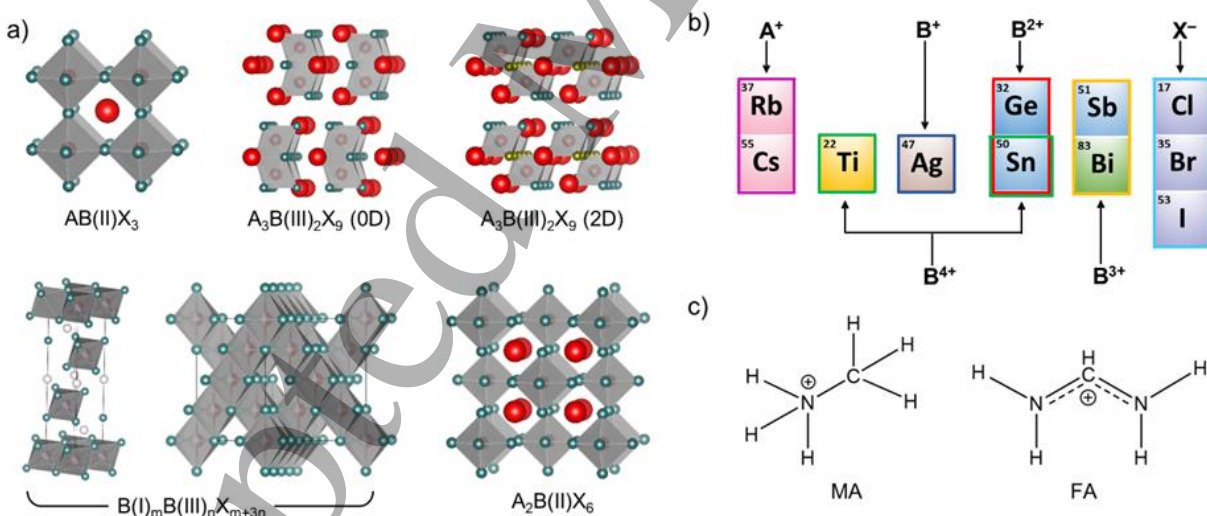


**Figure 1.** a) Representative structures of lead-free perovskites and derivatives. Alongside the standard perovskite structure with a formula  $\text{AB(II)X}_3$ , lower-dimensional perovskite derivatives have been pursued, such as the zero- and two-dimensional bismuth- and antimony-based  $\text{A}_3\text{B(III)}_2\text{X}_9$ . Silver-bismuth halides with a general formula  $\text{B(I)}_m\text{B(III)}_n\text{X}_{m+3n}$  have also been explored. Another representative class consists of vacancy-ordered double perovskites with a formula  $\text{A}_2\text{B(II)X}_6$ . Common b) inorganic and c) constituents of lead-free perovskites. MA: methylammonium. FA: formamidinium. Adapted from Ref. [1] under the terms of a [CC BY 4.0 open-access license](https://creativecommons.org/licenses/by/4.0/).

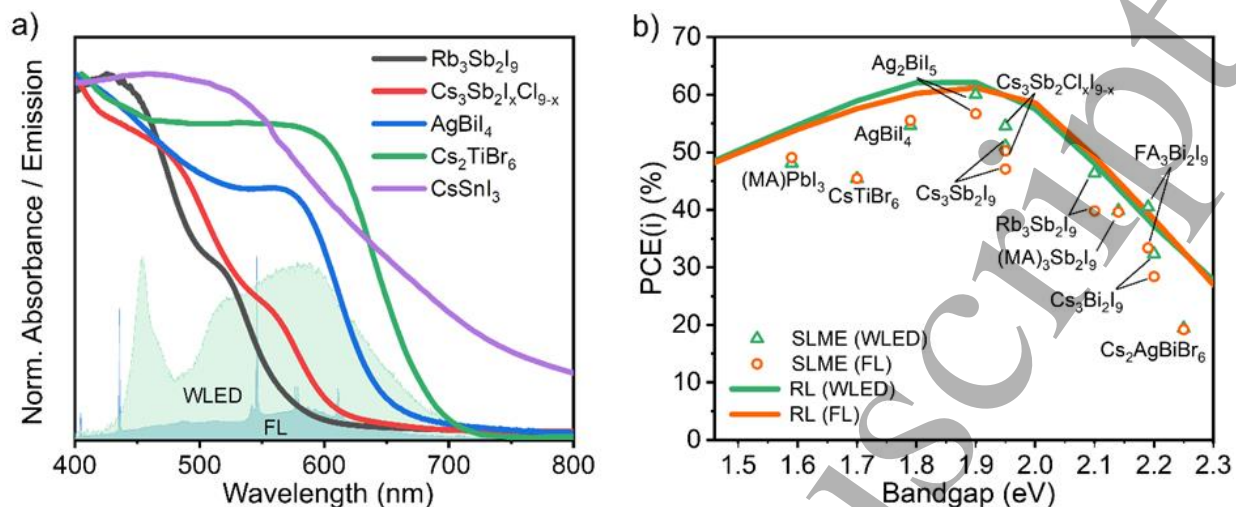


**Figure 2.** a) Absorbance spectra of representative lead-free perovskites and emission spectra of common indoor light sources (WLED: white LED; FL: fluorescent lamp) [1], [3], [5], [18]. b) Calculated PCE values of representative lead-free perovskites in the radiative limit (RL) and spectroscopic limited maximum efficiencies (SLMEs) under indoor illumination (adapted from Ref. [5] under the terms of a [CC BY 4.0 open-access license](#)).

### Current and Future Challenges

The success of lead-free-perovskite IPV will depend on their ability to reliably deliver IPV efficiencies well above mainstream a-Si:H, while allowing scalable manufacturing at a fraction of the cost and with lower environmental impacts, as detailed in the following.

**Efficiency.** Calculations have revealed that many lead-free perovskites could ultimately achieve PCE(i) values of up to  $\cong 60\%$  (**Figure 2b**) [5]. Therefore, a major challenge is to bridge the gap between current device efficiencies and this theoretical limit by developing suitable materials-, processing-, and device-based strategies. While tin-based perovskites have thus far delivered the highest PCE(i) values to date, importantly, their bandgaps are far from the IPV optimum (i.e., 1.9 eV). By contrast, while antimony- and bismuth-based compounds have considerable IPV potential due to their bandgaps being close to the IPV optimum, in the forms explored to date, these absorbers are characterized by non-ideal microstructures and comparatively low mobility-lifetime products, which reduces their charge collection efficiency. Additionally, the limited understanding of their electronic defects and interfacial properties prevents the rational development of suitable passivation treatments and the identification of charge transport layers for efficient charge extraction. Finally, while the PCE(i) of lead-free-perovskite IPV has been typically reported at illumination levels of 1000 lx, real-world applications involve illuminances down to 50 lx, which makes it critical to develop lead-free perovskite layers with particularly low bulk and interfacial defect concentrations.

**Stability.** Tin-based perovskites proper (i.e.,  $\text{ASnX}_3$  compounds, with  $\text{A}^+$  being a monovalent cation and  $\text{X}^-$  a halide anion) suffer from severe instability in air due to the oxidation of  $\text{Sn}^{2+}$  into  $\text{Sn}^{4+}$ . Despite recent advances, this still represents a key challenge to their adoption in real-world applications. By contrast, antimony- and bismuth-based compounds have generally demonstrated a much better stability profile; however, their behaviour under real-world operating conditions has not been assessed to date.

**Upscaling.** The lead-free-perovskite IPV demonstrated to date had active areas in the  $\text{mm}^2$  range; additionally, they were processed by spin-coating, which does not lend itself to large-scale manufacturing. Therefore, an important challenge is to achieve high photovoltaic performance over large areas and with acceptable uniformity and yield via scalable manufacturing methods.

1  
2  
3 *Cost.* The solution-processability of many lead-free perovskites points to their potential to deliver IPV at  
4 a lower cost than current commercial technology. However, it will be critical to pursue high-throughput  
5 manufacturing methods to achieve this objective.

6 *Environmental Impacts.* While their lead-free nature gives them a significant edge compared to their lead-  
7 based counterparts in terms of eco-friendliness, a detailed understanding of their potential sustainability  
8 hotspots and toxicity profiles is still lacking.  
9

### 10 11 **Advances in Science and Technology to Meet Challenges**

12 The full realization of the potential of lead-free-perovskite IPV requires advances in materials and process  
13 engineering as well as in characterization and physical insight.

14 *Materials and process engineering.* The promising performance of tin-based perovskites prompts the  
15 development of compounds of this class with bandgaps  $\cong 1.9$  eV, alongside the investigation of processing  
16 protocols and additives that could fully inhibit the oxidation of  $\text{Sn}^{+2}$  in these materials. In regard to  
17 antimony- and bismuth-based perovskites, a key priority is to develop strategies for the control of the  
18 crystallization process to achieve compact films with grain size greater than 1  $\mu\text{m}$  and favourable  
19 crystalline orientation. Moreover, it is essential to develop processing protocols for the passivation of bulk  
20 and interfacial defects in these materials to extend their carrier lifetimes well above the 10 ns range.  
21 Beyond the compounds developed to date, progress in lead-free-perovskite IPV would also benefit from  
22 the investigation of alternative lead-free compositions with high stability and defect tolerance, while  
23 delivering bandgaps of around 1.9 eV. Regardless of the absorber composition, the realization of high-  
24 performance lead-free-perovskite IPV suitable for real-world applications will also require the  
25 development of charge transport layers with adequate energy level alignment for efficient charge  
26 extraction, as well as the adoption of large-area deposition methods compatible with roll-to-roll  
27 processing.  
28

29 *Characterization and Physical Insight.* Pursuing the systematic characterisation and understanding of the  
30 oxidation mechanisms—at all stages of device fabrication and under real-world operating conditions—  
31 will be crucial for the advancement of IPV based on tin-based perovskites. Moreover, progress in bismuth-  
32 and antimony-based IPV will require the identification of the bulk defect levels currently limiting the  
33 carrier lifetimes in antimony- and bismuth-based perovskites, as well as the characterization of charge  
34 transport in these materials and the quantification of its limiting factors and the impact of anisotropy.  
35 Furthermore, the investigation of excitonic effects in these materials is essential to quantify their impact  
36 on the photogeneration efficiency under photogeneration rates in the range relevant to IPV operation.  
37  
38

### 39 40 **Concluding Remarks**

41 While still in its infancy, research in lead-free-perovskite IPV has already demonstrated efficiencies  
42 competitive or well above commercial IPV technology, highlighting the IPV potential of this family of  
43 materials. Moreover, their superior eco-friendliness compared to their lead-based counterparts makes  
44 them particularly attractive for IPV, given the tighter constraints in terms of material toxicity that hold for  
45 technologies to be deployed in consumer products. In fact, the ultimate IPV performance limits of lead-  
46 free-perovskite IPV (up to 60 % for certain compositions) are far from being reached, which highlights a  
47 considerable opportunity for future improvements. To fully realize their IPV potential, it will be necessary  
48 to engineer these materials and their processing for optimum absorption, superior microstructure, and  
49 low defect density over large areas, but also to pursue the systematic characterization and understanding  
50 of their fundamental optoelectronic properties and degradation mechanisms. Once these challenges are  
51 overcome, it is foreseeable that lead-free perovskites will play an important role as an easy-to-make, low-  
52 cost IPV technology with a promising sustainability profile.  
53  
54

### 55 56 **Acknowledgements**

57  
58  
59  
60



V. P. acknowledges funding from Simon Fraser University FRG 12-27. V. P. is thankful to Javith Mohammed Jailani for support in the revision process.

## References

- [1] V. Pecunia, L. G. Occhipinti, A. Chakraborty, Y. Pan, and Y. Peng, "Lead-free halide perovskite photovoltaics: Challenges, open questions, and opportunities," *APL Mater*, vol. 8, no. 10, p. 100901, Oct. 2020, doi: 10.1063/5.0022271.
- [2] Y. Peng *et al.*, "Enhanced photoconversion efficiency in cesium-antimony-halide perovskite derivatives by tuning crystallographic dimensionality," *Appl Mater Today*, vol. 19, p. 100637, Jun. 2020, doi: 10.1016/j.apmt.2020.100637.
- [3] J. Mei, M. Liu, P. Vivo, and V. Pecunia, "Two-Dimensional Antimony-Based Perovskite-Inspired Materials for High-Performance Self-Powered Photodetectors," *Adv Funct Mater*, vol. 31, no. 50, p. 2106295, Dec. 2021, doi: 10.1002/adfm.202106295.
- [4] V. Pecunia, L. G. Occhipinti, and R. L. Z. Hoyer, "Emerging Indoor Photovoltaic Technologies for Sustainable Internet of Things," *Adv Energy Mater*, vol. 11, no. 29, p. 2100698, Aug. 2021, doi: 10.1002/aenm.202100698.
- [5] Y. Peng *et al.*, "Lead-Free Perovskite-Inspired Absorbers for Indoor Photovoltaics," *Adv Energy Mater*, vol. 11, no. 1, p. 2002761, Jan. 2021, doi: 10.1002/aenm.202002761.
- [6] N. Lamminen *et al.*, "Triple A-Site Cation Mixing in 2D Perovskite-Inspired Antimony Halide Absorbers for Efficient Indoor Photovoltaics," *Adv Energy Mater*, vol. 13, no. 4, p. 2203175, Jan. 2023, doi: 10.1002/aenm.202203175.
- [7] L. Portilla *et al.*, "Wirelessly powered large-area electronics for the Internet of Things," *Nat Electron*, Dec. 2022, doi: 10.1038/s41928-022-00898-5.
- [8] A. Chakraborty, N. Pai, J. Zhao, B. R. Tuttle, A. N. Simonov, and V. Pecunia, "Rudorffites and Beyond: Perovskite-Inspired Silver/Copper Pnictohalides for Next-Generation Environmentally Friendly Photovoltaics and Optoelectronics," *Adv Funct Mater*, vol. 32, no. 36, p. 2203300, 2022 doi: 10.1002/adfm.202203300.
- [9] F. Li, Y. Wang, K. Xia, R. L. Z. Hoyer, and V. Pecunia, "Microstructural and photoconversion efficiency enhancement of compact films of lead-free perovskite derivative Rb<sub>3</sub>Sb<sub>3</sub>I<sub>9</sub>," *J Mater Chem A Mater*, vol. 8, no. 8, pp. 4396–4406, 2020, doi: 10.1039/C9TA13352F.
- [10] I. Turkevych, S. Kazaoui, N. Shirakawa, and N. Fukuda, "Potential of AgBi<sub>4</sub> rudorffites for indoor photovoltaic energy harvesters in autonomous environmental nanosensors," *Jpn J Appl Phys*, vol. 60, no. SC, p. SCCE06, Jun. 2021, doi: 10.35848/1347-4065/abf2a5.
- [11] G. K. Grandhi *et al.*, "Enhancing the Microstructure of Perovskite-Inspired Cu-Ag-Bi-I Absorber for Efficient Indoor Photovoltaics," *Small*, p. 2203768, Jul. 2022, doi: 10.1002/smll.202203768.
- [12] G. K. Grandhi, S. Toikkonen, B. Al-Anesi, V. Pecunia, and P. Vivo, "Perovskite-inspired Cu<sub>2</sub>AgBi<sub>6</sub> for mesoscopic indoor photovoltaics under realistic low-light intensity conditions," *Sustain Energy Fuels*, vol. 7, no. 1, pp. 66–73, 2023, doi: 10.1039/D2SE00995A.
- [13] B. Al-Anesi *et al.*, "Antimony-bismuth alloying: the key to a major boost in the efficiency of lead-free perovskite-inspired indoor photovoltaics," *ChemRxiv*, 2023, doi: 10.26434/chemrxiv-2023-nb5jj.
- [14] A. Singh *et al.*, "Panchromatic heterojunction solar cells for Pb-free all-inorganic antimony based perovskite," *Chemical Engineering Journal*, vol. 419, p. 129424, Sep. 2021, doi: 10.1016/j.cej.2021.129424.
- [15] Z. Ding, R. Zhao, Y. Yu, and J. Liu, "All-polymer indoor photovoltaics with high open-circuit voltage," *J Mater Chem A Mater*, vol. 7, no. 46, pp. 26533–26539, 2019, doi: 10.1039/C9TA10040G.

- 1  
2  
3 [16] J.-J. Cao *et al.*, “Multifunctional potassium thiocyanate interlayer for eco-friendly tin perovskite  
4 indoor and outdoor photovoltaics,” *Chemical Engineering Journal*, vol. 433, p. 133832, Apr. 2022,  
5 doi: 10.1016/j.cej.2021.133832.  
6  
7 [17] W.-F. Yang *et al.*, “Suppressed oxidation of tin perovskite by Catechin for eco-friendly indoor  
8 photovoltaics,” *Appl Phys Lett*, vol. 118, no. 2, p. 023501, Jan. 2021, doi: 10.1063/5.0032951.  
9  
10 [18] V. Pecunia *et al.*, “Assessing the Impact of Defects on Lead-Free Perovskite-Inspired Photovoltaics  
11 via Photoinduced Current Transient Spectroscopy,” *Adv Energy Mater*, vol. 11, no. 22, p. 2003968,  
12 Jun. 2021, doi: 10.1002/aenm.202003968.  
13  
14  
15  
16

## 2.9 Quantum-dot absorbers for indoor photovoltaics

17 Benxuan Li<sup>1,2</sup>, Yiwen Wang<sup>3</sup>, Zhe Li<sup>3</sup> and Bo Hou<sup>4</sup>

18 <sup>1</sup> International Collaborative Laboratory of 2D Materials for Optoelectronics Science and Technology of  
19 Ministry of Education, Institute of Microscale Optoelectronics, Shenzhen University, Shenzhen 518060,  
20 China  
21

22 <sup>2</sup> Electrical Engineering Division, Engineering Department, University of Cambridge, 9 JJ Thomson  
23 Avenue, Cambridge CB3 0FA, UK  
24

25 <sup>3</sup> School of Engineering and Materials Science, Queen Mary University of London, London E1 4NS, UK  
26

27 <sup>4</sup> Department of Physics and Astronomy, Cardiff University, Cardiff CF24 3AA, UK  
28

### Status

29 Based on the detailed balance limit applied to artificial indoor lighting spectra, the optimal bandgap for  
30 indoor photovoltaics (IPVs) is 1.9 eV.[1,2] (Fig. 1 presents indoor lighting sources and AM 1.5 solar spectra)  
31 Therefore, new technologies based on absorbers with tunable bandgap, such as perovskites and quantum  
32 dots (QDs), have been developed for IPVs. [3-5] Amongst these, QDs are theoretically the most promising  
33 absorber materials because they could potentially overcome the Shockley–Queisser limit in IPVs owing to  
34 the unique quantum confinement effect and multiple exciton generation.[6] To date, lead chalcogenides  
35 and lead halide perovskites QDs are the mainstream absorbers in QD-based solar cells, whereas QD-based  
36 IPVs are still in an emerging state. As shown in Fig. 1, several QDs cover desirable absorption ranges for  
37 photovoltaics, and some have shown satisfying efficiency in QD-based IPVs.[4] Meanwhile, the  
38 manufacturing cost of QD-based photovoltaic technologies is becoming competitive due to the mass  
39 production of QD HDTVs, where solution-processed QDs are employed via spin-coating, spray-coating,  
40 and blade coating methods. However, the QD absorbers in most reported high-performance QD IPVs are  
41 based on heavy metals such as lead and cadmium.[7] Recently, heavy metal-free QDs have achieved more  
42 than 15% efficiency in QD sensitised solar cells (QDSSCs),[8] but high QD loading and novel redox system  
43 remain a barrier for the IPVs.  
44  
45  
46  
47  
48  
49  
50  
51  
52  
53  
54  
55  
56  
57  
58  
59  
60

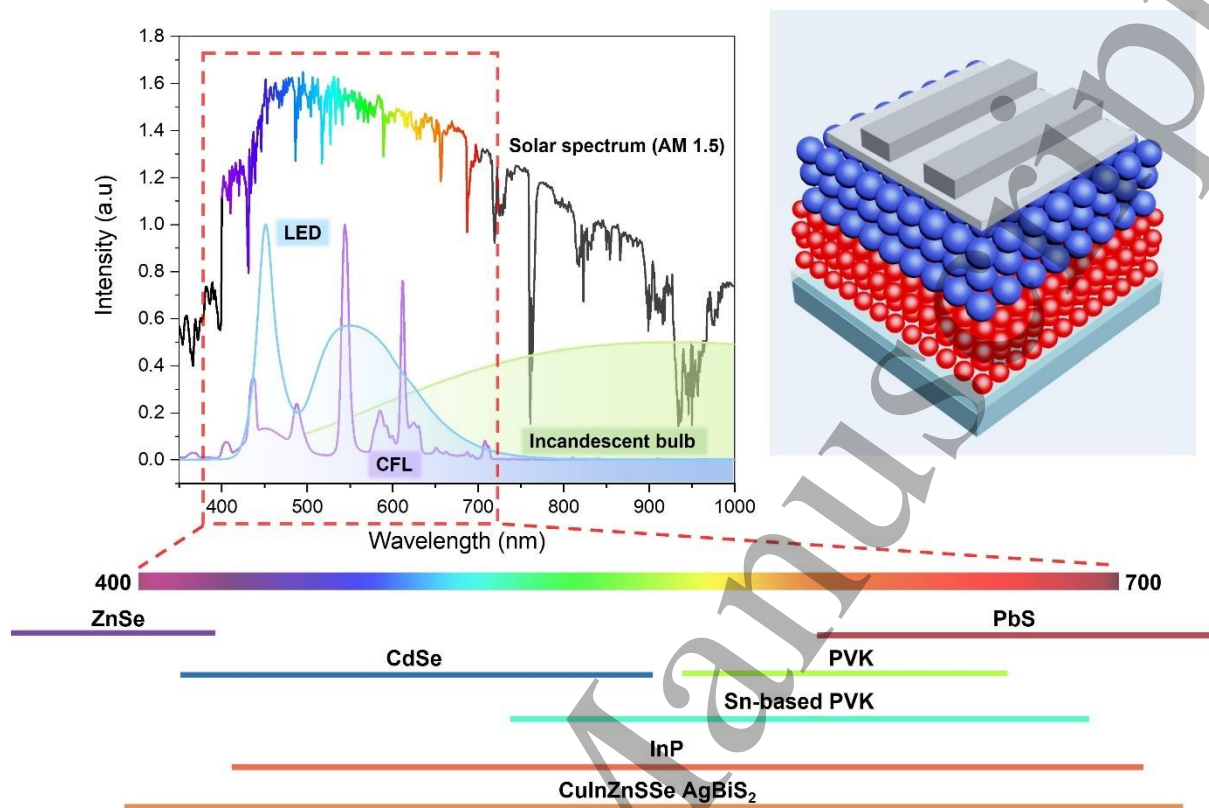


Figure 1 - Spectra comparison of typical indoor lighting and the AM 1.5 standard solar spectrum, with the absorbance of the mentioned QD materials (left panel) and a typical p-n QD-based solar cell architecture (right panel). AM 1.5 data is from National Renewable Energy Laboratory (NREL), and indoor lighting spectra are from National Centers for Environmental Information (NCEI) and normalised.

### Current and Future Challenges

Currently, QD-based solar cells are mainly in two categories: lead chalcogenides (PbX, X = S, Se) and lead halide perovskites (PVK). Large Bohr exciton radius in PbX QDs are suitable for IPV application, rendering efficient light absorption and charge transport. Besides size-dependent photophysical properties, PVK QDs feature more defect tolerance than PbX QDs, resulting in less energy loss such as photovoltage deficiency in devices. Although heavy metal Pb is dominant in both PbX and PVK QDs due to the essential role of its  $6s^2$  orbitals, enabling direct bandgap transition and stable crystal dimension, the technology is now moving towards eco-friendly QD materials such as  $\text{AgBiS}_2$ ,  $\text{CuInZnSSe}$ , Sn-based PVK and InP nanocrystals (Fig. 1). Very recently,  $\text{CuInZnSSe}$  QDs employed as organic replacements in dye-sensitised solar cells (DSSCs) have shown very promising performance (solar cells PCE >15%). [8] However, QD DSSCs still suffer from device instability deriving from the liquid electrolyte, poor interdot carrier mobility due to capped long ligands, and high QD loading and corrosion of QD by the electrolyte. Moreover, there is no report to date on IPV using eco-friendly QDs. [9]

Several issues remain in developing QD IPV. i) Long-chain organic ligands are adopted to provide QDs with good dispersion and stability. However, long-chain ligands prevent sufficient interdot charge transport, and improper removal of the long ligands can generate surface defects, phase transition, and degradation of QDs. The conventional layer-by-layer (LBL) process is time-consuming and material-costly, which is unsuitable for large-scale manufacturing. Besides, high-quality QD deposition cannot be

1  
2  
3 guaranteed in QD DSSCs by chemical bath deposition or successive ionic layer adsorption and reaction. ii)  
4 The Schottky junction and the depleted heterojunction structure have several issues: relatively low charge  
5 collection efficiency, Fermi-level pinning effect, energy level tuning and insufficient charge carrier  
6 extraction. iii) QD-based indoor cells may undergo different open-circuit voltage loss and degradation  
7 mechanisms compared to reported conditions under AM 1.5 irradiation. Due to the significant overlap of  
8 indoor PV with human life, the source of heavy metals (Pb, Cd) and nanoparticles (QDs) present a  
9 particular risk to the built environment and the human body.[10]  
10

### 11 **Advances in Science and Technology to Meet Challenges**

12 Advances in surface modification and synthesis routes have opened the door to more stable QDs. Apart  
13 from short ligands such as organic thiols and amines, inorganic halides are introduced for both PbX and  
14 PVK QDs, passivating the trap sites and improving the device performance. In addition, the solution-phase  
15 ligand exchange strategy can substitute for LBL and the solid-state ligand exchange method. In this way,  
16 large-scale QD IPV fabrication becomes feasible using prepared QD inks to form a controllable absorber  
17 layer. In addition, capping-ligand-induced self-assembly and QD secondary deposition have been  
18 developed to increase the QD loading in QDSSCs and thus realise desirable device performance.  
19 Furthermore, inkjet printing, spray coating, blade coating, and slot-die coating are widely used methods  
20 for manufacturing QD-based optoelectronic devices, which is also practical for QD-based IPV.  
21  
22  
23

24 Using homo- and heterojunction QD composite architectures can increase carrier diffusion length of QDs  
25 and active layer thickness, thus enhancing indoor device performance. Using size-dependent quantum  
26 confinement, the different bandgaps of PVK and PbX QDs can be used as front and back cells to form  
27 tandem IPV. Electron transfer layer (ETL) and HTL (hole transport layer) also play a critical role in  
28 achieving good device performance, so elaborate interface engineering should be adopted between ETL,  
29 QD and HTL. For instance, CsPbI<sub>3</sub> QDs can be coupled with n-type transition metal oxide (TiO<sub>2</sub> or SnO<sub>2</sub>)  
30 and p-type organic HTLs (Spiro-OMeTAD, PTB7 or PTAA) to form P-i-N geometry. Device stability can be  
31 improved by passivation on the QD layers and device encapsulation that hinders the penetration of  
32 oxygen and moisture. However, comprehensive stability research of QD IPV is required to assess their  
33 tolerance to stressors such as moisture, heat, and light soaking. For instance, photoelectrons will not be  
34 fully generated to fill trap states under dim indoor lighting compared to AM 1.5 conditions, which may  
35 accelerate device degradation. Regarding QDSSCs, an interesting alternative could be all-solid-state  
36 devices where conventional liquid polysulfide redox could be substituted. Since IPV target indoor and  
37 portable applications, ecotoxicity is an essential consideration.[10] Thus, eco-friendly QDs such as AgBiS<sub>2</sub>,  
38 CuInZnSe, Sn- and Ge-based PVK are more desirable than their heavy metal-based counterparts.  
39  
40  
41

### 42 **Concluding Remarks**

43 The emerging QD synthesis, engineering and cell fabrication technologies have demonstrated enormous  
44 potential for developing IPV. Recently, our group reported the first PbS-based QD IPV device, exhibiting  
45 a promising IPV PCE of 19.5% under fluorescent illumination but lagging behind the expected maximum  
46 IPV PCE (52%).[4] Several challenges remain before the final commercialisation of QD-based IPV. From a  
47 device perspective, more studies are required on a homo- or heterojunction and band-aligned tandem  
48 configuration. From a materials perspective, it is necessary to develop a more efficient ligand exchange  
49 approach for QD film fabrication and proper interface engineering to maintain low trap states between  
50 layers. Moreover, comprehensive ecotoxicity studies are required to understand QD leaching  
51 pathways.[10] With rapid advances in materials (metal chalcogenides, halides, phosphides, and nitrides)  
52 and devices (Tandem, QD-DSSC), it is envisaged that QD-based IPV will soon realise their full potential  
53 for commercialisation.  
54  
55  
56  
57  
58  
59  
60

## Acknowledgements

Bo Hou acknowledges the financial support from the Cardiff University, Engineering and Physical Sciences Research Council (EPSRC, EP/V039717/1) and Royal Society of Chemistry (E21-9668828170).

## References

- [1] I. Mathews, S. N. Kantareddy, T. Buonassisi, and I. M. Peters, "Technology and market perspective for indoor photovoltaic cells," *Joule*, vol. 3, no. 6, pp. 1415-1426, 2019.
- [2] M. Freunek, M. Freunek, and L. M. Reindl, "Maximum efficiencies of indoor photovoltaic devices," *IEEE Journal of Photovoltaics*, vol. 3, no. 1, pp. 59-64, 2013, doi: 10.1109/JPHOTOV.2012.2225023.
- [3] H. K. H. Lee, Z. Li, J. R. Durrant, and W. C. Tsoi, "Is organic photovoltaics promising for indoor applications?," *Applied Physics Letters*, vol. 108, no. 25, p. 253301, 2016, doi: 10.1063/1.4954268.
- [4] B. Hou *et al.*, "Multiphoton Absorption Stimulated Metal Chalcogenide Quantum Dot Solar Cells under Ambient and Concentrated Irradiance," *Advanced Functional Materials*, <https://doi.org/10.1002/adfm.202004563> vol. 30, no. 39, p. 2004563, 2020/09/01 2020, doi: <https://doi.org/10.1002/adfm.202004563>.
- [5] B. Li, B. Hou, and G. A. J. Amaratunga, "Indoor photovoltaics, The Next Big Trend in solution-processed solar cells," *InfoMat*, vol. 3, no. 5, pp. 445-459, 2021, doi: <https://doi.org/10.1002/inf2.12180>.
- [6] O. E. Semonin *et al.*, "Peak External Photocurrent Quantum Efficiency Exceeding 100% via MEG in a Quantum Dot Solar Cell," *Science*, vol. 334, no. 6062, pp. 1530-1533, 2011, doi: 10.1126/science.1209845.
- [7] M.-J. Choi *et al.*, "Cascade surface modification of colloidal quantum dot inks enables efficient bulk homojunction photovoltaics," *Nature Communications*, vol. 11, no. 1, p. 103, 2020/01/03 2020, doi: 10.1038/s41467-019-13437-2.
- [8] H. Song *et al.*, "Improving the Efficiency of Quantum Dot Sensitized Solar Cells beyond 15% via Secondary Deposition," *Journal of the American Chemical Society*, vol. 143, no. 12, pp. 4790-4800, 2021/03/31 2021, doi: 10.1021/jacs.1c01214.
- [9] T. Kim, S. Lim, S. Yun, S. Jeong, T. Park, and J. Choi, "Design Strategy of Quantum Dot Thin-Film Solar Cells," *Small*, <https://doi.org/10.1002/sml.202002460> vol. 16, no. 45, p. 2002460, 2020/11/01 2020, doi: <https://doi.org/10.1002/sml.202002460>.
- [10] D. Yan *et al.*, "Lead Leaching of Perovskite Solar Cells in Aqueous Environments: A Quantitative Investigation," *Solar RRL*, vol. n/a, no. n/a, doi: <https://doi.org/10.1002/solr.202200332>.

## 2.10 Accurate characterization of indoor photovoltaic performance

Behrang H. Hamadani

National Institute of Standards and Technology, USA

### Status

It is well understood that the standard reporting condition (SRC, air mass (AM) 1.5 global/ 25°C/ 1000 W/m<sup>2</sup>) for measurement of photovoltaic (PV) solar cells is not relevant for ambient indoor PV (IPV) measurements [1]–[3]. Both the spectrum and the total irradiance of many artificial indoor light sources are significantly different from the AM 1.5 spectral irradiance. Unfortunately, no international standards or broadly adopted guidelines exist to clearly outline the measurement procedure to characterize and report the electrical performance of IPV devices. Hence, problems begin to arise when various



laboratories report or compare the performance parameters of their IPV devices under common light sources such as fluorescent or white light emitting diode (LED) lighting. Currently, most laboratories report their IPV performance parameters under a light source that has been measured with a Lux meter, with the light intensity reported in the illuminance unit, lx ( $\text{lm}/\text{m}^2$ ). Typically, 1000 lx or fractions of it are considered appropriate for IPV measurements. However, it has been clearly demonstrated that illuminance is not an appropriate quantity for measuring and comparing IPV results so long as the precise reference spectrum remains undefined [4]. In some cases, an 18 % discrepancy in the short circuit current ( $I_{sc}$ ) may be reported under nominally similar lighting types at the same lux value, i.e., 1000 lx. It turns out the spectral distribution of the light source must also be considered. Adopting standards that clearly define the spectral irradiance profile of a given light source would help researchers conduct more accurate electrical measurements, even if lux continues to be used for measuring the light intensity. However, a more accurate method would involve extending the traditional reference-cell based method to IPV measurements under indoor lighting conditions. In short, reducing measurement uncertainties under well-defined reporting conditions (RC) would help advance the growing field of IPV and allow materials and device architects to better focus their efforts in developing high-efficiency devices, fine-tuned to specific ambient lighting profiles.

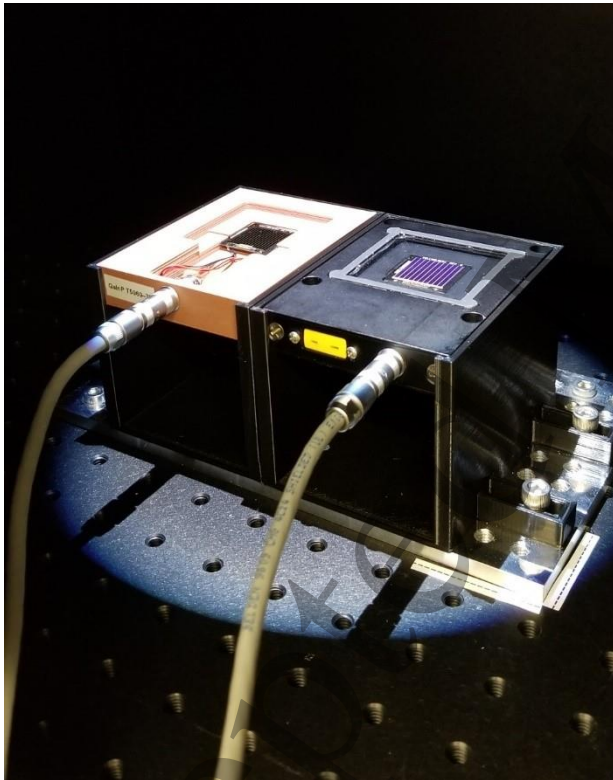


**Figure 1.** For IPV current vs. voltage measurements, a calibrated reference cell (right) is placed next to the IPV cell (left) and used to measure and adjust the effective irradiance of the incident LED light. The objective is to measure and report the IPV electrical performance parameters under a pre-defined reporting condition.

### Current and Future Challenges

When it comes to accurate electrical characterization of PV devices, the biggest challenge is related to the accurate (low uncertainty) measurement of the irradiance of the light source used to perform the current vs. voltage (I-V) measurement. In an ideal world, all researchers would use the same exact light source

1  
2  
3 with the same spectral and angular distribution. In this case, the intensity of the illumination incident on  
4 the cell could be measured and adjusted with a calibrated lux meter, spectroradiometer, reference solar  
5 cell or a similar equipment without any concerns or errors. However, indoor light sources or even solar  
6 simulators come in all sorts of spectral variations. Therefore, inter-comparison among different labs would  
7 be difficult unless everyone agreed on using one or a multitude of reference spectra for reporting results,  
8 much like we currently do with the AM 1.5 G or AM 0 spectra, as codified in ASTM or International  
9 Electrotechnical Commission (IEC) standards [5]. For indoor PV measurements, a reference spectrum has  
10 not yet been broadly adopted, although some steps towards that goal have been taken recently [6]. The  
11 challenge is that even if one agrees for their device to be traceable to a certain reference spectrum,  
12 achieving that exact illumination condition inside the laboratory is often unrealistic because spectral  
13 irradiance of artificial light sources vary significantly among manufacturers. Therefore, a universal  
14 protocol must be developed to allow each researcher to measure and adjust their light intensity such that  
15 everyone exposes their test specimen to the same exact *effective* irradiance when measuring I-V curves  
16 no matter the source of the illumination. For air mass 1.5 measurements, it is now universally accepted  
17 that the lowest uncertainty method to achieve traceability to this reference condition is accomplished  
18 through the use of a reference solar cell that has been calibrated by a primary national metrology institute  
19 or a secondary ISO-certified lab under a specific RC. There are currently efforts under way at some  
20 metrology institutes to extend this method to IPV measurements, but to do that, one or more appropriate  
21 reference spectra has to be adopted through international standard organizations.  
22  
23  
24

### 25 **Advances in Science and Technology to Meet Challenges**

26 Efforts are currently under way to meet the challenges discussed above. Recently, the standard SEMI  
27 PV80-0218 [6], Specification of Indoor Lighting Simulator Requirements for Emerging Photovoltaic was  
28 published, which clearly defined the normalized spectral distribution of five light sources adopted for IPV  
29 measurements from the International Commission of Illumination (CIE). These sources include illuminant  
30 A, which is a standard incandescent light bulb, and illuminant TL 84, which is a tri-band fluorescent lamp.  
31 Although the actual test method as described in this standard is still based on lux meter measurements,  
32 the methodology outlined will help reduce discrepancies between measurements. A more accurate  
33 method, however, is based on the use of a reference solar cell that has been specifically calibrated under  
34 a RC defined by one of the light sources in PV80-0218 or newly designated light sources. Such a calibrated  
35 reference solar cell can now be obtained from the National Institute of Standards and Technology in the  
36 USA. NIST uses the absolute irradiance spectral responsivity method to calibrate an appropriate reference  
37 solar cell under any adopted reference spectrum, including three unique NIST-proposed reference spectra  
38 based on white LEDs of different correlated color temperatures [4]. The chosen reference spectra are in  
39 absolute spectral irradiance (units:  $W/m^2 \times nm$ ) and they are designed such that they correspond to a total  
40 illuminance of 1000 lx. Because the integrated irradiance value incident on the cell is known for a given  
41 RC, power conversion efficiency can be easily computed, a task that is hard to achieve with low uncertainty  
42 if one only used lux to quantify the incident light intensity.  
43  
44  
45  
46  
47  
48  
49  
50  
51  
52  
53  
54  
55  
56  
57  
58  
59  
60



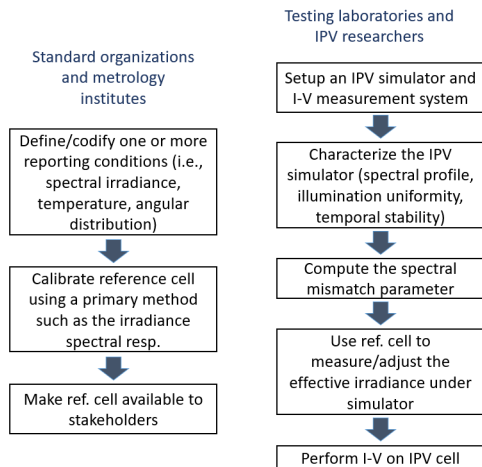


**Figure 2.** Under this proposed approach, standard organizations such as the ASTM would draft the necessary new standards for defining IPV reporting conditions and the metrology institutes would calibrate reference cells under the published RCs. The testing labs or individual researchers will then use their in-house IPV simulators and the reference cells to carry out traceable I-V measurements.

The complete procedure on how to use a calibrated reference cell to perform accurate I-V measurements traceable to a given RC has been published and is conceptually very similar to how we do I-V measurements under the SRC [4], [7]. The flowcharts in Fig. 2 outline the steps needed for accomplishing a traceable IPV measurement metrology. We believe relative expanded uncertainties ( $K = 2$ ) of 2 % or lower is easily achievable with this technique for electrical performance measurements of IPV cells.

### Concluding Remarks

In conclusion, significant effort is under way to establish and formulate a well-defined metrology for electrical performance characterization of IPV cells. Given the significant market penetration and growth of IPV in recent years for energy harvesting under a variety of lighting conditions [8], it is imperative that *accurate* and *traceable* measurement procedures are followed when evaluating and reporting the performance parameters of these devices. Recent interlab-comparisons [9] have helped to better define and formulate the outline of this task but more inter-lab measurements among metrology institutes are needed to accelerate the progress towards standardization of IPV measurements.

### Acknowledgements

B. H. Hamadani would like to thank Dr Mark Campanelli of Intelligent Measurement Systems LLC and Dr Howard Yoon of NIST for continued interest and stimulating discussions regarding this work spanning the course of the last several years.

### References

- [1] J. F. Randall and J. Jacot, "Is AM1.5 applicable in practice? Modelling eight photovoltaic materials with respect to light intensity and two spectra," *Renew. Energy*, vol. 28, no. 12, pp. 1851–1864, Oct. 2003.
- [2] M. Freunek, M. Freunek, and L. M. Reindl, "Maximum efficiencies of indoor photovoltaic devices," *IEEE J. Photovoltaics*, vol. 3, no. 1, pp. 59–64, Jan. 2013.
- [3] B. Minnaert and P. Veelaert, "A Proposal for Typical Artificial Light Sources for the Characterization of Indoor Photovoltaic Applications," *Energies*, vol. 7, no. 3, pp. 1500–1516, Mar. 2014.
- [4] B. H. Hamadani and M. B. Campanelli, "Photovoltaic Characterization Under Artificial Low Irradiance Conditions Using Reference Solar Cells," *IEEE J. Photovoltaics*, vol. 10, no. 4, pp. 1119–1125, Jul. 2020.

- [5] IEC 60904-3, "Photovoltaic Devices – Part 3: Measurement Principles for Terrestrial Photovoltaic (PV) Solar Devices with Reference Spectral Irradiance Data. 2008.
- [6] SEMI PV80-0218 Specification of Indoor Lighting Simulator Requirements for Emerging Photovoltaic. 2018.
- [7] B. H. Hamadani and B. Dougherty, "Solar Cell Characterization," in *Semiconductor Materials for Solar Photovoltaic Cells*, 2016, pp. 229–245.
- [8] I. Mathews, S. N. Kantareddy, T. Buonassisi, and I. M. Peters, "Technology and Market Perspective for Indoor Photovoltaic Cells," *Joule*, vol. 3, no. 6, pp. 1415–1426, Jun. 2019.
- [9] B. Hamadani, Y.-S. Long, M.-A. Tsai, and T.-C. Wu, "Interlaboratory Comparison of Solar Cell Measurements Under Low Indoor Lighting Conditions," *IEEE J. Photovoltaics*, vol. 11, no. 6, pp. 1430–1435, Nov. 2021.

### 3. Materials for Piezoelectric Energy Harvesting

#### 3.1 Introduction to Piezoelectric Energy Harvesting – Lead-based oxide perovskites

Emmanuel Defay<sup>1</sup>, Veronika Kovacova<sup>1</sup> and Sebastjan Glinsek<sup>1</sup>  
Luxembourg Institute of Science and Technology

##### Status

A piezoelectric energy harvester is a device that can absorb elastic work ( $W_{elast}$ ) and convert this mechanical energy into electric energy. If we consider a 1D-model and a piezoelectric material with  $E_D$  its Young's modulus at constant charge (the largest one) and  $S_{max}$  the maximum strain it can withstand, the maximum  $W_{elas}$  stored in this piezoelectric material is  $W_{elas,max} = \frac{1}{2}E_D S_{max}^2$ . This work is then converted in electric work  $W_{elec}$  via the piezoelectric effect. The electromechanical coupling  $k$  enables quantifying  $W_{elec} = k^2 W_{elas}$ . Consequently, the maximum electric work - per volume unit - that a piezoelectric material can deliver is

$$W_{elec,max} = \frac{1}{2}k^2 E_D S_{max}^2 \quad \text{equation 1}$$

This simple equation stands whatever the design, the structure, or the material. It corresponds to the energy enabled by one stroke. Hence, Table 1 depicts a broad picture of nowadays' state-of-the-art

regarding an upper bound of the electric energy that can be generated by prototypical piezoelectric materials that are estimated from this 1D model. Here we considered the best configuration possible regarding the coupling coefficient, which means the compression mode, enabling the use of  $k_{33}$ , which is generally the largest one. It is, however, difficult to use such coefficient in practice because bulk ceramics, the best piezoelectrics, are stiff materials and we generally prefer using softer structures such as membranes or cantilevers, better adapted to collect vibrations in the low frequency spectrum. This in turn considerably decreases the effective coupling coefficient. It is nonetheless interesting to contemplate the upper bound of piezoelectrics because it reveals their real potential at maximum. The three main things revealed by Table 1 are: 1) the range of maximum energy harvester performances of typical piezoelectric materials encompasses three orders of magnitude, 2) the best possible material is a lead-based single crystal perovskite material that combines large strain and large electromechanical coupling and 3) PZT films can withstand larger strain than bulk, which infers higher harvesting potential. In fact, lead-based oxide perovskite materials remain the best piezoelectric materials despite tremendous efforts to find lead-free alternatives with the same properties.

Table 1: State of the art energy-harvesting characteristics of the main materials.

Material	Young's Modulus $E_D$ (GPa)	Max. strain $S_{max}$ (%)	Coupling coefficient $k_{max}^2$	Electric Work $W_{elec,max}$ (mJ cm <sup>-3</sup> )
Pb(Mg,Nb)O <sub>3</sub> -PbTiO <sub>3</sub> single crystal [1]	18	1.7	0.81	2110
Pb(Zr,Ti)O <sub>3</sub> films [2,3]	80	0.5	0.5	500
(K,Na)NbO <sub>3</sub> bulk [4,5]	70	0.46	0.40	296
Pb(Zr,Ti)O <sub>3</sub> 5H bulk [6]	50	0.175	0.56	43
P(VDF-TrFE) [7]	4	1.44	0.04	16.6
AlN [8]	300	0.028	0.07	0.82
Sc doped AlN	200	0.028	0.12	0.94

### Current and Future Challenges

In realistic devices, Table 1's ranking is different because of practical limitations. Indeed, P(VDF-TrFE), AlN and PZT films-based energy harvesters are well represented in the literature because these materials are better suited to standard devices such as cantilevers [5-8]. The main issue in using the best materials could be phrased as a mismatch in mechanical impedance. Bulk piezoceramics are stiff and brittle. Therefore, finding harvesting conditions enabling a perfect impedance matching is scarce. Compliant structures are much better adapted to large strain and resonant conditions. This infers that piezo materials must be deposited or transferred on these well-adapted structures. This has been the case for a few decades with PZT buzzers or PZT/steel bilayers [9], associating an excellent piezo with a substrate able to withstand large strain. This leads to unprecedented, harvested power area density beyond 1 mW cm<sup>-2</sup> in resonant structures, as shown in Figure 1 [7]. Doing the same with single crystals or lead-free piezoelectrics remains a big challenge, though our 1D-model reveals the potential of these materials.

To go further, as suggested by our previous figure of 1 mW cm<sup>-2</sup>, we have to consider figures-of-merit that are based on practical devices that are most of the time related to vibrations in order to harvest more energy. A good description of these devices is provided by the following equation of the power density  $P_H$  (in W cm<sup>-2</sup>) of a cantilever that reads [7]

$$P_H = \frac{e_{31,eff}^2}{2\varepsilon} \pi f S^2 V. \quad \text{equation 2}$$

$e_{31,eff}$  is the transverse effective piezoelectric coefficient,  $\varepsilon$  the dielectric constant,  $f$  the vibration frequency,  $S$  the longitudinal strain in the piezoelectric layer and  $V$  the volume of active piezoelectric material. Here the electric field is along the transverse direction (direction 3). This figure of merit is very similar to equation 1 because  $e_{31,eff}^2/\varepsilon = k^2 E_D$ . Equation 2 enables focusing 1) on materials properties that are practical to measure, namely  $e_{31,eff}^2$  and  $\varepsilon$  and 2) on the extrinsic parameters, namely the **frequency**, the imposed **strain** and the **volume** of active material.

Our ideal energy harvester therefore contains a substantial volume (large  $V$ ) of a piezoelectric material with high piezoelectric properties (high  $e_{31,eff}$ ), low dielectric constant (low  $\varepsilon$ ) and is able to withstand large strain (large  $S$ ). Note that we could also use a pure longitudinal configuration, such as compression-extension, that would enable using  $e_{33}$  instead of  $e_{31}$  in equation 2. Strain would then be along direction 3.

### Advances in Science and Technology to Meet Challenges

Let us note that frequency cannot really be a parameter because mechanical and vibration energies in the environment lie in the low frequency range, typically below 100 Hz.

Here are the main ideas to carry on improving piezo-based energy harvesters.

#### 1. Higher $e_{31,eff}$ and lower $\varepsilon$

As suggested in Table 1, the best piezoelectric materials are based on lead and have perfect crystallographic structure. As mentioned, relying only on bulk ceramics is not an option because they are not well adapted to large strain. We need to consider films, and ideally epitaxial/highly oriented ones. Crystalline orientation plays also a paramount role in increasing  $e_{31,eff}$ , 100 being the most desired orientation in PZT layers. Improving piezo coefficients generally also increases  $\varepsilon$ . However, a proper stress management in the layer enables inducing a powerful imprint in the material, which in turn decreases  $\varepsilon$ .

#### 2. Larger volume

The inset in Figure 1 clearly shows that the power area density is proportional to the thickness of piezoelectric material. This essentially disqualifies very thin films for energy harvesting, as long as one considers 1 mW cm<sup>-2</sup> as the power density target. Large thickness of piezo generates high voltage, which is not easy to take full advantage of. Therefore, multilayers with intercalated electrodes fabricated via screen printing and aerosol jet have to be considered.

#### 3. Larger strain

As seen in equations 1 and 2, strain has a positive quadratic effect on harvested energy. This is why, despite a low coupling factor, P(VDF-TrFE) can make energy harvesters with power density close to 1 mW cm<sup>-2</sup>. One field of investigation to increase strain is to mix lead-based piezoelectrics with polymers and make composites. Another interesting approach consists in preparing a structure able to optimize the strain all along the piezoelectric material. It is referred to as compliant mechanism [10]. Finally, using substrates compatible with large strains, such as polymers, are very interesting. Piezoelectrics are generally prepared on stiff and brittle substrates able to withstand very high temperature, typically beyond 900 °C (see figure 1). Therefore, transferring top quality piezoelectric layers on compliant substrates is a fundamental approach. An alternative way is to crystallize the piezoelectric layers directly on polymers by using innovative chemistry, laser or photonic annealing.

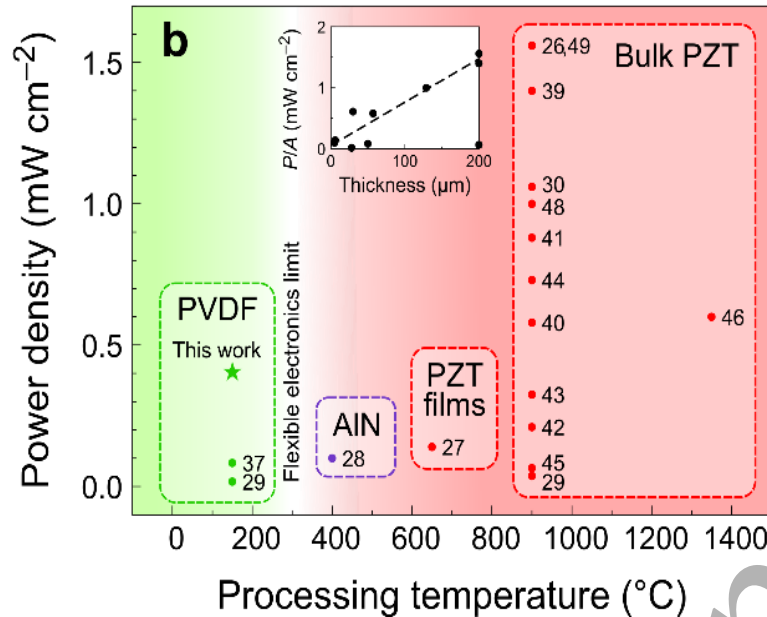


Figure 1 – Power density in  $\text{mW cm}^{-2}$  of existing energy harvesters based on polymers (PVDF), AlN, PZT films and bulk PZT. They are classified according to their maximum processing temperature. The inset underlines the clear role played by the thickness (and therefore the volume) of the active piezoelectric layer on harvested power density (figure from [7], with authorization from Elsevier. The numbers in the figure refer to the references in [7]).

### Concluding Remarks

The simple figures of merit proposed in this road map enable figuring out the four parameters to improve in piezoelectric energy harvesters, and more specifically in lead-based piezoelectric materials. These four parameters are the piezoelectric coefficients - notably the transverse one, which matters the most in vibrating energy harvesters -, the dielectric constant, the only one to decrease in order to improve electromechanical coupling, the volume of piezoelectric material and finally the maximum strain that the piezoelectric material can withstand. Harvested energy as large as  $2 \text{ J cm}^{-3}$  per stroke can be predicted if all these parameters could be optimized.

### Acknowledgements

The authors acknowledge the Luxembourg National Fund (FNR) (grant number INTER/ANR/18/12618689/HARVESTORE/Defay).

### References

- [1] S. E. Park, T. R. Shrotr, Ultrahigh strain and piezoelectric behavior in relaxor based ferroelectric single crystals. *J. Appl. Phys.* 82, 1804–1811 (1997). doi:10.1063/1.365983
- [2] Yeo, H.G., Ma, X., Rahn, C., and Trolrier-McKinstry, S. (2016). Efficient piezoelectric energy harvesters utilizing (001) textured bimorph PZT films on flexible metal foils. *Adv. Funct. Mater.* 26, 5940–5946.
- [3] K. Coleman, J. Walker, T. Beechem, and S. Trolrier-McKinstry, Effect of stresses on the dielectric and piezoelectric properties of  $\text{Pb}(\text{Zr}_{0.52}\text{Ti}_{0.48})\text{O}_3$  thin films, *J. Appl. Phys.* 126, 034101 (2019); <https://doi.org/10.1063/1.5095765>

- [4] Jun Ou-Yang, Benpeng Zhu, Yue Zhang, Shi Chen, Xiaofei Yang & Wei Wei, New KNN-based lead-free piezoelectric ceramic for high-frequency ultrasound transducer applications, *Applied Physics A* volume 118, 1177–1181 (2015)
- [5] Jigong Hao, Bo Shen, Jiwei Zhai, Chunze Liu, Xiaolong Li, and Xingyu Gao, Switching of morphotropic phase boundary and large strain response in lead-free ternary  $(\text{Bi}_{0.5}\text{Na}_{0.5})\text{TiO}_3$ – $(\text{K}_{0.5}\text{Bi}_{0.5})\text{TiO}_3$ – $(\text{K}_{0.5}\text{Na}_{0.5})\text{NbO}_3$  system, *Journal of Applied Physics* 113, 114106 (2013); <https://doi.org/10.1063/1.4795511>
- [6] Thomas R. Shrout, Seung Eek Eagle Park, Clive A. Randall, Joseph Shepard, Laurie B. Hackenberger, Dave J. Pickrell, Wesley S. Hackenberger, Recent advances in piezoelectric materials Proceedings Volume 3241, *Smart Materials, Structures, and Integrated Systems*; (1997) <https://doi.org/10.1117/12.293509>
- [7] Nicolas Godard, Lucas Alliol, Antoine Latour, Sebastjan Glinsek, Mathieu Gerard, Jerome Polesel, Fabrice Domingues Dos Santos, and Emmanuel Defay, 1-mW Vibration Energy Harvester Based on a Cantilever with Printed Polymer Multilayers, *Cell Reports Physical Science* (2020), <https://doi.org/10.1016/j.xcrp.2020.100068>
- [8] Ricart, T., Lassagne, P.-P., Boisseau, S., Despesse, G., Lefevre, A., Billard, C., Fanget, S., and Defay, E. (2011). Macro energy harvester based on aluminium nitride thin films. In 2011 IEEE International Ultrasonics Symposium (IEEE), pp. 1928–1931.
- [9] Roundy, S., and Wright, P.K. (2004). A piezoelectric vibration based generator for wireless electronics. *Smart Mater. Struct.* 13, 1131–1142.
- [10] Ma, X., Wilson, A., Rahn, C.D., and Trolier-McKinstry, S. (2016). Efficient energy harvesting using piezoelectric compliant mechanisms: theory and experiment. *J. Vib. Acoust.* 138, 021005.

### 3.2 Lead-free oxide perovskites for Piezoelectric Energy Harvesting

Yang Bai

Microelectronics Research Unit, Faculty of Information Technology and Electrical Engineering, University of Oulu, FI-90570 Oulu, Finland

#### Status

Initial studies of lead-free oxide perovskites for piezoelectricity date to the early 2000s and intensive research in the recent two decades has been triggered by the European Union’s legislation (EU-Directive 2002/95/EC) on the restriction of hazardous substances (widely known as the RoHS) [1]. In the case of piezoelectrics, the hazardous element refers to lead in the dominant PZT ( $\text{Pb}(\text{Zr},\text{Ti})\text{O}_3$ ) family where over 60 wt.% of lead is present in a compound. Oxide perovskites possess overwhelmingly higher performance among all piezoelectrics, due to which most research efforts have been put on searching for high-performance lead-free piezoelectrics from oxide perovskites. Looking at some key individual parameters such as piezoelectric charge coefficient ( $d$ ) and electromechanical coupling factor ( $k$ ), lead-free oxide perovskites are nowadays considered comparable to the PZT family if carefully designed in composition, microstructure, fabrication and post-processing [2].

For the time being, piezoelectric components account for only far below 1 % of the entire market influenced by the RoHS regulations. However, considering the rapid development of piezoelectric energy harvesters and their potential applications in the ubiquitous IoT industry, sustainable and environmentally

friendly piezoelectrics will weigh considerably more. This offers lead-free piezoelectrics an opportunity to flourish. Although there are many good lead-free piezoelectrics in laboratory, since they are not fully commercialized as is the PZT family, researchers such as device and system engineers at later stages in the value chain of piezoelectric energy harvesting have few options to choose from. It is admitted that design of energy harvesting systems is strongly case-by-case from materials to devices and systems [3]. Without a large selection pool of lead-free piezoelectrics, energy harvesting technologies built on top can hardly advance.

### Current and Future Challenges

Most of the state of the art still envisage conventional actuators, sensors and transducers as applications of lead-free piezoelectrics. However, the design and engineering of piezoelectric performance for energy harvesting set distinguishing criteria. In line with lead-based counterparts, the piezoelectric energy harvesting figure of merit (FOM) defines the capability of kinetic-electric energy conversion working at off-resonance while  $k$  and quality factor ( $Q$ ) determine the energy conversion efficiency at the resonance.

Ideally, FOM needs to be maximized, which brings the first issue.  $FOM = d^2/\epsilon$  where  $\epsilon$  is the material's permittivity. However, in well-sintered piezoelectric ceramics and well-grown single crystals, not only  $d$  and  $\epsilon$  evolve proportionally in the same direction but for lead-free piezoelectrics large  $d$  is achieved at a higher cost of  $\epsilon$  compared to the case of lead-based counterparts. This significantly degrades the FOM values of lead-free piezoelectrics. Meanwhile,  $k$  and  $Q$  change in opposite directions and thus  $k \cdot Q$  must be optimized. It is widely agreed that piezoelectric single crystals exhibit the best electromechanical properties, therefore, Figure 1 summarizes and compares lead-based and lead-free single crystals in terms of FOM and  $k$  by taking the 33-mode as an example.

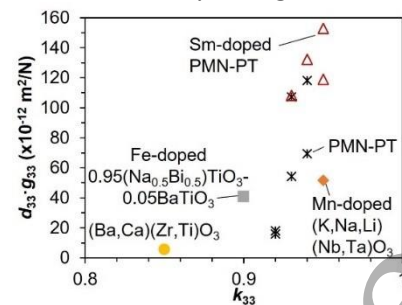


Figure 1. Selection of top-performing lead-based and lead-free piezoelectric single crystals in terms of energy harvesting-related parameters (data extracted from [2,4]). PMN-PT:  $Pb(Mg_{1/3}Nb_{2/3})-PbTiO_3$ .

It is obvious that the champion lead-free oxide perovskites can only reach approximately 50 % of the performance provided by lead-based counterparts, despite comparable  $k$  values. The situation is similar for ceramics with the best-performing lead-free  $(Ba,Ca)(Zr,Ti)O_3$  (BCZT) showing only 70-80% of the FOM and  $k$  values of the lead-based Sm-doped  $Pb(Mg_{1/3}Nb_{2/3})O_3-PbTiO_3$  [2,5]. These facts bring the crucial challenge of top performances for lead-free oxide perovskites which is urgently needed to be addressed especially for energy harvesting due to the crude requirement of output capabilities and efficiencies originated from the piezoelectric components. To the state of the art, comprehensive engineering of FOM,  $k$  and  $Q$  with energy harvesting as the target application, is insufficient.

### Advances in Science and Technology to Meet Challenges



1  
2  
3 Tremendous efforts are needed to keep improving the champion performance of lead-free oxide  
4 perovskites. This has always been the mutual aim in the lead-free piezoelectric community but  
5 considerably more attention should be paid to energy harvesting-related material properties as discussed  
6 above. The key to this still lies on finding the most appropriate environmentally friendly A- and B-site  
7 cations that give the largest possible lattice distortion as well as proper MPB (morphotropic phase  
8 boundary). Rödel et al. [6] have instructed what elements can be truly regarded as environmentally  
9 friendly. Apart from lead, elements such as antimony which has been frequently adopted as a dopant in  
10 lead-free compositions also need to be avoided. This leaves even a smaller room to optimize the  
11 compositions and thus MPB. Zheng et al. [2] has provided a systematic review of how to design a proper  
12 MPB for lead-free piezoelectrics.  
13  
14

15 Compositional optimization via experimental works is tedious and resource/time consuming. In the  
16 meantime, the use of density functional theory (DFT), multiscale modelling and machine learning to  
17 predict properties of oxide perovskite structures is rising [7]. Computation drastically increases the pace  
18 and effectiveness of material screening, discovery and development. These methods should be extended  
19 to the prediction of piezoelectric properties. The complexity of piezoelectric behaviours sensitively  
20 influenced by grains and boundary conditions is an essential issue to be addressed in simulation models  
21 before the adoption of computational methods in practical design and search of new lead-free  
22 piezoelectrics.  
23  
24

25 Application of lead-free piezoelectrics in energy harvesting is not only defined by top performance of the  
26 material family. Trade-offs between cost of raw materials and processing, working temperature range,  
27 and dynamic behaviours in the kinetic working conditions, also needs to be balanced. There are three  
28 promising compositions, BCZT-based, KNN ((K,Na)NbO<sub>3</sub>)-based and NBT ((Na,Bi)TiO<sub>3</sub>)-based. The BCZT-  
29 based ceramics enjoy comparable FOM values to those of the PZT family, and even better k-Q values [2,8].  
30 The PZT-based ceramics are the benchmark for lead-free piezoelectrics due to the seemingly best balance  
31 between cost and performance. The cost of BCZT is estimated to be similar to PZT [6] and for this reason,  
32 the BCZT-based is the most competitive lead-free candidate for energy harvesting at close to room  
33 temperature (Curie temperature < 100 °C). The KNN-based has higher Curie temperatures thus a broader  
34 working temperature range (up to 400 °C) [2]. Recent breakthroughs on multisource energy harvesting  
35 also provide the KNN-based an opportunity to evolve towards multifunctional components [3,9]. The NBT-  
36 based has the highest fracture toughness and strength, almost doubling that of the PZT family [10]. This  
37 feature is specifically beneficial in energy harvesting where high input kinetic energy (e.g., high  
38 acceleration) is present.  
39  
40

41 As mentioned above, piezoelectric energy harvesting is case-by-case design. This requires close  
42 collaboration among researchers of materials, devices and systems. Communal efforts should be made to  
43 answer research questions in the future:  
44

- 45 • In what exact use cases can lead-free piezoelectric energy harvesters win, given that the  
46 material performance might not be excellent but the device and system can work better  
47 thanks to, e.g., higher fracture toughness, higher working temperature, and clever duty-cycle  
48 design [3]? Advanced computational methods will be a great stimulator in this progress.
- 49 • Can the development of novel processing methods, such as solid-state crystal growth  
50 (SSCG) and room-temperature densification of ceramics, be used to create industrially  
51 compatible piezoelectric energy harvesters that cannot be achieved by the lead-based  
52 counterparts? This question mainly considers the cost and energy efficiency of the material  
53 processing methods.  
54  
55  
56  
57  
58  
59  
60

## Concluding Remarks

Lead-free oxide perovskite piezoelectrics promote sustainability and environmental friendliness. This can probably be a ground that, regulated by legislations and pushed by the global trend on climate actions, the industries and users could accept compromised device/system performances. However, lead-free piezoelectric energy harvesting does not necessarily mean compromise as being thought. On the contrary, as lead-free piezoelectrics have not been deeply integrated in mature industrial value chains, energy harvesting is a market where they can take the timely lead from the beginning of the commercialization hype. To realize this, we need to expand materials research extensively into electronics and systems. Each new material should have had a defined use case in certain energy harvesting system already at the stage of material design and engineering.

## References

- [1] J. Rödel and J-F Li, "Lead-free piezoceramics: Status and perspectives", *MRS Bull.*, vol. 43, pp. 576-580, 2018.
- [2] T. Zheng, J. Wu, D. Xiao and J. Zhu, "Recent development in lead-free perovskite piezoelectric bulk materials", *Prog. Mater. Sci.*, vol. 98, pp. 552-624, 2018.
- [3] Y. Bai, H. Jantunen and J. Juuti, "Energy harvesting research: The road from single source to multisource", *Adv. Mater.*, vol. 30, iss. 34, no. 1707271, 2018.
- [4] F. Li, M.J. Cabral, B. Xu, Z. Cheng, E. Dickey, J.M. Lebeau, J. Wang, J. Luo, S. Taylor, W. Hackenberger, L. Bellaiche, Z. Xu, L-Q Chen, T.R. Shrout and S. Zhang, "Giant piezoelectricity of Sm-doped  $\text{Pb}(\text{Mg}_{1/3}\text{Nb}_{2/3})\text{O}_3\text{-PbTiO}_3$  single crystals", *Science*, vol. 364, iss. 6437, pp. 264-268, 2019.
- [5] F. Li, D. Lin, Z. Chen, Z. Cheng, J. Wang, C. Li, Z. Xu, Q. Huang, X. Liao, L-Q Chen, T.R. Shrout and S. Zhang, "Ultrahigh piezoelectricity in ferroelectric ceramics by design", *Nat. Mater.*, vol. 17, pp. 349-354, 2018.
- [6] J. Rödel, W.J. Klaus, T.P. Seifert, E-M Anton, T. Granzow and D. Damjanovic, "Perspective on the development of lead-free piezoelectrics", *J. Am. Ceram. Soc.*, vol. 92, iss. 6, pp. 1153-1177, 2009.
- [7] Y. Bai and I. Grinberg (ed.), *Ferroelectrics: Advances in fundamental studies and emerging applications*, IOP Publishing, to be published.
- [8] Y. Bai, "Vibrational energy harvesting using piezoelectric ceramics and free-standing thick-film structures", *Ph.D. Thesis*, University of Birmingham, 2015.
- [9] Y. Bai, "Electro-ceramic material component, its manufacturing method and method of converting energy", *Patents and patent application*, PCT/FI2020/050810 (granted 2021), GB 2593105 (granted 2022), US 17/633,322 (filed 2022).
- [10] J. Rödel, "Piezoelectric materials and applications", *Lecture notes*, University of Oulu, 27 May 2022.

## 3.3 Nanostructured Inorganics for Piezoelectric Energy Harvesting

Da Bin Kim and Yong Soo Cho

Department of Materials Science and Engineering, Yonsei University, Seoul 03722, Republic of Korea

**ORCID:** Da Bin Kim: 0000-0002-1162-7429 / Yong Soo Cho: 0000-0002-1601-6395

## Status

The technology for piezoelectric energy harvesting has traditionally evolved in microelectromechanical systems based on thin-film cantilevers composed of piezoelectric perovskite oxides on Si substrates, wherein vibrational mechanical sources are mainly concerned with specific resonance frequencies. Inorganic nanostructures with unique electrical and physical characteristics have been introduced as

1  
2  
3 nonconventional alternatives for harvesting electromechanical energy, particularly using flexible polymer  
4 substrates that enable the utilization of unprecedented mechanical sources, such as bending, twisting,  
5 stretching, and pressing. Interestingly, the advantages of using various mechanical inputs in flexible  
6 environments have created an extensive range of state-of-the-art applications, including physiological  
7 power generation, self-powered flexible systems, wearable tactile devices, and biomedical sensors, all of  
8 which use electromechanical coupling with low-power generation in nanoscale materials [1,2].  
9

10  
11 Piezoelectric energy harvesters on nanoscale platforms are commonly called piezoelectric  
12 nanogenerators. For the last 20 years, nanoscale wurtzite ZnO has acted as a critical benchmark for  
13 representing earlier nanogenerators owing to its facile fabrication in the form of nanostructures, e.g.,  
14 nanowires, nanorods, and nanofibers, its excellent crystallinity even at room temperature, and its high  
15 piezoelectricity. Harvesting outcomes in nanogenerators often outpace the output values of traditional  
16 thin-film cantilevers in terms of voltage and power density, accompanied by lower sensitivity to  
17 temperature and frequency owing to the non-ferroelectric nature of ZnO with no phase transition. Other  
18 inorganic piezoelectric materials, such as  $\text{Pb}(\text{Zr,Ti})\text{O}_3$ ,  $(\text{K,Na})\text{NbO}_3$ ,  $\text{BaTiO}_3$ , GaN, and perovskite halides,  
19 have also been employed in various nanoscale structures with promising power-conversion efficiencies  
20 [2,3].  
21  
22

23 Because piezoelectricity is directly related to the enhanced dipole moments and polarization depending  
24 on the direction of the applied mechanical source, high-performance harvesters require the deliberate  
25 manipulation of the lattice strain in nanocrystals and the device architecture, as well as the proper  
26 adjustment of electrodes. The mechanisms that enable the extension of the lattice strain with applied  
27 stress in inorganic nanostructures may differ from the typical octahedral elongation of permanent dipoles  
28 in perovskite oxides, depending on the type of material and structure. For example, ZnO has a hexagonal  
29 structure without permanent dipoles and absorbs mechanical stress through the stretching of its  $\text{ZnO}_5$   
30 units [4]. For polymer-matrix nanocomposites incorporating inorganic nanoparticles, a more nuanced  
31 understanding of piezoelectricity and energy conversion with the contribution of individual constituents  
32 is required.  
33  
34

### 35 **Current and Future Challenges**

36 The choice of appropriate piezoelectric materials is critical for achieving high energy conversion. Because  
37 perovskite oxide materials must be processed above 700 °C for high crystallinity, stand-alone flexible  
38 harvesting systems using perovskite oxides on a plastic substrate have rarely been reported. Most  
39 common nanostructures for piezoelectric energy generation utilize an array of vertically aligned ZnO  
40 nanorods as fabricated from a seed layer by typical hydrothermal methods, which can be processed below  
41 100 °C on a plastic substrate. This vertical nanostructure can be ideally utilized for out-of-plane lattice  
42 extension with applied tensile strain in structures with the top and bottom electrode layers. In figure 1a,  
43 the effective piezoelectric coefficient  $d_{33,eff}$  values of the ZnO nanostructures are plotted with respect to  
44 the nanostructure dimensions, particularly for different ZnO morphologies and other nanomaterials. With  
45 some exceptions, the majority of  $d_{33,eff}$  values were less than 30 pm V<sup>-1</sup>, regardless of the nanostructures  
46 or materials. Specifically, the performance projections of selected ZnO-nanorod-based nanogenerators in  
47 terms of the output voltage and current density are shown in figure 1b, which are also classified by the  
48 mechanical input source, such as pressing, bending, and vibration. Most of the performance outcomes  
49 are less than 4 V and 1,000 nA cm<sup>-2</sup>, but some reach maximum values of ~7 V and ~2,500 nA cm<sup>-2</sup>. The  
50 harvesting output strongly depends on the type of mechanical input and the dimensions of the ZnO  
51 nanorods (figure 1c), where dimensions of ~50–200 nm deliver viable performance outcomes owing to  
52 more effective energy conversion with higher deflectivity.  
53  
54  
55  
56  
57  
58  
59  
60

1  
2  
3 Because of the difficulty in forming nanorods or nanowires for flexible systems, other perovskite oxide  
4 materials have been commonly used as nanoscale fillers in polymer-matrix composites based on films or  
5 nanofibers. A higher content of piezoelectric filler induces a larger piezoelectric response while  
6 maintaining the resilience of the polymer matrix to accommodate a higher mechanical stimulus. For  
7 example,  $\text{Pb}(\text{Zr},\text{Ti})\text{O}_3$  nanoparticles in a polymer matrix improved the harvesting characteristics, delivering  
8 outputs of 8.15 V and  $956 \text{ mW cm}^{-3}$  [5]. Particularly, with additional metallic inclusions, piezoelectric  
9 energy generation was increased by extra space-charge polarization at the metal-polymer interfaces, in  
10 addition to the contributions of piezoelectric nanoparticles [6].  
11  
12  
13  
14

### 15 **Advances in Science and Technology to Meet Challenges**

16 Significant efforts have been made to overcome the limited energy-harvesting performance of inorganic  
17 nanostructures, which include the modulation of lattice strain, the modification of nanostructures, and  
18 the use of nonconventional piezoelectric materials (figure 2a). Strain engineering may be a promising  
19 approach for significant harvesting enhancement by inducing dipole extension under tensile strain. For  
20 example, a planar stretching strain of  $\sim 4.87\%$  was reported to produce anisotropic lattice strain in a ZnO  
21 nanorod array, increasing the output voltage by  $\sim 90\%$  [4]. Ideal generator devices must be designed with  
22 appropriate sample dimensions for optimal performance. In the case of nanocomposites,  
23 nonconventional nanoscale fillers, such as perovskite halides and carbon nanotubes, have recently been  
24 reported to exhibit outstanding performance. For instance,  $\text{CsPbBr}_3$  halide nanocrystals embedded in  
25 polymer nanofibers delivered  $\sim 103 \text{ V}$  and  $\sim 170 \text{ mA cm}^{-2}$  with one-point pressing [6]. The performance of  
26 selected nanocomposites is projected in terms of their output voltage and current density in figure 2b.  
27  
28

29 Perovskite halide materials have recently attracted significant interest as high-performance  
30 nanogenerators based on thin films or nanoscale constituents. For example, inorganic  $\text{CsSnI}_3$  multi-layered  
31 films with the  $\sim 100 \text{ nm}$  Cu interlayers demonstrated impressive outcomes of  $\sim 22.9 \text{ V}$  and  $1.2 \text{ mA}$  [7]. As  
32 another recent example of inorganic nanostructures, two-dimensional dichalcogenide materials ranging  
33 in thickness from a single atomic layer up to a few nanometers have been introduced as potential  
34 piezoelectric nanogenerators. The energy-harvesting outcomes of a large-area monolayer  $\text{MoS}_2$  film  
35 reached  $\sim 0.4 \text{ V}$  and  $\sim 40.7 \text{ nA}$  with optimal domain configurations relative to the position of the  
36 interdigitated electrodes [8].  
37  
38

39 Applications using inorganic nanostructures have been extended to self-powered wearable systems with  
40 diverse functionalities, which may also be suitable for artificial intelligence and machine learning systems  
41 interfacing with human motions and activities [9,10]. Nanofiber-based composite generators have been  
42 extensively investigated as patches or woven fabrics for driving low-power devices or converting physical  
43 motion into electrical signals. In this regard, biocompatibility and long-term reliability must be seriously  
44 considered.  
45  
46  
47  
48

### 49 **Concluding Remarks**

50 Piezoelectric energy harvesters based on nanostructured inorganic materials have a relatively short  
51 history. Since the early intensive investigations on adopting ZnO-based nanostructures based on different  
52 energy-conversion mechanisms, unprecedented device structures and inorganic nanomaterials have been  
53 extensively explored. Nanostructured inorganic materials may be the sole choice for developing flexible  
54 and wearable systems that require self-powered energy sources as a consequence of interactions to  
55 diverse mechanical inputs. The exploration of halide perovskite materials, novel nanocomposites, and  
56  
57  
58  
59  
60

atomic-scale structures in related fields is currently driving scientific efforts to understand piezoelectricity and the mechanism of electromechanical energy conversion in unexplored material systems. A critical issue in the field of piezoelectric energy harvesting may lie in the non-standardized measurements, which makes it difficult to compare widely scattered reported values, even in similar devices. Nanostructured inorganics are expected to provide unique solutions for future high-efficiency electromechanical energy-harvesting devices.

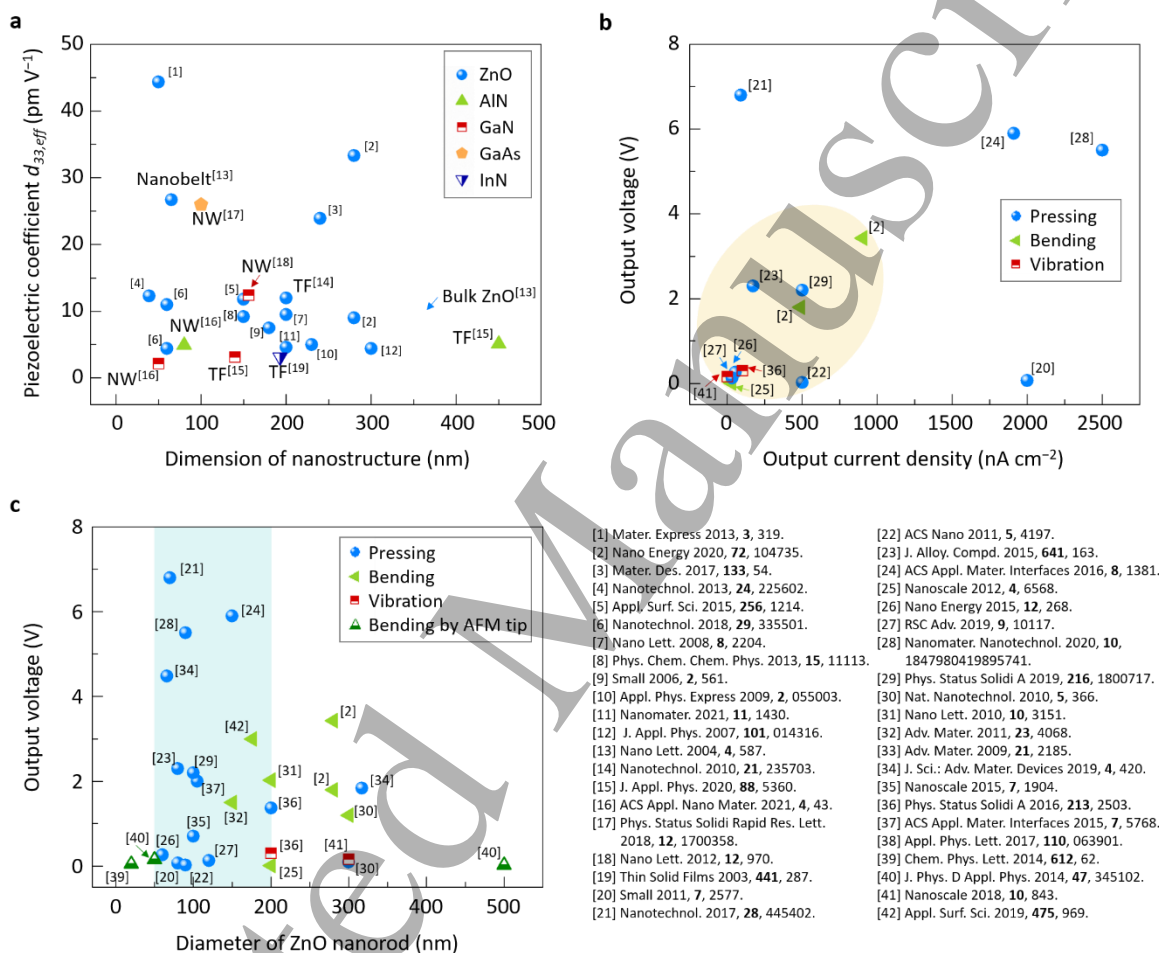


**Figure 1.** (a) Effective piezoelectric coefficient  $d_{33,eff}$  reported for the nanostructured inorganic materials as a function of the nanostructure dimensions. Unspecified blue dots are based on ZnO nanorods with dimensions specified on the x-axis, which means the diameter of the nanorods. For other types of nanostructures, the dimension is the film thickness for thin films and the width for wires. (b) Output voltage versus output current density for reported ZnO-nanorod-based energy harvesters depending on the type of mechanical input source (labeled with different colors). (c) Output voltage versus the ZnO nanorod diameter reported for ZnO-nanorod-based energy harvesters, labeled with different mechanical input sources.

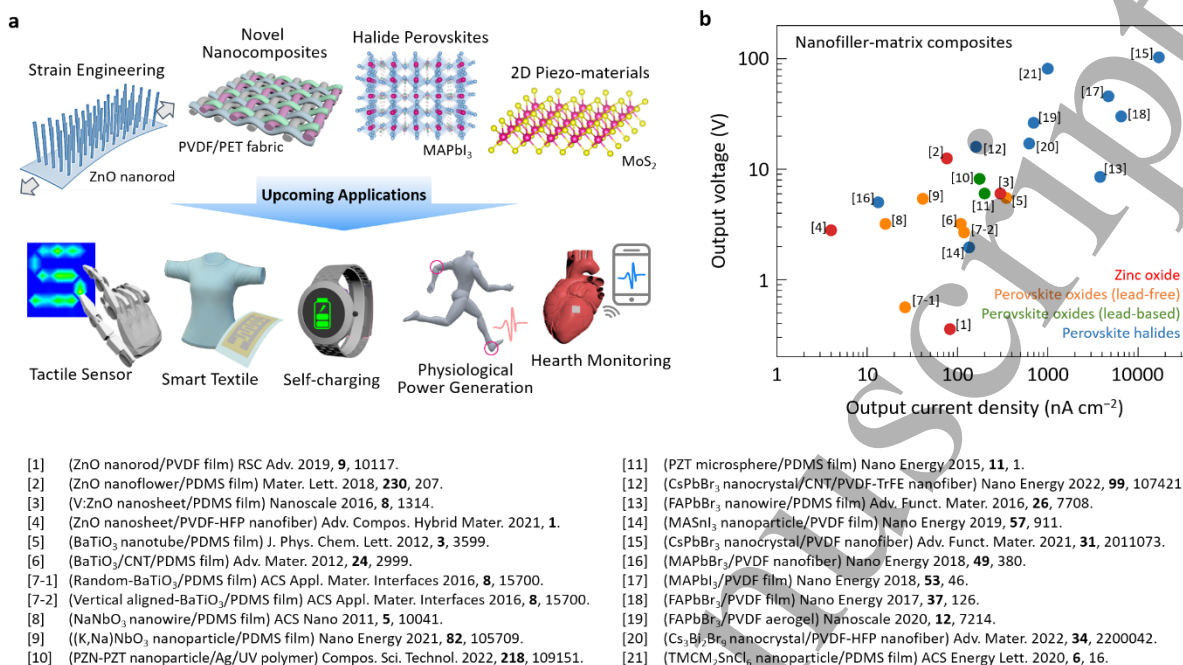


**Figure 2.** (a) Schematic illustration of recent experimental approaches using strain engineering, multifunctional nanocomposites, halide perovskites, and atomic-scale materials, in efforts to develop new piezoelectric energy harvesting platforms for upcoming applications such as physiological power generation, self-powered systems, wearable tactile devices, and biomedical use. (b) Projections of the output voltage and current density values reported for the nanocomposites incorporating inorganic nanoscale fillers.

## Acknowledgements

Financial support through grants from the National Research Foundation of Korea (NRF-2016M3A7B4910151 and NRF-2020M3D1A2102913) is acknowledged.

## References

- [1] Cao X, Xiong Y, Sun J, Zhu X, Sun Q and Wang Z L 2021 Piezoelectric nanogenerators derived self-powered sensors for multifunctional applications and artificial intelligence *Adv. Funct. Mater.* **31** 2102983
- [2] Mahapatra S D, Mohapatra P C, Aria A I, Christie G C, Mishra Y K, Hofmann S and Thakur V K 2021 Piezoelectric materials for energy harvesting and sensing applications: roadmap for future smart materials *Adv. Sci.* **8** 2100864
- [3] Pandey R K, Dutta J, Brahma S, Rao B and Liu C 2021 Review on ZnO-based piezotronics and piezoelectric nanogenerators: aspects of piezopotential and screening effect *J. Phys. Mater.* **4** 044011
- [4] Choi H J, Jung Y S, Han J and Cho Y S 2020 In-situ stretching strain-driven high piezoelectricity and enhanced electromechanical energy harvesting performance of a ZnO nanorod-array structure *Nano Energy* **72** 104735
- [5] Kim D B, Kim S W, Kim Y E, Choi H J and Cho Y S 2022 Room-temperature processed Ag/Pb(Zn<sub>1/3</sub>Nb<sub>2/3</sub>)O<sub>3</sub>-Pb(Zr<sub>0.5</sub>Ti<sub>0.5</sub>)O<sub>3</sub>-based composites for printable piezoelectric energy harvesters *Compos. Sci. Technol.* **218** 109151
- [6] Chen H, Zhou L, Fang Z, Wang S, Yang T, Zhu L, Hou X, Wang H and Wang Z L 2021 Piezoelectric nanogenerator based on in situ growth all-inorganic CsPbBr<sub>3</sub> perovskite nanocrystals in PVDF fibers with long-term stability *Adv Funct Mater* **31** 2011073
- [7] Kim D B, Park K S, Park S J and Cho Y S 2022 Microampere-level piezoelectric energy generation in Pb-free inorganic halide thin-film multilayers with Cu interlayers *Nano Energy* **92** 106785
- [8] Jung Y S, Choi H J, Park S H, Kim D, Park S and Cho Y S 2022 Nanoampere-level piezoelectric energy harvesting of lithography-free centimeter-scale MoS<sub>2</sub> monolayer film generators *Small* **18** 2200184
- [9] Zhang C, Fan W, Wang S, Wang Q, Zhang Y and Dong K 2021 Recent progress of wearable piezoelectric nanogenerators *ACS Appl. Electron. Mater.* **3** 2449-67



[10] Han J, Kim D B, Kim J H, Kim S W, Ahn B U and Cho Y S 2022 Origin of high piezoelectricity in carbon nanotube/halide nanocrystal/P(VDF-TrFE) composite nanofibers designed for bending-energy harvesters and pressure sensors *Nano Energy* **99** 107421

### 3.4 Nitrides for Piezoelectric Energy Harvesting

Agnė Žukauskaitė and Stephan Barth

Fraunhofer Institute for Organic Electronics, Electron Beam and Plasma Technology FEP

#### Status

This section is focused on wurtzitic nitrides, i.e. aluminum nitride (AlN) and aluminum scandium nitride ( $\text{Al}_{1-x}\text{Sc}_x\text{N}$ , AlScN) as well as other similar ternary and quaternary AlN-based alloys. Piezoelectric nitrides are attractive for various applications, including the energy harvesting due to low dielectric constants, good mechanical properties, CMOS compatibility, as well as high temperature stability. The main method of synthesis is magnetron sputtering, which is very scalable and inexpensive. Furthermore, in contrast to PZT-like materials, piezoelectric nitrides with non-centrosymmetric wurtzite structure do not need to be poled as they exhibit permanent polarization along the c-axis (Fig.1(a)). Until 2009, when the first paper about enhanced piezoelectric properties of aluminium scandium nitride (AlScN) was published [1], aluminium nitride (AlN) was the main nitride considered for its piezoelectric properties. However, it suffered from relatively low  $d_{33}$  value of  $\sim 4\text{-}6$  pC/N. High acoustic velocity made it worthwhile for RF applications, but in energy harvesting it was not very competitive with lead zirconium titanate ( $\text{Pb}(\text{Zr}_x\text{Ti}_{1-x})\text{O}_3$ , PZT)-like materials. Now, with the emergence of AlScN (up to  $d_{33} = 31.6$  pC/N reported for  $\text{Al}_{0.59}\text{Sc}_{0.41}\text{N}$  [2]), nitrides are also being considered a viable option for energy harvesting, especially where CMOS integration plays a role or where high-temperature poling step would damage a soft substrate so PZT can't be used. Power generation output of AlScN harvesters can reach relatively high values, e.g.  $>1$  mW in the 25-55 Hz range at Sc concentration of 39% [3]. An additional advantage is the possibility for use in high temperature applications, as the Curie temperature of PZT materials is not so high ( $T_c$  of PZT  $< 400$  °C, much lower for "soft" material) whereas AlN or AlScN are stable at much higher temperatures [4]. AlScN and other ternary or quaternary nitrides with enhanced piezoelectric properties is a relatively new and very actively growing scientific field.

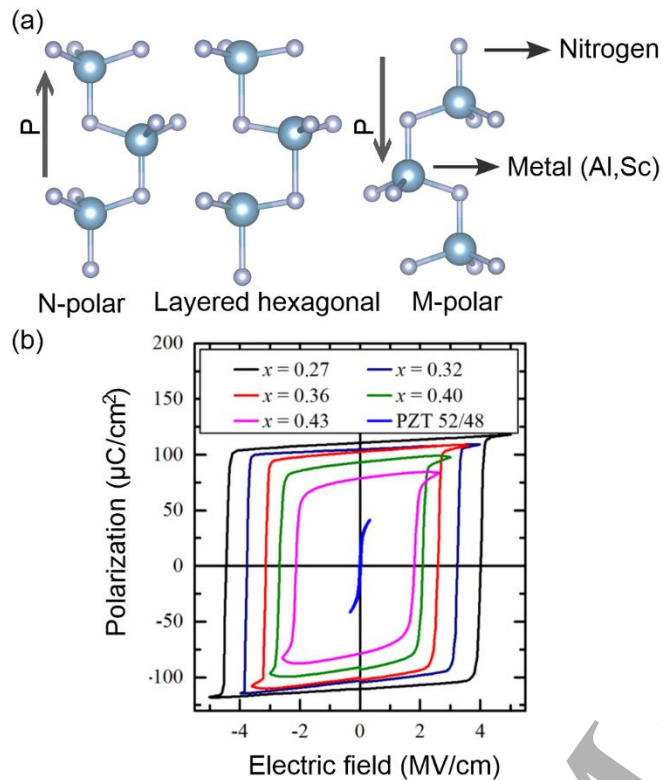


**Figure 1.** (a) Wurtzite nitrogen- and metal-polar Al<sub>x</sub>N structure, as well as predicted layered hexagonal structure of Al<sub>1-x</sub>Sc<sub>x</sub>N, (b) P-E loops for ferroelectric Al<sub>1-x</sub>Sc<sub>x</sub>N with  $x=0.27, 0.32, 0.36, 0.40, 0.43$ , as well as PZT 52/48. Reproduced with the permission of AIP Publishing from Ref [5].

### Current and Future Challenges

Due to high costs of Sc raw material, active search for alternatives is still on-going, with various ternary and even quaternary nitrides being investigated (Fig. 2). However, they did not surpass AlScN yet. Further theoretical and experimental search for other similar nitrides with enhanced properties is ongoing, with multiple research papers published every year.

Due to the metastability of AlScN [6], the material is prone to formation of abnormally oriented grains (AOG) [7] as well as elemental segregation and parasitic cubic inclusions when Sc content is over 40%, so there is a physical limit for Sc incorporation before AlScN stops being wurtzite [6]. Other AlN-based ternary nitrides suffer from the same problems. As with all thin-film based piezoelectric materials, strain engineering and adhesion are also to be taken into consideration. So at the moment, the most effort is still concentrated in the material synthesis and the different aspects of it as well as understanding how to achieve highest material quality to assist with high-yield device fabrication.

Another challenge is actually the structuring of AlScN layers as the conventional methods used for AlN have a drop in etching rate (e.g. ion-milling) or significantly high lateral etching rate (e.g. KOH-based wet etching), so additional considerations have to be taken into account during the device fabrication. Even less is known about working with other ternary nitrides mentioned in the previous section. In the end, to maximize the output power will require new discoveries in material and process knowledge, improved device architecture and even the choosing of the right substrate for a specific frequency region. Moreover, for very high frequency applications the film thickness has to be decreased, so achieving high crystalline quality of the film would require additional attention.

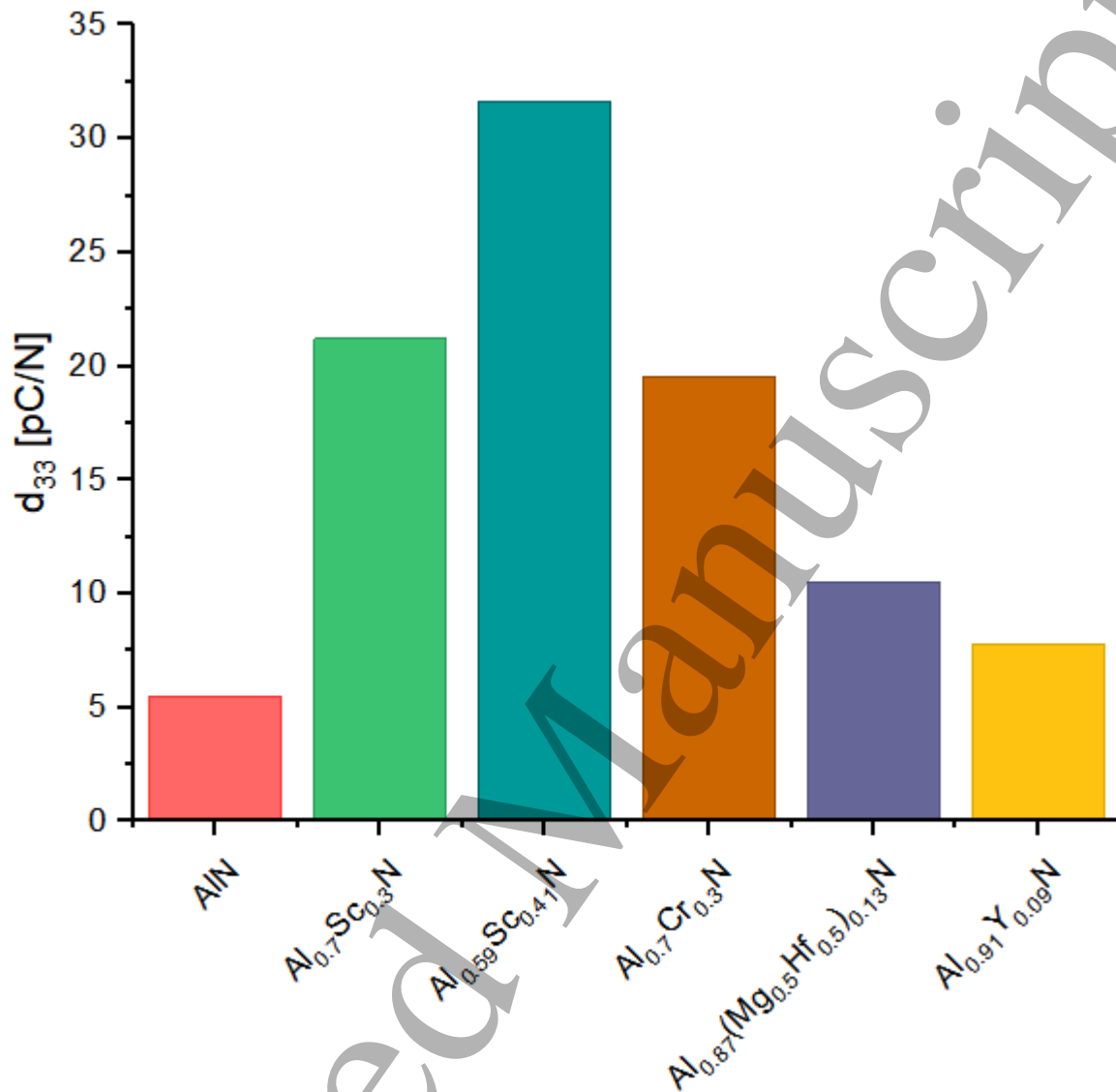


**Figure 2.** Comparison of piezoelectric coefficient  $d_{33}$  for AlN and various ternary and quaternary AlN-based piezoelectric nitrides [2, 8, 9, 10].

### Advances in Science and Technology to Meet Challenges

As the AlScN and other ternaries or quaternaries are still relatively new materials, discoveries about various material constants, behaviour under specific conditions or how the piezoelectric, mechanical, dielectric, optical, and other material properties are changing as a function of composition are still being made. For example, recently it was demonstrated, that due to the reduced energy barrier between the two polarization states of metastable AlScN the energy required for metal and nitrogen planes to switch their positions along  $c$  axis becomes very low, and as a result, under certain conditions AlScN is also ferroelectric [5] (Fig. 1(b)). As the switching is reversible, this would potentially allow to design hybrid cantilever-based energy harvesters that could dynamically switch between two modes: lower-output at higher frequency (unimorph) and higher-output at lower frequency (bimorph). For ultra-thin highly-crystalline nitride thin films, magnetron sputter epitaxy (MSE)[2] is gaining more attention in the

community as well. In addition, new and better harvester designs, e.g. hybrid piezoelectric-electromagnetic, multi-degree-of-freedom or nanowire energy harvesters are being developed where integration of nitride-based materials would be of relevance.

### Concluding Remarks

To conclude, the discovery of AlScN as the first nitride with such high piezoelectric coefficient and high electromechanical coupling triggered an avalanche in the studies of metastable nitrides for various applications, including energy harvesting. The challenges of fabrication of AlScN-based devices are being actively investigated by the scientific community as well as the industry. Pronounced formation of abnormally oriented grains and potential for elemental segregation add additional limitations to the process window.

Under specific circumstances, where high-temperature stability, low environmental impact (lead-free) and CMOS compatibility play a dominating role, this new family of enhanced piezoelectric materials offers a lot of potential for compact, thin-film based energy harvesters. New discovery of the ferroelectric properties of AlScN will also allow for designing more advanced and dynamic broadband harvesters.

### Acknowledgements

S. Barth acknowledges the financial support by projects funded by the European regional development fund (ERDF) and the Free State of Saxony under Grant no: 100206218, Term: 01.02.2015 - 31.01.2018 („DANAE - Dünnschicht- und Abgleichtechnologien für die nanoskalige Akustoelektronik“) and Grant no.: 100347675, Term 01.02.2019 – 31.12.2021 („TASG - Tragbare, Autarke und Kompakte Strom Generatoren“).

### References

- [1] M. Akiyama, T. Kamohara, K. Kano, A. Teshigahara, Y. Takeuchi, and N. Kawahara, “Enhancement of piezoelectric response in scandium aluminum nitride alloy thin films prepared by dual reactive cosputtering,” *Advanced Materials*, vol. 21, pp. 593–596, 2009.
- [2] Y. Lu, M. Reusch, N. Kurz, A. Ding, T. Christoph, M. Prescher, L. Kirste, O. Ambacher, and A. Žukauskaitė, “Elastic modulus and coefficient of thermal expansion of piezoelectric  $\text{Al}_{1-x}\text{Sc}_x\text{N}$  (up to  $x = 0.41$ ) thin films,” *APL Materials*, vol. 6, 076105, 2018.
- [3] S. Barth, H. Nizard, J. Göller, P. Spies, and H. Bartzsch, “AlScN-dünnschichten auf Metallsubstraten für Energy Harvesting Anwendungen,” *Proceedings of 11. EASS Tagung Energieautonome Sensorsysteme*, 05. - 06. July 2022, Erfurt, Germany, pp. 62–24.
- [4] E. Österlund, G. Ross, M. A. Caro, M. Paulasto-Kröckel, A. Hollmann, M. Klaus, M. Meixner, C. Genzel, P. Koppinen, T. Pensala, A. Žukauskaitė, and M. Trebala, “Stability and residual stresses of sputtered wurtzite AlScN thin films,” *Physical Review Materials*, vol. 5, 035001, 2021.
- [5] S. Fichtner, N. Wolff, F. Lofink, L. Kienle, and B. Wagner, “AlScN: A III-V semiconductor based ferroelectric,” *Journal of Applied Physics*, vol. 125, 114103, 2019.
- [6] C. Höglund, J. Birch, B. Alling, J. Bareno, Z. Czigány, P. O. Å. Persson, G. Wingqvist, A. Žukauskaitė, and L. Hultman, “Wurtzite structure  $\text{Sc}_{1-x}\text{Al}_x\text{N}$  solid solution films grown by reactive magnetron sputter epitaxy: Structural characterization and first-principles calculations,” *Journal of Applied Physics*, vol. 107, 123515, 2010.
- [7] C. S. Sandu, F. Parsapour, S. Mertin, V. Pashchenko, R. Matloub, T. LaGrange, B. Heinz, and P. Muralt, “Abnormal grain growth in AlScN thin films induced by complexion formation at crystallite interfaces,” *physica status solidi (a)*, vol. 216, 1800569, 2019.

- [8] S. Manna, K. R. Talley, P. Gorai, J. Mangum, A. Zakutayev, G. L. Brennecke, V. Stevanovic, and C. V. Ciobanu, "Enhanced piezoelectric response of AlN via CrN alloying," *Physical Review Applied*, vol. 9, no. 3, 034026, 2018.
- [9] T. Yokoyama, Y. Iwazaki, Y. Onda, Y. Sasajima, T. Nishihara, and M. Ueda, "Highly piezoelectric co-doped AlN thin films for wideband FBAR applications," *2014 IEEE International Ultrasonics Symposium (IUS)*, pp. 281–288, Sep 2014.
- [10] M. Schlögl, M. Schneider, and U. Schmid, "Piezoelectricity in  $Y_{0.09}Al_{0.91}N$  thin films," *Materials Science and Engineering: B*, vol. 276, 115543, 2022.

### 3.5 2D Materials for Piezoelectric Energy Harvesting

Feng Ru Fan<sup>1</sup> and Wenzhuo Wu<sup>2</sup>

<sup>1</sup> College of Chemistry and Chemical Engineering, Xiamen University, China

<sup>2</sup> School of Industrial Engineering, Purdue University, USA

#### Status

Traditional piezoelectric energy harvesters fall short in several crucial respects that would make them ideal for the emerging applications in wearables, robotics, etc. Progress in piezoelectric nanogenerator (PENG) has been aided by recent advances in both science and technology that leverage the unique characteristics of 2D materials<sup>2</sup>. Unlike bulk or thin-film materials, 2D materials can endure enormous strain and allow wide strain tunability due to their atomically thin geometries and superior mechanical features. Theoretical and experimental efforts suggest that many 2D materials, including transition metal dichalcogenides (e.g.,  $MoS_2$ ), monochalcogenide group (e.g., SnS), and others, exhibit strong intrinsic piezoelectricity from their noncentrosymmetric lattices<sup>3</sup>. The piezoelectric constant, a key piezoelectric figures of merit, for some 2D materials (e.g., SnS, GeS, etc.) is in the range of 75-250 pm/V (ref<sup>4</sup>), comparable to the piezoelectric constants of bulk piezoelectrics. The direct mechanical-to-electrical transduction of both static and dynamic signals makes these materials promising for application in PENGs with ultrathin form factors<sup>5</sup>. The reported power output for 2D materials based PENG is in the range of mW/m<sup>2</sup> (ref<sup>6</sup>). While there are many of recent papers that provide in-depth analyses of developments in related fields, our goal here is to give a more concise discussion focused on our perspectives on the potential and challenges in these areas.

#### Current and Future Challenges

Despite remarkable progress in related fields, challenges remain on the path toward the production, integration, and deployment of 2D materials based PENG. Inducing consistent piezoelectric responses by applying external macroscopic mechanical strain is a significant challenge. The following elements contribute significantly to this problem: (1) most of these 2D materials have symmetries that cause in-plane piezoelectricity<sup>7</sup>; (2) the ionic nature of these materials causes orientation-dependent piezoelectric responses; and (3) due to synthesis and/or assembly constraints, these materials are frequently placed on the host substrate with little or no control over the in-plane orientations. Even though a wide variety of 2D materials have been predicted to exhibit intrinsic piezoelectricity, most of these materials have not yet been studied experimentally due to the challenges associated with current methods of preparing these materials<sup>8</sup>. The ability to scale up the preparation of related 2D materials with the necessary yield and qualities is limited by constraints in growth substrates and process conditions. Furthermore, due to the material's symmetry, significant difficulties in process control arise when the thickness of a 2D piezoelectric material varies by even a single atomic layer<sup>2</sup>, rendering the material non-piezoelectric. Because of their atomic thickness, 2D materials are highly sensitive to their surroundings (and possibly unstable). It has been found that 2D materials' carrier concentration may be dramatically altered by

environmental doping, which in turn can have a profound effect on their piezoelectric behavior due to charge screening<sup>9</sup>.

### **Advances in Science and Technology to Meet Challenges**

The above barriers also create a wealth of research opportunities. Due to the reduced dimensions of 2D materials, their piezoelectricity is robust and easily accessible compared to its bulk counterpart. In contrast to conventional piezoelectrics, which are brittle and insulating, 2D piezoelectric materials can host significant strain-induced electric field couplings due to the 2D limit's extraordinarily high Coulomb interactions. The strong coupling of piezoelectricity to a variety of solid-state excitations including charges, photons, and spins in 2D systems provide undiscovered prospects for pursuing fascinating science at the atomically thin limit. The hybridization of these processes within PENG's operations might promote interest in the study of new sciences and facilitate the creation of novel device designs. The thin thickness of 2D materials also increases the occurrence of flexoelectricity, a physical phenomenon that can produce electrical polarizations with inhomogeneous deformation even in centrosymmetric lattices<sup>10</sup>. Understanding the impact of flexoelectricity on 2D materials based PENGs is anticipated to facilitate the development of high-performance energy devices using a broader range of atomically thin materials.

Technology developments in material design and nanomanufacturing have opened the door to the possibility of mass-producing substrate-independent, high-performance 2D materials with designer characteristics<sup>11</sup>. By combining theoretical and experimental examination of the interfacial characteristics of 2D materials and electrode, we may get insight into phenomena such as the impact of metals and electrode configurations on charge transfer/transport in metal-2D material contacts. Such understanding is crucial for the rational design and optimization of future PENGs. The potential to allow innovative device ideas and applications in PENGs is only one of many reasons why it is crucial to understand the underlying doping process and defect chemistry in 2D materials. The physics-based design and development of 2D PENGs relies on quantitative in situ and in operando characterizations of 2D materials under controlled straining circumstances to provide the vitally needed fundamental insights and experimental toolkit. Designing and fabricating 2D heterostructured artificial crystals can generate new device physics and create a plethora of new functions. The ultrathin nature and robust mechanical properties of 2D materials make them a candidate for 3D devices, which might result in a myriad of unique capabilities and enhanced performance in comparison to their planar counterparts. For such 3D integration, the discovery, development, and fabrication of 2D materials with high out-of-plane piezoelectricity are desirable<sup>9</sup>.

### **Concluding Remarks**

Theoretical and experimental progress in 2D materials based PENGs is expected to be sparked by the development of convergent techniques that bridge fields like advanced manufacturing, data science, material science, device physics, chemistry, etc. A concerted effort by the research community might assist several areas related to atomically thin materials' science and technology, such as piezoelectricity, semiconductor devices, ferroelectricity, and quantum physics.

### **Acknowledgements**

*W. Z. W. acknowledges the College of Engineering and School of Industrial Engineering at Purdue University for the Ravi and Eleanor Talwar Rising Star Professorship. F. R. F. acknowledges Nanqiang Young Top-notch Talent Fellowship from Xiamen University.*



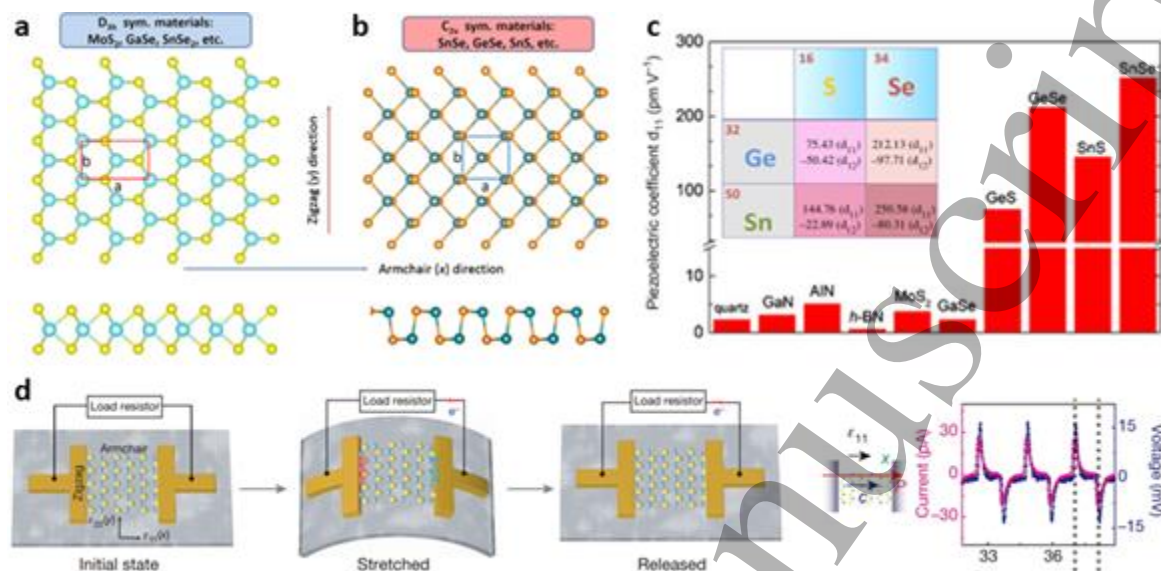


**Figure 1. Working mechanism and performance of 2D materials-based PENGs.** The top and side views of the (a) ball-stick atomic structure of  $D_{3h}$  hexagonal monolayer, and the (b) ball-stick atomic structure of  $C_{2v}$  orthorhombic monolayer. (c) In-plane piezoelectric coefficient ( $d_{11}$ ) between conventional piezoelectrics and group IV monochalcogenides. Reproduced with permission from Ref 4. Copyright 2015 APL. (d) Working mechanism and output of monolayer MoS<sub>2</sub>-based piezoelectric device. Reproduced with permission from Ref 2. Copyright 2014 Springer Nature.

## References

1. Z. L. Wang and J. Song, *Science*, 2006, **312**, 242.
2. W. Wu, L. Wang, Y. Li, F. Zhang, L. Lin, S. Niu, D. Chenet, X. Zhang, Y. Hao, T. F. Heinz, J. Hone and Z. L. Wang, *Nature*, 2014, **514**, 470-+.
3. W. Wu and Z. L. Wang, *Nature Reviews Materials*, 2016, 16031.
4. R. Fei, W. Li, J. Li and L. Yang, *Applied Physics Letters*, 2015, **107**, 173104.
5. S. K. Kim, R. Bhatia, T.-H. Kim, D. Seol, J. H. Kim, H. Kim, W. Seung, Y. Kim, Y. H. Lee and S.-W. Kim, *Nano Energy*, 2016, **22**, 483-489.
6. M. H. Lee and W. Wu, *Advanced Materials Technologies*, 2022, **n/a**, 2101623.
7. K.-A. N. Duerloo, M. T. Ong and E. J. Reed, *The Journal of Physical Chemistry Letters*, 2012, **3**, 2871-2876.
8. M. N. Blonsky, H. L. Zhuang, A. K. Singh and R. G. Hennig, *ACS Nano*, 2015, **9**, 9885-9891.
9. C. Cui, F. Xue, W.-J. Hu and L.-J. Li, *npj 2D Materials and Applications*, 2018, **2**, 18.
10. L. Wang, S. Liu, X. Feng, C. Zhang, L. Zhu, J. Zhai, Y. Qin and Z. L. Wang, *Nature Nanotechnology*, 2020, **15**, 661-667.
11. Y. Wang, G. Qiu, Q. Wang, Y. Liu, Y. Du, R. Wang, M. J. Kim, P. D. Ye and W. Wu, *Nature Electronics*, 2018, **1**.



### 3.6 Organics for Piezoelectric Energy Harvesting

Pedro Costa<sup>1,2</sup>, Javier del Campo<sup>3,4</sup> and Senentxu Lanceros-Mendez<sup>1,2,3,4</sup>

<sup>1</sup>Physics Centre of Minho and Porto Universities (CF-UM-UP), University of Minho 4710-053 Braga, Portugal

<sup>2</sup>Laboratory of Physics for Materials and Emergent Technologies, LapMET

<sup>3</sup>BCMaterials, Basque Center for Materials, Applications and Nanostructures, UPV/EHU Science Park, 48940 Leioa, Spain;

<sup>4</sup>IKERBASQUE, Basque Foundation for Science, 48009 Bilbao, Spain

#### Status

Piezoelectricity was discovered by the Curie brothers in 1880 [1] while studying several materials, including organic ones such as cane sugar or tartaric acid. The piezoelectric effect is widely applied to sensor/actuator devices and to generate electricity. In this regard, wasted mechanical energy can be harvested to supply low-power electronic devices ( $\mu\text{W}$  to  $\text{mW}$  range) [1].

Piezoelectric materials, which typically display non-centrosymmetric crystalline structures, can be also present in specific amorphous organic materials. Generally, organic piezoelectric materials are characterized by lower piezoelectric constants, lower electromechanical coupling factors, and lower Curie temperature than their inorganic counterparts. In contrast, they present outstanding mechanical properties, can be processed in large areas, are flexible and can take a variety of shapes, including spheres, fibres or membranes [1].

Most piezoelectric polymers are semi-crystalline, though there are also amorphous ones. The piezoelectric effect in organic polymers is originated in the macromolecular structure and conformation together with their orientation and packaging [1], where a poling process is typically necessary to create or optimize their piezoelectric response.

The most studied organic piezoelectric polymers are polyvinylidene fluoride (PVDF) and its copolymers, which present the highest piezoelectric response up to date (Figure 1) [2]. Semicrystalline PVDF and their copolymers present distinct crystalline phases, being the  $\beta$ -phase the electroactive one with the highest dipolar moment per unit cell ( $8 \times 10^{-30}$  C.m) [2]. The piezoelectric coefficients of PVDF range from  $8 < d_{31} < 30$  and  $-24 < d_{33} < -140$  pC/N, respectively [2]. Other polymers with piezoelectric properties include polyamides (odd-nylons, being nylon-11 the most studied) with  $d_{31} < 12$  pC/N [3].

Biopolymers typically display piezoelectric coefficients between  $0.1 < d_{14} < 2$  pC/N. These include polysaccharides (such as cellulose or chitin) and proteins (such as collagen or keratin) [4]. On the other hand, the piezoelectricity in amino acid single crystals can reach outstanding piezoelectric responses, such as 178 and 25 pC/N, respectively, for  $\beta$ -glycine and hydroxy-L-proline [5].

Piezoelectric polymers can be easily processed by solvent-based methods, including electrospinning, spin-coating, screen-printing or ink-jet printing, among others, but also from the melt: melt spinning, high-pressure melt crystallization, extrusion or injection provide a wide variety of shapes [1]. Among the different techniques, electrospinning provides larger piezoelectric coefficients because of the specific materials orientation during the process. Also, to optimize the piezoelectric coefficients and corresponding energy harvesting capability, poling (in order of MV/m) are usually applied in a post-processing step. The potential applications of the materials include energy harvesting from body

movements, transportation, roadway, bridges, vehicles, tyres, engine or suspension, wind and ocean waves, among others.

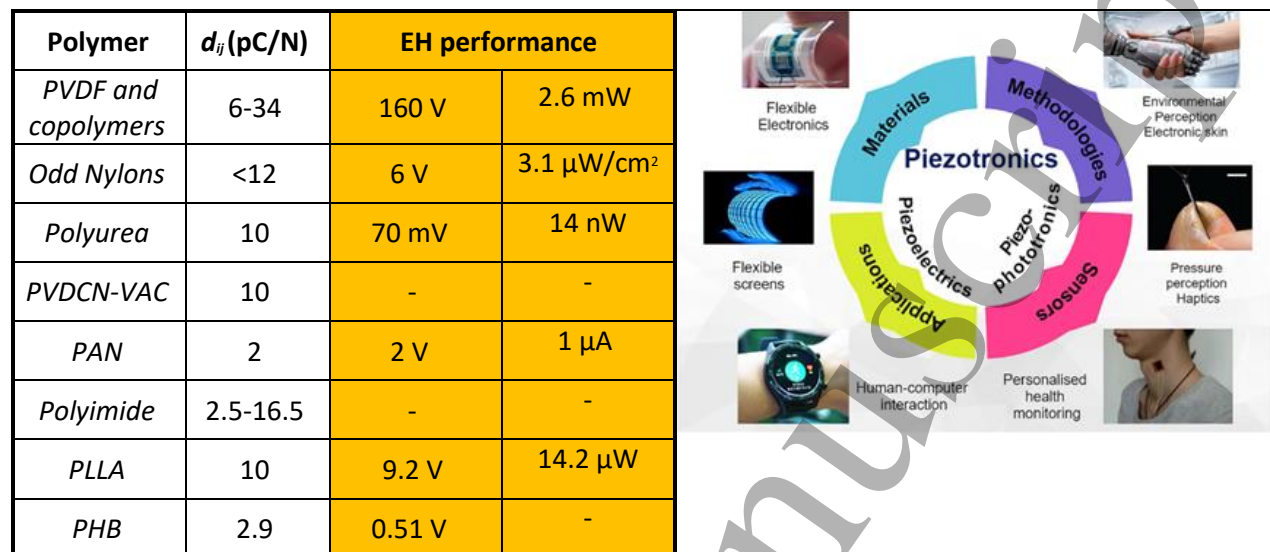


Figure 1- Left: Piezoelectric coefficients of representative polymers and their performance for energy harvesting [1, 6, 7]. Right: Future prospects of piezotronics [8].

### Current and Future Challenges

Organic piezoelectrics show lower piezoelectric output than inorganic ones [1], but they are flexible, mouldable, can be processed by additive manufacturing in a variety of geometries, and are less expensive as they can be processed without advanced facilities.

The piezoelectricity of PVDF was first discovered by Kawai in 1969 [4] in stretched and poled films. In subsequent years, the research in PVDF and copolymers and in nylons was extensively performed [4]. Materials processing optimization led to piezoelectric coefficients (pC/N) for PVDF of  $d_{33}=-24$  to  $-34$  pC/N, and for the copolymers of poly(vinylidene fluoride-trifluoroethylene), PVDF-TrFE,  $d_{33}=-25$  to  $-40$  pC/N; poly(vinylidene fluoride-co-hexafluoropropylene), PVDF-HFP,  $d_{33}=-24$  pC/N; poly(vinylidene fluoride-co-chlorotrifluoroethylene), PVDF-CTFE,  $d_{33}=-140$  pC/N. Further, the introduction of small amounts (<2 mol %) of fluorinated alkyne monomers in the relaxor ferroelectric poly(vinylidene fluoride-trifluoroethylene-chlorofluoroethylene), PVDF-TrFE-CFE, terpolymer leads to an ultrahigh electromechanical coupling, with a  $d_{33}> 1000$  pC/N [9], competitive with the ones of ceramic materials. For nylon-11 the piezoelectric response is  $d_{31}<12$  pC/N [3]. Poly(L-lactide) (PLLA), with  $d_{14}=12$  pC/N was discovered by Fukada in 1991 [1] and is relevant for medical applications due to their biodegradable characteristics. Natural materials with shear piezoelectric properties include silk and cellulose, with  $d_{14}=-1.5$  and  $0.2$  pC/N, respectively [4], being biological piezoelectricity first reported for bone. Biological materials present lower piezoelectric coefficients (below 2 pC/N) and have been scarcely used for energy harvesting [5].

Organic biomaterials such as collagen can generate up to 10 V and  $4.15 \mu$ W/cm<sup>2</sup> [1] but most biomaterials working as energy harvesters show lower performance than traditional polymers. Nevertheless, their multifunctionality and sensing abilities are suitable for smart biomedical systems [5].

PVDF-based materials are the most explored materials as harvesting devices, mainly in cantilever beam geometry (unimorph or bimorph) and rotary harvesters but also in pressure or force modes, and the output power generated typically reach up to tens of  $\mu$ W to some mW [1, 10]. PVDF-TrFE is the most used

1  
2  
3 polymer due to its improved piezoelectric coefficient [2]. The main advantage of these systems is the wide  
4 range of potential energy sources: rain over a PVDF film can generate several Volts and  $\mu\text{W}$  [10] while  
5 roadway applications may lead to 60 V, 18  $\mu\text{A}$  and 0.2 W of output power [1] using electroactive PVDF.  
6

7  
8 The need for flexible, low power energy harvesting systems has strongly increased in recent times due to  
9 market growth of small and autonomous electronic devices [1]. To optimize the generated energy  
10 harvesting devices it is mandatory combine two aspects: composite materials to maximize the energy per  
11 unit, and hybrid devices combining different active principles, such as the piezoelectric with triboelectric,  
12 pyroelectric or photovoltaic capabilities [8]. Lead-free piezoelectric ceramics with  $d_{33}$  larger than 100 [1]  
13 combined with ferroelectric polymers increase the device performance several times [1], while  
14 maintaining processability and flexibility. Polymer composites reinforced with ceramic fillers or  
15 nanocrystals can enhanced their performance several times generating of output power [7]. Poling the  
16 samples also increases the output performance of the devices.  
17

### 18 **Advances in Science and Technology to Meet Challenges**

19 Three important areas where scientific advances will create opportunities for piezoelectric energy  
20 harvesters (PEH) to meet societal and technological challenges (Figure 2) are (i) materials and processes,  
21 (ii) integration into multifunctional components and (iii) more efficient devices with lower power  
22 demands.  
23

24  
25 Despite the advantages of organic or polymeric materials compared to ceramic ones, they face important  
26 drawbacks such as low piezoelectric coefficients, relatively poor thermal stability, and limited durability.  
27 These limitations define future avenues for new technology development. New composite materials  
28 combining polymeric piezoelectric materials, ceramics and metal oxides are one way forward to improve  
29 piezoelectric properties. Another intriguing opportunity is presented by the use of micro- and nano-  
30 patterned structures [8] as a means to improve both mechanical and electrical properties of these  
31 materials. Here the challenge rests in scaling up the process to enable large area applications.  
32

33  
34 Self-powered devices provide the third area where organic PEH may find important opportunities. Current  
35 harvesting devices require the integration of several components such as the piezoelectric component, a  
36 rectifying unit, and a battery or other form of energy storage. The development of new materials and  
37 smarter device architecture could lead to the integration of several of these functions in a single  
38 component, which will lead to higher miniaturization levels and facilitate the integration of PEH units  
39 particularly in small and autonomous devices. Self-powered sensors are a particular case in which the  
40 PEH unit output is actually used as the readout of an event of interest. For instance, in structural health  
41 monitoring, an important application area for piezoelectric materials, either alone or in combination with  
42 other energy generation and storage systems.  
43

44  
45 Last, one of the most cited limitations of organic piezoelectric energy harvesters is their low power output,  
46 but it can be expected to increase over the coming years though advance materials design and  
47 development, supported by machine learning strategies, among others. We often think about the  
48 improvements needed in one technology in relation to present circumstances, missing the parallel  
49 development occurring in other areas. Thus, advances in ultra-low-power electronics and energy storage  
50 will provide new opportunities for organic PEH materials sooner than anticipated. While this kind of  
51 technological progress lies beyond piezoelectrics, it will eventually determine the most suitable  
52 opportunities.  
53  
54  
55  
56  
57  
58  
59  
60

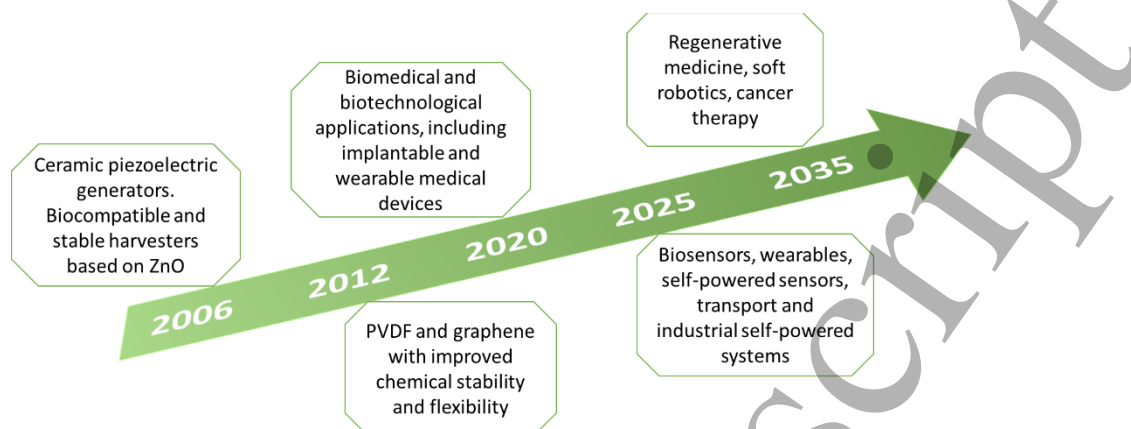


Figure 2- Proposed roadmap for 3D printed PENG development from its first implementation to the near future. Based on [11].

### Concluding Remarks

Piezoelectricity has been a fruitful area of research and applications since its discovery over a century ago. Their ability to exchange mechanical and electrical energy makes piezoelectric materials extremely relevant in sensing and energy harvesting. Although organic piezoelectric materials display lower piezoelectric constants than their inorganic counterparts, their flexibility and compatibility with additive manufacturing processes makes them very attractive for a large variety of applications. The obvious way forward is improving piezoelectric response, thermal stability and durability. However, new architectures leading to multifunctional components, particularly self-powered ones, will open design avenues for new devices. Last, while performance gains in organic PEH are important, one must keep an eye on the decreasing power needs of new low-power electronics and nanodevices, which may provide new opportunities sooner, or in areas other than expected. While most applications of piezoelectric sensors today may be in structural monitoring, applications in health and biomedicine will also play a decisive role in the future.

### Acknowledgements

The authors thank the Fundação para a Ciência e Tecnologia for financial support: Strategic Project UID/FIS/04650/2021 and grant SFRH/BPD/110914/2015 (P.C.); funding by Spanish State Research Agency (AEI) and the European Regional Development Fund (ERFD): project PID2019-106099RB-C43/AEI/10.13039/501100011033; BIDEKO Project, funded by MCIN/AEI, NextGenerationEU, PRTR; and from the Basque Government Industry Department under the ELKARTEK program.

### References

- [1] N. Sezer and M. Koç, "A comprehensive review on the state-of-the-art of piezoelectric energy harvesting," *Nano Energy*, vol. 80, p. 105567, 2021/02/01/ 2021.
- [2] P. Martins, A. C. Lopes, and S. Lanceros-Mendez, "Electroactive phases of poly(vinylidene fluoride): Determination, processing and applications," *Progress in Polymer Science*, vol. 39, pp. 683-706, 2014/04/01/ 2014.
- [3] K. Maity and D. Mandal, "Chapter Seven - Piezoelectric polymers and composites for multifunctional materials," in *Advanced Lightweight Multifunctional Materials*, P. Costa, C. M. Costa, and S. Lanceros-Mendez, Eds., ed: Woodhead Publishing, 2021, pp. 239-282.

- [4] E. Fukada, "History and recent progress in piezoelectric polymers," *IEEE Transactions on Ultrasonics, Ferroelectrics, and Frequency Control*, vol. 47, pp. 1277-1290, 2000.
- [5] S. Guerin, S. A. M. Tofail, and D. Thompson, "Organic piezoelectric materials: milestones and potential," *NPG Asia Materials*, vol. 11, p. 10, 2019/03/07 2019.
- [6] C. Wan and C. R. Bowen, "Multiscale-structuring of polyvinylidene fluoride for energy harvesting: the impact of molecular-, micro- and macro-structure," *Journal of Materials Chemistry A*, vol. 5, pp. 3091-3128, 2017.
- [7] S. Mishra, L. Unnikrishnan, S. K. Nayak, and S. Mohanty, "Advances in Piezoelectric Polymer Composites for Energy Harvesting Applications: A Systematic Review," *Macromolecular Materials and Engineering*, vol. 304, p. 1800463, 2019.
- [8] Y. Wu, Y. Ma, H. Zheng, and S. Ramakrishna, "Piezoelectric materials for flexible and wearable electronics: A review," *Materials & Design*, vol. 211, p. 110164, 2021/12/01/ 2021.
- [9] X. Chen, H. Qin, X. Qian, W. Zhu, B. Li, B. Zhang, *et al.*, "Relaxor ferroelectric polymer exhibits ultrahigh electromechanical coupling at low electric field," *Science*, vol. 375, pp. 1418-1422, 2022.
- [10] Y. Bai, H. Jantunen, and J. Juuti, "Energy Harvesting Research: The Road from Single Source to Multisource," *Advanced Materials*, vol. 30, p. 1707271, 2018.
- [11] M. A. P. Mahmud, P. Adhikary, A. Zolfagharian, S. Adams, A. Kaynak, and A. Z. Kouzani, "Advanced Design, Fabrication, and Applications of 3D-Printable Piezoelectric Nanogenerators," *Electronic Materials Letters*, vol. 18, pp. 129-144, 2022/03/01 2022.

### 3.7 Bio-inspired materials for piezoelectric energy harvesting

Hamideh Khanbareh

Department of Mechanical Engineering, University of Bath

#### Status

In the field of piezoelectric energy harvesting the term "bio-inspired" has been referred to different groups of materials and systems depending on their origin or application. In recent years research has been focused on i) biological piezoelectric materials (such as amino acids/peptides/proteins [1], [2], ii) polysaccharides [3], iii) animal-derived polymers such as silk [4] and collagen [5], iv) biomimetic porous materials such as sea sponge and bone [6], v) bio-waste [7] and vi) energy harvesting mechanisms inspired by nature [8].

Cellulose is a biodegradable polymer with a piezoelectric coefficient of 26–60 pC/N. Mandal [4] fabricated a cellulose microfiber and polydimethylsiloxane (PDMS) composite piezoelectric generator. With hand punching, it produced an open circuit voltage of ~30 V and short circuit current of ~500 nA, and a power density of 9.0  $\mu\text{W}/\text{cm}^3$ . Maiti *et al.* [3] developed self-poled aligned cellulose fibrous with a piezoelectric coefficient of 2.8 pC/N. The fabricated generator produced a voltage, current, power density, and energy conversion efficiency of 18 V, 166 nA, 1.7  $\mu\text{W}/\text{cm}^2$ , and 61.7%, respectively. Zheng *et al.* [9] fabricated an aerogel cellulose and PDMS composite nanogenerator with an open circuit voltage of 60.2 V, a short circuit current of 10.1  $\mu\text{A}$ , and a power density of 6.3  $\text{mW}/\text{cm}^3$  at 10 Hz.

Sea sponge composed of soft fibrils and hard skeletons that combines high elasticity and toughness has inspired Zhang *et al.* [10] to create a 3D interconnected porous structure of (Ba,Ca)(Zr,Ti)O<sub>3</sub> piezoceramics and elastomer-based composite piezoelectric generator with enhanced mechanical and piezoelectric performance compared to those of a randomly dispersed particle-based composites. The output voltage, current density, and power density of 25 V, 550 nA/cm<sup>2</sup> and 2.6  $\text{mW}/\text{cm}^2$ , respectively, were achieved when compressed by 12%.



1  
2  
3  
4 Ghosh [7] developed a piezoelectric nanogenerator based on fish swim bladder. It consisted of highly  
5 ordered self-aligned collagen nanofibrils and it could convert stress from a human finger (1.4 MPa) into  
6 electricity with an open circuit voltage, short circuit current, and power density of 10 V, 51 nA, and 4.15  
7  $\mu\text{W}/\text{cm}^2$ . Karan et al. [11] showed that the bio-waste eggshell could be used to build a nanogenerator,  
8 with an output voltage of 26.4 V, 63% energy conversion efficiency, and 1.45 mA current with a power  
9 density of 238.2  $\text{mW}/\text{cm}^3$  under 81.6 kPa. Alluri et al. [12] used flexible and transparent aloe-vera films  
10 with a  $d_{33}$  of 6.5 pm/V to create an energy harvester and reported to generate sufficient electric charge to  
11 act as a self-powered sensor for human finger monitoring.  
12  
13

#### 14 **Current and Future Challenges**

15 Bio-inspired natural materials exhibit promising piezoelectric properties as well as biocompatibility,  
16 biodegradability, flexibility, and durability. These are highly desired in most applications especially in  
17 healthcare and human-machine interface. However, this area of research is still in its infancy and open for  
18 the exploration of more novel biomaterials. These materials can help decrease toxic e-wastes generated  
19 by the use of electrochemical batteries or lead-containing piezoelectric materials.  
20

21 Biomolecules like amino acids possess chiral symmetry, while protein-based polymers (silk and collagen)  
22 and polysaccharides (cellulose and chitin) have low-symmetric helical structures, exhibiting intriguing  
23 piezoelectric effect. Although most of these bio-inspired piezoelectric materials have an inferior  
24 piezoelectric performance compared to the classic counterparts, additional control over the orientation  
25 and polarisation direction are expected to significantly improve their electromechanical coupling enabling  
26 future transducers with biodegradable properties.  
27  
28

#### 29 **Advances in Science and Technology to Meet Challenges**

30 To overcome the inferior piezoelectric performance of bioinspired piezoelectric materials special  
31 attention has been given to uniaxial ferroelectric biomolecules with peculiar domain structure and record  
32 high piezoelectric voltage coefficients. [1] The key to significant improvement of properties in these  
33 materials lies in controlling nanoscale ferroelectricity in crystalline biomolecules as shown in the case of  
34  $\beta$ -Glycine. [13], [14]. Self-assembly of organic ferroelectrics (such as  $\beta$ -glycine) with preferred orientation  
35 of polarisation axes has been shown as an effective method in improving the materials properties. [14]  
36 The importance of molecular simulations of polarisation switching on nanoscale be over emphasised,  
37 which open pathways to creating novel classes of bioelectronic materials and devices.  
38  
39

#### 40 **Concluding Remarks**

41 In addition to widely researched organic and inorganic piezoelectric materials, plenty of biological  
42 materials are composed of piezoelectric components. In addition, their non-toxic, biocompatible, and  
43 recyclable nature, have paved the way for their application in energy harvesting devices. Due to the  
44 growing interest in mechanical energy harvesting for healthcare and implantable devices as well as the  
45 environmental concerns related to the inorganic piezoelectric ceramics, more and more designs have  
46 been inspired by the materials and processes that offer functionality as well as biodegradability and  
47 seamless interfacing with the human body. Bio-inspired materials are promising candidates for future  
48 transducers as they offer a unique combination of the desired features. Research is focusing on improving  
49 the electromechanical performance by means of controlling the materials crystal structure,  
50 microstructure and the polarisation direction while maintaining biodegradability.  
51  
52

#### 53 **Acknowledgements**

54 This research is funded by the RCH studentship through University of Bath Alumni.  
55  
56  
57  
58  
59  
60



## References

- [1] A. Kholkin, N. Amdursky, I. Bdikin, E. Gazit, and G. Rosenman, "Strong piezoelectricity in bioinspired peptide nanotubes," *ACS Nano*, vol. 4, no. 2, pp. 610–614, 2010.
- [2] S. Guerin *et al.*, "Racemic Amino Acid Piezoelectric Transducer," *Phys. Rev. Lett.*, vol. 122, no. 4, p. 047701, Jan. 2019.
- [3] S. Maiti, S. K. Karan, J. K. Kim, and B. B. Khatua, "Nature Driven Bio-Piezoelectric/Triboelectric Nanogenerator as Next-Generation Green Energy Harvester for Smart and Pollution Free Society," *Adv. Energy Mater.*, vol. 9, no. 9, pp. 1–41, 2019.
- [4] J. Li, Y. Long, F. Yang, and X. Wang, "Degradable piezoelectric biomaterials for wearable and implantable bioelectronics," *Curr. Opin. Solid State Mater. Sci.*, vol. 24, no. 1, p. 100806, Feb. 2020.
- [5] D. Denning *et al.*, "Piezoelectric Tensor of Collagen Fibrils Determined at the Nanoscale," *ACS Biomater. Sci. Eng.*, vol. 3, no. 6, pp. 929–935, Jun. 2017.
- [6] Y. Zhang *et al.*, "Ferroelectret materials and devices for energy harvesting applications," *Nano Energy*, vol. 57, 2019.
- [7] S. K. Ghosh and D. Mandal, "Efficient natural piezoelectric nanogenerator: Electricity generation from fish swim bladder," *Nano Energy*, vol. 28, pp. 356–365, 2016.
- [8] J. Ma *et al.*, "Dye wastewater treatment driven by cyclically heating/ cooling the poled (K<sub>0.5</sub>Na<sub>0.5</sub>)NbO<sub>3</sub> pyroelectric crystal catalyst," *J. Clean. Prod.*, vol. 276, p. 124218, 2020.
- [9] Q. Zheng, H. Zhang, H. Mi, Z. Cai, Z. Ma, and S. Gong, "High-performance flexible piezoelectric nanogenerators consisting of porous cellulose nanofibril (CNF)/poly(dimethylsiloxane) (PDMS) aerogel films," *Nano Energy*, vol. 26, pp. 504–512, 2016.
- [10] Y. Zhang *et al.*, "Bioinspired elastic piezoelectric composites for high-performance mechanical energy harvesting," *J. Mater. Chem. A*, vol. 6, no. 30, pp. 14546–14552, 2018.
- [11] S. K. Karan *et al.*, "Nature driven spider silk as high energy conversion efficient bio-piezoelectric nanogenerator," *Nano Energy*, vol. 49, pp. 655–666, Jul. 2018.
- [12] N. R. Alluri, N. P. Maria Joseph Raj, G. Khandelwal, V. Vivekananthan, and S. J. Kim, "Aloe vera: A tropical desert plant to harness the mechanical energy by triboelectric and piezoelectric approaches," *Nano Energy*, vol. 73, no. March, p. 104767, 2020.
- [13] A. Heredia *et al.*, "Nanoscale Ferroelectricity in Crystalline  $\gamma$ -Glycine," *Adv. Funct. Mater.*, vol. 22, no. 14, pp. 2996–3003, Jul. 2012.
- [14] E. Seyedhosseini *et al.*, "Self-Assembly of Organic Ferroelectrics by Evaporative Dewetting: A Case of  $\beta$ -Glycine," *ACS Appl. Mater. Interfaces*, vol. 9, no. 23, pp. 20029–20037, Jun. 2017.

## 4. Materials for Triboelectric Energy Harvesting

### 4.1 Introduction to materials for triboelectric energy harvesting

Zhong Lin Wang

School of Materials Science and Engineering, Georgia Institute of Technology, Atlanta, GA, 30332-0245, USA

#### **Triboelectric nanogenerators**

Triboelectric nanogenerator (TENG) was first invented by Wang's group in 2012 for converting randomly distributed, irregular, and wasted low-frequency energy into electric power.[1,2] TENG relies on the coupling effect of contact-electrification and electrostatic induction that converts low-amplitude mechanical energy into electric power.[3] Different from the traditional electromagnetic generator, TENG is a field that uses Maxwell's displacement current as the driving force for effectively converting mechanical energy into electric power/signal. According to SCI data base, there are more than 8400 authors distributed across 62 countries and regions, who are engaged in TENG research. TENG is a field of focus of research that is truly multidisciplinary and across field, with application in wearable electronics, medical science, security, environmental science, infrastructure monitoring, robotics and internet of things.

TENG has four basic working modes: the contact-separation mode, lateral sliding mode, single-electrode mode, and free-standing mode (see Fig. 1) [4,5]. TENG has a broad application as micro-nano power source, self-powered sensors, blue energy and high voltage sources, covering area from medical science, wearable electronics, flexible electronics, security, human-machine interfaces and even environmental science [6-12]. Let us take the contact-separation mode TENG shown in Fig. 1a as an example. Under the mechanical pull-press force acting in vertical direction, the two dielectric layers are periodically contacted and separated. The two surfaces have opposite electrostatic charges owing to contact electrification effect. A change in spatial distribution of the media, surface electrostatic charge density, as well as the distance between the two electrodes, results in a variation of electric field in space, which is a form of displacement current that generates an output conduction current across the load connected between the two electrodes. As a general case, the media boundaries here do vary with time, and we need to derive the Maxwell's equations for moving charged media.

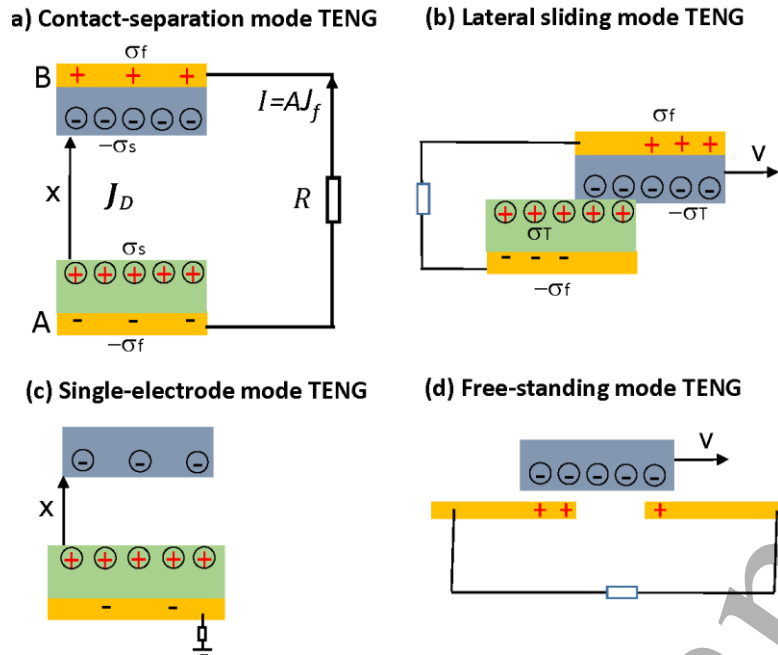


Figure 1. Schematics showing the four modes of triboelectric nanogenerators based on coupling effect of triboelectrification and electrostatic induction, for effectively harvesting high entropy energy in our living environment.

### Theory of triboelectric nanogenerators

The driving force for the TENG is the Maxwell's displacement current, which is caused by a time variation of electric field plus a media polarization term. In the case of TENGs, triboelectric charges are produced on surfaces simply due to CE between two different materials. To account for the contribution made by the contact electrification induced electrostatic charges in the Maxwell's equations, an additional term  $\mathbf{P}_s$ , called mechano-driven produced polarization, is added in displacement vector  $\mathbf{D}$  by Wang in 2017 [13], that is:

$$\mathbf{D} = \varepsilon_0 \mathbf{E} + \mathbf{P} + \mathbf{P}_s \quad (1)$$

Here, the first term polarization vector  $\mathbf{P}$  is due to the existence of an external electric field, and the added term  $\mathbf{P}_s$  is mainly due to the existence of the surface charges that are independent of the presence of electric field and the relative movement of the media. Substituting Eq. (1) into Maxwell's equations, and define

$$\mathbf{D}' = \varepsilon_0 \mathbf{E} + \mathbf{P} \quad (2)$$

The reformulated Maxwell's equations are [14]:

$$\nabla \cdot \mathbf{D}' = \rho_f - \nabla \cdot \mathbf{P}_s \quad (3.1)$$

$$\nabla \cdot \mathbf{B} = 0 \quad (3.2)$$

$$\nabla \times \mathbf{E} = -\frac{\partial \mathbf{B}}{\partial t} \quad (3.3)$$

$$\nabla \times \mathbf{H} = \mathbf{J} + \frac{\partial \mathbf{P}_s}{\partial t} + \frac{\partial \mathbf{D}'}{\partial t} \quad (3.4)$$

In Eq. (3.4),  $\frac{\partial \mathbf{D}'}{\partial t}$  represents the displacement current due to time variation electric field and the electric field induced medium polarization. The second term  $\frac{\partial \mathbf{P}_s}{\partial t}$  is the displacement current due to non-electric field but owing to external strain field. The first term is dominant at high frequency for wireless communication, while the second term is the low frequency or quasi-static term that is responsible for the energy generation (Fig. 2). The term that contributes to the output current of TENG is related to the driving force of  $\frac{\partial \mathbf{P}_s}{\partial t}$ , which is simply named as the *Wang term* in the displacement current. In general cases, the two terms are approximately decoupled and can be treated independently. However, if the external triggering frequency is rather high, so that the two terms  $\frac{\partial \mathbf{D}'}{\partial t}$  and  $\frac{\partial \mathbf{P}_s}{\partial t}$  can be effectively coupled, the interference between the two term can be significant, but such case may occur in MHz - GHz range.

The conventional Maxwell's equations are for media whose boundaries and volumes are fixed and at stationary. But for cases that involve moving media and time-dependent configuration, such as the case in TENG, the equations have to be expanded. Starting from the integral forms of the four physics laws, Wang has derived the expanded Maxwell's equations in differential form by assuming that the medium is moving as a rigid translation object with acceleration. If the relativistic effect is ignored, the Maxwell's equation for a mechano-driven slow-moving media system is given by [15]:

$$\nabla \cdot \mathbf{D}' = \rho_f - \nabla \cdot \mathbf{P}_s \quad (4a)$$

$$\nabla \cdot \mathbf{B} = 0 \quad (4b)$$

$$\nabla \times (\mathbf{E} - \mathbf{v} \times \mathbf{B}) = -\frac{\partial \mathbf{B}}{\partial t} \quad (4c)$$

$$\nabla \times [\mathbf{H} + \mathbf{v} \times (\mathbf{D}' + \mathbf{P}_s)] = \mathbf{J}_f + \rho_f \mathbf{v} + \frac{\partial \mathbf{P}_s}{\partial t} + \frac{\partial \mathbf{D}'}{\partial t} \quad (4d)$$

These equations are most useful for describing the electromagnetic behaviour of moving media with acceleration. expanded equations are the most comprehensive governing equations including both electromagnetic interaction and power generation as well as their coupling.

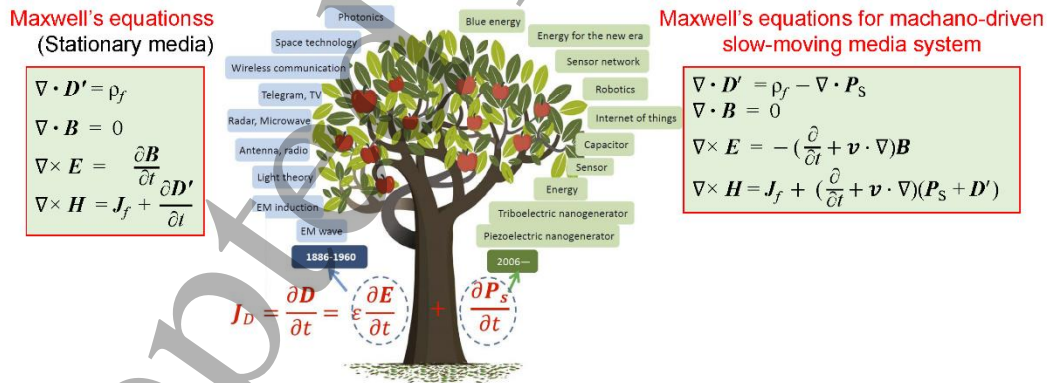


Figure 2. The conventional Maxwell's equations are for media whose boundaries and volumes are fixed and stationary. The Maxwell's equations for a mechano-driven slow-moving media system are further developed with including the polarization density term  $\mathbf{P}_s$  in displacement vector. These equations apply to media that moves with an acceleration in non-inertia frame of references.

### Materials for Triboelectric nanogenerators

Since triboelectrification is a universal effect that applies to almost all materials and their related phases [16-17]. The choice of materials for TENG is rather wide and unrestricted. In such a case, one can choose materials that fit the work environment the best, such as polymers, biodegradable materials, cellular

1  
2  
3 materials etc. In general, choices of materials need to satisfy four requirements. First, rational design of  
4 the materials surface is important. We found that a flat surface may not give the highest TENG output  
5 because the contact between two flat surface may not reach atomic level, especially with the presence  
6 of some surface micro-size dust particles. A too rough surface will reduce the effective contact area at  
7 the atomic level. Therefore, an optimization has to be carried out to maximize the 3D contact of the two  
8 surfaces, especially at atomic level contact, at which the charge transfer occurs. Secondly, from our  
9 theoretical analysis, the displacement current is related to materials permittivity so is the output  
10 voltage. A high  $k$  material would result in stronger electrostatic screening, which may reduce the output  
11 power. A low  $k$  material may not retain the required mechanical strength for the operation of the  
12 device.  
13  
14

15  
16 Thirdly, the surface charge density is the most important factor that governs the output power, because  
17 the output power is proportional to the square of the surface charge density. In general, each material  
18 has its own upper limit for holding the charges, which in most of the cases is limited by the strength of  
19 discharge in air. A great effort has been made to develop methodologies for enhancing the charge  
20 density on surfaces, including surface texturation [18] charge injection, oblique nanostructure  
21 construction [19], and charge transportation and storage along dielectric material [20] The surface  
22 charge density is normally limited by the breakdown voltage of a surface, so that it is normally in the  
23 order of  $\sim 250 \mu\text{C m}^{-2}$ . Recently, a new strategy by binding charges in floating conductive layers is  
24 developed, and the bound charges are generated using a charge pump design that can be a normal  
25 TENG [21-22]. The effective charge density can be greatly boosted to  $1.02 \text{ mC m}^{-2}$  in ambient conditions.  
26 Improved design of the pumping idea has further increased the charge density up to  $2.38 \text{ mC m}^{-2}$  based  
27 on optimization of contact status [23].  
28  
29

30  
31 Lastly, a key challenge is to reduce the wearing of materials and enhancing the durability of TENG. With  
32 considering the facts that the tribo-charges would remain on insulator surfaces for hours at  
33 conventional condition, a continuous rubbing between the two surfaces is unnecessary. Therefore, by a  
34 mechanical designing that allows the TENG to automatically switch between two modes depending on  
35 the rotation speed/frequency, the durability can be extensively extended [24-25]. The second approach  
36 is to amplifying the operation frequency by structure design. The triggering energy from water wave can  
37 be stored as potential energy using a pendulum structure, so that an extended oscillation at a high  
38 frequency can largely enhance the energy conversion efficiency [26]. Such design has been extended for  
39 harvesting water wave energy, and an energy conversion efficiency over 28% has been achieved [27].  
40 Lastly, by choosing an oil that has the smallest dielectric permittivity, such as squalene and paraffin oil,  
41 the performance of the lateral-sliding mode TENG is largely preserved and even improved. The  
42 lubricated TENG is able to give an output power that is 10 times of that of the unlubricated TENG [28].  
43 This study opens a new approach for extending the lifetime and stability of TENGs.  
44  
45  
46  
47  
48  
49  
50  
51  
52  
53  
54  
55  
56  
57  
58  
59  
60

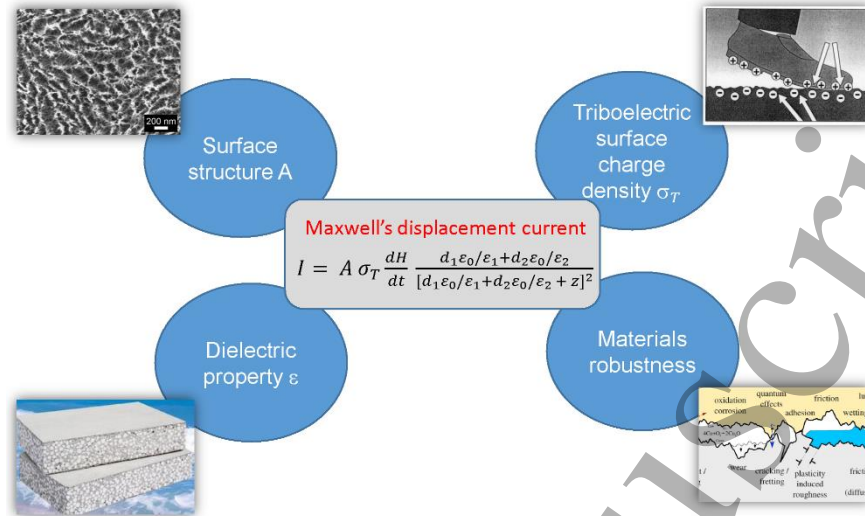


Figure 3. The choice of materials for TENG and the basic challenges in order to maximize its output power.

## References

- <sup>1</sup> F. R. Fan, Z. Q. Tian, Z. L. Wang, *Nano Energy* **2012**, *1*, 328.
- <sup>2</sup> Z.L. Wang "From contact electrification to triboelectric nanogenerators" (Review), *Report on Progress in Physics*, **84** (2021) 096502; <https://doi.org/10.1088/1361-6633/ac0a50>
- <sup>3</sup> Z. L. Wang, L. Lin, J. Chen. S.M. Niu, Y.L. Zi, *Triboelectric Nanogenerators*, Springer, Switzerland, 2016.
- <sup>4</sup> F. Fan, Z. Tian and Z. L. Wang, Flexible triboelectric generator, *Nano Energy* **1**, 328, (2012).
- <sup>5</sup> Z.L. Wang, From contact electrification to triboelectric nanogenerators, *Report on Progress in Physics*, **84**, 096502(2021)
- <sup>6</sup> R. Hinchet, H. Yoon, H. Ryu, M. Kim, E. Choi, D. Kim, S. Kim, Transcutaneous ultrasound energy harvesting using capacitive triboelectric technology, *Science*, **365**, 491, (2019).
- <sup>7</sup> Y. Wang, W. Gong, Q. Zhang, H. Wang, J. Brugger, All-fiber hybrid piezoelectric-enhanced triboelectric nanogenerator for wearable gesture monitoring, *Nano Energy*, **48**, 152, (2018).
- <sup>8</sup> Z. L. Wang, New wave power, *Nature* **542**, 159, (2017).
- <sup>9</sup> Y. Choi, Q. Jing, A. Datta, C. Boughey and S. Kar-Narayan, A triboelectric generator based on self-poled Nylon-11 nanowires fabricated by gas-flow assisted template wetting, *Energy Environ. Sci.* **10**, 2180, (2017).
- <sup>10</sup> W. Xu, H. Zheng, Y. Liu, X. Zhou, C. Zhang, Y. Song, X. Deng, M. Leung, Z. Yang, R. X. Xu, Z. L. Wang, X. Zeng, Z. Wang, A droplet-based electricity generator with high instantaneous power density, *Nature* **578**, 392, (2020).



- 1  
2  
3  
4  
5  
6  
7  
8  
9  
10  
11  
12  
13  
14  
15  
16  
17  
18  
19  
20  
21  
22  
23  
24  
25  
26  
27  
28  
29  
30  
31  
32  
33  
34  
35  
36  
37  
38  
39  
40  
41  
42  
43  
44  
45  
46  
47  
48  
49  
50  
51  
52  
53  
54  
55  
56  
57  
58  
59  
60
- <sup>11</sup> Z. L. Wang, Triboelectric Nanogenerators as New Energy Technology for Self-Powered Systems and as Active Mechanical and Chemical Sensors, *ACS Nano* **7**, 9533, (2013).
- <sup>12</sup> Z. L. Wang, J. Chen, L. Lin, Progress in triboelectric nanogenerators as new energy technology and self-powered sensors, *Energy Environ. Sci.* **8**, 2250, (2015).
- <sup>13</sup> Z. L. Wang, *Mater. Today* **2017**, *20*, 74.
- <sup>14</sup> Z.L. Wang, "On the first principle theory of nanaogenerators from Maxwell's equations", *Nano Energy*, **68** (2020) 104272
- <sup>15</sup> Zhong Lin Wang " On the expanded Maxwell's equations for moving charged media system – general theory, mathematical solutions and applications in TENG", *Materials Today*, 52 (2022) 348-363
- <sup>16</sup> Z.L. Wang and A.C. Wang "On the origin of contact electrification", *Materials Today*, **30** (2019) 34-51
- <sup>17</sup> S. Lin, X. Chen and Z.L. Wang "Contact-electrification at liquid-solid interface", *Chemical Review*, **122** (2022) 5209-5232
- <sup>18</sup> Y. Zheng, L. Cheng, M. Yuan, Z. Wang, L. Zhang, Y. Qin, T. Jing, An electrospun nanowire-based triboelectric nanogenerator and its application in a fully self-powered UV detector, *Nanoscale*, **6** (2014) 7842-7846.
- <sup>19</sup> L. Zhang, C. Su, L. Cheng, N. Cui, L. Gu, Y. Qin, R. Yang, F. Zhou, Enhancing the performance of textile triboelectric nanogenerators with oblique microrod arrays for wearable energy harvesting, *ACS Appl. Mater. Interfaces*, **11** (2019) 26824-26829.
- <sup>20</sup> N. Cui, J. Liu, Y. Lei, L. Gu, Q. Xu, S. Liu, Y. Qin, High-performance triboelectric nanogenerator with a rationally designed friction layer structure, *ACS Appl. Energy Mater.*, **1** (2018) 2891-2897.
- <sup>21</sup> L. Xu, T.Z. Bu, X.D. Yang, C. Zhang, Z.L. Wang, Ultrahigh charge density realized by charge pumping at ambient conditions for triboelectric nanogenerators, *Nano Energy*, **49** (2018) 625-633.
- <sup>22</sup> L. Cheng, Q. Xu, Y. Zheng, X. Jia, Y. Qin, A self-improving triboelectric nanogenerator with improved charge density and increased charge accumulation speed, *Nat. Commun.*, **9** (2018) 1-8.
- <sup>23</sup> W. Liu, Z. Wang, G. Wang, G. Liu, J. Chen, X. Pu, Y. Xi, X. Wang, H. Guo, C. Hu, Integrated charge excitation triboelectric nanogenerator, *Nat. Commun.*, **10** (2019) 1-9.
- <sup>24</sup> S. Li, S. Wang, Y. Zi, Z. Wen, L. Lin, G. Zhang, Z.L. Wang, Largely improving the robustness and lifetime of triboelectric nanogenerators through automatic transition between contact and noncontact working states, *ACS Nano*, **9** (2015) 7479-7487.
- <sup>25</sup> Z. Lin, B. Zhang, H. Zou, Z. Wu, H. Guo, Y. Zhang, J. Yang, Z.L. Wang, Rationally designed rotation triboelectric nanogenerators with much extended lifetime and durability, *Nano Energy*, **68** (2020) 104378.

1  
2  
3 <sup>26</sup> Z. Lin, B. Zhang, H. Guo, Z. Wu, H. Zou, J. Yang, Z.L. Wang, Super-robust and frequency-multiplied  
4 triboelectric nanogenerator for efficient harvesting water and wind energy, *Nano Energy*, 64 (2019)  
5 103908.  
6

7  
8 <sup>27</sup> T. Jiang, H. Pang, J. An, P. Lu, Y. Feng, X. Liang, W. Zhong, Z.L. Wang, Robust Swing-Structured  
9 Triboelectric Nanogenerator for Efficient Blue Energy Harvesting, *Adv. Energy Mater.*, 10 (2020)  
10 2000064.  
11

12 <sup>28</sup> J. Wu, Y. Xi, Y. Shi, Toward wear-resistive, highly durable and high performance triboelectric  
13 nanogenerator through interface liquid lubrication, *Nano Energy*, 72 (2020) 104659.  
14  
15

## 16 **4.2 Synthetic polymers for triboelectric energy harvesting**

17 Xiong Pu and Caofeng Pan

18 Beijing Institute of Nanoenergy and Nanosystems, Chinese Academy of Sciences  
19  
20

### 21 **Status**

22 Synthetic polymers play a crucial role in triboelectric nanogenerators (TENG). A TENG typically contains  
23 triboelectrification materials and electrode materials. Polymers could be designed to fulfill either of the  
24 two functions. Dielectric or insulating polymers are the most utilized triboelectrification materials, as the  
25 electrostatic charges could not be easily dissipated on their surfaces. Semiconducting polymers has  
26 recently been found to generate triboelectric energy through a tribovoltaic effect, different from the  
27 electrostatic induction effect for insulating polymers.[1] Sliding motions were found to excite electron-  
28 hole pairs at the interfaces of the semiconductors, in analogous to the photovoltaic effect. Conducting  
29 polymers, either electronic conductors or ionic conductors, can be applied as the electrode materials of  
30 the TENG. All-polymer or all-polymer-composite TENGs have been reported. Therefore, it is easily  
31 understood that the properties of the polymers can significantly affect the performances and  
32 functionalities of the TENG. Current research on the TENG, from the perspective of polymer materials,  
33 has two trends. On the one hand, investigations are carried out to improve the electrical outputs of the  
34 TENG by optimizing the polymer materials. The output voltage and power of a TENG are typically positively  
35 proportional to the static charge quantities maintained on the surface of the electrification polymers.  
36 Materials engineering is then the core concern to boost the output. On the other hand, attention is also  
37 paid to enriching the functionalities of the TENG through polymer designs. Many functions can be  
38 obtained by appropriately design the structures of the polymers involved in a TENG device, such as  
39 stretchability, wearability, transparency, self-healing capability, biocompatibility, and biodegradability.  
40  
41  
42  
43

### 44 **Current and Future Challenges**

45 The core challenge of the TENG is to achieve high electrical power output. Therefore, it is of prime  
46 importance to increase the electrostatic charge quantities on the surface of electrification polymers. It is  
47 recently demonstrated that electron transfer between two different polymers account for the contact  
48 electrification effect due to the difference in their work functions.[2] This charge transfer process leads to  
49 either positively or negatively charged surfaces. The larger difference of the two materials in the  
50 triboelectric series table leads to the possibly higher electrostatic charge quantities. However, this  
51 empirical rule does not provide reliable quantitative guidance for the TENG designs, and fundamental  
52 understanding on the relationship between the polymer structures and electrification properties remains  
53 challenging. Furthermore, the TENG output could also be determined by the air breakdown limit and the  
54 dielectric breakdown limit. The former one is the reason why the TENG is seriously degraded under humid  
55  
56  
57  
58  
59  
60

environment, as the high humidity lowers the air breakdown limit and accelerates the dissipation of electrostatic charges; the latter one could attribute to the dilemma in electrification layer design, that improving the dielectric constant is beneficial for the higher TENG output but it also lowers dielectric breakdown limit. Therefore, hydrophobic polymer materials could be considered to alleviate the effect of humidity, or the suitable waterproof package should be designed, which is very important for TENGs applied for the water wave energy harvesting. Another challenge is the wearing resistance of the polymers especially for the sliding-mode TENGs, though the contact-separation-mode TENGs have been demonstrated to be viable for long term durability. As for functional polymer materials for TENGs, such as stretchable and self-healable polymers, the durability and scalable fabrication are yet to be demonstrated.

### **Advances in Science and Technology to Meet Challenges**

Progress in the following aspects are mainly needed to address these challenges. First, fundamental studies are conducted to understand the mechanism of electrification processes at the solid-solid, solid-liquid and even solid-gas interfaces.[3] Meantime, the origin of the electricity generation has also been systematically investigated, finding that the output current is due to the Maxwell's displacement current, i.e. the time-varying electric field of surface charges.[4] These efforts on fundamental understandings are crucial for future materials or devices optimizations. Second, quantitative descriptions of the relationship between materials/structures and the electrical outputs have been systematically studied. The figure of merit of a TENG has been proposed.[5] The electrification properties of a large number of polymer materials have been studied, trying to quantitatively establish the triboelectric series.[6] Fundamental studies have also been performed to correlate the polymer structures with the electrification behaviors.[7] Third, a series of different strategies have been attempted to improve the output performances. In order to increase the surface charge quantities, the electrification polymers can be chemically modified with desired functional groups to tune the electrification capabilities; the surface can be patterned with morphology at different scales to increase the effective electrification areas; inorganic fillers with high dielectric constant were added to polymer-based composite to enhance the outputs; approaches were proposed to pre-charge the polymer surface with static charges, such as corona discharging method; excitation circuits were designed to boost the surface charge quantities.[8] Considering the importance of the surface charge quantity, the output performances can simply be evaluated or compared based on it. The reported state-of-art surface charge density reaches  $\sim 8.8$  mC/m<sup>2</sup>. [9] Other than these progresses, intensive studies have also been conducted to enrich the functionalities of the TENG through polymer materials innovation. Polymeric ionic hydrogels were designed as either electrode or even electrification materials for fulfill multifunctionalities, such as stretchability, self-healing capability and transparency.[10] Biodegradable or bioabsorbable polymers were designed and fabricated for realizing implantable energy harvesters. Through polymer materials engineering, the TENGs can be designed into fibers, yarns, thin films, fabrics, bracelets, eyeglass frames, swimsuits, socks, shoes, 3D printed objects, and so on. The demonstrated versatility of the TENGs ensures the great potential applications in a variety of areas.

### **Concluding Remarks**

In summary, a variety of polymer materials could play important roles in triboelectric energy harvesting. Not only improvement in output performance but also enrichment in the functionalities can be achieved through polymer materials engineering. The TENG research field is attracting increasing attention worldwide, which makes this field a hotspot and promotes fast progresses. In particular, more polymer specialists are contributing to this field. As the challenges and opportunities are getting better understood, breakthroughs in practical applications are optimistically anticipated in the near future.

## Acknowledgements

This work was supported by the National Key R&D Project from the Minister of Science and Technology (2021YFA1201603).

## References

- [1] J. Meng, Z. H. Guo, C. Pan, L. Wang, C. Chang, L. Li, X. Pu, and Z. L. Wang, "Flexible Textile Direct-Current Generator Based on the Tribovoltaic Effect at Dynamic Metal-Semiconducting Polymer Interfaces," *ACS Energy Letters*, vol. 6, no. 7, pp. 2442-2450, 2021.
- [2] C. Xu, Y. Zi, A. C. Wang, H. Zou, Y. Dai, X. He, P. Wang, Y.-C. Wang, P. Feng, D. Li, and Z. L. Wang, "On the Electron-Transfer Mechanism in the Contact-Electrification Effect," *Advanced Materials*, vol. 30, no. 15, p. 1706790, 2018.
- [3] Z. L. Wang and A. C. Wang, "On the origin of contact-electrification," *Materials Today*, vol. 30, pp. 34-51, 2019.
- [4] Z. L. Wang, "On Maxwell's displacement current for energy and sensors: the origin of nanogenerators," *Materials Today*, vol. 20, no. 2, pp. 74-82, 2017.
- [5] Y. Zi, S. Niu, J. Wang, Z. Wen, W. Tang, and Z. L. Wang, "Standards and figure-of-merits for quantifying the performance of triboelectric nanogenerators," *Nature communications*, vol. 6, no. 1, p. 8376, 2015.
- [6] H. Zou, Y. Zhang, L. Guo, P. Wang, X. He, G. Dai, H. Zheng, C. Chen, A. C. Wang, C. Xu, and Z. L. Wang, "Quantifying the triboelectric series," *Nature communications*, vol. 10, no. 1, p. 1427, 2019.
- [7] X. Zhang, L. Chen, Y. Jiang, W. Lim, and S. Soh, "Rationalizing the Triboelectric Series of Polymers," *Chemistry of Materials*, vol. 31, no. 5, pp. 1473-1478, 2019.
- [8] W. Liu, Z. Wang, G. Wang, G. Liu, J. Chen, X. Pu, Y. Xi, X. Wang, H. Guo, C. Hu, and Z. L. Wang, "Integrated charge excitation triboelectric nanogenerator," *Nature communications*, vol. 10, no. 1, p. 1426, 2019.
- [9] Z. Zhao, L. Zhou, S. Li, D. Liu, Y. Li, Y. Gao, Y. Liu, Y. Dai, J. Wang, and Z. L. Wang, "Selection rules of triboelectric materials for direct-current triboelectric nanogenerator," *Nature communications*, vol. 12, no. 1, p. 4686, 2021.
- [10] X. Pu, M. Liu, X. Chen, J. Sun, C. Du, Y. Zhang, J. Zhai, W. Hu, and Z. L. Wang, "Ultrastretchable, transparent triboelectric nanogenerator as electronic skin for biomechanical energy harvesting and tactile sensing," *Science Advances*, vol. 3, no. 5, p. e1700015, 2017.

## 4.3 Nanocomposites for triboelectric energy harvesting

Renyun Zhang

Department of Natural Sciences, Mid Sweden University

### Status

Traditional dielectric materials such as polymers have well-known mechanical and dielectric properties. These well-known properties allow us to study the mechanisms behind triboelectrification and apply them in triboelectric nanogenerators (TEGs) [1]. These properties are commonly found with pure polymer materials, and theoretical explanations could be developed due to the simplicity of the composition. These properties become more complicated if the pure polymers are composited with other materials, such as nanoparticles and nanowires. Despite the complex properties, nanocomposites bring new opportunities for studies of TEGs because they enable tuning of the properties, such as dielectric constant, surface roughness, mechanical strength, conductivity, flexibility, and transparency.

The reasons why nanocomposite materials are so important for TENGs can be explained with the theoretical model for the output current density [2]. The equation for current density can be divided into three parts [3] (Figure 1).  $P_1$  is the triboelectric charge on the surface that represents the charge affinity of a dielectric material. By forming a nanocomposite, the charge affinity can be changed so that more charges are transported during triboelectrification [4].  $P_2$  is related to operational aspects of TENGs, such as force, frequency, and speed. The mechanical properties of the triboelectric materials can have a great impact on operation of the TENG. By compositing with other materials, the mechanical strength, flexibility and friction constant of the dielectric material can be tuned [5].  $P_3$  is the electrostatic induction that decides directly how much induction charge can be created on the back electrode. The dielectric constant of the materials plays an important role here [6], and this is also a challenge for future studies.

Nanocomposites that have been studied in TENGs have inorganic–organic (I–O), inorganic–inorganic (I–I), and organic–organic (O–O) compositions [7]. The I–O type of nanocomposites are mainly studied because the inorganic and organic parts of the composites have different properties that establish new properties in the nanocomposites and therefore enhance the output of the TENG. The output power densities of nanocomposites constituting TENGs are lower than those of pure polymeric materials, partly due to the emphases put on other advances, such as flexibility and durability. However, as our understanding of the properties of nanocomposites increases, higher output power densities are expected.

$$J_D \approx \underbrace{\left[ \sigma_T \right]}_{(P_1)} \underbrace{\left[ \frac{dH}{dt} \right]}_{(P_2) \text{ Device}} \underbrace{\left[ \frac{d_1 \epsilon_0 / \epsilon_1 + d_2 \epsilon_0 / \epsilon_2}{(d_1 \epsilon_0 / \epsilon_1 + d_2 \epsilon_0 / \epsilon_2 + z)^2} \right]}_{(P_3)}$$

Triboelectric effect      Electrostatic induction

**Figure 1.** Deconstructed current density showing the three parts of the triboelectric effect; ( $P_1$ ), device ( $P_2$ ), and electrostatic induction ( $P_3$ ). Reproduced from ref [3] under CC BY 4.0

### Current and Future Challenges

The challenges remaining for application of nanocomposites for triboelectric energy harvesting involve development of theories and fabrication of nanocomposite materials with desired triboelectric properties.

The challenge in developing theoretical models has two aspects: one is the understanding of charge transport during a triboelectrification process, and the other is the understanding of how the properties of a dielectric material change after it is composited with a nanomaterial. Current models built to explain charge transport were designed for materials with known band structures or orbitals that make electron transfer predictable. However, the complex chemical and physical compositions of nanocomposites make the band structures and orbitals difficult to define, especially when organic dielectric materials are composited with inorganic nanomaterials. Regarding the second challenge, it seems that there is no good theoretical model comparable to the empirical models derived from experiments for predicting the dielectric properties of nanocomposites. The theoretical models [8] most typically applied are used to simulate the dielectric constant of the nanocomposite, including the series mixing model and Lichtnecker



logarithmic model. However, these models still generate errors in predicting the dielectric constants of nanocomposites. Figure 2 shows the  $P_3$  value of a TENG using nanocomposites as triboelectric materials. As the figure shows, the two plotted models exhibit similar trends, but the  $P_3$  values could be significantly different. That said, better models are needed to enable more accurate predictions.

The challenge that remains for fabrication of nanocomposites with excellent triboelectric effects is in designing systematic experiments. Many studies have successfully produced nanocomposites for use in TENGs. However, in most cases, one type of nanocomposite is made, despite the ratios of compositing parts being tuned. Such studies are successful but contribute relatively little to development of the theoretical models discussed above. On the other hand, a more systematic study demands more financial and human resources.

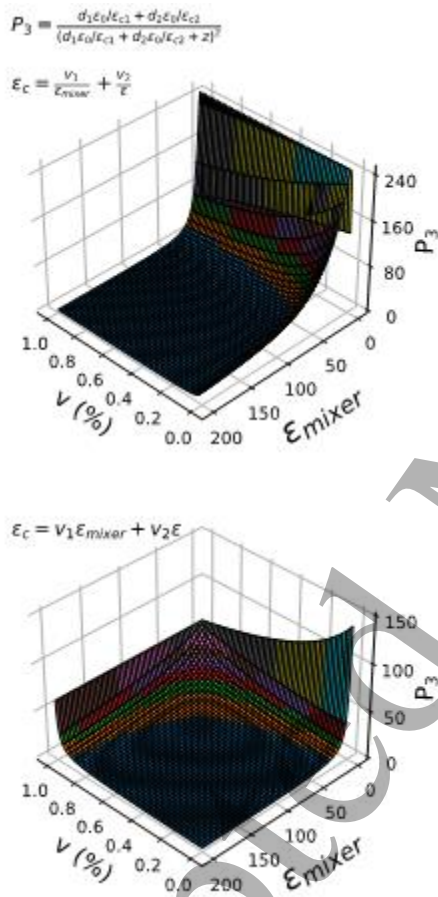


**Figure 2.** Simulated  $P_3$  values based on the series mixing model (top) and the simplified model (bottom).  $v_1$  and  $v_2$  are the volume fractions of the components in a nanocomposite, and  $v_1 + v_2 = 1$ . The thicknesses of the dielectric materials,  $d_1$  and  $d_2$ , were set at 0.1 mm, and the distance,  $z$ , between the triboelectric surfaces was set at 1 mm.

### Advances in Science and Technology to Meet Challenges

Current nanocomposites studied for use in TENGs are usually prepared by physically mixing the components. This procedure creates only physical contact between the components. A more advanced way is to create bonds between the components with or without linkages. Chemically, it is not very difficult to create such bonds, since many types of nanocomposites have been made from inorganic–inorganic, inorganic–organic, and organic–organic combinations. The question is whether the resulting



nanocomposites could be processed further to develop good mechanical properties for use in TENGs. A benefit of this strategy is that the properties of the nanocomposite become more predictable. Moreover, quantum chemical theories can be applied to simulate or calculate molecular properties, such as the highest occupied molecular orbital (HOMO) and the lowest unoccupied molecular orbital (LUMO) [9]. The success of this strategy would contribute to our understanding of triboelectrification because one could design a nanocomposite, simulate its properties, and compare them with results from instrumental characterisations.

Modern characterisation techniques, such as Kelvin probe force microscopy (KPFM) [10], could allow us to understand the triboelectric properties of the nanocomposites. KPFM could provide information about the local dielectric properties of nanocomposites that would indicate how triboelectric charges are generated and distributed. Such information would lead to syntheses of nanocomposites with strong triboelectric effects.

### Concluding Remarks

Nanocomposite dielectric materials offer new opportunities to understand the fundamentals of triboelectrification and develop high-performance TENGs for energy harvesting and self-powered sensing. Unlike pure engineering polymers that have limited ranges in which to tune the chemical composition, the methods for making nanocomposites allow researchers to design structures both chemically and physically. The outcomes of experimental studies will supply evidence needed to develop advanced theories and models. This will help to explain the mechanisms of triboelectrification and support the design of new nanocomposites for TENGs exhibiting higher performance. To achieve such goals, there is a need for input from research areas other than material science and engineering, including chemical synthesis, quantum chemistry and electronics.

### Acknowledgements

We appreciate financial support from the Promobilia Stiftelsen and the Swedish Knowledge Foundation.

### References

- [1] Z. L. Wang and A. C. Wang, "On the origin of contact-electrification," *Mater. Today*, vol. 30, pp. 34–51, Nov. 2019, doi: 10.1016/j.mattod.2019.05.016.
- [2] Z. L. Wang, "On Maxwell's displacement current for energy and sensors: the origin of nanogenerators," *Mater. Today*, vol. 20, no. 2, pp. 74–82, 2017, doi: 10.1016/j.mattod.2016.12.001.
- [3] R. Zhang and H. Olin, "Material choices for triboelectric nanogenerators: A critical review," *EcoMat*, vol. 2, no. 4, p. eom2.12062, Dec. 2020, doi: 10.1002/eom2.12062.
- [4] N. Soin *et al.*, "High performance triboelectric nanogenerators based on phase-inversion piezoelectric membranes of poly(vinylidene fluoride)-zinc stannate (PVDF-ZnSnO<sub>3</sub>) and polyamide-6 (PA6)," *Nano Energy*, vol. 30, no. October, pp. 470–480, 2016, doi: 10.1016/j.nanoen.2016.10.040.
- [5] J. S. Im and I. K. Park, "Mechanically Robust Magnetic Fe<sub>3</sub>O<sub>4</sub> Nanoparticle/Polyvinylidene Fluoride Composite Nanofiber and Its Application in a Triboelectric Nanogenerator," *ACS Appl. Mater. Interfaces*, vol. 10, no. 30, pp. 25660–25665, 2018, doi: 10.1021/acsami.8b07621.
- [6] Z. Zheng, D. Yu, and Y. Guo, "Dielectric Modulated Glass Fiber Fabric-Based Single Electrode Triboelectric Nanogenerator for Efficient Biomechanical Energy Harvesting," *Adv. Funct. Mater.*, vol. 31, no. 32, p. 2102431, Aug. 2021, doi: 10.1002/adfm.202102431.

- [7] R. Zhang, J. Örtengren, M. Hummelgård, M. Olsen, H. Andersson, and H. Olin, "A review of the advances in composites/nanocomposites for triboelectric nanogenerators," *Nanotechnology*, vol. 33, no. 21, p. 212003, May 2022, doi: 10.1088/1361-6528/ac4b7b.
- [8] X. Kang *et al.*, "Boosting performances of triboelectric nanogenerators by optimizing dielectric properties and thickness of electrification layer," *RSC Adv.*, vol. 10, no. 30, pp. 17752–17759, 2020, doi: 10.1039/d0ra02181d.
- [9] M. Meunier and N. Quirke, "Molecular modeling of electron trapping in polymer insulators," *J. Chem. Phys.*, vol. 113, no. 1, pp. 369–376, Jul. 2000, doi: 10.1063/1.481802.
- [10] N. Balke, P. Maksymovych, S. Jesse, I. I. Kravchenko, Q. Li, and S. V. Kalinin, "Exploring Local Electrostatic Effects with Scanning Probe Microscopy: Implications for Piezoresponse Force Microscopy and Triboelectricity," *ACS Nano*, vol. 8, no. 10, pp. 10229–10236, Oct. 2014, doi: 10.1021/nn505176a.

#### 4.4 Nanoparticles, Surface texturing and functionalization for triboelectric energy harvesting

Jing Xu, Xun Zhao, Yihao Zhou, Guorui Chen, Trinny Tat, Il Woo Ock and Jun Chen  
University of California, Los Angeles

##### Status

The performance of a TENG at the macroscale is determined by multifaceted interface properties and material properties at the nanoscale [1]. Therefore, nanoscale modifications that can manipulate the active interfacial area or electron transfer capacity of the materials are critical to ensuring high-performance TENGs [2,3]. Based on this, various physical, chemical, and hybrid strategies are proposed and developed substantially to engineer the tribo-materials at the nanoscale to improve the mechanical-to-electrical conversion of TENGs, as shown in Fig.1. Among them, *physical modifications* is the most widely adopted approach which includes two means: non-additive modifications and additive modifications. Non-additive physical modifications mainly refer to the morphology engineering of tribo-materials which can increase the effective contact area by introducing surface nanostructures and microstructures. Additive physical modifications can enhance the performance of TENGs by introducing extra nanomaterials to make dielectric composite contact layers for increasing the surface charge density and reducing the triboelectric loss. By using physical modifications, a relative voltage enhancement of >10 times can be realized, indicating that physical modifications are efficient strategies to increase the output performance of TENGs. Another efficient strategy to improve the performance of TENGs is *chemical modification*. Chemical modifications involve surface or bulk chemistry to tune the electron-donating or -accepting ability and thus increase the surface charge density. Basically, the most representative chemical modifications are functional chemical groups grafting and ion implanting [4]. Functional chemical groups with a higher possibility to accept or donate electrons can be grafted on the tribo-materials surfaces and change the surface charge density through self-assembled monolayers, wet chemical reaction, etc. [5] In

1  
2  
3 addition, ion implantation can also effectively manipulate the surface charge density through direct ion  
4 injection or ion doping. [6] In this way, chemical modifications yield significant enhancement for both  
5 output current and voltage of TENGs and maintain the desired performance for a long time, thereby  
6 expanding the available material choices in the triboelectric series to fabricate high-performance TENGs.  
7 Besides these, the modifications involving more than one approach belong to *hybrid modifications*, which  
8 can combine the merits of different modification approaches and therefore can demonstrate a higher  
9 performance enhancement for TENGs.  
10

### 11 12 **Current and Future Challenges**

13 Even though efforts and developments have been made to enhance the output performance of TENGs by  
14 introducing modifications at the nanoscale, there are still challenges and opportunities in this research  
15 direction in the current stage. *Firstly*, for non-additive physical modifications, the correlation between the  
16 introduced surface nano/microstructure and output performance of TENGs is not fully understood.  
17 Although in previous studies, introducing nano/microstructures to tribo-materials surfaces is thought to  
18 be able to improve the performance of TENG by increasing the effective contact area, more analysis of  
19 different geometric sizes and shapes (i.e., zero-dimensional (0D) nanoparticles, 1D nanowires, 2D  
20 nanoflakes, and more complex 3D structures) should be performed to summarize a more universal  
21 strategy for TENG surface structure design. In addition, for additive physical modifications, the theories  
22 describing the enhancement effect of additives (e.g., nanoparticles, nanowires, nanoflakes) remain  
23 unverified. As summarized in some research, additives can increase the output performance of TENGs by  
24 tuning the dielectric constant, preventing triboelectric loss, forming micro-capacitors, etc. [5] However,  
25 the true functions of additives can be more complex than consideration since the enhancement effects of  
26 one additive may come from more than one aspect. *Secondly*, for chemical modifications, the durability  
27 still needs to be improved in the future. The surfaces treated by chemical modifications, including  
28 functional group grafting, ion injection, etc. are prone to lose efficacy during mechanical abrasions.  
29 Systematic studies on suitable operation modes and pre-prepared methods like post-packing may help to  
30 realize robust chemically modified TENGs. *Last but not least*, comprehensive criteria for TENGs  
31 performance evaluation have not been established yet which means it is still a challenge to directly  
32 compare modification approaches. Although various performance metrics, including output voltage,  
33 current, power density, etc. have been reported in TENG modification studies, more comprehensive and  
34 scientific evaluation criteria need to be introduced which may take materials selection, mechanical energy  
35 input, and other vital performance enhancement effects into consideration. These challenges coming with  
36 opportunities are worth exploring and will give valuable guidance to design efficient and robust TENGs  
37 with high performance in the future.  
38  
39  
40  
41

### 42 **Advances in Science and Technology to Meet Challenges**

43 Significant progress has been made through physical, chemical, and hybrid modification methods to  
44 enhance the output performance of TENGs. Challenges and opportunities coexist in this research direction  
45 which is favorable and promising in every TENG application from energy harvesting to biomedical therapy.  
46 Some perspectives can be proposed and discussed as follow to provide possible inspirations for future  
47 studies in this field:  
48

- 49 1. *Theoretical guidance*. Theories require further development in order to guide the design  
50 of new modification methods. At the current stage, the correlation of nano/microstructures with  
51 output performance, the enhancement effect of additive nanomaterials, and the fundamental  
52 physics of the charge transfer process in contact electrification are still not fully understood. More  
53 calculations and simulations are required to provide a better understanding of both working  
54 principles and modification methods for high-performance TENG design.  
55  
56  
57  
58  
59  
60

2.  
3. *New materials introduction.* At present, most of the studies focus on adding various modifications to polymer and metal since they are typical tribo-materials that display excellent triboelectric properties and are indispensable in TENG design. However, many possible tribo-materials, i.e., semiconductors, remain largely unexplored. It is expected to see the introduction of more materials and new modification methods to TENGs design in the future since it will be favorable for the development of multifunctional TENGs with expanded application fields.

3. *Modification method combinations.* Although many hybrid approaches have been demonstrated in previous research, there are still opportunities in this field. How to wisely choose suitable combinations of various modification approaches that can not only maximize the performance but also create multifunctional TENGs need further studies.

4. *Biotechniques and biomaterials.* With the rapid development of biotechniques and biomaterials, it will be excited to see their applications in TENG. For example, genetic engineering has shown its potential to tune the electron-donating ability of silk fibroin which may be helpful for tribo-materials modification. The development and exploration require the efforts of scientists across multidisciplinary fields.

5. *Evaluation criteria.* A unified and comprehensive assessment system of TENG modification approaches is urgently needed to evaluate their performance and give guidance to TENG design in the future.

### Concluding Remarks

Nanoscale modifications have been widely adopted to improve the performance of TENGs, with paramount importance to energy harvesting. Significant progress has been made through physical, chemical, and hybrid modification methods. Challenges and opportunities coexist in these research directions, including theoretical guidance, new materials introduction, modification methods combinations, biotechniques and biomaterials, and evaluation criteria. Therefore, more in-depth studies of nanoscale modifications for TENGs are desirable and need the synergetic efforts of researchers from different backgrounds such as materials science, chemistry, physics, and engineering. It is hoped that this article can help beginners get familiar with modification methods for TENG and provide possible inspiration for future studies in this field.

### Acknowledgements

The authors acknowledge the Henry Samueli School of Engineering & Applied Science and the Department of Bioengineering at the University of California, Los Angeles for the startup support.

### References

- [1] J. Chen, "Triboelectric Nanogenerators", Ph.D. Dissertation, Georgia Institute of Technology, Atlanta, GA, USA, 2016. Available online: <https://smartech.gatech.edu/handle/1853/54956> (accessed on 20 March 2022).
- [2] S.-H. Shin *et al.*, "Formation of triboelectric series via atomic-level surface functionalization for triboelectric energy harvesting", *ACS Nano*, vol. 11, pp. 6131–6138, 2017.
- [3] A. Ahmed *et al.*, "Toward high-performance triboelectric nanogenerators by engineering interfaces at the nanoscale: looking into the future research roadmap", *Adv. Mater. Technol.*, vol. 5, no. 11, pp. 2000520, 2020.
- [4] J. Xu, Y. Zou, A. Nashalian and J. Chen, "Leverage surface chemistry for high-performance triboelectric nanogenerators", *Front. Chem.*, vol. 8, pp. 577327, 2020.
- [5] Y. Zhou, W. Deng, J. Xu, and J. Chen, "Engineering materials at the nanoscale for triboelectric nanogenerators", *Cell Rep.Phys.Sci.*, vol. 1, no. 8, pp. 100142, 2020.

- [6] Z.-H. Lin *et al.*, "A selfpowered triboelectric nanosensor for mercury ion detection", *Angew. Chem. Int. Ed. Engl.*, vol. 52, pp. 5065–5069, 2013.

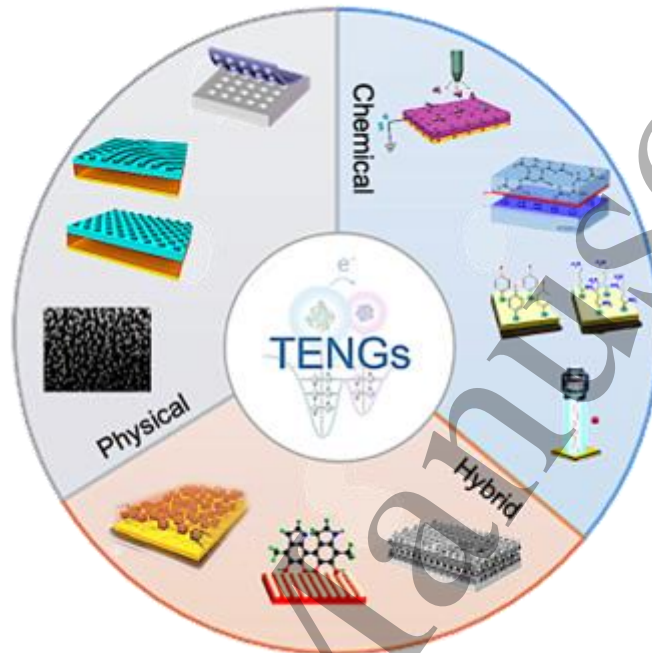


Figure 1. Outline of the current modification methods. Outline of the modification methods including physical, chemical, and hybrid approaches to enhance the performance of TENGs.

#### 4.5 Nature-inspired materials for triboelectric energy harvesting

Sontyana Adonijah Graham and Jae Su Yu

Department of Electronics and Information Convergence Engineering. Kyung Hee University. 1732 Deogyong-daero, Giheung-gu, Yongin-Si, Gyeonggi-do 17104, Republic of Korea

##### Status

Nature-inspired triboelectric materials (NITMs) are a potential candidate for the design of triboelectric energy harvesters (TEEHs) due to their distinguishing characteristics such as triboelectricity, piezoelectricity, biocompatibility, biodegradability, and non-toxicity. However, using synthetic triboelectric materials is difficult to create an eco-friendly environment because they are mostly derivatives of petroleum products/plastic induced components. Thus, they have mostly low degradation ability, high recycling difficulty, poor remodelling ability, and toxicity.[1] Zheng *et al.* first time reported a fully biodegradable TEEH, but this was fabricated using a synthetic polymer which is expensive and also may cause potential harm when implanted.[2] For this reason, the fabricated TEEHs using the NITMs could

efficiently reduce the cost and enhance biocompatibility and eco-friendliness. The NITMs have been proven to be applicable in various nanogenerator applications to energy harvesting, medical treatments, self-powered systems, etc.[3] The NITMs-based TEEHs/hybrid devices can produce high power density, making them applicable in an energy storage system to power electronic gadgets.[1] Generally, NITM can be classified into polysaccharides and proteins. The polysaccharides have a long chain of polymeric carbohydrates composed of monosaccharide units bound together by glycosidic linkages. They originate from various natural sources such as plants, algae, animals, bacteria, and fungal. Figure 1a shows various NITMs previously reported to be employed in the TEEH.[1, 3] The other sources of NITMs are proteins. Figure 1b shows various natural-inspired proteins used in the fabrication of TEEHs.[4] There are four different TEEH fabrication techniques while using naturally-derived bio-materials, which include electrospinning, 3D printing, inkjet printing, spray pyrolysis, and casting. Investigating the NITMs to make them sustainable and reliable in the TEEH technology could promote the next-generation electronics to rely on renewable energy and create eco-friendly surroundings.

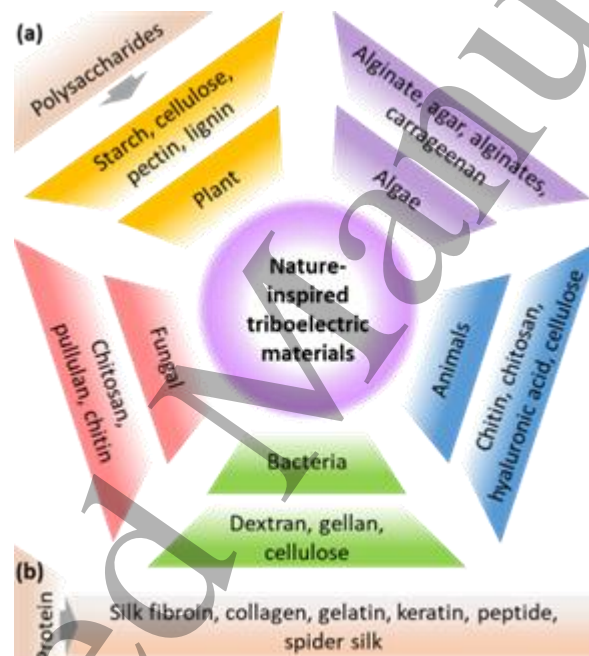


**Figure 1.** Various nature-inspired triboelectric materials classified according to their type and origin.

### Current and Future Challenges

Compared to the synthetic triboelectric materials, the NITMs have a great practical engineering application due to their low cost, simple production, high availability, etc. However, using the NITMs has a few challenges to be resolved for commercialization. Most of the commonly used triboelectric materials in the fabrication of TEEHs to achieve high performance are plastic products based on petrochemical production. For example, polytetrafluoroethylene, polydimethylsiloxane, fluorinated ethylene propylene, and polyvinylidene fluoride have very unique characteristics of high durability, low density, high corrosion resistance, and many more.[1] It is well known that the work function of the triboelectric materials is highly important for the electrical performance of TEEHs. However, the work function of NITMs is low when compared to other synthetic materials used in the TEEH fabrication (Figure 2a). This can be



1  
2  
3 enhanced by hybridizing the NITMs with other materials.[5-7] Most of the NITMs are positively charged  
4 triboelectric materials and their electron affinity is also very low. The electrical performance can be  
5 enhanced by surface engineering, chemical modification, or combining the NITMs with biocompatible  
6 polymers (Figure 2b).[7] The output power density is considered the general criteria to facilitate the  
7 performance comparison between NITMs. Figure 2c shows the output power density of the various  
8 NITMs-based TEEHs. The output power densities of most of the NITMs are very weak, which makes it very  
9 difficult to power electronics. However, when the NITMs were combined with biocompatible polymers,  
10 enhanced electrical output was observed.[7] The currently used NITMs shown in Figure 1 lack the  
11 properties of high durability. Unfortunately, external environment conditions such as temperature and  
12 humidity also highly affect the electrical performance of the NITMs- based TEEHs.[5] As shown in Figure  
13 2d, the electric output of TEEHs decreases with humidity furthermore, so making the NITMs or fabricating  
14 the TEEHs sustainable in harsh environments is challenging.[8] TEEHs can be protected from the  
15 environment by various techniques such as fully packing the device, functionalization, and surface  
16 patterning/making the film surface hydrophobic. On the other hand, environmental humidity can also be  
17 taken as a positive factor via chemical modifications to improve the electrical performance of the  
18 TEEHs.[9]  
19  
20  
21

### 22 **Advances in Science and Technology to Meet Challenges**

23 The NITMs-based TEEHs have a few challenges that need to be resolved. Although bio-TEEHs are made of  
24 NITMs, most of their used electrode materials are synthetic materials, thus limiting the fabrication of  
25 complete biodegradable devices. Thus, bio-conductive electrodes could be investigated. Compared to the  
26 stable electrical performance and output power density of synthetic TEEHs, the performance of NITM-  
27 based TEEHs is significantly low. This could be resolved by improving the triboelectric material properties  
28 and developing novel device fabrication techniques. There is a high potential for the NITMs to be  
29 applicable in implantable devices such as the in-vivo application as sensors and harvesters. However, the  
30 current investigations are not sufficient enough to reach the need. The limitations are due to the large  
31 size, not sustainability and compatibility. This issue can be overcome by integrating the NITMs-based  
32 TEEHs with the micro- and nanoelectromechanical system technologies. The sensitivity and accuracy of the  
33 TEEHs are still challenging, especially in biomedical applications. The slight discrepancy in the value could  
34 misdiagnose or misinform the patient's condition, which could be solved by improving the sensing  
35 accuracy and response time of the TEEHs by modulating the NITM and the device structures. Since most  
36 of the NITMs functioning in-vivo or in-vitro produce low power, and thus it is very difficult to be used in a  
37 self-powered energy system. Therefore, low energy consuming circuits can be investigated to integrate  
38 with the low output power-producing TEEHs. Many of the biocompatible triboelectric nanogenerators are  
39 not fabricated with biocompatible materials.[10] The use of NITMs could resolve this issue because of  
40 their non-toxic and biocompatible characteristics. The NITMs-based TEEHs have a high demand in the field  
41 of implantable medical devices for long-term in-vivo diagnosis and therapy. These can be applied in  
42 various fields including sensors, gastric simulators, cardia pacemakers, and cardioverter-defibrillators as  
43 well as bone, deep brain, and nerve stimulation. The power source of most of the implanted devices has  
44 relied on rechargeable batteries, However, the internal heat, capacity loss, and battery failure are a series  
45 of problems. Replacing the battery in the implanted devices is also difficult, and efficient NITMs-based  
46 TEEHs could function as a continuous power source. Furthermore, the future roadmap of the NITMs-based  
47 TEEHs is shown in Figure 2e.[10]  
48  
49  
50  
51  
52  
53  
54  
55  
56  
57  
58  
59  
60

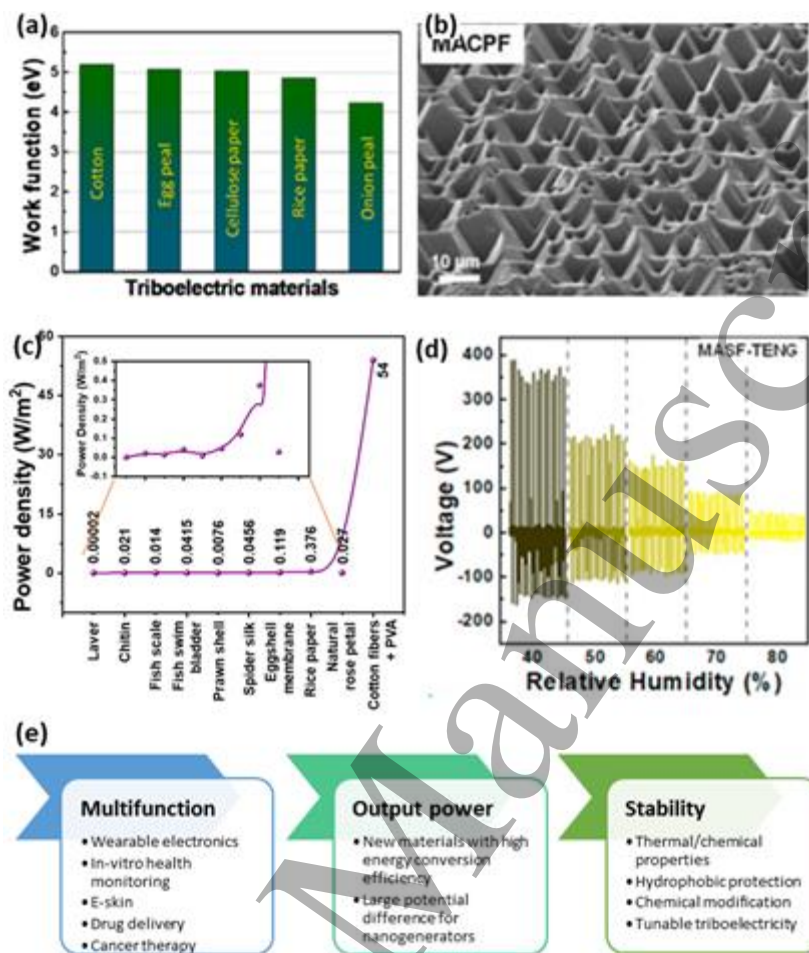


**Figure 2.** (a) Work function of various NITMs. Reproduced with permission [5] Copyright 2021, Elsevier. (b) Surface modification of the NITMs to improve the harvesting ability. Reproduced with permission [7] Copyright 2019, Elsevier. (c) Electrical performance of the NITMs-based TEEHs, influenced by the environmental humidity. Reproduced with permission [8] Copyright 2020, Elsevier. (d) Output power density of various NITMs-based TEEHs. (e) Future roadmap of the NITMs-based TEEHs.

### Concluding Remarks

Employing the NITMs with biocompatibility and eco-friendly feature to create an eco-friendly energy harvesting system is one of the advanced technologies to support the non-pollution and creation of an ecological environment. The NITMs-based TEEHs have a high potential for mass production because of their eco-friendly feature, low cost, and abundantly available raw materials. Unfortunately, the current research may not be sufficient enough to commercialize the NITMs for energy harvesting due to the above-mentioned issues. Nevertheless, the incorporation of NITMs into the TEEH technology could be very useful for eco-friendly energy harvesting system and also promote them for next-generation electronics. This future roadmap of the NITMs-based TEEHs might provide a deep insight into the field of triboelectric energy harvesting and further benefit various other technologies.

### Acknowledgements

This work was supported by the National Research Foundation of Korea (NRF) grant funded by the Korean government (MSIP) (No. 2018R1A6A1A03025708).

## References

- [1] X. Li, C. Jiang, Y. Ying, and J. Ping, "Biotriboelectric nanogenerators: materials, structures, and applications," *Advanced Energy Materials*, vol. 10, no. 44, p. 2002001, 2020.
- [2] Q. Zheng *et al.*, "Biodegradable triboelectric nanogenerator as a life-time designed implantable power source," *Science advances*, vol. 2, no. 3, p. e1501478, 2016.
- [3] L. Cao, X. Qiu, Q. Jiao, P. Zhao, J. Li, and Y. Wei, "Polysaccharides and proteins-based nanogenerator for energy harvesting and sensing: A review," *International Journal of Biological Macromolecules*, vol. 173, pp. 225-243, 2021.
- [4] D. W. Kim, S.-W. Kim, and U. Jeong, "Lipids: Source of Static Electricity of Regenerative Natural Substances and Nondestructive Energy Harvesting," *Advanced Materials*, vol. 30, no. 52, p. 1804949, 2018.
- [5] S. A. Graham, S. C. Chandrarathna, H. Patnam, P. Manchi, J.-W. Lee, and J. S. Yu, "Harsh environment-tolerant and robust triboelectric nanogenerators for mechanical-energy harvesting, sensing, and energy storage in a smart home," *Nano Energy*, vol. 80, p. 105547, 2021.
- [6] H. Zou *et al.*, "Quantifying and understanding the triboelectric series of inorganic non-metallic materials," *Nature communications*, vol. 11, no. 1, pp. 1-7, 2020.
- [7] S. A. Graham, B. Dudem, A. R. Mule, H. Patnam, and J. S. Yu, "Engineering squandered cotton into eco-benign microarchitected triboelectric films for sustainable and highly efficient mechanical energy harvesting," *Nano Energy*, vol. 61, pp. 505-516, 2019.
- [8] B. Dudem *et al.*, "Exploring the theoretical and experimental optimization of high-performance triboelectric nanogenerators using microarchitected silk cocoon films," *Nano Energy*, vol. 74, p. 104882, 2020.
- [9] N. Wang, Y. Zheng, Y. Feng, F. Zhou, and D. Wang, "Biofilm material based triboelectric nanogenerator with high output performance in 95% humidity environment," *Nano Energy*, vol. 77, p. 105088, 2020.
- [10] Y.-M. Wang *et al.*, "Fabrication and application of biocompatible nanogenerators," *Iscience*, vol. 24, no. 4, p. 102274, 2021.

## 4.6 MXenes materials for triboelectric energy harvesting

Ling-Zhi Huang, Dan-Dan Li and Ming-Guo Ma

Research Center of Biomass Clean Utilization, College of Materials Science and Technology, Beijing Forestry University, Beijing 100083, PR China

Triboelectric nanogenerators (TENGs) technology can directly convert irregular and tiny low-frequency mechanical energy in the environment into electrical energy [1]. MXenes are considered to be ideal candidates for triboelectric layers and conductive electrodes in TENGs due to their high electrical conductivity, hydrophilic surfaces, and abundant surface functional groups (-OH, -O, and -F) [2]. For example, MXene was used as the active material and indium tin oxide (PET-ITO) film as the top electrode of TENGs [3]. In addition, MXenes can also be used as effective filler together with other triboelectronegative materials such as polyvinylidene fluoride (PVDF), polytetrafluoroethylene (PTFE), and silicone rubber to improve dielectric property. For instance, Bhatta *et al.* [4] prepared MXene-PVDF TENGs with the increase dielectric constant and surface charge density. Moreover, MXenes can be used to replace metals as the TENGs electrode due to their high conductivity. Besides  $Ti_3C_2T_x$ , MXene-based TENGs,  $V_2CT_x$  and  $Nb_2CT_x$ , MXene were also applied to synthesize TENGs. MXene-based TENGs show great applications potential in energy collection and self-powered sensors, as shown in **Figure 1**. Combining

various advantages of MXenes, TENGs can be fabricated into lightweight and miniaturized devices to supply power for small electronic and meet the urgent needs of sustainable energy supply. In Cao's work [5], the cellulose nanofibers/MXene liquid electrode-based TENGs (CM-TENGs) were obtained using elastic silicone rubber as both packaging material and triboelectrification layer. A flexible stretchable TENGs were achieved using MXene/PVA hydrogels as electrodes [6]. MXene-based TENGs can be utilized as self-powered tactile sensors to monitor body motions such as wrist, elbow, and finger movement. The self-powered sensors also need high sensitivity and stretchability to meet the requirements of practical applications. A fabric-assisted MXene/silicon nanocomposite friction nanogenerator (DSC-TENG) was developed for self-powered human-motion sensors and wearable electronics [7]. Cao et al. [8] prepared stretchable crumpled MXene film TENGs based pressure/strain sensor with high sensitivity for wireless human motion detection. The MXene-based TENGs have promising applications in the fields of selective  $\text{NH}_3$  or  $\text{NO}_2$  gas sensor [9], humidity sensing [10], biomechanical sensing, personal thermoregulatory device, intelligent agriculture, etc. All the mentioned above reports indicate the immense potential of MXene-based TENGs.

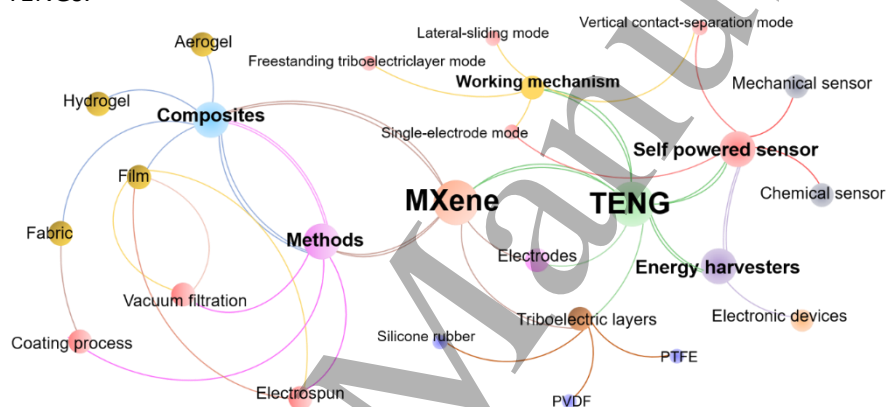


**Figure 1.** Overview of this research update for MXene-based triboelectric nanogenerators (MXene-based TENGs).

### Current and Future Challenges

Although the exploration of MXene-based TENGs only began about 5 years ago, this is a rapidly expanding field due to the applications of MXenes as negative triboelectric materials and replace traditional metal electrodes. Usually, the mechanical energy in the environment is intermittent, resulting in unstable output performance of MXene-based TENGs, which affects the power supply for small electronic devices. Initially, the interest in MXenes was mainly for energy storage, conductive electrodes, electromagnetic shielding, etc. However, integration with energy storage devices such as supercapacitors is a promising development direction. Thereinto, TENGs provide a new idea for the next generation of wearable electronic devices by converting the mechanical energy of human motion into electrical energy and storing it in electrochemical devices. However, the applications of flexible functional MXene-based TENGs for athlete health monitoring and auxiliary training have not widely reported yet. Secondly, MXenes usually undergo rapid oxidation/degradation reaction in air and water, mainly forming  $\text{TiO}_2$ . High stability is a necessary condition for the practical application of MXene-based TENGs. Therefore, further research could pay more attention to improving the stability of MXene and its composites, so as to bring stable output performance and reliable stability to TENGs. Moreover, besides  $\text{Ti}_3\text{C}_2\text{T}_x$  MXene-based TENGs, various types of MXene-based TENGs should be developed to design TENGs. In addition, fluorinated reagents are inevitably used in the synthesis process. Therefore, there is an urgent need to explore ways to control the morphology and termination groups of MXene and green and fluorine-free synthesis methods in the future. Third, we should carefully explore the stretching strategy for scalable production of wearable MXene-based TENGs to meet the actual requirements for practical applications in wearable

1  
2  
3 electronic devices. Fourth, the self-powered sensors based on MXene-based TENGs face complex and  
4 diverse application context in practice, mainly because the complex environment affects the stability of  
5 the output performance of TENGs. For example, the presence of water vapor and temperature driving in  
6 the environment will lead to the loss of surface charge on the MXenes triboelectric materials, thus  
7 reducing the output performance of the sensors. It is still a great challenge to design wearable MXene-  
8 based TENGs with long-term stability under extreme conditions such as severe cold. The limited stretching  
9 degree of composites and slow response to external stimuli greatly limit the practical application of  
10 MXene-based TENGs. Therefore, it is necessary to continue to explore and solve these problems.  
11  
12  
13

#### 14 **Advances in Science and Technology to Meet Challenges**

15 So far, more than 30 kinds of MXenes have been synthesized experimentally, showing promising  
16 applications in MXene-based TENGs. For example, a general Lewis acidic etching route was developed to  
17 prepare MXenes with enhanced electrochemical performance in non-aqueous electrolyte. MXene-based  
18 TENGs with unique structure and excellent properties can be designed by simulation calculation. In situ  
19 characterization technologies, such as in situ XRD, SEM, neutron diffraction, etc, are helpful to understand  
20 the change process of MXene-based TENGs in real time. Theoretical calculation and experimental  
21 verification should be used to reveal the interaction mechanism among MXene-based TENGs. The multi-  
22 scale delamination feature is related to the design strategies widely existing in nature, which means the  
23 toughening mechanism related to the micro/nano structural features of MXene-based TENGs. Bionic  
24 strategies such as bionic materials, bionic structures, and functional bionics solves the problems by  
25 learning from nature. The bellow methods and types maybe effectively solve the problem that MXene-  
26 based TENGs cannot be stretched. On the one hand, MXenes can be composited with flexible materials  
27 such as polydimethylsiloxane (PDMS), elastic silicone rubber, polymer, and biomass to prepare stretchable  
28 MXene-based TENGs. On the other hand, MXene-based TENGs displayed various types, such as hydrogel,  
29 aerogel, fiber, films, paper, and textile. Noteworthy, the construction of special structure (crumpled  
30 structure, Kirigami structure, and braided structure, sandwich structure, Janus structure, etc) can also  
31 endows the stretchability of brittle materials. Emerging preparation strategies help to obtain MXene-  
32 based TENGs with ideal properties, such as 3D printing or additive manufacturing, spatially confined  
33 growth, surface imprinting technology, click chemistry, etc. The composite is a promising route to increase  
34 the stability of MXenes with graphene oxide, carbon nanotubes, metal-organic framework [9], noble  
35 metal, etc. Therefore, the development of appropriate packaging materials and packaging technology is  
36 one of the key issues to solve the problem of stability in the near future. MXene-based TENGs based on  
37 scenario can better meet the requirements of practical applications. In view of the complex environment  
38 factors, we suggest that MXene-based TENGs should be endowed with various specific functions in future  
39 research. For example, the environmental stability can be enhanced by introducing the hydrophobicity,  
40 flame retardancy, oxygen barrier, and other functions, while the output stability can be improved by  
41 introducing the self-healing and charge-storage capacity functions. Up to now, the fundamental  
42 performance of MXene-based TENGs self-powered sensor was only explored. However, it is unrealistic for  
43 the whole IOT system to work without any power supply. Therefore, we suggest to develop a multi-  
44 functional self-powered IOT system in the future, which can not only sense the stimulation in the external  
45 environment, but also obtain energy from the external environment.  
46  
47  
48  
49  
50

#### 51 **Concluding Remarks**

52 In summary, MXene-based TENGs has made a breakthrough in the research of energy collection and self-  
53 powered sensor. However, the common synthesis methods of MXenes will make the structure and surface  
54 functional groups out of control, further affecting the performance of MXene-based TENGs. In addition,  
55 fluorinated reagents are inevitably used in the synthesis process of MXene-based TENGs. Therefore, there  
56  
57  
58  
59  
60



is an urgent need to explore ways to control the morphology and termination groups of MXenes and green and fluorine-free synthesis methods in the future. Moreover, a major direction in the future is to select appropriate MXene-based TENGs to obtain self-powered sensors with high sensitivity and wide response range for practical applications in health monitoring, sports monitoring, and wearable devices. In general, MXenes and their composites still have broad research prospects in the field of TENGs. We believe that MXene-based TENGs will have a promising applications in the near future.

### Acknowledgements

The financial support from the National Key R&D Program of China (2019YFC1905901) and the Beijing Forestry University Outstanding Young Talent Cultivation Project (2019JQ03014) is gratefully acknowledged.

### References

- [1] F.R. Fan, Z.Q. Tian, Z.L. Wang, Flexible Triboelectric Generator, *Nano Energy* 1(2) (2012) 328-334.
- [2] C. Jiang, C. Wu, X. Li, Y. Yao, L. Lan, F. Zhao, Z. Ye, Y. Ying, J. Ping, All-electrospun Flexible Triboelectric Nanogenerator Based on Metallic MXene Nanosheets, *Nano Energy* 59 (2019) 268-276..
- [3] Y.C. Dong, S.S.K. Mallineni, K. Maleski, H. Behlow, V.N. Mochalin, A.M. Rao, Y. Gogotsi, R. Podila, Metallic MXenes: A New Family of Materials for Flexible Triboelectric Nanogenerators, *Nano Energy* 44 (2018) 103-110.
- [4] T. Bhatta, P. Maharjan, H. Cho, C. Park, S.H. Yoon, S. Sharma, M. Salauddin, M.T. Rahman, S.M.S. Rana, J.Y. Park, High-performance Triboelectric Nanogenerator based on MXene Functionalized Polyvinylidene Fluoride Composite Nanofibers, *Nano Energy* 81 (2021) 105670.
- [5] W.T. Cao, H. Ouyang, W. Xin, S.Y. Chao, C. Ma, Z. Li, F. Chen, M.G. Ma, A Stretchable Highoutput Triboelectric Nanogenerator Improved by MXene Liquid Electrode with High Electronegativity, *Adv. Funct. Mater.* 30(50) (2020) 2004181.
- [6] X.X. Luo, L.P. Zhu, Y.C. Wang, J.Y. Li, J.J. Nie, Z.L. Wang, A Flexible Multifunctional Triboelectric Nanogenerator Based on MXene/PVA Hydrogel, *Adv. Funct. Mater.* 31(38) (2021) 2104928.
- [7] M. Salauddin, S.M.S. Rana, M.T. Rahman, M. Sharifuzzaman, P. Maharjan, T. Bhatta, H. Cho, S.H. Lee, C. Park, K. Shrestha, S. Sharma, J.Y. Park, Fabric-Assisted MXene/Silicone Nanocomposite-Based Triboelectric Nanogenerators for Self-Powered Sensors and Wearable Electronics, *Adv. Funct. Mater.* 32(5) (2022) 2107143.
- [8] Y.L. Cao, Y.B. Guo, Z.X. Chen, W.F. Yang, K.R. Li, X.Y. He, J.M. Li, Highly Sensitive Self-Powered Pressure and Strain Sensor Based on Crumpled MXene Film for Wireless Human Motion Detection, *Nano Energy* 92 (2022) 106689.
- [9] D.Y. Wang, D.Z. Zhang, Y. Yang, Q. Mi, J.Z. Zhang, L.D. Yu, Multifunctional Latex/Polytetrafluoroethylene-Based Triboelectric Nanogenerator for Self-Powered Organ-like MXene/Metal–Organic Framework-Derived CuO Nanohybrid Ammonia Sensor, *ACS Nano* 15 (2021) 2911–2919.
- [10] P.D. Li, N. Su, Z.Y. Wang, J.S. Qiu, A  $Ti_3C_2T_x$  MXene-Based Energy-Harvesting Soft Actuator with Self-Powered Humidity Sensing and Real-Time Motion Tracking Capability, *ACS Nano* 15 (2021) 16811–16818.



## 4.7 Perovskite-based triboelectric nanogenerators

JiKui Luo

College of Information Science and Electronic Engineering, Zhejiang University, Hangzhou, 310027, China.

### Status

Perovskites, emerging as promising materials for electronic, optoelectronic and energy devices, have attracted considerable interests for the fabrication of TENGs, because their variety of electronic band structures, crystal formats and tuneable material properties etc., and both the inorganic and hybrid organic-inorganic perovskites have been explored.[1]

A TENG with a stretchable PVDF-copolymer nanofiber membrane-Ag tribolayer delivered a high open-circuit voltage ( $V_{oc}$ ) of  $\sim 400$  V. The nanofiber composite incorporated with  $Cs_3Bi_2Br_9$  nanoparticles was obtained by electrospinning.[2] The perovskite nanoparticles served as efficient electron acceptors and nucleating agents for crystallization.

Inorganic perovskite  $CsPbBaBr_3$ /PVDF TENG showed significant dependence of outputs on the Ba content due to the corresponding variation of properties. A  $V_{oc}$  of 220 V was achieved with a 0.09% Ba.[3]  $CsPbBr_3$  doped with I or Cl ions were further investigated for TENGs.  $V_{oc}$  up to 257V was obtained, attributing to the built-in electric field induced by the spontaneous polarization and alignment of dipoles.[4] However, the outputs are much smaller than expected. Four iron-based lead-free triple perovskites synthesized by sol-gel method were used to fabricate TENGs paired with Kapton. Despite the very high dielectric constants over 200, outputs of the TENGs were very small with  $V_{oc}$  less than 80 V.[10]

Hybrid perovskites ( $MAPbI_3$ ) were utilized to fabricate TENG-driven photodetectors paired with PTFE and a mesoporous  $TiO_2$  electron transport layer. TENG showed  $V_{oc}$  of 10 V in dark, and a 11% enhancement in both current and voltage outputs once being exposed to light.[5] By using an ultrathin pentacene layer on top of  $MAPbI_3$  as a hole transport layer, TENG outputs were improved by 55~58%.[6]  $MA_xPb_{1-x}I_3$  paired with a PA6 or PDMS layer was utilized to fabricate TENGs. The perovskites showed either positive or negative triboelectric features, depending on the pairing tribomaterial. Polarization and mobile charges in the perovskites would modulate surface charge density significantly, and increased  $V_{oc}$  from  $\sim 550$  to  $\sim 780$ V (reduced to  $\sim 380$ V) when being forward (reverse) polarized. Similarly,  $V_{oc}$  could be tuned largely from 380V to 695 V when the MAI to  $PbI_2$  ratio was changed from 0.4 to 3 due to the change of electron affinity etc.[7,8]

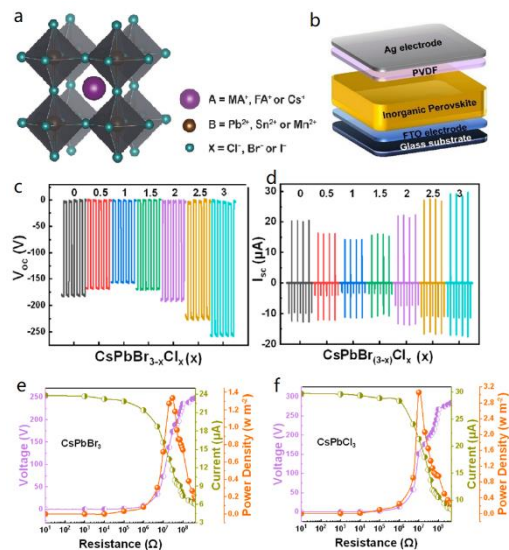


Figure 1. (a) Crystal structure of perovskites, (b) inorganic perovskite-based contact-mode TENG configuration and (c)&(d) voltage and current outputs; and (e)&(f) power output of the TENGs as a function of resistance.[3,4]

### Current and Future Challenges

TENG's outputs strongly depend on the tribomaterials. Perovskites possessing unique properties are expected to be the promising tribomaterials for TENGs. However, from the vast types of perovskite materials point of view, the relevant research activities are sparse.[1]

Varying composition ratio or percentage of metal ions of a perovskite could distinctly modify conductivity, electron affinity, piezoelectric property etc. These are anticipated to bring extra degrees of freedom to design new types of TENGs and self-driven sensors, and they are very effective in altering material properties[9]. However, the lack of systematic investigation and fundamental research have inhibited its progress, and most of the research relied on the trial-and-error approach with no theoretical guidance for material and device development.

Perovskites possess excellent optoelectronic properties and have been utilized to fabricate self-powered TENG-type photodetectors. But the low sensitivity and high dark current are the serious drawbacks for the photodetectors.[5] Theoretically, photogenerated carrier concentrations are orders of magnitudes higher than the tribo-charges, but the photo-enhanced triboelectric effect has not yet been clearly observed, requiring a thorough understanding of the mechanism and roles of the electron and hole transport layers, and optimal structural design.

Ferroelectricity is known to exist in some perovskites, and remnant polarization is in the range of a few mC/cm<sup>2</sup> for MAPbI<sub>3</sub>[7,8], which affects the piezoelectric property etc. Also, there are many mobile charges in perovskites. Change of both the dipoles and mobile charges under an electric field could modulate surface electronic state and potential of the perovskites. The challenges are on how to generate a high density of these charges and fix them on surfaces, so that to further enhance and stabilize performance of the TENGs.

Nanocomposites possess a range of excellent properties and have been utilized for fabricating high-performance TENGs. Similarly, perovskites have varieties of nanostructures, however, their nanocomposites are barely explored for TENGs, not even to mention very poorer performance. Some

piezoelectric nanoparticles could assist polarization and crystallization of piezo-phase of PVDF polymers, and has not been utilized for perovskite tribomaterials yet. The use of perovskite-polymer nanocomposites could boost the mechanical durability of perovskite TENGs, enabling the development of flexible TENGs-driven energy source and sensors.

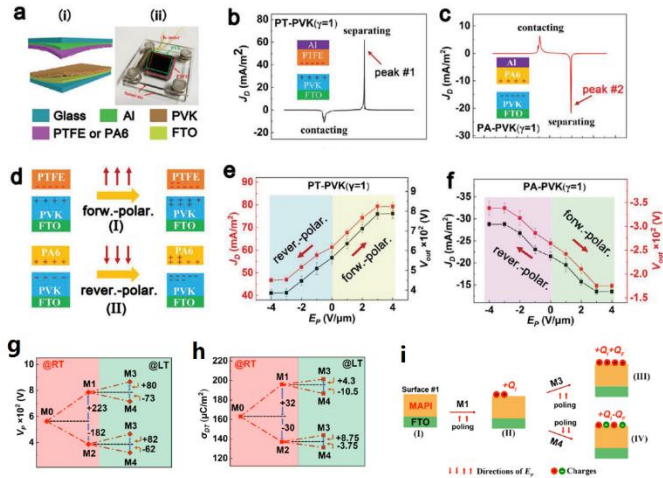


Figure 2. MAPbI<sub>3</sub>-based TENG in pairing with PTFE or PA6 layer. (a) the device configuration, (b)&(c) typical current outputs for these two types of TENGs with different polarities, (d) schematic of poling of perovskite (PVK), and (e)&(f) poling effect on TENG's outputs, (g)-(i) dipole charges and mobile charges in the perovskites could be added up and subtracted, leading to improvement or deterioration of TENG performance. (LT: low temp., 239 K, RT: room temp.) [7-9]

### Advances in Science and Technology to Meet Challenges

Although the application of perovskites has resulted in TENGs with attractive performance and increased the portfolio of tribo-series, the results have clearly indicated that the potential for perovskites-based TENGs is not realized yet. TENG performance largely depends on electron affinity, surface charge density and permittivity of the tribomaterials. Piezoelectric coefficient is also positively related to both spontaneous polarization and permittivity, thus the piezo and ferric properties of perovskites provide much room for designing materials for high-performance TENGs. The research on perovskites TENGs is at the very early stage, and many discoveries and innovations are yet to be made, in terms of new types of perovskites, tribomaterial combinations, new physics phenomenon, novel device structures and applications. The challenges are as follows.

1. To design high-performance TENG, it is necessary to understand fundamentals of perovskites, including electronic structures and dielectrics, piezoelectric and ferroelectric properties etc. and their relationships with composition ratios. The first principle methods should be applied to clarify perovskites properties and design tribomaterials with desirable properties for high-performance perovskites TENGs.
2. Perovskites is a material family with rich features, however, only a tiny portion of perovskites, mostly in the forms of thin film have been studied for TENG development. More and systematic experimental investigations are needed to clarify perovskites in terms of electron affinity, band structure, conductivity etc., so that suitable materials could be identified for TENGs.
3. Novel structural designs towards multifunctionalities with integrated electronic, optoelectronic, and piezoelectric effects are highly desirable for different application scenarios, particularly the self-driven sensors and photodetectors as perovskites have high light absorption coefficient and

photoconversion efficiency, and are sensitivity to broad light spectrum. This requires device modeling for the structure optimization.

4. Nanocomposites possess excellent properties such as large effective surface area, tunable properties, high piezoelectric constants etc. Perovskite nanocomposites are hardly explored for TENGs, thus there are great rooms for exploration and optimization. The material modelling and design approaches should be utilized for this research.

5. Further research could be conducted on lead-free perovskite for ecofriendly and sustainable development by replacing the lead element with other metal or even organic moiety.

### Concluding Remarks

Perovskites are a family of materials with numerous unique band structures, electronic, optoelectronic, piezoelectric and ferroelectric properties, thus, they could provide a rich source of materials for the exploration in multifunctional and high-performance TENGs. Although some perovskites have been investigated for the fabrication of TENGs, it is still at the very early stage, and much is yet to be done. Lack of fundamental understanding of the materials and systematic investigation of material properties are the obstacles that prevent the design of materials and TENGs with desirable properties and application scenarios. On the other hand, this provides great opportunities for scientists and engineers to make efforts on fundamental theories for materials and devices, material synthesis methods, methodologies for device design and fabrication process. It is highly envisaged that great successes will be made soon in the relevant areas, that contribute to the research community and society markedly.

### Acknowledgements.

This work was funded by Key Research Project of Zhejiang (LD22E030007) and Leading Goose" R&D Program of Zhejiang Province (No.2022C01136).

### References

- [1] R. Ding et al., "Recent advances in hybrid perovskite nanogenerators," *EcoMat*. Vol. 2, pp.12057, 2020.
- [2] F. Jiang et al., "Stretchable, Breathable, and Stable Lead-Free Perovskite/Polymer Nanofiber Composite for Hybrid Triboelectric and Piezoelectric Energy Harvesting," *Adv. Mater.*, Vol. 34, pp. 2200042, 2022.
- [3] Y. Wang et al. "The unique dielectricity of inorganic perovskites toward high-performance triboelectric nanogenerators,". *Nano Energy*. Vol. 69, pp. 104418. 2020;
- [4] X.P. Yu et al. "Halogen regulation of inorganic perovskites toward robust triboelectric nanogenerators and charging polarity series," *J. Mater. Chem. A*, vol. 8, pp. 14299, 2020.
- [5] L. Su et al. High-performance organolead halide perovskite-based self-powered triboelectric photodetector. *ACS Nano*. Vol. 9, pp. 11310-11316, 2015;
- [6] X.D. Yang et al., "Robust perovskite-based triboelectric nanogenerator enhanced by broadband light and interface engineering" *J. Mater. Sci.* vol. 54, pp. 9004–9016, (2019
- [7] S.Y. Huang et al., "Controlling Performance of Organic–Inorganic Hybrid Perovskite Triboelectric Nanogenerators via Chemical Composition Modulation and Electric Field-Induced Ion Migration," *Adv. Energy Mater.* Pp.2002470, 2020,
- [8] S.Y. Huang et al., "Surface electrical properties modulation by multimode polarizations inside hybrid perovskite films investigated through contact electrification effect," *Nano Energy* vol. 89 pp. 106318, 2021.
- [9] H.B. Wang et al., "Coexistence of Contact Electrification and Dynamic p–n Junction Modulation Effects in Triboelectrification", *ACS Appl Mater Interfaces*. Vol.14, no.26. pp.30410, 2022.
- [10] J. Kojcinovic et al. Nanocrystalline triple perovskite compounds  $A_3Fe_2BO_9$  (A = Sr, Ba; B = W, Te) with ferromagnetic and dielectric properties for triboelectric energy harvesting," *Mater. Chem. Front.*, vol. 6, pp.1116, 2022.

## 4.8 Towards self-powered woven wearables via triboelectric nanogenerators

Feng Jiang and Pooi See Lee

School of Materials Science and Engineering, Nanyang Technological University, 50 Nanyang Avenue, Singapore 639798, Singapore

### Status

Fibers and textiles, serving as promising materials for triboelectric nanogenerators (TENGs), endow the energy devices with excellent breathability, wearability, stretchability, and comfortability. The mature industrial production and abundant raw material selection also provide the fiber and textile-based TENGs with a desirable platform for device fabrication and customized design. Compared to the thin film or bulk structures, fibers and textiles have more sophisticated patterns and higher surface roughness, which can further satisfy the functionality and aesthetic requirements of wearable applications with enhanced triboelectric output.

Figure 1a shows different forms of fibers and textiles based on their various structural dimensions and fabrication methods.[1, 2] Fibers are the basic building blocks, which can be coiled alone or twisted with other fibers to form yarns. Different yarns can be further processed to construct a hierarchical structure with better mechanical strength. Finally, textiles can be prepared by combining different yarns through woven and knitted methods.[2] The first fiber-based TENG was proposed in 2014, which utilized cotton, carbon nanotube, and PTFE as raw materials to fabricate an entwined structure, conceptually confirming that fibers and textiles can be fabricated into efficient TENGs.[3] Since then, tremendous efforts have been made to optimize the device structure, output performance, and application scenarios of fiber and textile-based TENGs.[4]

The textile-based TENGs were not limited to traditional two-dimensional woven and knitted structures. The recently proposed 3D fabric and multilayer stacking structure offered new opportunities for multifunctional integration and structure optimization.[4] Some non-woven methods, such as electrospinning and 3D printing, were also developed to improve the structure and expand the functions of textile-based TENGs.[1] Apart from the structure design, electrical performance optimization is also significant to the fiber and textile-based TENGs. Extensive improvement strategies, such as micro/nanopatterned structure design, charge trapping, as well as intermediate layer embedding, have been explored to promote the triboelectric output of the devices.[2, 4] Currently, fiber and textile-based TENGs have also been widely applied in wearable electronics, self-powered sensors, as well as physiological health monitoring, exhibiting their huge potential in the field of smart textiles and human-machine interface.[2]



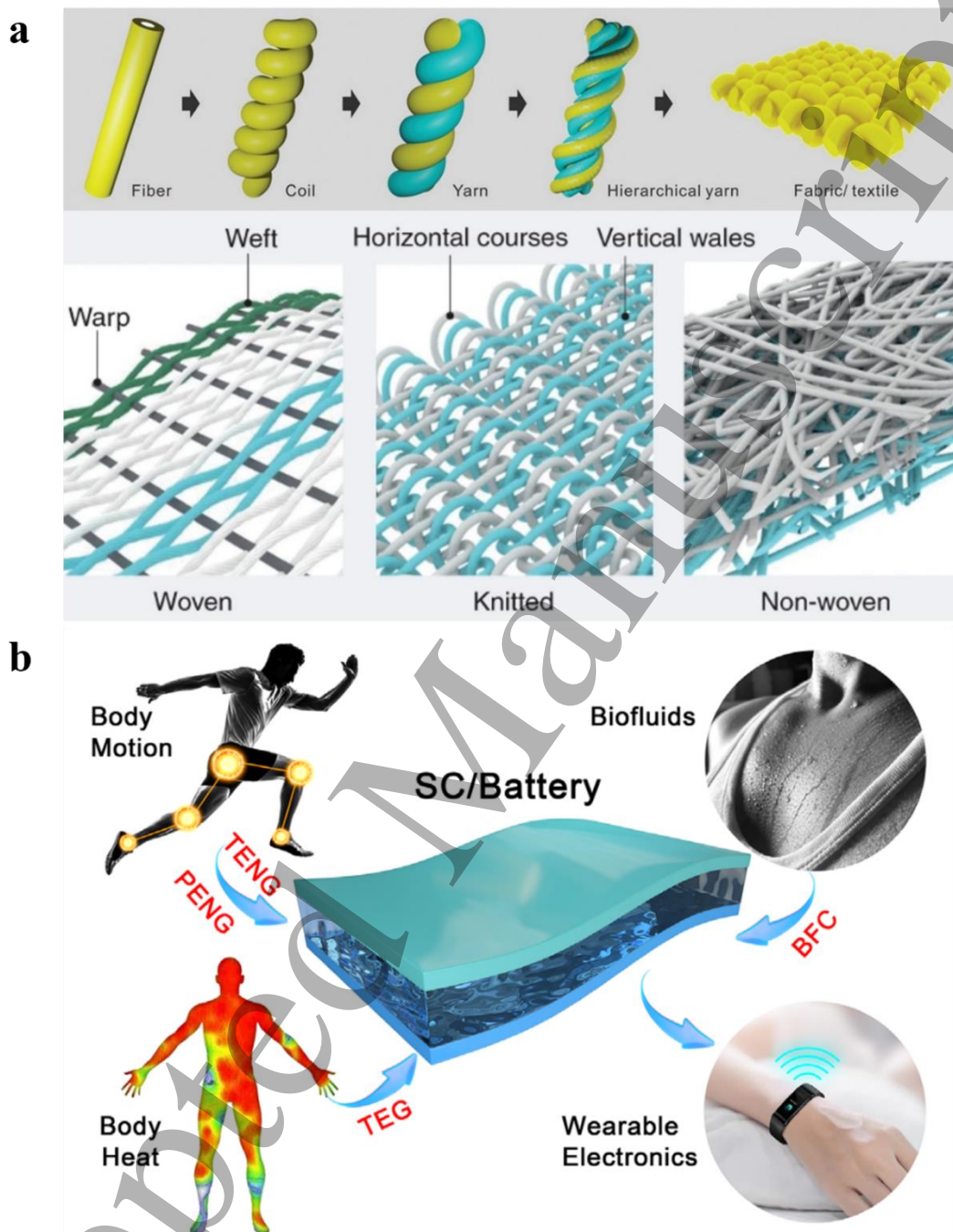


**Figure 1.** (a) Different forms of fibers/textiles based on their various structural dimensions and fabrication methods. Reprinted with permission from [1, 2]. (Springer Nature Customer Service Centre GmbH: Nature Electronics [1] (2022); [2] John Wiley & Sons. Copyright © 2021 WILEY-VCH Verlag GmbH KGaA & Co., Weinheim) (b) A wearable energy storage system via self-charged human-body bioenergy including body motions, heat, and biofluids. Reprinted with permission from [5]. John Wiley & Sons. Copyright © 2021 WILEY-VCH Verlag GmbH KGaA & Co., Weinheim.

### Current and Future Challenges



1  
2  
3 *Material innovation.* Fiber/textile-based TENGs, despite excellent progress in structure design and  
4 performance enhancement, are primarily focused on traditional materials, such as metal, carbon  
5 materials, Kapton (polyimide), silicone rubber, polytetrafluoroethylene (PTFE), and polyethylene  
6 terephthalate (PET). Although these materials are low-cost and easy to obtain, they are difficult to meet  
7 the harsher requirements of multifunctional smart textiles in modern society. Therefore, developing new  
8 materials is of significant importance to address the emerging issues, including biocompatibility,  
9 washability, waterproofness, self-healing ability, as well as a complex integration of electronic devices.  
10 Furthermore, the new materials should also be low-cost, sustainable, eco-friendly, air/moisture  
11 permeable, and thermally and mechanically stable, in order to tackle new challenges for the future  
12 development of fiber/textile-based TENGs.  
13

14  
15 *A hybrid and sustainable energy platform.* Fiber/textile-based TENGs are effective technologies that  
16 convert mechanical energy into electricity. However, with the growing amount of energy consumption  
17 and urgent demands for denser device integration, sole reliance on mechanical energy is not sufficient to  
18 satisfy the present power supply. Hence, it is necessary to construct a hybrid and sustainable energy  
19 platform that simultaneously collects different forms of energy, such as mechanical, solar, thermal, and  
20 biochemical energy. The existing challenges are still centered on how to prepare the hybrid energy devices  
21 in the fiber/textile form and efficiently integrate them into one garment without affecting their original  
22 breathability and comfortability. An overview of the storage of energy via self-charged human-body  
23 bioenergy is shown in Figure 1b.[5]  
24  
25

26  
27 *Mass production.* Low-cost and large-scale production of high-performance fiber/textile-based TENGs is  
28 one of the most important goals in this research field. However, most works remain in the laboratory  
29 stage. To accelerate the practical applications of smart textiles, more efforts should be made to establish  
30 industry standards and develop modular production lines. On one hand, systematic evaluation of device  
31 fabrication methods and performance measurements should be determined, serving as guidelines for the  
32 future design of fiber/textile-based TENGs. On the other hand, new equipment and manufacturing  
33 methods should also be developed for the mass production of fiber/textile-based TENGs. Even though  
34 traditional textile production is mature and industrialized, some novel processing requirements, such as  
35 conductive textile fabrication as well as assembly of conductive and functional textiles, still need further  
36 optimization and improvements.  
37

### 38 **Advances in Science and Technology to Meet Challenges**

39  
40 The electric output of fiber/textile-based TENGs is determined by the intrinsic physicochemical properties,  
41 surface roughness or micro/nanopatterns, as well as charge trapping or retention capacity of materials.  
42 Surface functionalization/modification via coating or printing is an effective method that bestows textiles  
43 with better performance and novel functions. For example, the surface of PET could be more negative  
44 and positive by functionalizing it with more fluorinated (electron-accepting elements) and aminated  
45 (electron-donating elements) molecules, respectively.[6] Moreover, the waterproofness and charge  
46 trapping capacity of fabric could be also enhanced by modifying their surface with functional fillers (e.g.,  
47 hydrophobic cellulose oleoyl ester nanoparticles for waterproofness improvement and black phosphorus  
48 for electron-trapping enhancement).[7] Therefore, designing new functional materials and combining  
49 them with textiles are prospective ways that endow the TENGs with higher output performance and more  
50 advantageous properties.  
51  
52

53 Integrating multiform energy harvesting and storage systems into one fabric is also promising for future  
54 smart textiles, allowing users to charge their electronic gadgets such as cell phones and laptops through  
55 their garments whenever and wherever they like. An ideal textile platform for multiform energy  
56  
57  
58  
59  
60

1  
2  
3 harvesting and storage is shown in Figure 2. Some pioneer works have been done to combine the  
4 fiber/textile-based TENGs with other energy generation and storage devices, including fiber/textile-based  
5 solar cells, lithium-ion batteries, as well as supercapacitors.[8, 9] However, these research works are still  
6 in the preliminary stage. Some critical challenges, such as high-efficiency power conversion, structural  
7 design, and device packaging, still need long-term exploration.  
8  
9

10 Advanced manufacturing processes are also needed to supplement traditional textile production and  
11 tailor to the new era of 5G, the Internet of Things, and artificial intelligence. At present, some preliminary  
12 efforts have been made to use 3D printing to directly fabricate porous and fiber-shape TENGs with high  
13 electric output and ultra-high flexibility.[10] These new manufacturing technologies not just make the  
14 fabrication process of fiber/textile-based energy devices more efficient and precise, but also provide a  
15 new platform for customized designs of smart textiles, bringing unprecedented opportunities and  
16 revolutionary progress to the whole textile industry.  
17  
18



46 **Figure 2.** Schematic illustration of a smart textile platform for multiform energy harvesting and storage. Reprinted  
47 with permission from [4]. Copyright 2020, ACS Publications.  
48

### 49 **Concluding Remarks**

50 Overall, much inspiring progress, from structure design and performance optimization to application  
51 development, has been made in the field of fiber/textile-based TENGs. Beyond the structure and  
52 performance improvement, more efforts should be focused on material innovation, hybrid energy system  
53 construction, multifunctional device integration, as well as the mass production of these fiber/textile-  
54 based energy devices. In the future, this emerging field will pave a fresh avenue toward the next-  
55 generation wearable electronics and smart textiles. These fiber/textile-based TENGs are easily combined  
56  
57  
58  
59  
60

with other energy technologies mentioned in this roadmap, including photovoltaic, piezoelectric, thermoelectric, and wireless devices, to construct a sustainable, safe, eco-friendly, and hybrid wearable energy system, offering new application scenarios in self-powered sensors, wearable power source, and personal healthcare.

### Acknowledgments

This work was supported by the Ministry of Education (MOE) Singapore, AcRF Tier 1 (Award no. RT15/20).

### References

- [1] A. Libanori, G. Chen, X. Zhao, Y. Zhou, and J. Chen, 2022 Smart textiles for personalized healthcare, *Nat. Electron.*, **5**, 142-156.
- [2] J. Xiong, J. Chen, and P. S. Lee, 2021 Functional Fibers and Fabrics for Soft Robotics, Wearables, and Human–Robot Interface, *Adv. Mater.*, **33**, 2002640.
- [3] J. Zhong *et al.*, 2014 Fiber-Based Generator for Wearable Electronics and Mobile Medication, *ACS Nano*, **8**, 6273-6280.
- [4] G. Chen, Y. Li, M. Bick, and J. Chen, 2020 Smart Textiles for Electricity Generation, *Chem. Rev.*, **120**, 3668-3720.
- [5] J. Lv, J. Chen, and P. S. Lee, 2021 Sustainable wearable energy storage devices self-charged by human-body bioenergy, *SusMat*, **1**, 285-302.
- [6] S.-H. Shin *et al.*, 2017 Formation of Triboelectric Series via Atomic-Level Surface Functionalization for Triboelectric Energy Harvesting, *ACS Nano*, **11**, 6131-6138.
- [7] J. Xiong *et al.*, 2018 Skin-touch-actuated textile-based triboelectric nanogenerator with black phosphorus for durable biomechanical energy harvesting, *Nat. Commun.*, **9**, 4280.
- [8] J. Chen *et al.*, 2016 Micro-cable structured textile for simultaneously harvesting solar and mechanical energy, *Nature Energy*, **1**, 16138.
- [9] J. Wang *et al.*, 2016 Sustainably powering wearable electronics solely by biomechanical energy, *Nat. Commun.*, **7**, 12744.
- [10] M. Zhang *et al.*, 2019 Printable Smart Pattern for Multifunctional Energy-Management E-Textile, *Matter*, **1**, 168-179.

## 4.9 Theoretical Investigations towards the Materials Optimization for Triboelectric Nanogenerators

Bhaskar Dudem, Venkateswaran Vivekananthan and S. Ravi P. Silva

Advanced Technology Institute, Department of Electrical and Electronic Engineering, University of Surrey, Surrey GU2 7XH, UK

### Status

Triboelectric Nanogenerators (TENGs) are at the forefront in terms of promising technologies for next-generation energy harvesting to power IOT electronics and self-powered sensing devices. TENGs generally work with four different modes, namely contact-separation mode, linear sliding mode, single electrode mode, and free-standing mode. For each different mode optimizing with the different counter electrode materials is key to high performance. Further, multifunctionality aspects such as energy storage, voltage regulation, and power modules can all be integrated with different components and comprise systems engineering of materials to external functionality. These TENG devices have several advantages such as high output generation under low frequency, cost-effectiveness, and simple fabrication techniques. The mechanism of power generation of TENGs is based on contact electrification and electrostatic induction by the charge separation between the triboelectric contact layers. Therefore, the two counter electrodes

in contact are crucial for high performance. So far, TENGs have been utilized for various applications such as bio-mechanical energy harvesting, water wave energy harvesting, vibration detection, photodetection, human-machine interfacing, chemical sensing, and the Internet of things (IoT). In each system, specific and unique materials have been used for the counter electrodes. In addition, TENGs have been coupled with piezoelectric energy harvesters and electromagnetic generators for boosting the electric output performance as well as coupled with the supercapacitors for extending its application in continuous powering up applications. As TENGs can be used in a set of wide applications, it is important to understand the underlying mechanism of power generation and material evaluation. In view of a better cost-effective analysis, the design of materials for a high throughput TENG is necessary prior to manufacturing. To achieve this the present review chapter discusses theoretical models such as the parallel-plate capacitor model (V-Q-x relationship), distance dependent electric field model (DDEF), and figure-of-merits (FOMs) as leading concepts together with any specific materials requirements. The parallel plate model is the most fundamental theoretical model which can be used to simulate the power generation of TENGs under a planar working configuration. Whereas the non-planar modes and configurations can be simulated using the DDEF models in which the distance dependence is considered rather than uniform all over the space. FOMs are introduced to standardize the evaluation of TENGs output performances, which influence the output performance of the TENGs with different parameters analysis. These models contribute towards the theoretical investigations of TENGs for the better optimization of parameters in the TENGs, which would help boost the electrical output performance of the TENGs and towards its utilization in various applications in the future. For each of these scenarios, specific materials would be needed, and the performance optimised based on the active materials in use.

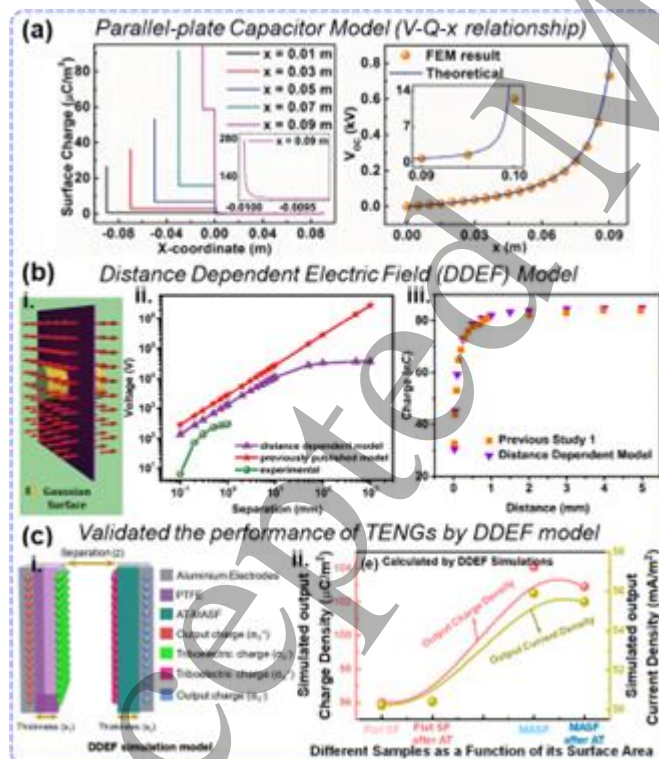


**Figure 1.** Theoretical models such as (a) parallel-plate capacitor model (V-Q-x relationship), (b) distance dependent electric field (DDEF) model, to simulate the output performance of triboelectric nanogenerators (TENGs). (c) DDEF model employed to validate the output performance of a silk biomaterial-based TENG.

## Current and Future Challenges



The current and future challenges are dependent on boosting the electrical output of the TENG device with accurate figure-of-merits by the influence of configuring the device parameters. The charges generated in the layers move to the metal electrodes and transfer through the external circuit to balance the potential difference [1]. The parallel plate model can be applied to the TENG devices having the planar configurations, which can be constructed upon two factors such as (1) the generated charges are distributed evenly on the counter materials surface and (2) the electrical field component, which is parallel to the plate should be neglected and there is one electric field perpendicular to the plate inside the dielectric [2]. In this case, the V-Q-x relationship is an important factor for the parallel plate capacitor model of the TENGs.

$$V = -1C(x)Q + V_{oc}(x) \quad V = -1CxQ + VOC(x)$$

Figure 1a shows the dielectric-to-dielectric model sliding mode TENG with the increase of  $x$  (lateral separation direction) the open circuit voltage ( $V_{oc}$ ) between the two electrodes also increases the  $V_{oc}$ - $x$  curve increases higher when  $x$  is approaching  $l$  (longitudinal direction). So, the peaks are higher when  $x=9$  cm, which is shown in Figure 1(a) meaning that the edge effect is more severe when  $x$  approaches to  $l$  [3]. Figure 1b shows the DDEF model with Figure 1(b-i) shows the electric field distribution perpendicular to an infinitely large, charged sheet which is derived from Gauss's law. Figure 1(b-ii) shows the comparison of prediction with the DDEF model compared with the previous models [4]. The DDEF model is further verified by comparing the electrical response of the metal-dielectric TENG reported against the DDEF model shown in Figure 1(b-iii) in which the output from both cases agrees with the DDEF predictions. As shown in Figure 1(c), the electrical output performance of a typical TENG developed through biowaste counter materials like silk cocoons was further validated by the DDEF model, where the electrodes responding to the induced charges on the other side of the triboelectric contact surfaces [5, 6]. The validation of performance was analysed with different silk polymers as a function of their surface area by recording the surface charge density and output current [7]. These studies are well matched with the experimental output performance, it also confirms that the TENGs output increases with an increase in triboelectric material's surface roughness owing to the increased surface area.

### Advances in Science and Technology to Meet Challenges

The challenges may be overcome by adopting proper power transfer equations and parameters in designing the TENG devices. The power transfer equation was used to predict the output behaviour of TENG under the contact separation working model.

$$K(t)_{\text{eff}} = LWG(t) = [1LW\pi(1\epsilon_a + 1\epsilon_b) \int y f(x) dx]^{-1} \quad K(t)_{\text{eff}} = LWG(t) = 1LW\pi 1\epsilon_a + 1\epsilon_b \int y f(x) dx - 1$$

The accuracy of the TENG power transfer equation was evaluated by comparing the output predictions with the DDEF model, and by directly solving the power transfer equation. Figure 2(a-i) describes the parameters of TENG in the power transfer equation [8]. Changing the load resistance causes the impedance ratio to vary and as a result the output current changes according to the change in load resistance, which depicts the relationship which is predicted in the power transfer theorem shown in Figure 2(a-ii).

Another challenge is quantifying the output performance of the TENG by adopting proper FOMs. The FOMs are usually comprised of structural and material FOMs, the corresponding method is described in Figure 2(b). Consider a linear sliding mode TENG in which both the absolute short-circuit transferred charges  $Q_{sc}(x)$  and the absolute open-circuit voltage  $V_{oc}(x)$  at  $x=0$  position are set to be 0. The definitions

of the displacement  $x$  and the two electrodes for an LS-mode TENG are illustrated in Figure 2(b-i). The maxima of  $Q_{SC,max}$  and  $V_{OC,max}$  are expected to be reached at  $x=x_{max}$  for these basic-mode TENGs. From the  $V-Q$  plot, we noticed that the operation of the TENG will go to its steady state after only a few periods as shown in Figure 2(b-ii), and thus we can directly focus on the output of the steady-state operation [9]. In Figure 2(b-iii) we noticed that for each 'cycles for energy output' (CEO), the total cycling charge  $Q_c$  was always less than the maximum transferred charges  $Q_{SC,max}$ , especially for cycles with large external load resistances. If we could maximize the  $Q_c$  to be  $Q_{SC,max}$  for these cycles, the output energy per cycle would be further enhanced. Figure 2(c) shows the force-displacement ( $F-x$ ) plot and voltage-charge ( $V-Q$ ) plot in TENGs with maximum energy output under infinite resistance [10]. The encircled area in  $F-x$  plot equals the mechanical energy input per cycle.

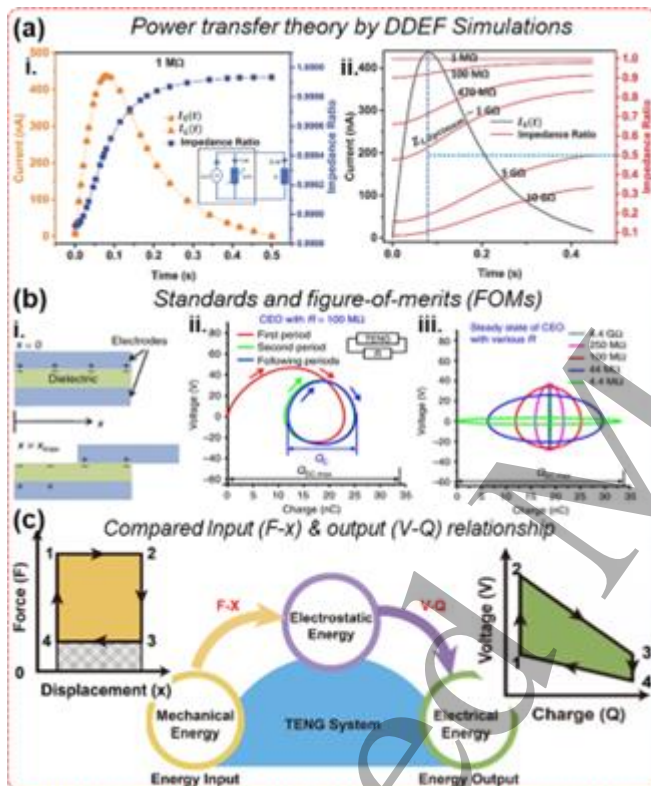


**Figure 2.** (a) Power transfer theory and (b) figure-of-merits studies to predict the output behaviour of TENGs. (c) A theoretical model to compare or simulate the input mechanical energy and derived the energy conversion efficiency of TENGs.

### Concluding Remarks

In summary, the present review briefly introduces the distinct theoretical models. These models are a guide to the optimization of materials and their structural features, fabrication processes, and experimental analysis of the TENGs, which could further be proposed for successful commercialization. The parallel plate capacitor and DDEF models suggest the use in the simulation of planar and non-planar materials-based TENG devices. The power transfer theory with DDEF models suggests the consideration of the impedance of the device and edge effects on counter materials to solve the problems in TENG design. In addition, the influence of triboelectric material's surface roughness in improving the electrical performance of the TENGs is also studied through DDEF and materials figure-of-merits. Supplementing to energy harvesting, TENGs have a great potential to use in Self-powered sensing and IoT applications, which warrants development in theories of working.



#### Acknowledgements

The authors would like to acknowledge the support from the EPSRC research project grant EP/S02106X/1 in providing the funding for this work.

#### References

- [1] Z. L. Wang, "On Maxwell's displacement current for energy and sensors: the origin of nanogenerators," *Materials Today*, vol. 20, no. 2, pp. 74-82, 2017/03/01/ 2017.
- [2] S. Niu *et al.*, "Theory of freestanding triboelectric-layer-based nanogenerators," *Nano Energy*, vol. 12, pp. 760-774, 2015/03/01/ 2015.
- [3] S. Niu *et al.*, "Theory of Sliding-Mode Triboelectric Nanogenerators", *Advanced Materials*, vol. 25, no. 43, pp. 6184-6193, 2013.
- [4] R. D. I. G. Dharmasena *et al.*, "Triboelectric nanogenerators: providing a fundamental framework," *Energy & Environmental Science*, vol. 10, no. 8, pp. 1801-1811, 2017.
- [5] B. Dudem *et al.*, "Wearable Triboelectric Nanogenerator from Waste Materials for Autonomous Information Transmission via Morse Code," *ACS Applied Materials & Interfaces*, vol. 14, no. 4, pp. 5328-5337, 2022/02/02 2022.
- [6] B. Dudem, S. A. Graham, R. D. I. G. Dharmasena, S. R. P. Silva, and J. S. Yu, "Natural silk-composite enabled versatile robust triboelectric nanogenerators for smart applications," *Nano Energy*, vol. 83, p. 105819, 2021/05/01/ 2021.
- [7] B. Dudem *et al.*, "Exploring the theoretical and experimental optimization of high-performance triboelectric nanogenerators using microarchitected silk cocoon films," *Nano Energy*, vol. 74, p. 104882, 2020/08/01/ 2020.
- [8] R. D. I. G. Dharmasena, J. H. B. Deane, and S. R. P. Silva, "Nature of Power Generation and Output Optimization Criteria for Triboelectric Nanogenerators," *Advanced Energy Materials*, vol. 8, no. 31, p. 1802190, 2018.
- [9] Y. Zi, S. Niu, J. Wang, Z. Wen, W. Tang, and Z. L. Wang, "Standards and figure-of-merits for quantifying the performance of triboelectric nanogenerators," *Nature Communications*, vol. 6, no. 1, p. 8376, 2015/09/25 2015.
- [10] G. Xu, X. Li, X. Xia, J. Fu, W. Ding, and Y. Zi, "On the force and energy conversion in triboelectric nanogenerators," *Nano Energy*, vol. 59, pp. 154-161, 2019/05/01/ 2019.

## 5. Materials for Thermoelectric Energy Harvesting

### 5.1 Introduction on Materials for Thermoelectric Energy Harvesting

Mercouri G. Kanatzidis<sup>1</sup> and Hongyao Xie<sup>1</sup>

Department of Materials Science and Engineering, Northwestern University, Evanston, IL, USA

In the past few decades, the realization has set in that over 65% of the energy we generate is wasted in the form of heat and low-cost effective technologies to reduce the losses are desired<sup>1-3</sup>. Thermoelectric materials offer an attractive solution for directly converting thermal energy into electrical power. If they can be successfully employed on a broad scale in waste heat harvesting, they will improve the efficiency of fossil fuel utilization. Moreover, thermoelectric materials can be used to sustainably charge portable/wearable electronics based on the temperature differences found indoors or between the human body and the ambient environment.

A thermoelectric device is a fully solid-state electronic device that can generate electricity from a hot source using the Seebeck effect. Vice versa, electricity can drive a thermoelectric device in reverse to work as a solid-state heat pump for refrigeration through the Peltier effect<sup>4</sup>. Thermoelectric devices are free of moving parts, run quietly, and can have excellent reliability and scalability in size and power. These advantages make it compatible with other energy-conversion technologies<sup>2</sup>.

A typical device utilizing this effect is shown in **Fig. 1a**. It is composed of one pair of n- and p-type thermoelectric materials. When a temperature gradient is applied across a material, the free charge carriers on the hot side absorb energy and tend to diffuse to the cold side. This migration of charge carriers builds up a net charge at the cold side until an equilibrium is reached between the diffusion potential and the electrostatic repulsion caused by the build-up of charge. Thus, an electric potential difference is produced between the hot side and cold side of the material. The performance of thermoelectric materials is defined by the dimensionless figure of merit  $ZT = S^2\sigma T/\kappa$ , where  $S$  is the Seebeck coefficient,  $\sigma$  is the electrical conductivity,  $T$  is the specific operating temperature and  $\kappa$  is the thermal conductivity<sup>5</sup>. The conversion efficiency/ $ZT$  relationship is shown in eq.1. On the other hand, the maximum power conversion efficiency (PCE,  $h$ ) of a thermoelectric device depends on the temperature difference between the hot ( $T_h$ ) and the cold source ( $T_c$ ), as well as the performance of the materials as follows<sup>6</sup>:

$$\eta = \left( \frac{T_h - T_c}{T_h} \right) \left[ \frac{\sqrt{1 + ZT_m} - 1}{\sqrt{1 + ZT_m} + (T_c / T_h)} \right]$$

Here the ratio of the temperature difference between the hot end and the cold end to  $T_h$  is the Carnot efficiency, and the  $ZT_m$  is the average  $ZT$  value between  $T_h$  and  $T_c$ . Thus, in practical applications, a large  $ZT$  averaged over a wide temperature range is more pragmatic than a high maximum  $ZT$  at a narrow temperature range. To make thermoelectrics competitive with other energy generation technologies, an average  $ZT$  value of  $\sim 3$  to 4 is needed<sup>2</sup>. If they are achieved, game-changing conversion efficiencies near 30% or more could be possible. However, although the maximum  $ZT$  values of 3.0 have been reached in such materials as SnSe<sup>7</sup>, the average  $ZT$  for most advanced thermoelectric materials is below 1.0 and the record-high value is about 1.7 in recent reports<sup>8</sup>.

Improving the  $ZT$  value of materials is the key to the thermoelectrics application. Based on the  $ZT$  expression, it is obvious that good thermoelectric materials should have a large Seebeck coefficient ( $S$ ),

1  
2  
3 high electrical conductivity ( $\sigma$ ), and poor thermal conductivity ( $\kappa$ ). The actual scientific challenge is that  
4 these transport properties are strongly interdependent through the carrier concentration ( $n$ ) and the  
5 carrier effective mass ( $m^*$ ), and maximizing one transport parameter would inevitably lead to the  
6 diminishing of the others<sup>6</sup>. On the other hand, the total thermal conductivity is generally composed of the  
7 lattice part ( $\kappa_l$ ) and the electronic part ( $\kappa_e$ ) as  $\kappa = \kappa_l + \kappa_e$ , and increasing the  $\sigma$  would also unavoidably leads  
8 to an increase in the  $\kappa_e$ .<sup>6</sup> Thus, the strong correlation between the heat and electronic transport properties  
9 makes the optimization of the average  $ZT$  challenging. The key to achieving high  $ZT$  values must be a  
10 synergistic optimization of these transport properties by tuning the carrier concentration to an optimized  
11 value, see **Fig. 1b**.  
12  
13

14 In the past two decades, tremendous progress has been made in understanding how to increase  $ZT$   
15 leading to many promising materials, with  $ZT$  values exceeding 2, **Fig. 1c**<sup>4</sup>. The most successful strategies  
16 in improving performance have been those that minimize thermal conductivity. The most well-known is  
17 the formation of in-situ nanostructured inclusions, **Fig. 1g**.<sup>9</sup> This was first demonstrated in the lead  
18 chalcogenide and then has been widely employed in many other material systems as a universally valid  
19 method. Since then, other important strategies have also been proposed to optimize the thermal  
20 conductivity for several specific materials, such as the rattling atom filling, liquid-like lattice, weak  
21 chemical bonding, and recently, the discordant atom doping<sup>3,10</sup>. Moreover, exploiting new materials with  
22 intrinsic low thermal conductivity is always an important research area for thermoelectrics.  
23  
24

25 For electronic property optimization, the most successful concept in the past decades could be the  
26 presence of several electronic bands of the same carrier type near the Fermi energy, also known as  
27 multiband convergence. When all these bands host multiple carrier pockets that participate in the  
28 electronic transport (**Fig. 1h**), they can enhance the Seebeck coefficient and the electrical conductivity<sup>2</sup>.  
29 This band convergence strategy has been widely implemented to achieve high performance, including the  
30 PbTe, PbSe and PbS, Mg<sub>2</sub>(SiSn), SnSe, CoSb<sub>3</sub>, and GeTe to name but a few<sup>2</sup>.  
31  
32

33 Among these compounds, PbTe is an outstanding mid-temperature range thermoelectric material in the  
34 past decades. Because of its unique electronic band structure and the successful application of  
35 nanostructuring strategy<sup>4</sup>, PbTe exhibits a very high thermoelectric performance in both p-type ( $ZT > 2.6$ )  
36 and n-type ( $ZT > 2$ ) forms<sup>1</sup>. On the other hand, the world record of  $ZT$  has recently been pushed to 3.1 by  
37 the SnSe compound. Because of the intrinsic ultralow thermal conductivity and the multiple electronic  
38 band structure. The maximum  $ZT$  value of  $\sim 3.0$  has been obtained in both p-type and n-type SnSe, raising  
39 expectations for SnSe-based thermoelectric devices in the near future<sup>1</sup>.  
40  
41

42 However, to further broaden the application of thermoelectrics and make it a more competitive energy  
43 technology. Future research should not simply focus on improving the maximum  $ZT$  of the material. Other  
44 important challenges that must be addressed are improving the average  $ZT$  of the materials, enhancing  
45 their mechanical strength and thermal stability, raising their toughness and fracture strength, exploring  
46 the approach for large-scale and high-quality material production (**Fig. 1i**), as well as developing the new  
47 device structure and fabrication techniques.<sup>1</sup>  
48  
49  
50  
51  
52  
53  
54  
55  
56  
57  
58  
59  
60

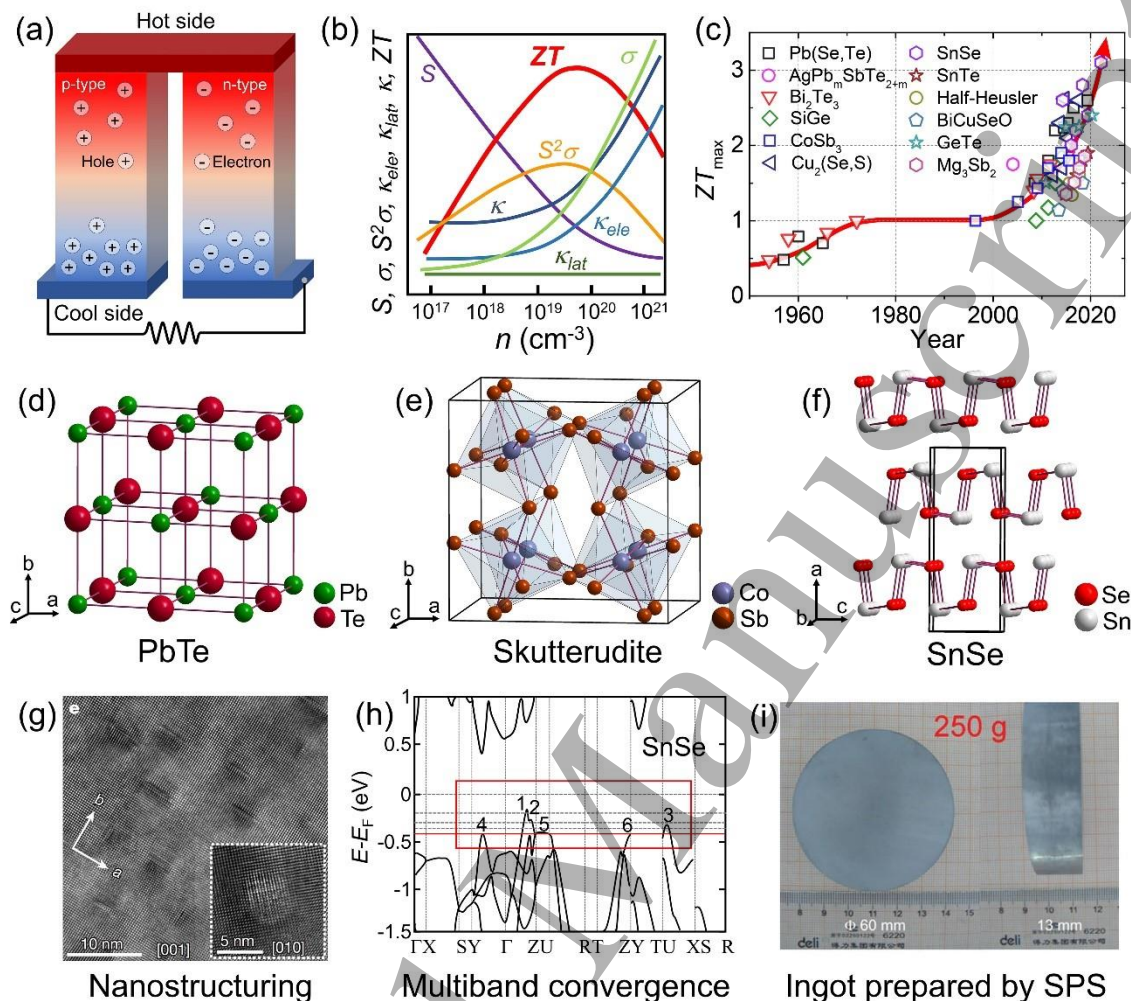


Figure 1 (a) Schematic illustrations of a thermoelectric device for power generation; (b) Schematic diagram showing the  $ZT$  value, and its related parameters change as a function of carrier concentration; (c) Progress timeline of maximum  $ZT$  progress in thermoelectric materials<sup>1</sup>. Crystal structure of (d)  $\text{PbTe}$ , (e) Skutterudite and (f)  $\text{SnSe}$ ; (g) TEM image showing the nanostructure in  $\text{PbTe}$ <sup>9</sup>; (h) The band structure of  $\text{SnSe}$  showing the multiple valence band convergence<sup>7</sup>; (i) Images of an thermoelectric ingot with the diameter of 60 mm and height of 13 mm prepared by SPS<sup>11</sup>.

## References

1. Yan, Q.; Kanatzidis, M. G., High-performance thermoelectrics and challenges for practical devices. *Nat Mater* **2021**.
2. He, J.; Tritt, T. M., Advances in thermoelectric materials research: Looking back and moving forward. *Science* **2017**, 357 (6358).
3. Tan, G.; Zhao, L. D.; Kanatzidis, M. G., Rationally Designing High-Performance Bulk Thermoelectric Materials. *Chemical reviews* **2016**, 116 (19), 12123-12149.
4. Su, X.; Wei, P.; Li, H.; Liu, W.; Yan, Y.; Li, P.; Su, C.; Xie, C.; Zhao, W.; Zhai, P.; Zhang, Q.; Tang, X.; Uher, C., Multi-Scale Microstructural Thermoelectric Materials: Transport Behavior, Non-Equilibrium Preparation, and Applications. *Adv Mater* **2017**.
5. Snyder, G. J.; Toberer, E. S., Complex thermoelectric materials. *Nat Mater* **2008**, 7 (2), 105-114.
6. Goldsmid, H. J., Introduction to Thermoelectricity. Springer Berlin Heidelberg: Heidelberg, 2016.



7. Zhao, L. D.; Lo, S. H.; Zhang, Y.; Sun, H.; Tan, G.; Uher, C.; Wolverton, C.; Dravid, V. P.; Kanatzidis, M. G., Ultralow thermal conductivity and high thermoelectric figure of merit in SnSe crystals. *Nature* **2014**, *508* (7496), 373-7.
8. Su, L.; Wang, D.; Wang, S.; Qin, B.; Wang, Y.; Qin, Y.; Jin, Y.; Chang, C.; Zhao, L.-D., High thermoelectric performance realized through manipulating layered phonon-electron decoupling. *Science* **2022**, *375* (6587), 1385-1389.
9. Biswas, K.; He, J.; Blum, I. D.; Wu, C. I.; Hogan, T. P.; Seidman, D. N.; Dravid, V. P.; Kanatzidis, M. G., High-performance bulk thermoelectrics with all-scale hierarchical architectures. *Nature* **2012**, *489* (7416), 414-8.
10. Zheng, Y.; Slade, T. J.; Hu, L.; Tan, X. Y.; Luo, Y.; Luo, Z. Z.; Xu, J.; Yan, Q.; Kanatzidis, M. G., Defect engineering in thermoelectric materials: what have we learned? *Chem Soc Rev* **2021**, *50* (16), 9022-9054.
11. Zheng, G.; Su, X.; Li, X.; Liang, T.; Xie, H.; She, X.; Yan, Y.; Uher, C.; Kanatzidis, M. G.; Tang, X., Toward High-Thermoelectric-Performance Large-Size Nanostructured BiSbTe Alloys via Optimization of Sintering-Temperature Distribution. *Advanced Energy Materials* **2016**, *6* (13), n/a-n/a.

## 5.2 Chalcogenides for thermoelectric energy harvesting

Xiao-Lei Shi and Zhi-Gang Chen

School of Chemistry and Physics, Queensland University of Technology, Brisbane, QLD 4000, Australia

### Status

Chalcogenide-based thermoelectric materials are important members of the thermoelectric family. Conventional thermoelectric chalcogenides such as  $\text{Bi}_2\text{Te}_{3-x}\text{Se}_x$ ,  $\text{Bi}_{2-x}\text{Sb}_x\text{Te}_3$ , and  $\text{PbTe}$ , have been widely applied in thermoelectric devices for various purposes such as commercial thermoelectric modules and radioisotope temperature-difference batteries [1]. In the last few years, a few thermoelectric chalcogenides with high experimental  $ZT$  values of  $>1.5$ , including  $\text{SnX}$ ,  $\text{Cu}_2\text{X}$ ,  $\text{Ag}_2\text{X}$ ,  $\text{ZnX}$ ,  $\text{In}_8\text{X}$ , and  $\text{GeX}$ , have been considerably developed ( $X = \text{S}, \text{Se}, \text{Te}$ ). Especially, some chalcogenides have exhibited outstanding  $ZT$ s of  $>2$  (Figure 1) or even reached  $ZT > 3$  [2, 3]. For example,  $\text{GeTe}$  is a promising material with high  $ZT$ s of  $>2$  within a wide temperature range from 500 K to 800 K, and the reported  $\text{GeTe}$ -based single-leg device showed a high  $\eta$  of 14 % [4].  $\text{Cu}_2\text{Se}$  is one of the most cost-effective thermoelectric materials with high  $ZT$  of up to 2.7 [5], and the reported prototype  $\text{Cu}_2\text{Se}$ -based TED showed a  $\eta$  of 9.1 % [6], indicating great potential for practical applications. High-entropy alloys based on chalcogenides are also rapidly developed with potentially high  $ZT$ s [7].

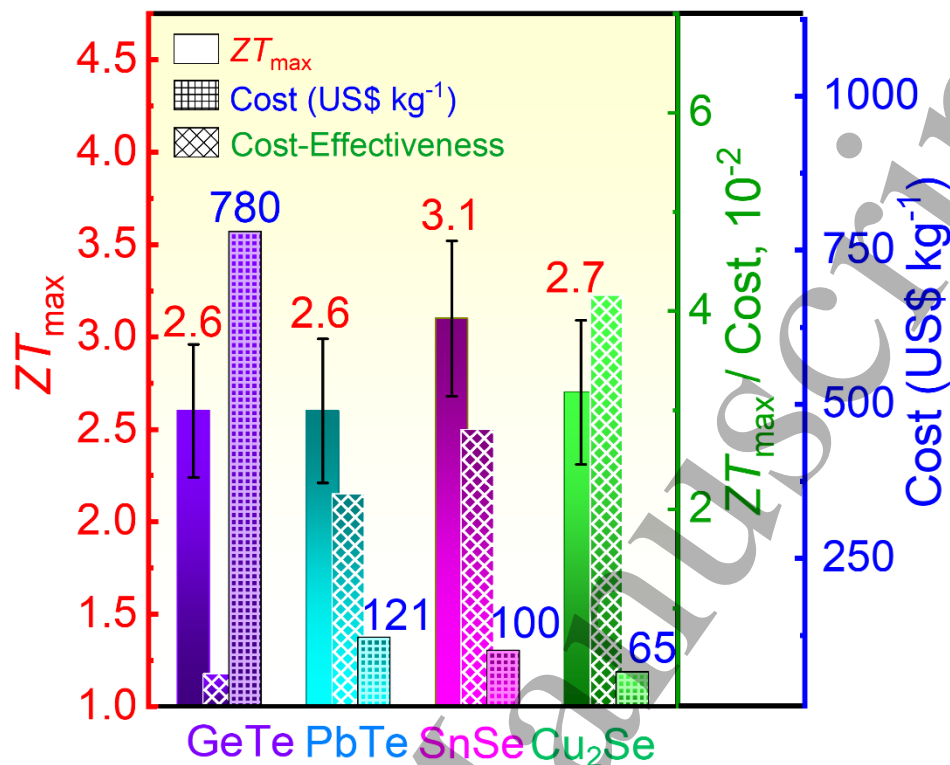


**Figure 1.** Comparison of their maximum  $ZT$  ( $ZT_{max}$ ), cost, and cost-effectiveness of typical chalcogenides [1].

### Current and Future Challenges

The supreme thermoelectric performance of advanced chalcogenides is mainly derived from their manipulable band structures with relatively narrow bandgaps, which are important to achieve high electrical conductivity and Seebeck coefficient. As well, chalcogenides usually exhibit relatively low thermal conductivity due to their unique crystal structures. However, despite their high  $ZT$ s, there is still a huge gap in employing them in practical devices for commercial use. The current and future challenges mainly include: i) low mechanical properties. Compared to other thermoelectric materials such as skutterudites, oxides, half-Heuslers, and silicides, chalcogenides usually exhibit relatively low mechanical properties due to their relatively weak bonding between metal cations and chalcogenide anions [1]. Considering that mechanical robust thermoelectric materials are significant for ensuring performance stability during device service, their mechanical properties must be further improved; ii) high cost. A few high-performing thermoelectric chalcogenides such as GeTe possess high costs derived from the expensive Ge that limits its future applications, therefore some alternatives need to be developed to reduce the cost but keep the high performance; iii) relatively low stability. Some chalcogenides such as Cu<sub>2</sub>Se and SnSe are not stable at very high temperatures because selenium is easily volatile, which limits their applications. Phase transition engineering should be a good resolution, but still needs a long-time attempt; iv) difficulties in applying these advanced chalcogenides into devices. Designing a useful thermoelectric device with both high performance and stability is tricky due to the coupled factors such as topology, structural optimization, electrode material selection, interlayer, n/p-materials pairing, filling material, and the reduction of internal thermal/electrical resistance. Such a device design is especially challenging when using newly developed chalcogenides because most of the above factors need to be re-adapted to exert the high thermoelectric properties of advanced chalcogenides. For example, it is difficult



1  
2  
3 to pair p-type GeTe and Cu<sub>2</sub>Se with suitable n-type legs in the devices because it is considerably difficult  
4 to realize n-type GeTe and Cu<sub>2</sub>Se with similar ZTs to their p-type counterparts. Therefore, considering the  
5 discussed challenges, developing practical thermoelectric devices composed of newly developed  
6 advanced chalcogenides is still a long way to go.  
7

### 8 **Advances in Science and Technology to Meet Challenges**

9 To achieve the goal of developing high-performance, cost-effective, and mechanical robust thermoelectric  
10 chalcogenides and related devices, there are many advances in science and technology to meet the  
11 challenges discussed above, as summarized below and in **Figure 2**:  
12  
13

14 1. Further improving the thermoelectric performance of chalcogenides to enhance the performance of  
15 their devices. Various band manipulation approaches such as alloying and doping with secondary  
16 elements/compounds can be applied to enhance the power factors by tuning appropriate electrical  
17 transport properties [8], and structure engineering can be used to strengthen the multi-wavelength  
18 phonon scattering and in turn, suppress the thermal conductivity [9]. Computational methods such as  
19 modelling and first-principles have been employed to design thermoelectric chalcogenides with promising  
20 ZTs or guide the improvement of current thermoelectric chalcogenides [10].  
21  
22

23 2. Boosting the mechanical properties as well as the stability of advanced chalcogenides to enhance the  
24 practical application values of their devices. As discussed above, phase transition engineering by doping  
25 or alloying is a good resolution to tackle the stability issue, while the routes to further improve the  
26 mechanical properties of chalcogenides can be referred to the strengthening mechanisms of conventional  
27 alloys, such as grain refinement, vacancy-induced dispersion hardening, and alloying with carbon  
28 nanotubes to strengthen the adjacent grain bonding like steel-reinforced concretes [1].  
29  
30

31 3. Rationally designing chalcogenides-based thermoelectric devices with both high performance and  
32 stability to meet the requirement of practical applications. Such a design needs to satisfy many coupled  
33 factors, including topological structures, electrode materials, transition layers, n/p-chalcogenides pairing,  
34 fillers, and stability test methods. Fortunately, mature commercial thermoelectric devices composed of  
35 conventional chalcogenides such as Bi<sub>2</sub>Te<sub>3</sub> can provide enough valuable experience to design the new-  
36 generation chalcogenides-based thermoelectric devices, while the rapid developed computational assist  
37 tools such as ANSYS can also help guide the device designs in terms of the electrical/thermal transport.  
38  
39

40 4. Broadening the types of chalcogenides-based thermoelectric devices for various application scenarios.  
41 In addition to conventional solid-state thermoelectric devices, high-performing chalcogenides can be  
42 developed to fabricate miniature or flexible/wearable thermoelectric devices, which target various  
43 application scenarios such as sustainably charging low-grade wearable electronics, or realize solid-state  
44 localized chip thermal management.  
45  
46  
47  
48  
49  
50  
51  
52  
53  
54  
55  
56  
57  
58  
59  
60

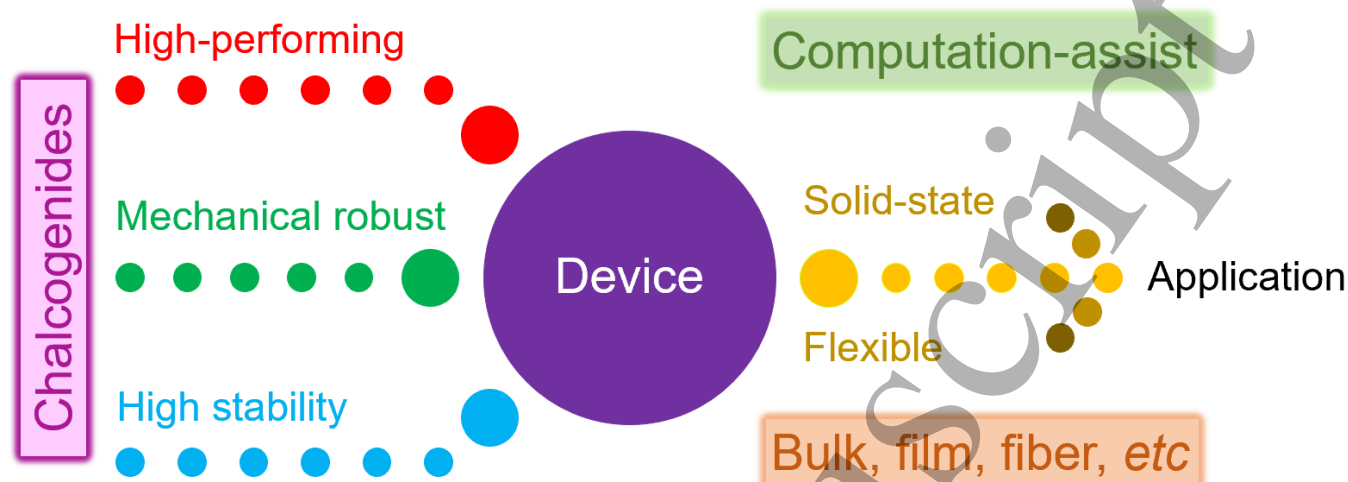


**Figure 2.** Key words for outlooks of designing high-performance, cost-effective, and mechanical robust thermoelectric chalcogenides and related devices.

### Concluding Remarks

Up to now, the performance of conventional thermoelectric chalcogenides has been considerably improved, while many advanced chalcogenides with significant thermoelectric potential have been newly found and developed, both benefited from the advanced strategies based on electronic band engineering and structural manipulation theories. Although there are still many issues that impede the practical appellations of these advanced chalcogenides in devices such as stability, mechanical property, and high cost, most of these challenges are expected to be resolved soon based on the already established knowledge and experience in device engineering as well as the continuously developed techniques from physics, chemistry, engineering, computer science, and data science.

### Acknowledgements

The authors thank the financial support from the Australian Research Council, QUT capacity building professor program, and HBIS-UQ Innovation Centre for Sustainable Steel (ICSS) project.

### References

- [1] Shi X-L, Zou J and Chen Z-G Advanced Thermoelectric Design: From Materials and Structures to Devices *Chem. Rev.* **120** 7399-515
- [2] Zhou C *et al* Polycrystalline SnSe with a thermoelectric figure of merit greater than the single crystal *Nat. Mater.* **20** 1378-84
- [3] Su L *et al* High thermoelectric performance realized through manipulating layered phonon-electron decoupling *Science* **375** 1385-9
- [4] Bu Z *et al* Realizing a 14% single-leg thermoelectric efficiency in GeTe alloys *Sci. Adv.* **7** eabf2738
- [5] Yang D *et al* Blocking Ion Migration Stabilizes the High Thermoelectric Performance in  $\text{Cu}_2\text{Se}$  Composites *Adv. Mater.* **32** 2003730
- [6] Qiu P *et al* High-Efficiency and Stable Thermoelectric Module Based on Liquid-Like Materials *Joule* **3** 1538-48
- [7] Jiang B *et al* High-entropy-stabilized chalcogenides with high thermoelectric performance *Science* **371** 830-4

- 1  
2  
3 [8] Pei Y, Shi X, LaLonde A, Wang H, Chen L and Snyder G J Convergence of Electronic Bands for High  
4 Performance Bulk Thermoelectrics *Nature* **473** 66-9  
5 [9] Zheng Y *et al* Defect engineering in thermoelectric materials: what have we learned? *Chem. Soc.*  
6 *Rev.* **50** 9022-54  
7 [10] Yang J *et al* On the Tuning of Electrical and Thermal Transport in Thermoelectrics: An Integrated  
8 Theory-Experiment Perspective *npj Comput. Mater.* **2** 15015  
9

### 11 5.3 - Full-Heuslers for thermoelectric energy harvesting

12 Alexander Riss<sup>1</sup>, Michael Parzer<sup>1</sup>, Fabian Garmroudi<sup>1</sup> and Ernst Bauer<sup>1</sup>  
13 Institute of Solid-State Physics, TU Wien, A-1040 Wien, Austria  
14  
15

#### 16 Status

17 In 1905, Friedrich Heusler submitted a manuscript entitled “Über magnetische Manganlegierungen”,  
18 where he first demonstrated that three non-magnetic elements (Cu, Mn, Al) form a ferromagnetic  
19 material in the  $X_2YZ$  stoichiometry [1]. Since then, thousands of cubic  $X_2YZ$  full-Heusler (FH) and XYZ half-  
20 Heusler (HH) compounds have been found, as their unique and simple crystal structure allows to host a  
21 large range of elements from the periodic table. As a result, Heusler compounds represent a material class  
22 which exhibits a multitude of interesting physical phenomena and tunable properties, such as band  
23 topology, half-metallicity, superconductivity or thermoelectricity. It was demonstrated that for both FH  
24 and HH compounds, the electronic properties are strongly dependent on the valence electron  
25 concentration  $n_v$ . The Slater-Pauling rule states that Heusler compounds with  $n_v = 6$  are non-magnetic  
26 semiconductors. Following this rule, many HH semiconductors were identified, with gap sizes up to several  
27 eV, making them excellent candidates for thermoelectric explorations, whereas FH compounds have been  
28 mostly studied with respect to their peculiar magnetic properties and half-metallicity [2]. Previously,  
29 however, the discoveries of a giant anomalous Nernst effect in several FH compounds sparked enormous  
30 interest [3]. While numerous FH semiconductors with excellent thermoelectric performance have been  
31 predicted theoretically, experiments so far identified only semi-metallic  $Fe_2VAl$  as a potential  
32 thermoelectric material.  
33  
34  
35

36  
37 Already in the early 2000s, Nishino and co-workers obtained large values of the Seebeck coefficient  $S$  and  
38 power factor  $PF$  in  $Fe_2VAl$  which they attributed to a deep pseudo gap in the vicinity of the Fermi energy  
39  $E_F$  [4]. Over the years, doping studies showed that the position of  $E_F$  of  $Fe_2VAl$  can be readily tuned by  
40 changing the carrier concentration  $n$ , depicted as black circles in Fig.1. Only recently, it has been  
41 demonstrated that the electronic structure itself can be severely modified, exhibiting remarkable tune-  
42 ability. By either opening the band gap [5] or incorporating narrow resonant or semi-localized impurity  
43 states at  $E_F$  [6,7], the Seebeck coefficient was significantly enhanced, compared to the conventional  $S(n)$   
44 behaviour (see coloured symbols, deviating from the black solid line in Fig.1). Consequently,  
45 thermoelectric power factors, 2 – 3 times larger than those of optimised  $Bi_2Te_3$  systems in the 0 – 100 °C  
46 range, have been achieved [5].  
47  
48  
49  
50  
51  
52  
53  
54  
55  
56  
57  
58  
59  
60

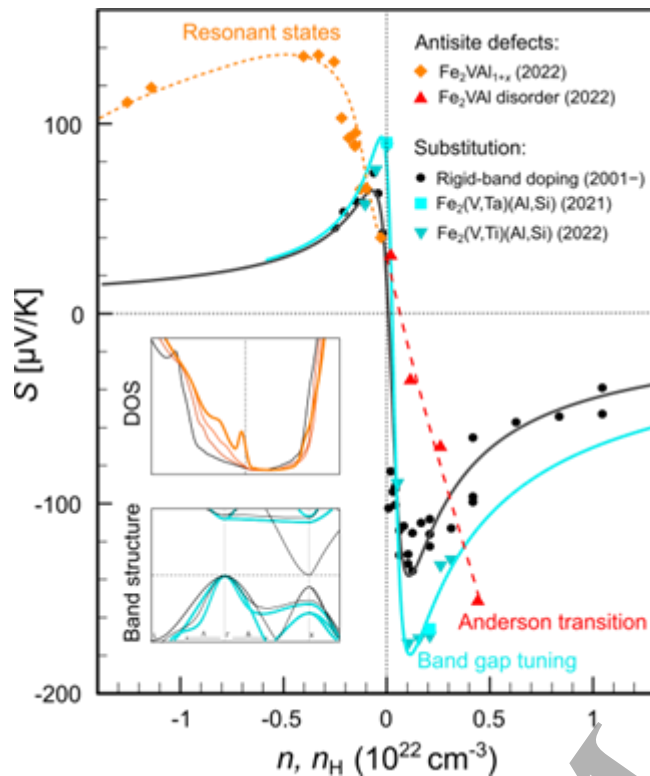


**Figure 1.** Carrier concentration dependence of the Seebeck coefficient of  $\text{Fe}_2\text{VAI}$ -based full-Heusler compounds. Black circles represent conventional doping studies, whereas colored symbols depict recent developments, tuning the electronic structure. Solid and dashed lines are guides to the eye. Insets show exemplary modifications of the density of states (DOS) and band structure features.

### Current and Future Challenges

Although FH systems possess excellent power factors (see Fig.2a), well above those of other state-of-the-art thermoelectric materials, and exhibit excellent mechanical and chemical properties, the overall thermoelectric performance of FHs is suffering from their large thermal conductivity,  $\kappa$ , prevalent in most of the FH family members. This is primarily a result of the simple crystal structure and stiff lattice, reflected in high values of the sound velocity  $v_s$ . As an example,  $\text{Fe}_2\text{VAI}$  demonstrates an average  $v_s = 5500$  m/s, while the sound velocity of  $\text{Bi}_2\text{Te}_3$  is  $v_s = 1750$  m/s, leading to a lattice thermal conductivity,  $\kappa_{\text{ph}}$ , being intrinsically at least 3 times larger for the FH compound.

Disorder and substitutions can lower  $\kappa_{\text{ph}}$  owing to scattering processes originated from mass and volume differences of the various ions on the respective lattice sites [8]. Reducing the dimensionality of FH compounds by thin film deposition or manipulating the nano- and microstructure can further decrease  $\kappa_{\text{ph}}$ . As shown in Fig.2b,  $\kappa_{\text{ph}}$  drops, from about  $25 \text{ Wm}^{-1}\text{K}^{-1}$  in pristine  $\text{Fe}_2\text{VAI}$ , to around  $4 \text{ Wm}^{-1}\text{K}^{-1}$  for severe off-stoichiometry [6] or heavy-element substitution [8], around  $2 \text{ Wm}^{-1}\text{K}^{-1}$  for thin films [9] and even down to  $1.2 \text{ Wm}^{-1}\text{K}^{-1}$  for severe plastic deformation [10]. However, the total thermal conductivities are still several times larger than those of other high-performance thermoelectric materials, owing to a sizeable electronic contribution  $\kappa_{\text{el}}$ , hindering the realization of high  $ZT$  values ( $ZT_{\text{max}} \approx 0.4$ ) [10]. A future challenge to improve  $ZT$  will therefore be to combine the novel electronic enhancement concepts for increasing the Seebeck coefficient with the above-mentioned strategies to substantially reduce  $\kappa_{\text{ph}}$ .

Apart from  $\text{Fe}_2\text{VAI}$ -based FH systems, current and future challenges involve the experimental realization of other theoretically predicted FH compounds with semiconducting properties. For instance, Fe-based

full-Heuslers, such as  $\text{Fe}_2\text{YZ}$  ( $Y = \text{Ti, Zr, Hf}$ ;  $Z = \text{Si, Ge, Sn}$ ) [11] and  $\text{Fe}_2\text{TaZ}$  ( $Z = \text{Al, Ga, In}$ ) [12] have been predicted to be semiconductors with very promising thermoelectric properties. Moreover, ultralow thermal conductivities and  $ZT = 2 - 5$  were predicted theoretically for a novel class of full-Heusler semiconductors  $\text{X}_2\text{YZ}$  ( $X = \text{Ca, Sr, Ba}$ ;  $Y = \text{Au, Ag}$ ;  $Z = \text{Sn, Pb, As, Sb, Bi}$ ) [13,14]. These predictions have yet to be confirmed experimentally.

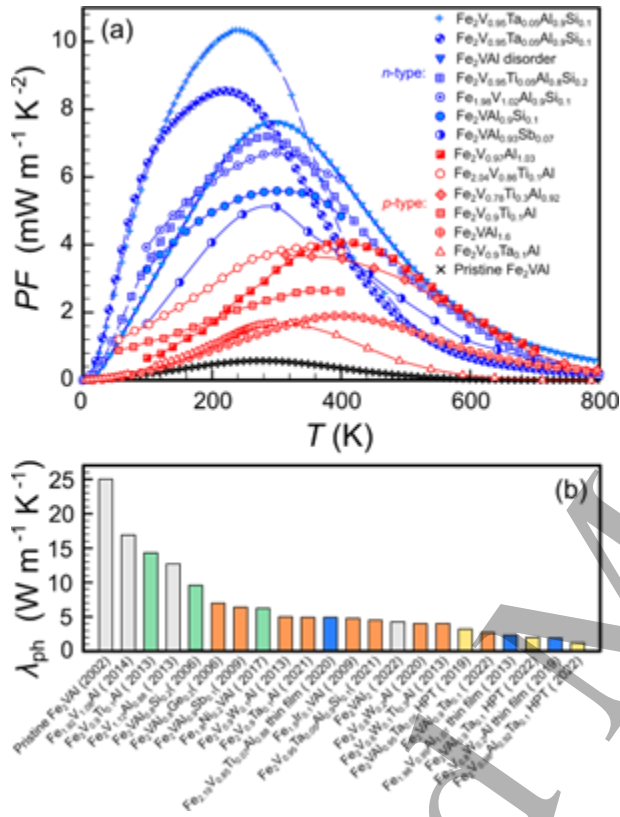


**Figure 2.** (a) Comparison of temperature-dependent power factors for  $p$ - and  $n$ -type  $\text{Fe}_2\text{VAI}$ -based full-Heusler compounds. (b) Room temperature lattice thermal conductivities of  $\text{Fe}_2\text{VAI}$  reduced by off-stoichiometry (grey), (heavy-)element substitution (green and orange), thin film deposition (blue) as well as nano-structuring via high-pressure torsion (yellow).

### Advances in Science and Technology to Meet Challenges

Record-high values of  $PF$  and  $ZT$  values have been recently reported for  $\text{Fe}_2\text{VAI}$ -based FH compounds, and new enhancement concepts were proposed over the last couple of years. In 2019, Hinterleitner et al. reported  $ZT > 5$  in a metastable Heusler thin film, due to a severe reduction of  $I_{\text{ph}}$  and an anomalously large Seebeck effect [9]. In the same year, Tsuji et al. showed that spin fluctuations can be utilized to increase the Seebeck coefficient of ferromagnetic Heusler alloys [15]. In 2022, Fukuta et al. demonstrated that high-pressure torsion is an effective and reproducible tool to reduce the grain size of  $\text{Fe}_2\text{VAI}$ -based systems towards the nanoscale, resulting in record-low values of  $I_{\text{ph}}$  [10]. Shortly after, Parzer et al. found ultrahigh solubility of Al antisites, leading to low  $I_{\text{ph}}$  and simultaneously to a promising enhancement of the Seebeck coefficient due to resonant states [6]. Later that year, Garmroudi et al. proposed a disorder-driven Anderson transition in an impurity band as a novel route to obtain high thermoelectric performance in  $\text{Fe}_2\text{VAI}$  [7]. This was achieved by an innovative approach of freezing the high-temperature disordered structure via thermal quenching. Both the deposition of thin films as well as the rapid thermal quenching technique can also be explored to potentially stabilize other FH-based semiconductor phases (see

previous section) with theoretically promising thermoelectric properties that have not yet been experimentally realized.

In addition, recent progress in fundamental thermoelectric research has identified significantly reduced Lorenz numbers  $L$  and violations of the Wiedemann-Franz (WF) law as a means of reducing the electronic part of the thermal conductivity  $\kappa_{el}$  in several nano-structured systems but also in topological materials. For instance, it has been estimated that  $L$  decreases by almost an order of magnitude in the ferromagnetic Weyl semimetal FH compound  $\text{Co}_2\text{MnAl}$  [16]. Since FH compounds often also have intrinsically large values of  $\kappa_{el}$  in addition to  $I_{ph}$ , violations of the WF law can be an especially promising approach to tackle the issue of high thermal conductivities in this material class. Upcoming research on full-Heusler thermoelectric materials would have a successful breakthrough if the electronic tuning concepts discussed in this review as well as a further reduction of  $I$  can be combined effectively.

### Concluding Remarks

Full-Heusler thermoelectric materials based on  $\text{Fe}_2\text{VAl}$  turn out to bear large potentials for being used in the 100°C temperature range for power generation, cooling, or wireless sensing in near future, thereby supersede today's commercially available materials based on  $\text{Bi}_2\text{Te}_3$ . Superior power factors and excellent mechanical properties, the easy synthesis and the non-poisonous and reasonably priced constituting elements, as well as their respective abundance will outplay  $\text{Bi}_2\text{Te}_3$  in this temperature regime, where globally the largest share of waste heat accumulates.

The flexibility of tuning the electronic structure of FHs, such as the band gap size or the density of states effective charge carrier mass and promising theoretical predictions concerning other FH compounds, which still remain to be experimentally verified, are outstanding assets of FHs. These encouraging results motivate further research on combining the established electronic-engineering and nano-structuring strategies – thus paving the road towards high  $ZT$  in full-Heusler systems.

### Acknowledgements

We thank the Japan Science and Technology Agency (JST), program MIRAI, JPMJMI19A1 and the Austrian Christian Doppler Laboratory for Thermoelectricity for financial support.

### References

- [1] Heusler F. (1903). "Über magnetische Manganlegierungen". Verhandlungen der Deutschen Physikalischen Gesellschaft (in German). 12: 219.
- [2] Graf, Tanja, Claudia Felser, and Stuart SP Parkin. "Simple rules for the understanding of Heusler compounds." Progress in Solid State Chemistry 39.1 (2011): 1-50.
- [3] Sakai, Akito, et al. "Giant anomalous Nernst effect and quantum-critical scaling in a ferromagnetic semimetal." Nature Physics 14.11 (2018): 1119-1124.
- [4] Nishino, Yoichi, et al. "Effect of off-stoichiometry on the transport properties of the Heusler-type  $\text{Fe}_2\text{VAl}$  compound." Physical Review B 63.23 (2001): 233303.
- [5] Garmroudi, Fabian, et al. "Large thermoelectric power factors by opening the band gap in semimetallic Heusler alloys." Materials Today Physics (2022): 100742.
- [6] Parzer, Michael, et al. "High solubility of Al and enhanced thermoelectric performance due to resonant states in  $\text{Fe}_2\text{VAl}_x$ ." Applied Physics Letters 120.7 (2022): 071901.
- [7] Garmroudi, Fabian, et al. "Anderson transition in stoichiometric  $\text{Fe}_2\text{VAl}$ : high thermoelectric performance from impurity bands. Nature Communications 13 (2022): 3599.
- [8] Hinterleitner, B., et al. "Stoichiometric and off-stoichiometric full Heusler  $\text{Fe}_2\text{V}_{1-x}\text{W}_x\text{Al}$  thermoelectric systems." Physical Review B 102.7 (2020): 075117.



- [9] Hinterleitner, B., et al. "Thermoelectric performance of a metastable thin-film Heusler alloy." *Nature* 576.7785 (2019): 85-90.
- [10] Fukuta, Kodai, et al. "Improving thermoelectric performance of Fe<sub>2</sub>VAl-based Heusler compounds via high-pressure torsion." *Applied Physics A* 128.3 (2022): 1-8.
- [11] Bilc, Daniel I., et al. "Low-dimensional transport and large thermoelectric power factors in bulk semiconductors by band engineering of highly directional electronic states." *Physical Review Letters* 114.13 (2015): 136601.
- [12] Khandy, Shakeel Ahmad, et al. "A case study of Fe<sub>2</sub>TaZ (Z= Al, Ga, In) Heusler alloys: hunt for half-metallic behavior and thermoelectricity." *RSC advances* 8.71 (2018): 40996-41002.
- [13] He, Jiangang, et al. "Ultralow thermal conductivity in full Heusler semiconductors." *Physical Review Letters* 117.4 (2016): 046602.
- [14] Wang, Shao-Fei, et al. "Intrinsic Ultralow Lattice Thermal Conductivity in the Full-Heusler Compound Ba<sub>2</sub>AgSb." *Physical Review Applied* 17.3 (2022): 034023.
- [15] Tsujii, Naohito, et al. "Observation of enhanced thermopower due to spin fluctuation in weak itinerant ferromagnet." *Science Advances* 5.2 (2019): eaat5935.
- [16] Robinson, Robert A., et al. "Large violation of the Wiedemann–Franz law in Heusler, ferromagnetic, Weyl semimetal Co<sub>2</sub>MnAl." *Journal of Physics D: Applied Physics* 54.45 (2021): 454001.

## 5.4 Half Heuslers for Thermoelectric Energy Harvesting

Duncan Zavanelli, Madison K. Brod, Muath Al Malki, G. Jeffrey Snyder

Department of Materials Science and Engineering, Northwestern University, Evanston, IL, USA

### Status

There are many classes of materials that are currently pursued as promising thermoelectric (TE) materials. The focus of most of these studies is improving the material figure of merit,  $zT$ , as a proxy for device efficiency. One promising group of potential materials are the half Heusler (hH) alloys with the formula XYZ, where X and Y are transition metals and Z is an element in the p block. The structure of HH alloys is shown in Figure 1 along with the  $zT$ s of state-of-the-art alloys. The current best performance gives  $zT$  values of up to 1.5 at high temperatures, showing excellent TE performance competitive with other materials. [1] These  $zT$  values arise from very large power factors, with alloying crucial to reduce thermal conductivity ( $\kappa$ ). [1] Current alloying strategies focus on increasing mass contrast to reduce  $\kappa$ , leading to high performance in alloys such as Ta<sub>x</sub>V<sub>1-x</sub>FeSb and Zr<sub>x</sub>Hf<sub>1-x</sub>NiSn. [1] Their high-power factors make hHs attractive for applications where total  $\kappa$  is fixed by geometric constraints.

Beyond their  $zT$ s, hH alloys provide other advantages over other TE systems that make them more important than just their  $zT$ . Other thermoelectric materials, such as PbTe, have limited usage despite reported  $zT$ s much higher than can be obtained with hHs. This is often a result of the inherent brittleness of many semiconductors, or a limited temperature range prohibiting high  $\Delta T$  values. hH alloys have been shown to have the highest creep resistance of all measured TE materials as well as excellent thermal stability [1,2]. As a result, HH alloys have their niche as the usable TE materials that have a unique combination of non-TE properties that make them much more practical than other materials. This ensures that they remain of great interest despite not being able to reach with some of the recently reported  $zT$ s of greater than 2 in other materials such as SnTe or PbTe. Future work into hH alloys is poised to focus on further understanding and optimizing the electronic structures, microstructures, alloying strategies, and mechanical properties of these alloys.

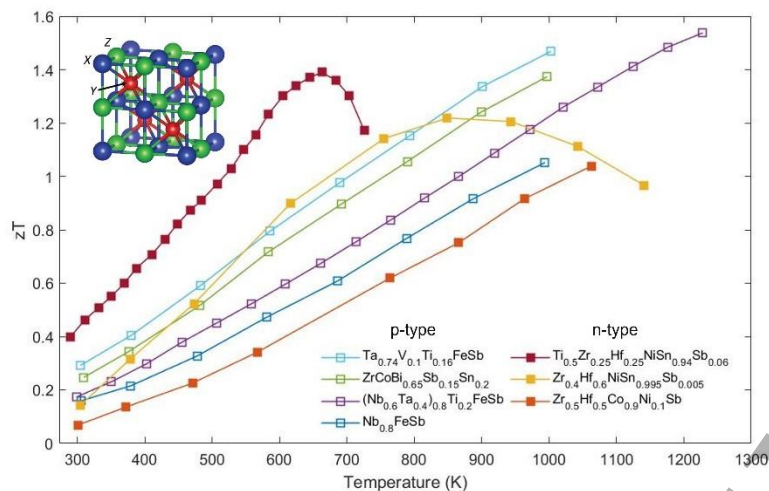


**Figure 1.**  $zT$  of highest performing p type and n type hH alloys from R. Quinn et al. [1] with an insert showing the hH structure adapted from Brod et al.. [6]

### Current and Future Challenges

The biggest challenge facing hH alloys is their comparatively poor TE performance in relation to current high performing materials. A promising route for improvement for both n-type and p-type hH thermoelectrics is via band engineering through alloying. Band engineering can improve the valley degeneracy,  $NV$ , of hH alloys.  $N$  is a characteristic of an electronic dispersion that describes the number of carrier pockets that contribute to electronic transport, and higher values of  $NV$  lead to better performance. Electronic bands with higher  $NV$  require band extrema at lower symmetry points in the Brillouin zones (BZ) of higher symmetry crystals and convergence between band extrema at different (or the same)  $k$ -points in the BZ [3].

There are opportunities to achieve high  $NV$  in both n-type and p-type hH thermoelectrics. For hH alloys, there are two competing CBMs at the X-point and three possible locations for the VBM at different  $k$ -points,  $\Gamma$ , L or W [4-6]. There are three symmetrically equivalent X-points, four L-points, six W-points, and one  $\Gamma$ -point in the BZ of an fcc crystal. Thus, the valley degeneracy of the CB edge can be improved engineering the bands such that the two competing CBMs at X are converged in energy, and the valley degeneracy of the VB edge can be improved by promoting a VBM at L or (ideally) W rather than at  $\Gamma$ , and/or by converging multiple of the competing VBMs. [5,6].

High-throughput DFT studies have discovered chemical trends describing the relative energy of the competing CBMs and VBMs that can help predict both end-member compounds and solid-solution alloys that have high  $NV$  based on the group number (valence) or electronegativity of the X, Y, and Z sites [4,5]. In alloys, the average group number difference can be tuned through aliovalent substitutions, while both aliovalent and isoelectronic substitutions can be used to tune the electronegativities. The chemical guidelines for engineering high  $NV$  can be understood by studying the chemical bonding that dominates the band edges [6]. Thus, the current challenge for improving hH alloys is to predict and synthesize these alloys predicted to have enhanced  $NV$ , such as p-type NbCoSn.

### Advances in Science and Technology to Meet Challenges

Along with the band engineering approach outlined above, alloying and microstructure strategies are needed to further reduce  $\kappa$  and optimize electronic properties. From Figure 1, the highest performing hH

alloys contain alloying elements, such as Ta on the Nb site in NbFeSb [1]. While many alloys have been explored, there are opportunities for systematic probes of the large compositional space open to hH alloys. Computational work has emerged to present alloy strategies, particularly showing that increasing the number of alloying elements does not necessarily lead to further reductions in  $\kappa$ . [7] The alloying elements need to increase mass contrast on a sublattice to reduce  $\kappa$ . These strategies could be combined with high throughput methods to rapidly screen promising compositions and discover optimal stoichiometries. However, this approach can be complicated by the presence of significant site disorder, particularly on the interstitial site, seen in hHs like ZrNiSn. [8]

Aside from alloying, hH alloy performance can be improved through microstructural understanding and control. Recent studies have shown dopant segregation to grain boundaries (GB) in hH alloys, with corresponding reduction of GB scattering. For example, Pt dopants in NbCoSn segregate to GBs, increasing the room temperature weighted mobility. [9] Dopant segregation can be used as a tool to enable GBs to reduce  $\kappa$  without harming electrical transport.

Until the performance of hH alloys is improved, their main advantage as TE materials is their mechanical properties. Superseding other classes of thermoelectric materials, hHs are known for their mechanical robustness and thermal stability in the mid-high temperature range.[10] This is depicted in high resistance to elastic deformation (average Young's modulus  $\sim 187$  GPa)[10] and the best reported creep resistance in TE materials (see Figure 2).[2] However, hH alloys, among most of the thermoelectric materials, lack the required fracture resistance that is essential to minimize the impact of expanding cracks initiated during processing or operation of the thermoelectric. Toughening mechanisms established for brittle ceramics, including fiber bridging, transformation toughening and crack tortuosity, can be applied to hHs, and thermoelectric materials in general, to enhance its fracture toughness without compromising the electronic properties.

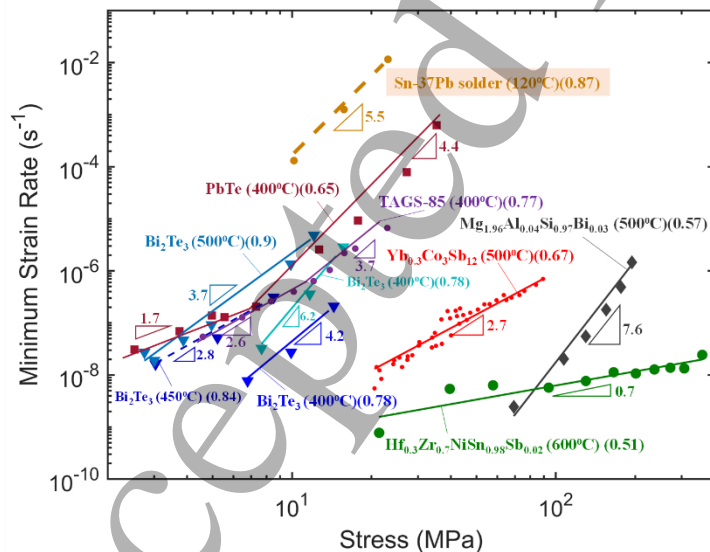


**Figure 2.** Comparison of creep rates between the hH ZrNiSn and other TE materials. Reproduced based on Malki et al. [2]

## Concluding Remarks

Half Heusler alloys feature competitive thermoelectric properties, as well as a path for further improvements through engineering their band structure. Despite not quite matching the current best reported  $zT$  values, the other inherent advantages of hH alloys make them the target of considerable interest for designing full thermoelectric modules. Their mechanical stability makes them more inherently usable than most brittle thermoelectrics. However, the high operating temperatures of half Heusler modules and resulting thermal stresses means there are challenges in creating stable robust modules. In summary, the current and past research has identified several high performing hH alloys based on NbFeSb and ZrNiSn and highlighted their anomalously good mechanical properties for TE materials. Future work should concentrate on further improving these alloys through band engineering strategies as well as improving the module stability with toughening strategies and an investigation of the interfaces between hHs and other components.

### Acknowledgements

D.Z., M.M, M.K.B. and G.J.S. acknowledge support from “Accelerated Discovery of Compositionally Complex Alloys for Direct Thermal Energy Conversion”, DOE Award DE-AC02-76SF00515 and award 70NANB19H005 from U.S. Department of Commerce, National Institute of Standards and Technology as part of the Center for Hierarchical Materials Design (CHi-MaD)

### References

1. R. J. Quinn and J.-W. G. Bos, “Advances in half-Heusler Alloys for thermoelectric power generation,” *Materials Advances*, vol. 2, no. 19, pp. 6246–6266, 2021. DOI:10.1039/D1MA00707F
2. M. Al Malki, X. Shi, P. Qiu, G. J. Snyder, and D. C. Dunand, “Creep behavior and post-creep thermoelectric performance of the N-type skutterudite alloy  $\text{yb}_0.3\text{co}_4\text{sb}_{12}$ ,” *Journal of Materiomics*, vol. 7, no. 1, pp. 89–97, 2021. DOI: 10.1016/j.jmat.2020.07.012
3. A. Zevalkink, D. M. Smiadak, J. L. Blackburn, A. J. Ferguson, M. L. Chabinyk, O. Delaire, J. Wang, K. Kovnir, J. Martin, L. T. Schelhas, T. D. Sparks, S. D. Kang, M. T. Dylla, G. J. Snyder, B. R. Ortiz, and E. S. Toberer, “A practical field guide to thermoelectrics: Fundamentals, synthesis, and characterization,” *Applied Physics Reviews*, vol. 5, no. 2, p. 021303, 2018. DOI: 10.1063/1.5021094
4. S. Guo, S. Anand, M. K. Brod, Y. Zhang, and G. J. Snyder, “Conduction band engineering of half-Heusler thermoelectrics using orbital chemistry,” *Journal of Materials Chemistry A*, vol. 10, no. 6, pp. 3051–3057, 2022. DOI: 10.1039/d1ta09377k
5. M. T. Dylla, A. Dunn, S. Anand, A. Jain, and G. J. Snyder, “Machine Learning Chemical Guidelines for engineering electronic structures in half-Heusler Thermoelectric Materials,” *Research*, vol. 2020, pp. 1–8, 2020. DOI: 10.34133/2020/6375171
6. M. K. Brod, S. Anand, and G. J. Snyder, “The importance of avoided crossings in Understanding High Valley degeneracy in half-Heusler Thermoelectric semiconductors,” *Advanced Electronic Materials*, vol. 8, no. 4, p. 2101367, 2022 DOI: 10.1002/aelm.202101367
7. R. Gurunathan, S. Sarker, C. Borg, J. Saal, L. Ward, A. Mehta, G. J. Snyder, “Mapping Thermoelectric Transport in a Multicomponent Alloy Space,” arXiv:2205.01520, 2022 DOI:10.48550/arXiv.2205.01520
8. H.-H. Xie, J.-L. Mi, L.-P. Hu, N. Lock, M. Chirstensen, C.-G. Fu, B. B. Iversen, X.-B. Zhao, and T.-J. Zhu, “Interrelation between atomic switching disorder and thermoelectric properties of ZRNiSn half-Heusler compounds,” *CrystEngComm*, vol. 14, no. 13, p. 4467, 2012. DOI:10.1039/C2CE25119A
9. T. Luo, F. Serrano-Sánchez, H. Bishara, S. Zhang, R. Bueno Villoro, J. J. Kuo, C. Felser, C. Scheu, G. J. Snyder, J. P. Best, G. Dehm, Y. Yu, D. Raabe, C. Fu, and B. Gault, “Dopant-segregation to grain boundaries controls electrical conductivity of N-Type NbCo(PT)Sn half-Heusler alloy mediating thermoelectric performance,” *Acta Materialia*, vol. 217, p. 117147, 2021. DOI: 10.1016/j.actamat.2021.117147

10. G. Rogl, A. Grytsiv, M. Gürth, A. Tavassoli, C. Ebner, A. Wünschek, S. Puchegger, V. Soprunyuk, W. Schranz, E. Bauer, H. Müller, M. Zehetbauer, and P. Rogl, "Mechanical properties of half-Heusler Alloys," *Acta Materialia*, vol. 107, pp. 178–195, 2016. DOI: 10.1016/j.actamat.2016.01.031

## 5.5 Clathrates for thermoelectric energy harvesting

Kirill Kovnir<sup>1,2</sup> and Susan M. Kauzlarich<sup>3</sup>

<sup>1</sup> Department of Chemistry, Iowa State University, Ames, IA 50011, USA

<sup>2</sup> US DOE Ames Laboratory, Ames, IA 50011, USA

<sup>3</sup> Department of Chemistry, University of California Davis, Davis, CA 95616, USA

### Status

Clathrates are cage structures with various guest occupying the centers of 20-28 vertex polyhedra. Inorganic clathrates can be comprised of almost all the elements from the periodic chart and the diversity of structures provide materials with properties ranging from semiconducting to superconducting with applications in energy conversion and storage [1-3]. This brief highlight will focus on thermoelectric energy conversion. Inorganic clathrates can be considered the quintessential "phonon-glass electron-crystal" (PGEC) materials as proposed originally by Slack because the large unit cell covalent framework can provide effective transport of charge carriers while guest atoms in the oversized polyhedra can rattle giving rise to scattering of heat-carrying phonons [4]. The tetrahedrally coordinated clathrate framework suits elements from group 14 well. Filling the clathrate cages with guest ions requires aliovalent substitution in the framework to maintain charge balance (Figure 1A). Conventional clathrates feature group 13 (or lower) and 14 elements in the framework with guest alkali, alkaline-earth, or rare-earth cations. Inverse clathrates host anionic guests from group 16 or 17 inside a framework composed of elements from group 14 and 15 or 16. In these two examples, the frameworks composed of group 13-14 elements can be considered electron deficient, and a cation is necessary to fill the guest sites, whereas in frameworks containing group 14-15 elements, an anion is necessary to compensate charge. The Si-containing clathrates are earth abundant lightweight compounds where the guest cation can have significant impact on the structure and properties. Depending on polyhedral cage types and connectivity the structure of clathrates is divided into different classes and most abundant and studied are type I ( $A_2B_6E_{46}$ ) and type II ( $A_{16}B_8E_{136}$ ) clathrates, A and B – guests, E – framework atoms (Figure 1B-C). The clathrates free from group 14 elements have been called "unconventional clathrates". Their frameworks are based on combination of group 11 or 12 or 13 and 15 elements allowing for substantial deviations from tetrahedral coordination of the framework resulting in structural and properties flexibility [5]. Unconventional clathrates show a variety of framework structures with guest ions (Figure 1D-E) and hold the promise of high figure of merit,  $zT$ , while being prepared from light elements with tunable transport properties.



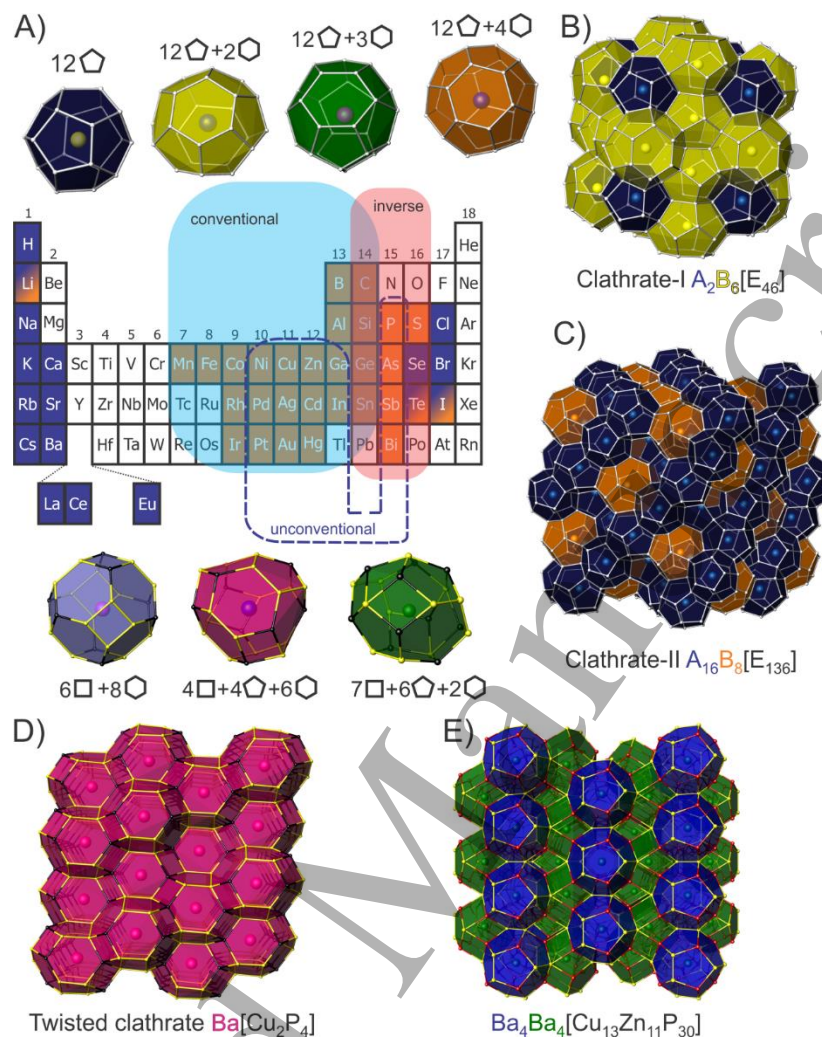


**Figure 1.** A) Periodic chart showing elements found in inorganic clathrates as guest atoms (blue cells) and framework atoms (orange cells). Highlighted rectangles show compositional areas for frameworks of conventional (cyan), inverse (pink), and unconventional (dotted) clathrates. Polyhedra found in conventional and inverse clathrates composed of pentagons and hexagons are shown on the top. In unconventional clathrates due to deviations from tetrahedral coordination additional polyhedra with square and trigonal faces may be found as those shown in the bottom. B-C) Polyhedral representation of the crystal structures of type I and II clathrates. D-E) Crystal structures of unconventional clathrates.

### Current and Future Challenges

Inorganic clathrates have structures that exhibit phonon glass electron crystal behavior. The framework provides a conduction path while the guest atoms scatter phonons and significantly reduce thermal conductivity. In addition, alio- and isovalent substitutions allow for band structure engineering and various elemental combinations providing a variety of adjustable band gaps. Many clathrate phases have been shown to have good thermoelectric properties (Figure 2) [2, 6] with the highest thermoelectric figure of merit,  $zT$ , reported to date of 1.35 for  $Ba_{16}Ga_{16}Ge_{30}$  at 823 K [7]. Several Sn-based clathrates exhibited similar  $zT$  in 1-1.3 range albeit at lower temperatures of 500-550 K. A significant number of conventional, inverse, and unconventional clathrate crystal structures have been reported and a limited number of properties investigated. Because many of these framework structures undergo significant expansion with temperature, obtaining dense pellets for measurement is a challenge.



Another challenge is to organize the data to provide a signpost toward the best compositions that may provide further improvements in thermoelectric conversion efficiencies. Zintl rules, electron transfer between the framework and guest atoms and the fulfillment of the electron octet, provides an excellent roadmap for proposing new combinations of elements but lack of detailed understanding of guest-host interactions limits the predictive property outcomes of this simple electron counting formalism. Compositions and structural features of the frameworks are well understood by covalent or polar covalent bonding between atoms. For clathrates based on group 14 elements, frameworks stability (and thermoelectric application temperature) correlates with strength of homoatomic covalent E-E bond: Si-based frameworks are stable up to 900-1200°C while most of Sn-based clathrates decomposes above 600°C. This is emphasized by the absence of high-temperature Sn-based clathrate thermoelectrics (Figure 2). Si clathrates readily form charge-unbalanced compositions, which prevents widespread investigations of Si clathrates for thermoelectric applications, as control over carrier concentration is difficult to achieve. Unconventional clathrates with polar-covalent bonding exhibit intermediate stability in the range of 600-900°C. The understanding and interpretation of defects and their interplay with stability and transport properties remains a challenge [8]. As mentioned above, guest-host interactions are a key issue for study. PGEC concept postulates the independence of the heat and charge transport, but in clathrates strong host-guest interaction may arise and affect properties [9]. Even with these caveats, an exciting challenge is to design new materials with earth abundant elements that may provide high thermoelectric efficiencies at high temperatures and are stable in air.

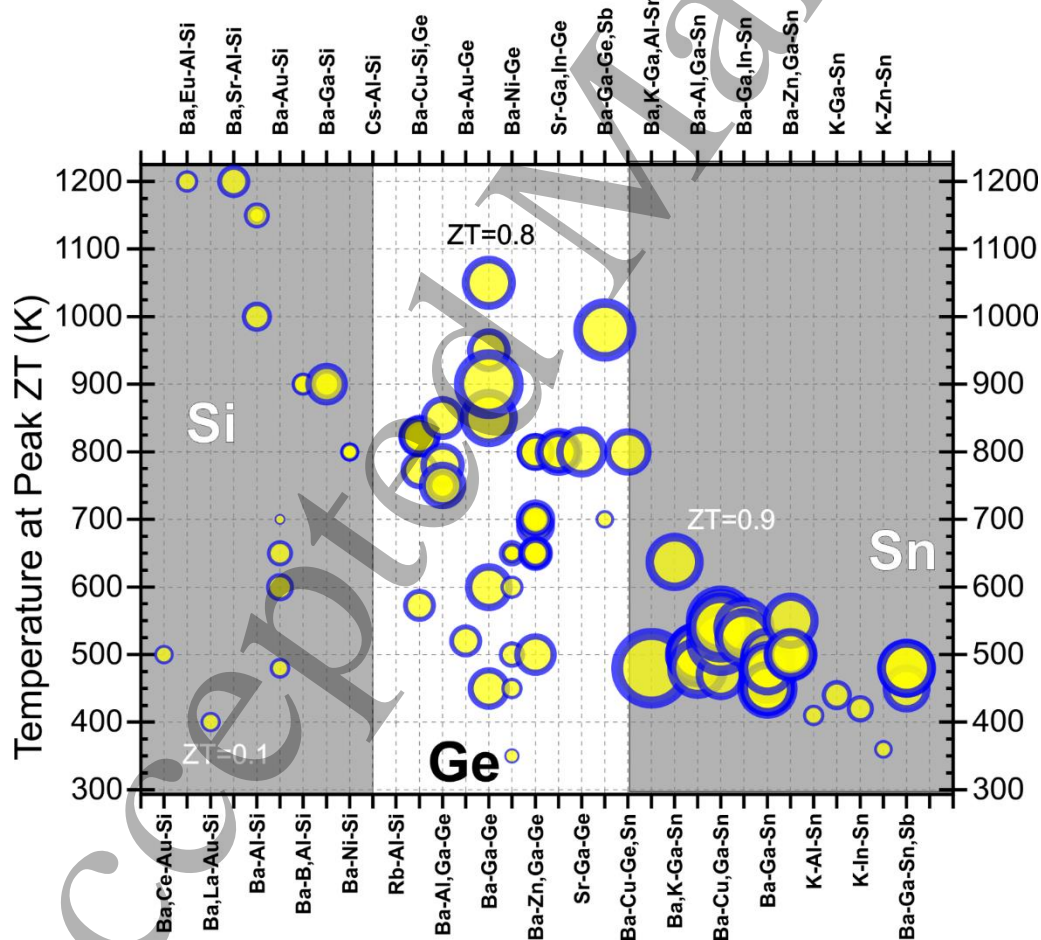


**Figure 2.** Values of maximum ZT for selected conventional clathrates. The temperature at maximum ZT is shown on the vertical axis. Maximum ZT value is encoded in diameter of the circular symbol used. Few ZT values are shown for references. Note, that stability of the framework defines the temperature ranges used for transport properties characterization.

### Advances in Science and Technology to Meet Challenges

Although clathrates display a large diversity of structure and properties, most are restricted to low temperatures and modest ZT's. Therefore, an important challenge for the field is to design and synthesize materials with better properties, eventually leading to applications. An important fundamental science priority is a development of new synthetic approaches to high purity materials where composition can be controlled with high fidelity [10]. Theoretical calculations on the defect structures and understanding their impact on properties is a challenge. Clathrates are often described as highly symmetric cubic structures with some disorder in the framework due to the presence of either vacancies or two or more elements of different chemical nature. More thorough studies shown that bonding preferences of the framework forming elements results in either short-range or long-range ordering which impacts the electronic structure and transport properties. Proper modeling of such complex structures requires a detailed characterization where X-ray and neutron high resolution powder and single crystal diffraction in combination with total scattering and local probes such as EXAFS and scanning-transmission electron microscopy may reveal true structure. The latter is crucial for the proper computational description of electronic structure and properties prediction. High throughput theoretical calculations may provide a breakthrough by identifying underlying components of these complex framework structures that can lead to high thermoelectric efficiencies.

### Concluding Remarks

There is a myriad combination of possible elements that give rise to clathrate phases and progress has been considerable. A good understanding of electron counting requirements of compounds synthesized to date frames the design of semiconducting properties that may provide good thermoelectric properties. Theory has a significant role to play in providing guideposts towards new materials with good thermoelectric properties. However, there is still a significant phase space unexplored with high prospects of finding efficient thermoelectric materials. In addition, because of the possibilities of superconductivity, photovoltaics and energy storage applications, these properties are also worthy of investigation.

### Acknowledgements

SMK acknowledges NSF DMR-2001156 for funding. KK acknowledges support by the U.S. Department of Energy, Office of Basic Energy Sciences, Division of Materials Science and Engineering, grant DE-SC0022288.

### References

- [1] A. V. Shevelkov, "Thermoelectric Power Generation by Clathrates.," *Thermoelectrics for Power Generation - A Look at Trends in the Technology*, S. Skipidarov and M. Nikitin, Eds., London: IntechOpen, 2016. [Online]. Available: <https://www.intechopen.com/chapters/52634> doi: 10.5772/65600

- [2] J. Dolyniuk, B. Owens-Baird, J. Wang, J. V. Zaikina, and K. Kovnir, "Clathrate Thermoelectrics," *Materials Science & Engineering: R: Reports*, vol. 108, pp. 1-46, 2016. [Online]. Available: <https://doi.org/10.1016/j.mser.2016.08.001>.
- [3] S. M. Kauzlarich, F. Sui, and C. J. Perez, "Earth Abundant Element Type I Clathrate Phases," *Materials (Basel)*, vol. 9, no. 9, Aug 23 2016, doi: 10.3390/ma9090714.
- [4] T. Takabatake, K. Suekuni, T. Nakayama, and E. Kaneshita, "Phonon-glass electron-crystal thermoelectric clathrates: Experiments and theory," *Reviews of Modern Physics*, vol. 86, no. 2, pp. 669-716, 2014, doi: 10.1103/RevModPhys.86.669.
- [5] J. Wang, J. A. Dolyniuk, and K. Kovnir, "Unconventional Clathrates with Transition Metal-Phosphorus Frameworks," *Acc Chem Res*, vol. 51, no. 1, pp. 31-39, Jan 16 2018, doi: 10.1021/acs.accounts.7b00469.
- [6] R. Freer, D. Ekren, T. Ghosh, K. Biswas, P. Qiu, S. Wan, L. D. Chen, S. Han, C. Fu, T.-J. Zhu, A. K. M. Ashiquzzaman Shawon, A. Zevalkink, K. Imasato, G. J. Snyder, M. Ozen, K. Saglik, U. Aydemir, R. Cardoso-Gil, E. Svanidze, R. Funahashi, A. V. Powell, S. Mukherjee, S. Tippireddy, P. Vaqueiro, F. Gascoin, T. Kyratsi, P. Sauerschnig, and T. Mori, "Key Properties of Inorganic Thermoelectric Materials – Tables (Version 1)," *J. Phys. Energy*, vol. 4, no. 2, 2022, doi: 10.1088/2515-7655/ac49dc.
- [7] L.-H. Wang and L.-S. Chang, "Thermoelectric properties of p-type  $Ba_8Ga_{16}Ge_{30}$  type-I clathrate compounds prepared by the vertical bridgman method.," *J. Alloys & Compounds*, vol. 722, pp. 644-650, 2017. [Online]. Available: <https://www.sciencedirect.com/science/article/abs/pii/S0925838817321096>.
- [8] A. Bhattacharya, C. Carbogno, B. Böhme, M. Baitinger, Y. Grin, and S. M., "Formation of Vacancies in Si- and Ge-based Clathrates: Role of Electron Localization and Symmetry Breaking," *Phys. Rev. Lett.*, vol. 118, p. 236401, 2017. [Online]. Available: <https://doi.org/10.1103/PhysRevLett.118.236401>.
- [9] J. Wang, J. Dolyniuk, E. Krenkel, J. L. Niedziela, M. A. Tanatar, E. Timmons, T. Lanigan-Atkins, H. Zhou, Y. Cheng, A. J. Ramirez-Cuesta, D. L. Schlagel, U. S. Kaluarachchi, L.-L. Wang, S. L. Bud'ko, P. C. Canfield, R. Prozorov, O. Delaire, and K. Kovnir, "Clathrate  $BaNi_2P_4$ : An interplay of heat and charge transport due to strong host-guest interactions," *Chem. Mater.*, vol. 32, pp. 7935-7940, 2020. [Online]. Available: <https://doi.org/10.1021/acs.chemmater.0c02758>.
- [10] W. D. C. B. Gunatilleke, O. P. Ojo, H. Poddig, and G. S. Nolas, "Synthesis and characterization of phase-pure clathrate-II  $Rb_{12.9}Si_{136}$ ," *Journal of Solid State Chemistry*, vol. 311, 2022, doi: 10.1016/j.jssc.2022.123152.

## 5.6 Skutterudites for thermoelectric energy harvesting

Ctirad Uher

Department of Physics, University of Michigan, Ann Arbor, Michigan 48109, United States

### Status

In 1994, Prof. Slack pointed out that skutterudites are an excellent example of his Phonon-Glass-Electron-Crystal (PGEC) paradigm [1]. Since that time, researchers worldwide have focused on the development of this interesting class of thermoelectrics [2]. Moreover, many car-manufacturing companies saw a great potential in capturing the waste heat from engines, converting it to electricity, and, ultimately, improving the millage. Further appeal of skutterudites has been their non-toxic and readily available chemical elements. Skutterudites are binary compounds  $MX_3$ , with M being column 9 transition metals Co, Rh, and

Ir, while X are pnictogen elements P, As, and Sb. All nine combinations of M and X exist, and they crystallize in the bcc structure in the space group  $Im\bar{3}$ .

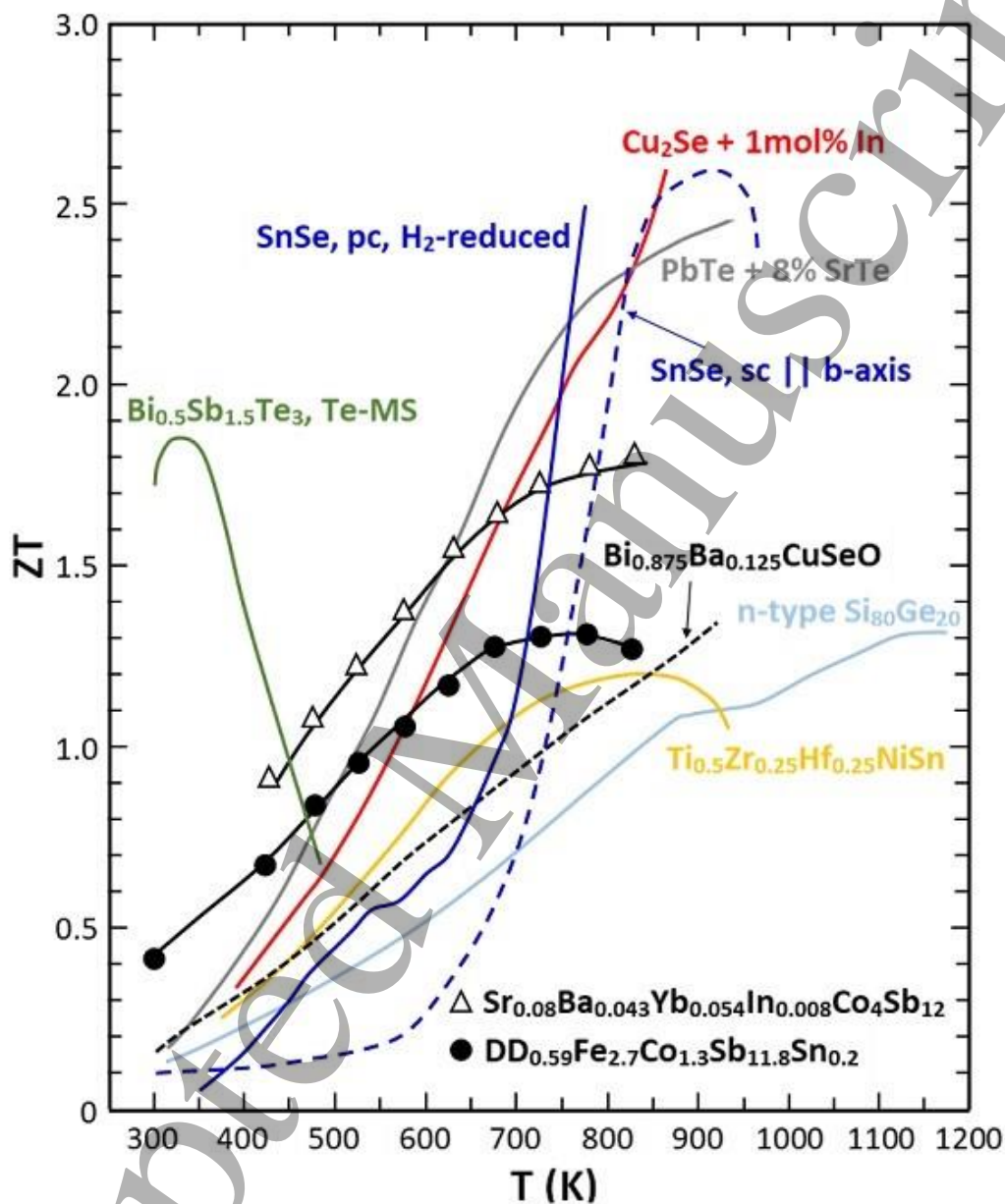


Figure 1: Comparison of the best n-type skutterudites, designated with upside unfilled triangles, Rogl et al. Acta Mater. 95 (2015) 201, and the best p-type skutterudites indicated by black solid circles, Rogl et al. Acta Mater. 91 (2015) 227, with other high-performing thermoelectrics. In the mid-temperature range 500 K -900 K, skutterudites are an excellent choice for thermoelectric modules.

The prominent feature of skutterudites are two large structural voids. When filled with foreign ions, filled skutterudites result [3] that are of interest to thermoelectricity due to their outstanding electronic properties. Moreover, filling, particularly with multiple kinds of filler species, is exceptionally effective in suppressing the thermal conductivity by affecting a broader range of phonon frequencies. Combining excellent electronic properties and very low lattice thermal conductivities makes filled skutterudites

1  
2  
3 outstanding thermoelectric materials for power generation applications. Although the interest of the car  
4 companies in thermoelectricity has recently fizzled out as they shifted their attention to electrically driven  
5 cars, filled skutterudites maintain their position as premier thermoelectrics for waste heat recovery in the  
6 temperature range between 500 K – 850 K, where there are plentiful sources of waste industrial heat  
7 waiting to be captured, Fig.1.  
8

### 9 10 **Current and Future Challenges**

11 The current state-of-the-art skutterudites developed in the laboratories worldwide have achieved  
12 outstanding thermoelectric performance with  $ZT \sim 1.8$  for n-type skutterudite [4,5], further enhanced to  
13  $ZT \sim 2$  upon applying high-pressure torsion [6]. The best p-type forms of the structure have attained a  
14 somewhat lower but still very competitive  $ZT \sim 1.3$  [7]. Moreover, skutterudites are mechanically very  
15 robust and machineable. A long-standing puzzle concerning n-type skutterudites, namely their high  
16 Seebeck coefficients at high carrier densities of  $\sim 10^{21} \text{ cm}^{-3}$ , has been solved recently by DFT calculations  
17 combined with detailed measurements of the temperature dependent optical absorption [8, 9]. The data  
18 revealed the existence of a nearby-lying second conduction minimum that descends with temperature  
19 and converges with the G-point conduction band minimum, Fig.2. The convergence dramatically enhances  
20 the valley degeneracy and the density of states effective mass, thus assuring high electrical conductivity  
21 with no penalty to the Seebeck coefficient. Concerns regarding sublimation of Sb and oxidation when  
22 operated in air at elevated temperatures have been mitigated by applying thin protective electrically  
23 insulating coatings, such as aerogels and enamels. The major problem concerning skutterudites is the  
24 inability to transfer the outstanding laboratory results to a large-scale manufacturing setting and fabricate  
25 highly efficient skutterudite-based thermoelectric modules. This is partly due to the poorer performance  
26 of materials prepared in large batches and due to high contact resistances introduced during the assembly  
27 of modules. Nevertheless, modules with the efficiency exceeding 10% have been demonstrated [10].  
28  
29  
30

### 31 **Advances in Science and Technology to Meet Challenges**

32 To improve the thermoelectric energy conversion of skutterudites, advances must be made on several  
33 fronts. The performance of p-type skutterudites should be improved to match closely the performance of  
34 their n-type cousins. Detailed DFT calculations combined with doping studies should explore a possibility  
35 of band convergence within the valence band manifold. For all forms of skutterudites, optimal  
36 microstructures should be identified (grain size and its orientation) that minimize electrical resistivity yet  
37 very effectively scatter the heat conducting phonons, and ways to realize such microstructures in actual  
38 samples should be explored. The key point is that such optimal microstructures must be stable at  
39 temperatures where skutterudites are expected to operate. An understanding must be gained why the  
40 performance of gram quantities of skutterudites prepared in laboratories are not replicated when the  
41 identical skutterudite is fabricated in kilogram quantities in a production setting. In the past, the bulk of  
42 research efforts have focused on finding the best performing skutterudite compounds with little regard  
43 how such outstanding materials will function in efficient thermoelectric modules. The much less  
44 glamorous tasks of finding how to metallize skutterudites, how to make low resistance contact, how to  
45 mitigate differential thermal expansion between n- and p-type elements, and how to protect the couple's  
46 legs in a hostile environment when operating in air at high temperatures were not adequately considered.  
47 These more engineering tasks must become of prime focus to fully utilize the great potential of  
48 skutterudites and fabricate efficient, reliable, and inexpensive skutterudite-based thermoelectric  
49 modules.  
50  
51  
52  
53  
54  
55  
56  
57  
58  
59  
60



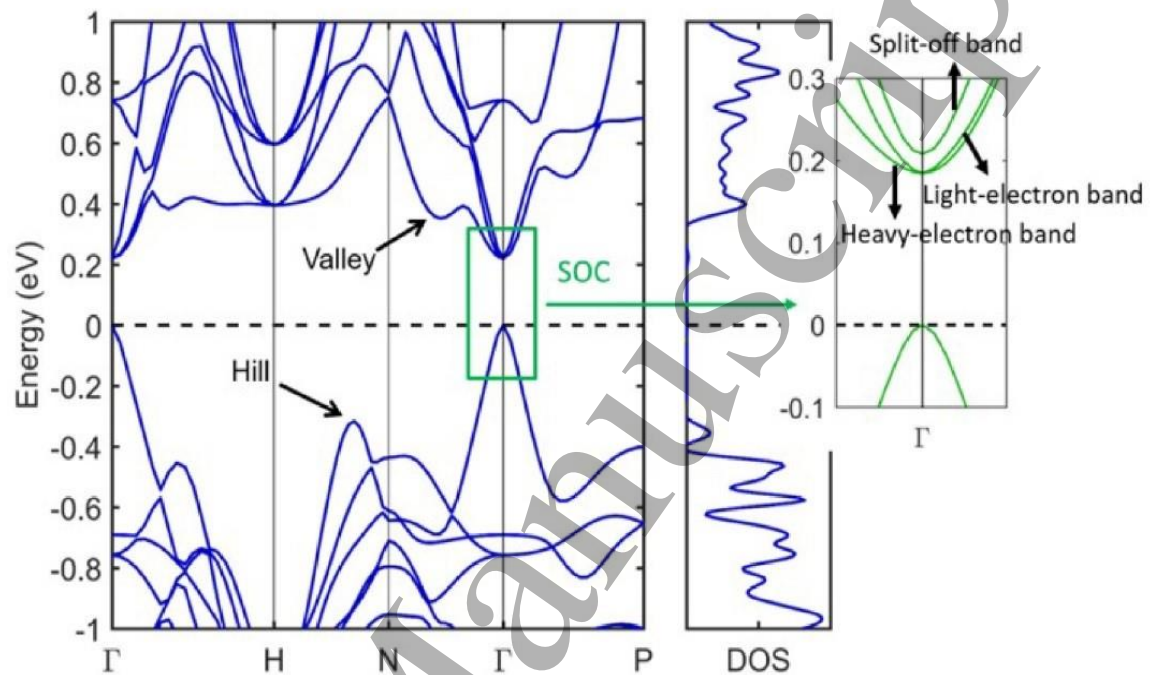


Figure 2: Band structure of skutterudites highlighting the closely lying conduction bands, the band edges of which converge with increasing temperature to the G-point conduction band. Reproduced from C.Z. Hu et al., *Physical Review B* 95 (2017) 165204. Reproduced with permission from the American Physical Society.

### Concluding Remarks

Some twenty-five years of research have resulted in n- and p-type skutterudites that have the thermoelectric figure of merit greatly exceeding values of unity. Moreover, skutterudites are among the best thermoelectrics as far as the mechanical properties are concerned and are even machineable. Thin protective electrically insulating coatings, such as aerogels and enamels, solved problems with Sb sublimation and oxidation. These are outstanding laboratory achievements. The problem is that they have not transferred readily to a large-scale manufacturing setting where detailed issues concerning the assembly of elements into reliable thermoelectric couples are dealt with. Indeed, one cannot buy skutterudite modules off the shelf because, simply, no one is manufacturing them. Yet, the modules fabricated by some of the larger research groups perform very well with efficiencies in excess of 10%. The shift of interests of the car manufacturers from gasoline engines to fully electric cars has been a major blow to funding of research on skutterudites. Nevertheless, there are numerous other sources of waste industrial heat in the temperature range between 500 K and 900 K where the efficient performance of skutterudites could make a great impact.

### Acknowledgements

My work on skutterudites was funded chiefly by the U.S. Office of Naval Research, and the U.S. Department of Energy.

### References



- [1] G.A. Slack, New materials and performance limits for thermoelectric cooling, in: D.M. Rowe (Ed.), CRC Handbook of Thermoelectrics, CRC Press, Boca Raton, FL, (1995), p. 407.
- [2] C. Uher in Thermoelectric Skutterudites, CRC Press, Taylor & Francis Group, Boca Raton, FL (2021).
- [3] W. Jeitschko, D.J. Braun, LaFe<sub>4</sub>P<sub>12</sub> with filled CoAs<sub>3</sub>-type structure and isotypic lanthanoid-transition metal polyphosphides, Acta Crystallogr. B33 (1977) 3401.
- [4] X. Shi, J. Yang, J.R. Salvador, M.F. Chi, J.Y. Cho, H. Wang, S.Q. Bai, J.H. Yang, W.Q. Zhang, L.D. Chen, Multiple-filled skutterudites: high thermoelectric figure of merit through separately optimizing electrical and thermal transports, J. Amer. Chem. Soc. 133 (2011) 7837.
- [5] G. Rogl, A. Grytsiv, K. Yubuta, S. Puchegger, E. Bauer, C. Raja, R.C. Mallik, P. Rogl, In-doped multifilled n-type skutterudites with  $ZT = 1.8$ , Acta Mater. 95 (2015) 201.
- [6] G. Rogl, A. Grytsiv, P. Rogl, N. Peranio, E. Bauer, M. Zehetbauer, O. Eibl, n-Type skutterudites (R,Ba,Yb)<sub>y</sub>Co<sub>4</sub>Sb<sub>12</sub> (R = Sr, La, Mm, DD, SrMm, SrDD) approaching  $ZT \approx 2.0$ , Acta Mater. 63 (2014) 30.
- [7] G. Rogl, A. Grytsiv, P. Heinrich, E. Bauer, P. Kumar, N. Peranio, O. Eibl, J. Horky, M. Zehetbauer, P. Rogl, New bulk p-type skutterudites DD<sub>0.7</sub>Fe<sub>2.7</sub>Co<sub>1.3</sub>Sb<sub>12-x</sub>X<sub>x</sub> (X = Ge, Sn) reaching  $ZT > 1.3$ , Acta Mater. 91 (2015) 227.
- [8] C.Z. Hu, X.Y. Zeng, Y.F. Liu, M.H. Zhou, H.J. Zhao, T.M. Tritt, J. He, J. Jakowski, P.R.C. Kent, J.S. Huang, B.G. Sumpter, Phys. Rev. B 95 (2017) 165204.
- [9] Y.L. Tang, Z.M. Gibbs, L.A. Agapito, G. Li, H.-S. Kim, M.B. Nardelli, S. Curtarolo, G.J. Snyder, Nat. Mater. 14 (2015) 1223.
- [10] Q.H. Zhang, J.C. Liao, Y.S. Tang, M. Gu, C. Ming, P.F. Qiu, S.Q. Bai, X. Shi, C. Uher, L.D. Chen, Energy Environ. Sci. 10 (2017) 956.

## 5.7 Oxides for thermoelectric energy harvesting

Jinle Lan<sup>1</sup> and Yuan-Hua Lin<sup>2</sup>

<sup>1</sup>State Key Laboratory of Organic-Inorganic Composites, College of Materials Science and Engineering, Beijing University of Chemical Technology, North Third Ring Road 15, Chaoyang District, Beijing 100029, P. R. China

<sup>2</sup>State Key Laboratory of New Ceramics and Fine Processing, School of Materials Science and Engineering, Tsinghua University, Shuangqing Road 30, Haidian District, Beijing 100084, P. R. China

### Status

To date, state-of-the-art thermoelectric (TE) materials usually contain toxic, scarce and expensive metal elements (e.g., Pb, Te, Sb). The practical applications of these materials are restricted by the poor thermal and chemical stability at high temperature as well as high cost. After the discovery of NaCo<sub>2</sub>O<sub>4</sub> single crystals with high TE potential performance by Terasaki *et al.*,<sup>1</sup> many oxides such as Ca<sub>3</sub>Co<sub>4</sub>O<sub>9</sub><sup>2</sup>, ZnO, CaMnO<sub>3</sub> and SrTiO<sub>3</sub>, were carefully investigated for TE applications. These types of oxides have proven to be very promising for high temperature TE application, which are thermally and chemically stable in air at high temperature. These oxides are easy to prepare, low cost raw materials and eco-friendly, which have drawn considerable attention in the TE community. However, the TE performance of oxides especially the polycrystallines have relatively low  $ZT$  values, which is ascribed to low electrical conductivity and high thermal conductivity caused by high grain boundary resistance and strong ionic bonding (Figure.1). So far, some layered structure oxides have outstanding performance, giving some hope for further development. The p-type oxide TE materials, Co-based oxide material Ca<sub>3</sub>Co<sub>4</sub>O<sub>9</sub> has been intensively investigated due to low thermal conductivity originated from its misfitted structure and high Seebeck coefficient by the plus spin entropy. The highest  $ZT$  value of Ca<sub>3</sub>Co<sub>4</sub>O<sub>9</sub>  $\sim 0.90$  at 1073 K was achieved by grain boundary

engineering.<sup>3</sup> BiCuSeO oxyselenides have been reported to exhibit intrinsic low lattice thermal conductivity and high ZT value.<sup>4</sup> Recently, a recorded thermoelectric performance with  $ZT > 1.5$  at 873 K has been achieved for Pb, Ca dual doped BiCuSeO oxyselenide ceramics.<sup>5</sup>

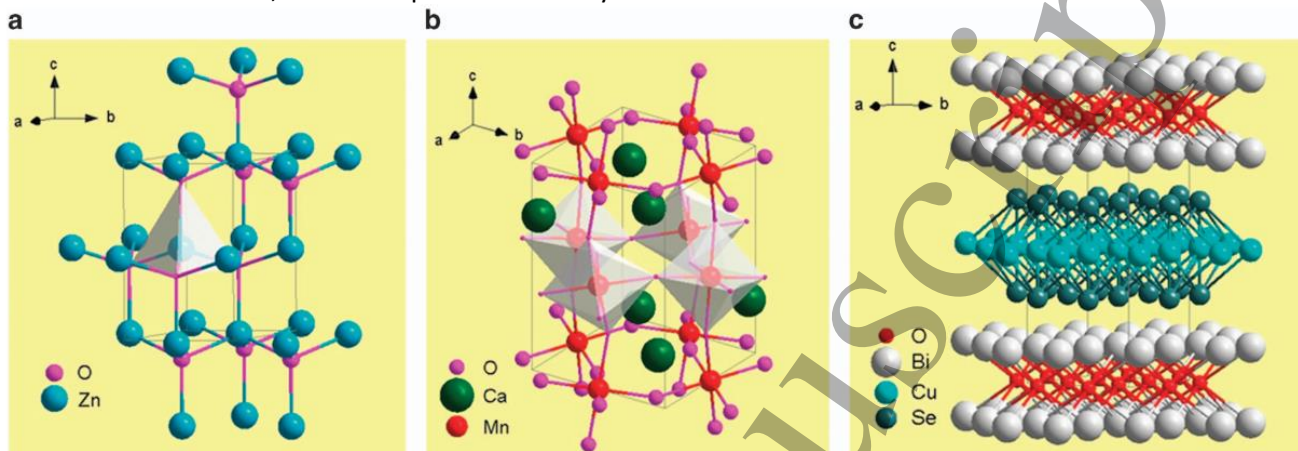


Figure 1. The crystal structure of (a) simple wurtzite oxide-based materials: ZnO (P63mc), (b) perovskite oxides: CaMnO<sub>3</sub> (Pbnm) and (c) layered oxides: BiCuSeO (P4/nmm).

### Current and Future Challenges

In the field of oxide-based thermoelectric materials, several challenges appear. Here, we highlight a few key challenges:

- The strong ionicity in the bonds between light oxide atoms with other atoms leads to intrinsically small carrier mobility  $\mu$  and carrier concentration  $n$ . Besides, strong bonds in oxides also make the lattice distortions be suppressed, and the vibrations of atoms are rarely disturbed, which further results in relatively high lattice thermal conductivity  $\kappa_l$ . Thus, except Ca<sub>3</sub>Co<sub>4</sub>O<sub>9</sub>,<sup>2,j</sup> Bi<sub>2</sub>O<sub>2</sub>Se<sup>6</sup>, and BiCuSeO<sup>4</sup>, most of oxide thermoelectrics exhibit poor ZT value around 0.1~0.4. Therefore, it is an open question for the TE community to design the proper crystal structure for the novel oxide materials.
- Grain boundary engineering with dopant segregations or carbon addition (e.g. graphene, CNTs and graphite) have been proved to be a robust strategy to achieve “phonon glass- electron crystal” behavior in oxides, which even outperform single crystal-like charge transport in polycrystalline oxides. The open question is how to clearly resolve and manipulate the atomic structure of grain boundaries to achieve desirable properties.<sup>7,8</sup>
- To decouple the electrical and thermal properties, the “phonon glass- electron crystal” concept proposed by Slack can be realized in the materials with layered structures. Two-dimensional (2D) layered materials exhibit artificial super-lattice structure, which possess short phonon mean free paths due to the strong phonon scattering in lattice-scale without deteriorating the electric transport. The layered oxygen-containing thermoelectric materials (e.g., Ca<sub>3</sub>Co<sub>4</sub>O<sub>9</sub>, BiCuSeO and Bi<sub>2</sub>O<sub>2</sub>Se), were intensively investigated due to their low  $\kappa$  value originated from misfitted structures and impressive high carrier mobility. Nevertheless, the electronic and phonon mechanism has not been fully understood, especially in the effect of in-plane and out-plane structures of the sublayers in the materials.
- In non-oxide thermoelectric devices, the effects of air and high temperature have always limited the practical application of the device. Oxide ceramics are considered to promising high temperature application due to their excellent thermal stability and strong oxidation resistance. The first prototype all-oxide thermoelectric device was fabricated using Gd-doped Ca<sub>3</sub>Co<sub>4</sub>O<sub>9</sub> p-

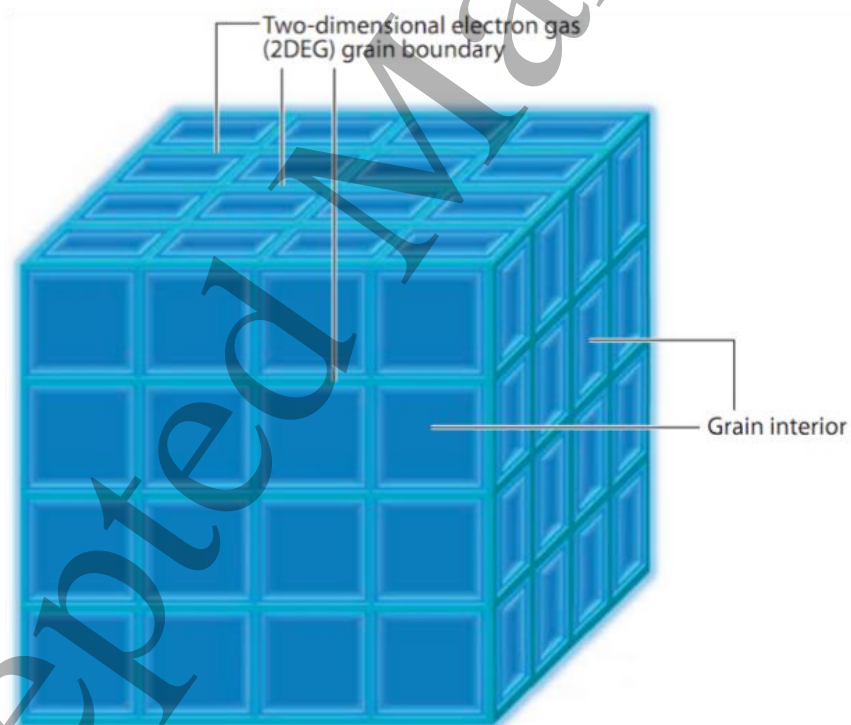
1  
2  
3 type legs and La-doped  $\text{CaMnO}_3$  n-type legs on a fin in 2001.<sup>9</sup> This device proved to be operable  
4 for more than two weeks in air showing high durability. The challenge is that few new works  
5 concerned on oxide thermoelectric devices have been reported during the last decade.  
6

### 7 **Advances in Science and Technology to Meet Challenges**

8 To address the challenges mentioned above, key strategies are required to boost the development of  
9 oxide thermoelectrics. Efforts must continue to design and synthesize new materials with complex  
10 structure and high bonding covalency, searching beyond oxyselenides and cobaltites.  
11

12  
13 To shed more light on the optimized properties for the existing materials system, strategies including band  
14 gap tuning, modulation doping, texturing and nanocompositing should be carefully investigated. A brick  
15 and mortar type structure of ceramics with two-dimensional electron gas grain boundary (Figure.2) are  
16 introduced to  $\text{SrTiO}_3$  system.<sup>10</sup> The predicted  $ZT$  value of this material can reach 1.13 at room temperature,  
17 an order of magnitude higher than the bulk value. This assumption may be realized through the fine-  
18 tuning grain boundary by two-dimensional materials (e.g. graphene) in the future.  
19

20  
21 In terms of technological advances, efforts should continue to intertwine interfacial and local properties  
22 characterization tools (e.g. atomic structure of grain boundaries). The all-oxide thermoelectric devices  
23 should be rational designed and tested in real waste-heat source condition in air.  
24



51 Figure. 2. Brick-and-mortar-type structure of  $\text{SrTiO}_3$  nanoceramics. 2DEG grain boundaries are  
52 shown in light blue. Grain interiors are shown in deep blue.<sup>10</sup>  
53  
54  
55  
56  
57  
58  
59  
60

### Concluding Remarks

During these two decades, great efforts have been made in oxide thermoelectric field, which make the  $ZT$  values surpass 1. Future work must combine the new crystal/bonding design concept and proper interfacial manipulation to achieve carrier mobility maximization and lattice thermal conductivity minimization properties. It is no doubt that the oxide thermoelectrics are becoming more and more important in the big thermoelectric family. With unique features like good chemical and thermal stabilities, oxide thermoelectric materials and devices are promising candidates for high temperature thermoelectric applications

### Acknowledgements

This work was financially supported by Basic Science Center Project of National Natural Science Foundation of China under grant No. 51788104 and National Science Foundation of China under grant No. 51772016 and 52172211.

### References

1. I., Terasaki, Y., Sasago, K., and Uchinokura: 'Large thermoelectric power in  $\text{NaCo}_2\text{O}_4$  single crystals', *Physical Review B*, 1997, 56, (20), pp. R12685–R12687
2. Shikano, M., and Funahashi, R.: 'Electrical and thermal properties of single-crystalline  $(\text{Ca}_2\text{CoO}_3)_x(\text{CoO})_{1-x}$  with a  $\text{Ca}_3\text{Co}_4\text{O}_9$  structure', *Applied Physics Letters*, 2003, 82, (12), pp. 1851-1853
3. Romo-De-La-Cruz, C.-O., Chen, Y., Liang, L., Williams, M., and Song, X.: 'Thermoelectric Oxide Ceramics Outperforming Single Crystals Enabled by Dopant Segregations', *Chemistry of Materials*, 2020, 32, (22), pp. 9730-9739
4. Lan, J.-L., Liu, Y.-C., Zhan, B., Lin, Y.-H., Zhang, B., Yuan, X., Zhang, W., Xu, W., and Nan, C.-W.: 'Enhanced Thermoelectric Properties of Pb-doped  $\text{BiCuSeO}$  Ceramics', *Advanced Materials*, 2013, 25, (36), pp. 5086-5090
5. Liu, Y., Zhao, L.-D., Zhu, Y., Liu, Y., Li, F., Yu, M., Liu, D.-B., Xu, W., Lin, Y.-H., and Nan, C.-W.: 'Synergistically Optimizing Electrical and Thermal Transport Properties of  $\text{BiCuSeO}$  via a Dual-Doping Approach', *Advanced Energy Materials*, 2016, 6, (9), pp. 1502423
6. Tan, X., Liu, Y., Liu, R., Zhou, Z., Liu, C., Lan, J.-L., Zhang, Q., Lin, Y.-H., and Nan, C.-W.: 'Synergistical Enhancement of Thermoelectric Properties in n-Type  $\text{Bi}_2\text{O}_2\text{Se}$  by Carrier Engineering and Hierarchical Microstructure', *Advanced Energy Materials*, 2019, 9, (31), pp. 1900354
7. Acharya, M., Jana, S.S., Ranjan, M., and Maiti, T.: 'High performance ( $ZT > 1$ ) n-type oxide thermoelectric composites from earth abundant materials', *Nano Energy*, 2021, 84, pp. 105905
8. Lin, Y., Dylla, M.T., Kuo, J.J., Male, J.P., Kinloch, I.A., Freer, R., and Snyder, G.J.: 'Graphene/Strontium Titanate: Approaching Single Crystal-Like Charge Transport in Polycrystalline Oxide Perovskite Nanocomposites through Grain Boundary Engineering', *Advanced Functional Materials*, 2020, 30, (12), pp. 1910079
9. Matsubara, I., Funahashi, R., Takeuchi, T., Sodeoka, S., Shimizu, T., and Ueno, K.: 'Fabrication of an all-oxide thermoelectric power generator', *Applied Physics Letters*, 2001, 78, (23), pp. 3627-3629
10. Zhang, R.-z., Wang, C.-l., Li, J.-c., and Koumoto, K.: 'Simulation of Thermoelectric Performance of Bulk  $\text{SrTiO}_3$  with Two-Dimensional Electron Gas Grain Boundaries', *Journal of the American Ceramic Society*, 2010, 93, (6), pp. 1677-1681

## 5.8 SiGe for thermoelectric energy harvesting

Luis Fonseca<sup>1</sup>, Alex Morata<sup>2</sup>, Marisol Martin-Gonzalez<sup>3</sup> and Giovanni Pennelli<sup>4</sup>

<sup>1</sup> Instituto de Microelectrónica de Barcelona (IMB-CNM, CSIC), C/Til·lers s/n (Campus UAB), Bellaterra, Barcelona, Spain

<sup>2</sup> Catalonia Institute for Energy Research (IREC), Jardins de Les Dones de Negre 1, 08930, Sant Adrià de Besòs, Barcelona, Spain

<sup>3</sup> Instituto de Micro y Nanotecnología (IMN-CNM-CSIC), C/ Isaac Newton 8, PTM, E-28760 Tres Cantos, Spain

<sup>4</sup> Dipartimento di Ingegneria della Informazione, Università di Pisa, Via G.Caruso, I-56122, Pisa, Italy

### Status

SiGe is an alloy of semiconductor nature and a very stable material that offers a good thermoelectric figure of merit ( $ZT = S^2 \cdot \sigma \cdot T / k$ ) in the mid-high range of temperature. It is the paramount example of the advantages thermoelectricity offers as a solid-state approach to robust, low maintenance and reliable heat harvesters without moving parts, providing long-term, unattended, autonomous supply of energy: Voyager 1 and 2, already in interstellar space (>18,000 million km), are still reporting thanks to the power supplied by them after 40 years of mission.

Back on Earth, SiGe is an environmentally friendly alternative to the materials that require exotic or even toxic elements, e.g. B, Te or Pb-containing materials, which are currently used in the market dominant devices. However, while SiGe systems are much superior to systems based on pure silicon, due to the alloy phonon scattering effect, germanium is not a very cheap material, so that conventional bulk monocrystalline SiGe systems do not offer future prospects for large-scale applications. SiGe belongs to the suite of the silicon family materials, though, and thus can be incorporated into mainstream silicon technology, which is the champion of scalable, miniaturized, and high-density features device making. This is a particularly worth avenue to explore in install & forget IoT scenarios to fulfil the promise of smarter (and more sustainable) environments. In these scenarios heat harvesters could replace primary batteries (or complement secondary batteries) for the provision of the desirable long-term energy autonomy given the widespread of waste heat sources. Since SiGe performance peaks at mid-high T, industrial IoT may be the appropriate market to address.

There are current efforts about going micro and even nano with SiGe. One approach is internally *nanostructuring bulk SiGe* to lower the Ge content, but still preserve or enhance ZT, and use it in the assembly of thermoelectric modules with dimensions comparable to commercial Bi<sub>2</sub>Te<sub>3</sub> ones. Another, it is engineering it into thinner holey membranes or nanomeshes [1] (e.g. using nanoporous alumina templates), as well as thin films, and low dimensional objects such as nanowires arrays [2,3] or bundles of *nanotubes* [4], as shown in Figure 1. This second approach better suits the silicon integration route and enables the possibility of *on-chip microfabricated TEGs*.



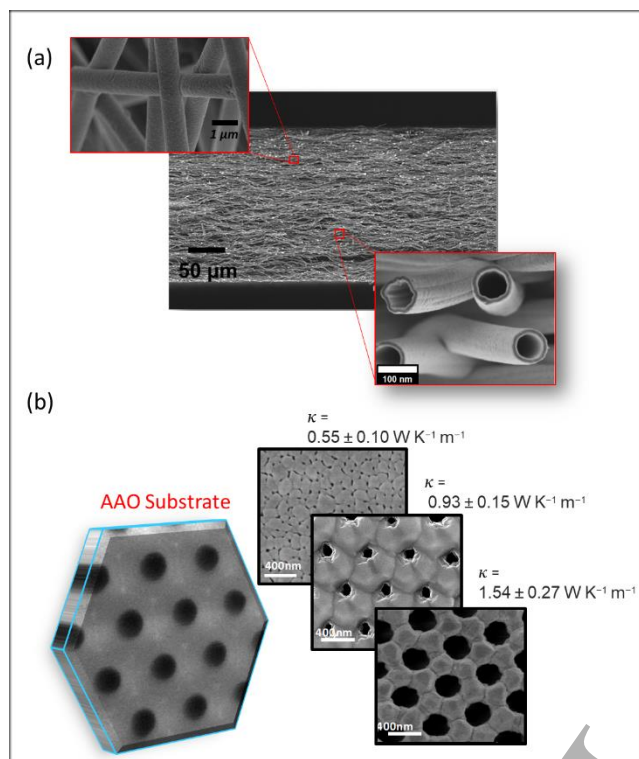


**Figure 1.** Thermoelectric materials based on low dimension SiGe nanostructure. a) Paper-like material formed of bundles of SiGe nanotubes. b) Hollow SiGe membranes using anodized alumina substrates. Different conditions allow tuning the thermal diffusion coefficient ( $\kappa$ )

### Current and Future Challenges

In a microenergy 'harvesting for IoT' scenario, *efficacy* (getting what it is needed from the ambient) prevails over *efficiency* (getting as much as possible). While there is still margin for improvement both at the materials processing level (e.g. optimum doping and nanostructure, homogeneity etc.), and at the device level (e.g. low thermal and electrical contacts, reduced thermal strain etc.), the feasibility of *effective* thermoelectric devices based on SiGe is not questioned. The main hindrances to take SiGe technologies out of their niche applications are the high Ge cost and the lack of scalable processing routes.

The integration of SiGe in silicon technologies has been pointed as a solution for mass production, while acutely reducing critical materials usage. The two available routes are Si MEMS and standard CMOS fabrication. In MEMS, *Silicon micromachining* can be used to fabricate silicon microplatforms able to convert vertical temperature gradients into internal lateral ones. These devices feature the so-called transversal architecture where low dimensional SiGe instances can be integrated flexibly [5], as shown in Figure 2. Alternatively, *entirely CMOS-compatible* approaches can be used for on-chip TEGs replicating the  $\pi$ -architecture of standard modules [6]. In this way, scalability of silicon technologies is fully exploited, but the length of the thermoelectric legs is functionally constrained to the range of thickness compatible with planar mainstream technologies.

One of the key points for the progress of thermoelectricity, also the one based in SiGe, is improving the default *performance of the material of choice* by optimizing the (normally mutually depending) magnitudes) of ZT. Local low dimensionality has been shown to *decrease thermal conductivity* due to

phonon scattering without affecting electric conductivity [7]. *Increasing the power factor ( $S^2 \cdot \sigma$ ) will be much convenient, too.* There are many theoretical and experimental advances in science and technology needed to relate material features (nanocrystallinity, defects, grain boundaries, alloying effects, meshing, metal decoration, roughness...) that could be engineered towards the *energy filtering* of carriers [8] and *phonon suppression* [9] leading to the independent optimization of ZT parameters.

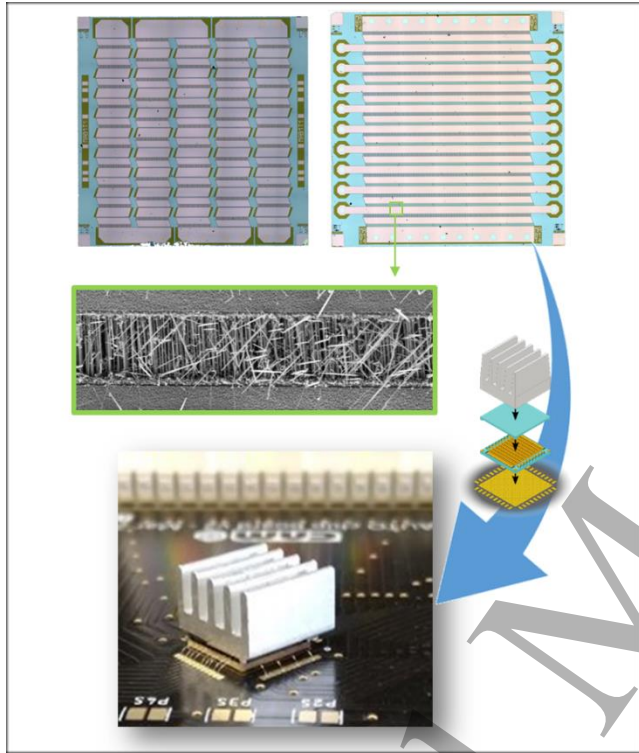


**Figure 2.** Silicon-micromachined thermoelectric generators. Top: two kinds of architectures with series and parallel connected uni-leg couples. Middle: detail of the active thermoelectric material based on aligned VLS growth nanowires. Bottom: sketch and final realization of a device with a heat dissipation element.

### Advances in Science and Technology to Meet Challenges

Interdisciplinary and complementary skills, ranging from semiconductor physics, chemistry, material science and nanotechnology, to the design, nanofabrication, and (thermal and electrical) characterisation of advanced nanodevices and nano-electromechanical systems (MEMS-NEMS) are required to succeed with the design, assembly and testing of SiGe-based prototypes completed with heat exchanger systems for green energy approaches.

*Multi-scale, multi-physics modelling* of thermal and electrical transport for the different avenues considered is needed. At current stage of development, improving the power factor and decreasing the internal resistance of the device should take precedence over lowering the thermal conductivity, which has a low starting value for SiGe. Theoretical predictions need to be validated. They will provide the precise guidelines for the fabrication of devices with maximized performance, either in micro or macromodule format. Such fabrication needs to be put to a test by defining a feasible *technological route*, using the toolbox of *bottom-up* and *top-down* processes accessible to silicon technologies, integrating the

1  
2  
3 engineered materials into d the appropriate architectures to transduce the available thermal gradients  
4 into usable power. The new materials and devices need to be characterized with refined versions of  
5 standard procedures or adhoc methods that are better adapted to the low dimensionality of the  
6 materials.  
7

8  
9 Of particular importance is the part of the technological route that assures a *good thermal coupling* with  
10 the heat source and the heat sink. The exposed surfaces are very small to be cooled off effectively by  
11 nature convection, so a *mesoscale assembly of a heat exchanger* is required. For on-chip micromachined  
12 approaches, which feature transverse architectures, both hot and cold areas are on the same surface  
13 level. This means that the assembly of the heat exchanger needs to be precise and mechanically controlled  
14 to make a gentle physical contact only with the cold parts of the suspended platforms [10].  
15

### 16 **Concluding Remarks**

17 TEGs based on nanostructured SiGe materials will eventually offer a wide variety of possible applications  
18 in the fields of microenergy harvesting and waste heat recovery. On the material side, they build up on  
19 availability, environmental sustainability and stability with aging. On the other hand, combining low-  
20 dimensional SiGe material systems with the maturity of silicon technologies paves the way of device  
21 integration, miniaturization and production scalability. A long and interdisciplinary route of theoretical  
22 and experimental work is still required in order to establish the guidelines that can lead to adequate  
23 performance improvements. These advances have to combine low thermal conductivity and high-power  
24 factor ( $S^2 \cdot \sigma$ ) and must sort out the full chain of nano-micro-meso integration issues that will allow such  
25 TEGs to reach technological maturity and thermally couple to the environment in the most productive  
26 way possible.  
27  
28  
29

### 30 **References**

- 31 [1] J.A. Perez-Taborda et al., "Ultra-low thermal conductivities in large-area Si-Ge nanomeshes for  
32 thermoelectric applications", *Scientific Reports* 6, 32778, 2016  
33 [2] I. Donmez-Noyan et al., "SiGe nanowire arrays based thermoelectric microgenerator", *Nano Energy*  
34 57, pp. 492-499, 2019  
35 [3] E. Dimaggio and G. Pennelli, "Reliable Fabrication of Metal Contacts on Silicon Nanowire Forests",  
36 *Nano Lett* 16, pp. 4348-4354, 2016  
37 [4] A. Morata et al., "Large-area and adaptable electrospun silicon-based thermoelectric nanomaterials  
38 with high energy conversion efficiencies", *Nature Communications* 9, 4759, 2018  
39 [5] M. Salleras et al., "Managing heat transfer issues for thermoelectric microgenerators" in *Heat Transfer*  
40 *- Design, Experimentation and Applications*, Ed. IntechOpen, 2021, ch 18, 23 pp  
41 [6] R. Dhawan, P. Madusanka and M. Lee, "Si<sub>0.97</sub>Ge<sub>0.03</sub> microelectronic thermoelectric generators with  
42 high power and voltage densities", *Nature Communications* 11, 4362, 2020  
43 [7] A.I. Hochbaum et al., "Enhanced thermoelectric performance of rough silicon nanowires", *Nature* 451,  
44 pp. 163-167, 2008  
45 [8] N. Neophytou et al., "Simultaneous increase in electrical conductivity and Seebeck coefficient in highly  
46 boron-doped nanocrystalline Si", *Nanotechnology* 24, 205402, 2013  
47 [9] J. Cuffe et al., "Reconstructing phonon mean free path contributions to thermal conductivity using  
48 nanoscale membranes", *Phys. Rev. B* 91, 245423, 2015  
49 [10] I. Donmez-Noyan et al., "All-silicon thermoelectric micro/nanogenerator including a heat exchanger  
50 for harvesting applications", *Journal of Power Sources* 413, pp. 125-133, 2019  
51  
52  
53  
54  
55  
56  
57  
58  
59  
60

## 5.9 Mg<sub>2</sub>IV (IV = Si, Ge and Sn)-based systems for thermoelectric energy harvesting

David Berthebaud<sup>1</sup> and Takao Mori<sup>2,3</sup>

<sup>1</sup> CNRS-Saint Gobain-NIMS, IRL 3629, LINK, National Institute for Materials Science (NIMS), 1-1 Namiki, Tsukuba, 305-0044 Japan

<sup>2</sup> National Institute for Materials Science (NIMS), WPI International Center for Materials Nanoarchitectonics (WPI-MANA), 1-1 Namiki, Tsukuba, 305-0044 Japan

<sup>3</sup> Graduate School of Pure and Applied Sciences, University of Tsukuba, Tennoudai 1-1-1, Tsukuba, 305-8671, Japan

### Status

Among potential thermoelectric materials for applications, Mg<sub>2</sub>IV(IV=Si, Ge and Sn)-based compounds have attracted a great deal of interest in the last couple decades as they combine great advantages such as versatility between n and p-type, in addition with their ZT value also able to reach unity or above, while they also are relatively light-weight and are composed of low-cost and abundant elements for the silicides and stannides [1,2]. They usually have been considered to be manufactured as an n-type leg associated with their p-type manganese counterpart; higher manganese silicide (HMS) [3], since until recently the thermoelectric properties of p-type Mg<sub>2</sub>IV materials were deemed to be rather low to be implemented in thermoelectric generators (TEG) [1]. Until the recent advances on p-type Mg<sub>2</sub>IV materials, tentative manufacturing of thermoelectric generators were mainly made on Mg<sub>2</sub>Si-based/HMS modules [3] which is a challenging task due to large differences in the mechanical properties of these two materials, as well as poorer resistance to oxidation under working conditions for the magnesium-based materials. The main disadvantage of using a manganese counterpart [4] to the Mg<sub>2</sub>Si-based materials in TEG fabrication is their large differences of coefficient of thermal expansion (CTE) which under high temperature differences cause a high level of mechanical stress ultimately leading to the reduction of the thermoelectric efficiency or its complete failure [3]. Various strategies have been considered to address these issues such as for example the fabrication of Mg<sub>2</sub>Si unileg structure thermoelectric modules. Since such modules are only made of n-type Mg<sub>2</sub>Si legs therefore they did not meet the mechanical failure issues due to CTE differences between n and p-type materials [5]. The unileg concept initially drew some interest for industrial application, but was ultimately not propelled forward, as the complex geometry involved in the unileg design appeared to greatly affect the power output of the module in a diminishing way [5]. Fortunately, in the last few years, the improvement of p-type Mg<sub>2</sub>(Si,Sn) thermoelectric properties [1] has revived interest in this material system with future hope of fabrication of a fully Mg<sub>2</sub>IV-based TEG.

### Current and Future Challenges

Even if the future of low-cost, lightweight, fully Mg<sub>2</sub>IV-based TEG is hopeful, many challenges remain to be overcome and addressed regarding these materials. Among those challenges, the trade-off between the improvement of the thermoelectric properties and the chemical stability, remains one of the most important, as it defines the final power output of the working modules. Indeed, in the Mg<sub>2</sub>IV-based materials, in order to control the n or p-type behaviour [1] or to achieve high figure of merit [2], complex doping strategy have been used involving for example 3 or 4 different elements on the anionic position [2], which comes with a cost concerning the chemical stability of the materials during working conditions or under temperature cycles, leading to phase segregations or decomposition of the involved materials. Sensitivity of Mg<sub>2</sub>X based materials toward oxidation has also been pointed out as an issue preventing these materials to be operable for a long period of time [3]. To address oxidation issues, coatings strategies have been considered to protect Mg<sub>2</sub>X against corrosion, such as for example a promising coating based on amorphous silicon oxycarbide SiOC which exhibit good mechanical and chemical stability [6]. If the current challenges concerning chemical stability and efficiency are overcome, large scale

1  
2  
3 synthesis/production of magnesium-based materials will also need to be further addressed. Indeed,  
4 magnesium metal can be explosive and flammable, therefore production with fast, safe and efficient  
5 methods need to be developed. So far classic solid state chemistry method or mechanical synthesis have  
6 shown to be efficient at a laboratory scale but are unpractical at the industrial scale. More exotic  
7 production techniques such as self-propagating high-temperature synthesis (SHS) or synthesis under  
8 microwave irradiation have been demonstrated as fast and efficient synthesis method, but these methods  
9 still come with high uncertainty concerning their reproducibility, up scalability, and safety.

### 11 12 **Advances in Science and Technology to Meet Challenges**

13 The energetic development and application of various enhancement principles & processes continue to  
14 promise further increase in the performance of thermoelectric materials in general. In addition to higher  
15 degree of control over various nano-microstructuring, defect engineering, etc. to achieve improved  
16 selective phonon scattering, better understanding of various band engineering to enhance the Seebeck  
17 coefficient, there have recently also been multidisciplinary efforts such as utilizing magnetism to enhance  
18 the thermoelectric properties. In this backdrop it is expected that the ZT of Mg<sub>2</sub>IV-based materials  
19 themselves will continue to show further improvement. As the different tools for property enhancement  
20 increase, it is also hoped that the requirement of stability mentioned above can be satisfied more readily.

21  
22  
23 The development of Mg<sub>2</sub>IV-based bulk TEG at mid-high temperatures for energy saving is an increasingly  
24 important target, because of the recent carbon neutral goals. In regard to the oxidation problem, the  
25 further development of protective coatings such as recently demonstrated [6], is a promising direction as  
26 mentioned above. As has been reviewed recently [7], the scientific issues and strategies regarding fast  
27 and energetically efficient synthesis methods such as solution-based, solvothermal, microwave-assisted,  
28 and mechanochemical synthesis are becoming clearer, and hopefully can be applied further for the mass  
29 production of the Mg<sub>2</sub>IV-based materials.

30  
31  
32 One new applicative direction which is not plagued by the oxidation problems described above, is the  
33 relatively low temperature IoT energy harvesting applications [8]. For an elementally abundant, light-  
34 weight system, which is starkly in contrast to conventionally used Bi<sub>2</sub>Te<sub>3</sub>-type materials, a quite high room  
35 temperature power factor of close to 2 mW/m/K<sup>2</sup> has been obtained for bulk and thin film Mg<sub>2</sub>Sn-based  
36 materials [9]. Typically, thin film materials exhibit significantly lower electrical conductivity and thereby  
37 lower power factors than their bulk counterparts, so this is a promising development. Toward IoT  
38 applications, an in-plane miniaturized TEG using Mg<sub>2</sub>Sn-type thin film was constructed utilizing industrially  
39 compatible microfabrication techniques of photolithography and dry etching. The microfabricated TEG  
40 exhibited a relatively high output voltage of 0.58 V and output power of 0.6 mW [10]. Further IoT oriented  
41 developments of the Mg<sub>2</sub>IV-based systems should continue.

### 42 43 44 **Concluding Remarks**

45 The Mg<sub>2</sub>IV (IV = Si, Ge and Sn)-based systems, especially for the silicide and stannide-based materials,  
46 represent attractive thermoelectric systems, for their high ZT reaching unity and above, versatility  
47 between n and p-type, while being relatively light-weight and composed of low-cost and abundant  
48 elements. In this section we have laid out several technological challenges for these materials which are  
49 expected to be possible to overcome, and to be a promising material to be applied, not just for the mid-  
50 high temperature energy saving power generation, but also energy harvesting to power the innumerable  
51 IoT sensors and devices.

### 52 53 54 **Acknowledgements**

55 *TM acknowledges support from JST Mirai Program grant JPMJM19A1.*  
56  
57  
58  
59  
60



## References

- [1] J. De Boor et al., Recent progress in p-type thermoelectric magnesium silicide based solid solutions, *Materials Today Energy*, 4, 105-121 (2017). <https://doi.org/10.1016/j.mtener.2017.04.002>
- [2] AU Khan, N Vlachos, T Kyratsi, High thermoelectric figure of merit of Mg<sub>2</sub>Si<sub>0.55</sub>Sn<sub>0.4</sub>Ge<sub>0.05</sub> materials doped with Bi and Sb, *Scripta Materialia*, 69, 606-609 (2013). <https://doi.org/10.1016/j.scriptamat.2013.07.008>
- [3] G. Skomedal, L. Holmgren, H. Middleton, IS Eremin, GN Isachenko, M. Jaegle, K. Tarantik, Ni. Vlachos, M. Manoli, T. Kyratsi, D. Berthebaud, N. Y Dao Truong, and F. Gascoin, Design, assembly and characterization of silicide-based thermoelectric modules, *Energy Conversion and Management*, 110, 13-21 (2016). <https://doi.org/10.1016/j.enconman.2015.11.068>
- [4] Y Miyazaki, Y Saito, K Hayashi, K Yubuta, and T Kajitani, Preparation and thermoelectric properties of a chimney-ladder (Mn<sub>1-x</sub>Fex) Si<sub>y</sub> ( $y \sim 1.7$ ) solid solution, *Japanese Journal of Applied Physics* 50, 035804 (2011). <https://doi.org/10.1143/JJAP.50.035804>
- [5] Takashi Nemoto et al., Development of an Mg<sub>2</sub>Si Unileg Thermoelectric Module Using Durable Sb-Doped Mg<sub>2</sub>Si Legs, *Journal of Electronic Materials*, 42, 2192–2197 (2013). <https://doi.org/10.1007/s11664-013-2569-0>
- [6] Pawel Nieroda et al., New high temperature amorphous protective coatings for Mg<sub>2</sub>Si thermoelectric material, *Ceramics International*, 45, 10230-10235 (2019). <https://doi.org/10.1016/j.ceramint.2019.02.075>
- [7] N. Nandihalli, D. Gregory, and T. Mori, Energy-saving pathways for thermoelectric nanomaterial synthesis: Hydrothermal/solvothermal, microwave-assisted, solution-based, and powder processing, *Advanced Science* in press.
- [8] I. Petsagkourakis, et al., Thermoelectric Materials and Applications for Energy Harvesting Power Generation, *Sci. Tech. Adv. Mater.*, 19, 836–862 (2018). <https://doi.org/10.1080/14686996.2018.1530938>
- [9] M. S. L. Lima, T. Aizawa, I. Ohkubo, T. Baba, T. Sakurai and T. Mori, “High power factor in epitaxial Mg<sub>2</sub>Sn thin films via Ga doping”, *Applied Physics Letters*, 119, 254101 (2021). <https://doi.org/10.1116/1.5122844>
- [10] I. Ohkubo et al., “Miniaturized in-plane p-type thermoelectric device composed of a II–IV semiconductor thin film prepared by microfabrication”, *Materials Today Energy*, in press. <https://doi.org/10.1016/j.mtener.2022.101075>

## 5.10 Zintl phases for thermoelectric energy harvesting

Robert J. Quinn<sup>1</sup> and Jan-Willem G. Bos<sup>1</sup>

<sup>1</sup>Institute of Chemical Sciences and Centre for Advanced Energy Storage and Recovery, School of Engineering and Physical Sciences, Heriot-Watt University, Edinburgh, EH14 4AS, UK.

### Status

Zintl phases can be defined as materials with ionic and covalently bonded substructures.<sup>1</sup> The presence of two types of bonding results from the transfer of valence electrons from electropositive metals to covalently bonded elements. Ideal Zintl phases (e.g., NaSi) are valence precise with all elements achieving either empty (Na<sup>+</sup>) or filled valence shells (tetrahedral [Si<sub>4</sub>]<sup>4-</sup> clusters). This directly leads to semiconducting behaviour, a key requirement for good thermoelectric properties.

Many of the known good thermoelectric materials, including the clathrates, half-Heuslers and skutterudites discussed elsewhere in this roadmap can be understood within the Zintl concept. The term Zintl thermoelectrics, is however, largely synonymous with antimonide materials.<sup>1,2</sup> Sb-based thermoelectrics first generated attention in the early 2000s and have  $zT > 1$  values for a wide range of compositions, as summarised in Figure 1.  $\text{Yb}_{14}\text{MnSb}_{11}$  (p-type) is one of the best materials for high temperatures, whilst n-type  $\text{Mg}_3(\text{Sb/Bi})_2$  is competitive with  $\text{Bi}_2\text{Te}_3$  near room temperature. Lower mass compositions based on P are starting to attract attention,<sup>3</sup> whilst As is likely of limited use due to its toxicity. Alloying with heavy Bi has been exploited to introduce mass disorder and to manipulate the electronic band structure. However, there are relatively few Bi-based Zintl compounds reported in structural databases.

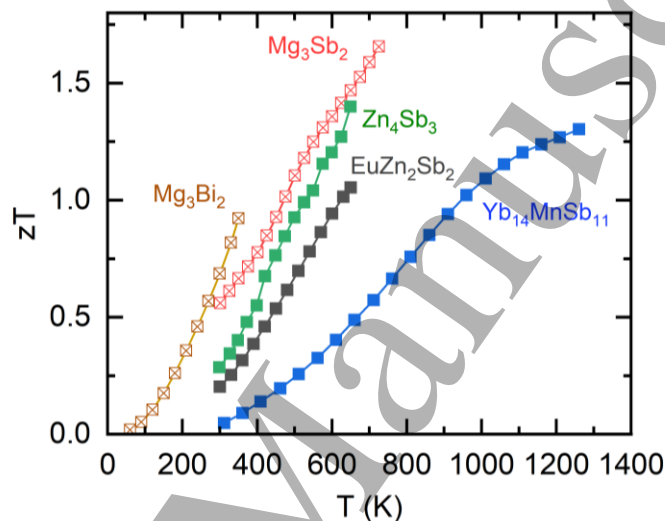


Figure 1. Thermoelectric figures of merit ( $zT$ ) for high performance Sb-based Zintl phases.  $\text{Mg}_3\text{Bi}_2$  (n-type) =  $\text{Mg}_{3.2}\text{Bi}_{1.28}\text{Sb}_{0.7}\text{Te}_{0.02}$ ;<sup>4</sup>  $\text{Mg}_3\text{Sb}_2$  (n-type) =  $\text{Mg}_3\text{Sb}_{1.48}\text{Bi}_{0.48}\text{Te}_{0.04}$ ;<sup>5</sup>  $\text{Zn}_4\text{Sb}_3$  (p-type) =  $(\text{Zn}_{3.98}\text{Pb}_{0.02}\text{Sb}_3)_{0.97}-(\text{Cu}_3\text{SbSe}_4)_{0.03}$ ;<sup>6</sup>  $\text{EuZn}_2\text{Sb}_2$  (p-type) =  $\text{EuZn}_{1.8}\text{Cd}_{0.2}\text{Sb}_2$ ;<sup>7</sup>  $\text{Yb}_{14}\text{MnSb}_{11}$  (p-type) =  $\text{Yb}_{14}\text{Mn}_{0.2}\text{Al}_{0.8}\text{Sb}_{11}$ .<sup>8</sup>

The first widely investigated high- $zT$  compositions were  $\text{Zn}_4\text{Sb}_3$  and  $\text{Yb}_{14}\text{MnSb}_{11}$ , achieving  $zT = 1.3$  at 670 K and at 1220 K, respectively (Fig. 1).<sup>6,8</sup> Both materials have complex structures with low lattice thermal conductivity, enabling good  $zT$  values from modest power factors  $S^2/\rho = 0.5\text{-}1.5 \text{ mW m}^{-1} \text{ K}^{-2}$ .  $\text{Yb}_{14}\text{MnSb}_{11}$  has a large unit cell, leading to many optical phonon modes with low heat propagation.  $\text{Zn}_4\text{Sb}_3$  is non-stoichiometric and contains interstitial Zn atoms that effectively reduce the thermal conductivity through structural disorder. Both materials have been the subject of intensive optimisation studies but are limited by their unique structures that limit the possibilities for chemical substitutions. By contrast, the layered  $\text{AZn}_2\text{Sb}_2$  ( $A = \text{Ca, Sr, Ba, Eu, Yb}$ ) phases are a large class of materials that offer wider opportunities for electronic and phonon engineering, achieving peak  $zT = 1.2$  at 700 K in samples with designed p-orbital degeneracy (Fig. 1).<sup>7</sup> The most recent breakthrough in the field of Zintl thermoelectrics is the discovery of high  $zT = 1.5$  at the relatively low temperature of 650 K in n-type  $\text{Mg}_3\text{Sb}_2$  in 2016 (Fig. 1).<sup>5,9</sup> This was remarkable because  $\text{Mg}_3\text{Sb}_2$  usually forms as a p-type material and careful control of the defect chemistry was required to achieve this. Current optimised Bi-rich compositions approach  $zT = 1$  at room temperature (Fig. 1) and may be a possible replacement for  $\text{Bi}_2\text{Te}_3$ . This is an exciting development, both for ambient temperature waste heat harvesting and thermoelectric cooling.<sup>4</sup>

### Current and Future Challenges

The reported  $zT$  and power factors ( $S^2/\rho$ ) can be used to estimate an upper limit on power output and efficiency of harvesting devices.<sup>10</sup> This is based on the “leg” performance of a single material with the performance reduced in generators, e.g., due to the imperfect matching of n- and p-type legs, parasitic losses due to electrical and thermal contacting, and the reduced fill fraction needed to avoid contact between legs. An overview of calculated power outputs and efficiencies for near ambient harvesting (300-310 K) and up to the stability limit of the materials is given in Fig. 2. This shows that high efficiencies are possible for large temperature differences, and that  $Mg_3(Sb/Bi)_2$  is promising for near ambient harvesting, both in terms of efficiency and power output. The relatively modest power output of the Zintl materials reflects the dominant impact of a low thermal conductivity, which in combination with modest  $S^2/\rho$ , enables the observed high  $zT$  values. Improving the electrical properties, whilst maintaining  $zT$ , would enable improved device power at comparable efficiency.

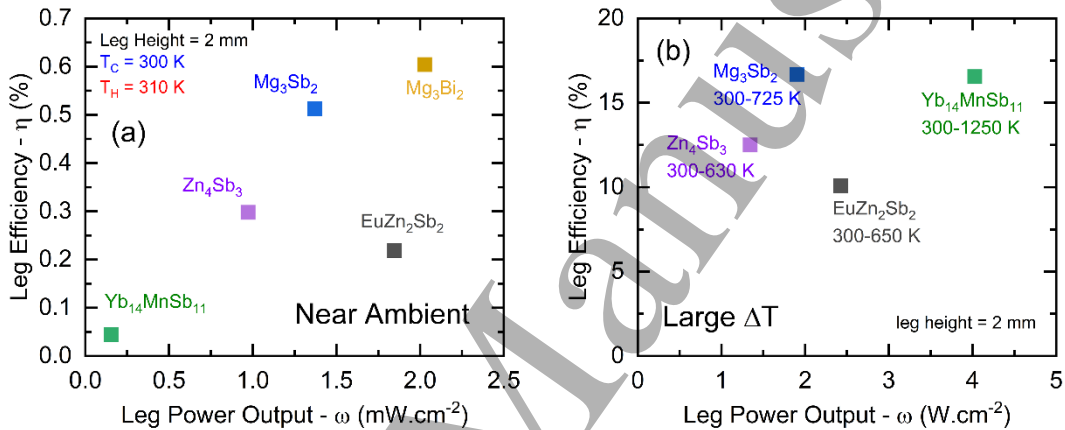


Figure 2. Calculated leg efficiencies and power outputs for the Sb-based Zintl compositions shown in Figure 1. Panel (a) shows calculated values for utilisation of a 300-310 gradient. Panel (b) shows leg efficiencies and power outputs up to the stability limit of the materials. Note that these values will be substantially reduced in generator devices and only reflect an upper limit on performance (based on the properties of a single material).

Two key challenges are to improve  $zT$  and the power output of the Zintl materials and to find matched n- and p-type pairs for use in generators. Achieving better power factors is linked to finding optimal electronic structures, enabling high mobilities and large Seebeck coefficients, and control of doping levels. Controlling the carrier-type is often difficult due to the presence of compensating “killer” defects. In the layered 122 phases, first principles calculations guided the preparation of band converged compositions, leading to increased power factors.<sup>7</sup> In  $Mg_3Sb_2$ , calculations identified a favourable conduction band structure with a highly degenerate pocket away from the usual high-symmetry directions, which underpins the outstanding n-type performance.<sup>5,9</sup> Progress has been made in controlling n-/p-type doping through improved materials growth, guided by defect chemistry calculations. This is illustrated by n-type  $Mg_3Sb_2$ : as grown, this composition is p-type, and it is difficult to access n-type compositions due to the presence of compensating Mg vacancy acceptor defects. The synthetic innovation was to grow the materials in Mg-rich conditions,<sup>9</sup> which suppresses formation of Mg vacancies, enabling the material to be n-type doped through chemical substitution.

### Advances in Science and Technology to Meet Challenges

The challenge in discovering the next generation of ultra-high performance Zintl phases is like other classes of thermoelectrics. At the fundamental level this boils down to finding materials that have highly favourable electronic and thermal band structures, and that allow for synergistic optimisation of the individual thermoelectric parameters. To some extent this is exemplified by the band engineered

1  
2  
3 AZn<sub>2</sub>Sb<sub>2</sub> phases and Mg<sub>3</sub>Sb<sub>2</sub>,<sup>5,7,9</sup> where calculations were used to guide experimental work. At a lower  
4 level of accuracy first principles calculations are used to screen structural databases and electronic band  
5 structures of materials are now readily available (e.g., from the Materials Project). The next step is to  
6 combine this with electronic transport calculations that go beyond the constant relaxation time  
7 approximation, enabling better predictions of  $S^2/\rho$ . Ab initio calculation of the thermal conductivity  
8 remains challenging but access to calculated elastic properties and velocity of sound data is a useful  
9 proxy for materials selection. Another area where first principles calculations can have a big impact is in  
10 the area of defect energetics. Here energy calculations can be used to identify favourable growth  
11 conditions (suppressing compensating defects) that enable highly controlled and targeted carrier  
12 doping. This has the potential to greatly reduce the amount of experimental work, especially for  
13 chemical systems with many components. From the experimental side, control of defect energetics in  
14 the Ca-Zn-Sb system has been explored, leading to a doubled  $zT = 1.1$  at 875 K for Ca<sub>9</sub>Zn<sub>4+x</sub>Sb<sub>9</sub>.<sup>11</sup> A  
15 notable feature of recent work is that many high-performance materials have been prepared by a route  
16 involving mechanical milling / alloying followed by rapid consolidation.<sup>4,5,9</sup> Further work developing  
17 alternative routes for materials growth, including low-temperature routes targeting metastable phases,  
18 is highly desirable. Another challenge that was highlighted by Mg<sub>3</sub>Sb<sub>2</sub> is the need to identify and  
19 eliminate grain boundary resistances, which can be achieved by exposure to Mg vapour.<sup>12</sup> This approach  
20 was directed by atom probe tomography that showed Mg deficiencies at grain boundaries, illustrating  
21 the need for detailed structural analysis to fully understand and optimise materials. Finally, there is a  
22 clear need for continued materials discovery, expanding the library of Zintl compounds and testing their  
23 properties.

24  
25  
26  
27  
28 Device fabrication and testing is the final step in the validation of a thermoelectric material. Several  
29 Zintl-phases have been tested in laboratory generator test devices (e.g., p-type Yb<sub>14</sub>MnSb<sub>11</sub> and Zn<sub>4</sub>Sb<sub>3</sub>,  
30 and n-type Mg<sub>3</sub>Sb<sub>2</sub>).<sup>4</sup> None are currently commercially applied and there is a need to develop matching  
31 n- and p-type pairs, including in terms of performance, mechanical properties and stability. The low  
32 thermal conductivity of Zintls is compatible with small temperature gradients in harvesting, whilst some  
33 of the difficulties of contacting Sb-based materials have been resolved in the extensive work on  
34 skutterudite generator modules.

### 35 36 37 **Concluding Remarks**

38 Major advances have been made since the first investigations in the early 2000s and a range of high-  
39 performing Zintl phases is available as illustrated in Figs. 1 and 2. Based on efficiency, the Zintl phases  
40 are amongst the leading thermoelectric materials and further work is therefore warranted. This should  
41 also focus on non-Sb systems, in particular phosphides that may support good electrical properties.

### 42 43 **Acknowledgements**

44 The Leverhulme Trust and EPSRC are acknowledged for supporting the work on thermoelectric  
45 materials.

### 46 47 **References**

- 48 1. Intermetallic Thermoelectrics – Design and Preparation of Half-Heuslers, Skutterudites and Zintl-type  
49 Materials. Jan-Willem G. Bos. Chapter 5, Inorganic Thermoelectric Materials (2021). DOI  
50 <https://doi.org/10.1039/9781788019590-00216>
  - 51 2. Zintl Phases: Recent Developments in Thermoelectrics and Future Outlook. Susan M. Kauzlarich, Alex  
52 Zevkink, Eric Toberer and G. Jeff Snyder. Chapter 1, Thermoelectric Materials and Devices (2016).  
53 <https://doi.org/10.1039/9781782624042-00001>
- 54  
55  
56  
57  
58  
59  
60

3. New sustainable ternary copper phosphide thermoelectrics. Quinn, R.J., Stevens, C., Long, H., et al. Chem. Commun. 58, 11811 (2022). <https://doi.org/10.1039/D2CC03154J>
4. High thermoelectric cooling performance of n-type  $\text{Mg}_3\text{Bi}_2$ -based materials. Jun Mao et al. Science 365, Issue 6452, pp 495-498. 2019. <https://www.science.org/doi/10.1126/science.aax7792>
5. Zhang, J., Song, L., Pedersen, S. et al. Discovery of high-performance low-cost n-type  $\text{Mg}_3\text{Sb}_2$ -based thermoelectric materials with multi-valley conduction bands. Nat Commun 8, 13901 (2017). <https://doi.org/10.1038/ncomms13901>
6. Zou, T., Qin, X., Zhang, Y. et al. Enhanced thermoelectric performance of  $\beta\text{-Zn}_4\text{Sb}_3$  based nanocomposites through combined effects of density of states resonance and carrier energy filtering. Sci Rep 5, 17803 (2015). <https://doi.org/10.1038/srep17803>
7. Zhang, J., Song, L., Madsen, G. et al. Designing high-performance layered thermoelectric materials through orbital engineering. Nat Commun 7, 10892 (2016). <https://doi.org/10.1038/ncomms10892>
8. Traversing the Metal-Insulator Transition in a Zintl Phase: Rational Enhancement of Thermoelectric Efficiency in  $\text{Yb}_{14}\text{Mn}_{1-x}\text{Al}_x\text{Sb}_{11}$ . Advanced Functional Materials 18, Volume 18 (2008). <https://doi.org/10.1002/adfm.200800298>
9. Isotropic Conduction Network and Defect Chemistry in  $\text{Mg}_{3+x}\text{Sb}_2$ -Based Layered Zintl Compounds with High Thermoelectric Performance. Hiromasa Tamaki, Hiroki K. Sato and Tsutomu Kanno. Advanced Materials 28, Issue 26 (2016). <https://doi.org/10.1002/adma.201603955>
10. Do we really need high thermoelectric figures of merit? A critical appraisal to the power conversion efficiency of thermoelectric materials. Dario Narducci. Appl Phys Lett 99, 102104 (2011) <https://doi.org/10.1063/1.3634018>
11. Achieving  $zT > 1$  in Inexpensive Zintl Phase  $\text{Ca}_9\text{Zn}_{4+x}\text{Sb}_9$  by Phase Boundary Mapping. Saneyuki Ohno, Umut Aydemir, Maximilian Amsler, Jan-Hendrik Pöhls, Sevan Chanakian, Alex Zevalkink, Mary Anne White, Sabah K. Bux, Chris Wolverton, G. Jeffrey Snyder. Advanced Materials, 27, Issue 20 (2017). <https://doi.org/10.1002/adfm.201606361>
12. Improvement of Low-Temperature  $zT$  in a  $\text{Mg}_3\text{Sb}_2$ - $\text{Mg}_3\text{Bi}_2$  Solid Solution via Mg-Vapor Annealing. Maxwell Wood, Jimmy Jiahong Kuo, Kazuki Imasato and Gerald Jeffrey Snyder. Advanced Materials 31, Issue 35 (2019). <https://doi.org/10.1002/adma.201902337>

## 5.11 Molybdenum-based cluster chalcogenides as high-temperature thermoelectric materials

Christophe Candolfi<sup>1</sup>, Patrick Gougeon<sup>2</sup>, Philippe Gall<sup>2</sup> and Bertrand Lenoir<sup>1</sup>

<sup>1</sup> Institut Jean Lamour, UMR 7198 CNRS – Université de Lorraine, 2 allée André Guinier-Campus ARTEM, BP 50840, 54011 Nancy Cedex, France

<sup>2</sup> Institut des Sciences Chimiques de Rennes, UMR 6226 CNRS – Université de Rennes 1 - INSA de Rennes, 11 allée de Beaulieu, CS 50837, F-35708 Rennes Cedex, France

### Status

Thermoelectric materials provide a versatile way to convert waste heat into electrical power from room to high temperatures. While most of them reach their optimum efficiency between 500 and 700°C, only a handful are able to operate beyond due to their limited thermal stability and/or melting point. Over the last two decades, several rare-earth-containing Zintl phases were



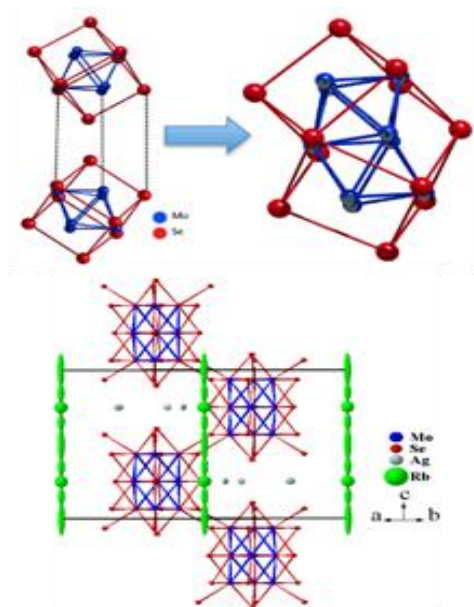


Figure 1. (upper panel) Example of two Mo<sub>6</sub>Se<sub>8</sub> units condensing to form a Mo<sub>9</sub>Se<sub>11</sub> cluster. (lower panel) Crystal structure of Ag<sub>3</sub>RbMo<sub>9</sub>Se<sub>11</sub> highlighting the extended electronic density of the Rb cations, a general characteristic of Mo-based cluster compounds.

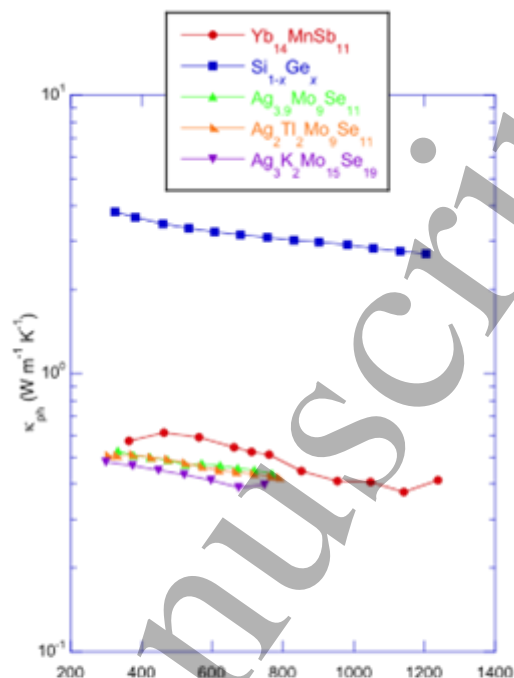


Figure 2. Temperature dependence of the lattice thermal conductivity  $\kappa_{ph}$  of various Mo-based cluster compounds compared to those of the Zintl phase Yb<sub>14</sub>MnSb<sub>11</sub> and the solid solution Si<sub>1-x</sub>Ge<sub>x</sub>.

demonstrated to outperform the state-of-the-art Si<sub>1-x</sub>Ge<sub>x</sub> alloys used in space applications [1-4]. Identifying novel materials with high thermoelectric performance and high melting points is desirable for both terrestrial and space applications. While the former would benefit from higher temperature differences yielding enhanced output power, such materials would also allow to reduce the amount of radioisotope heat-source fuel embarked in spacecrafts. In this context, Mo-based cluster compounds are particularly appealing due to their very high melting points, typically above 1800°C, and their promising thermoelectric properties [5-10], as first pointed out in Chevrel phases [9]. The crystal structure of these compounds are built up by a three-dimensional arrangement of Mo<sub>3n</sub>X<sub>3n+2</sub> clusters (X = S, Se or Te; n is an integer), the size and geometry of which can vary from 3 to more than 36 atoms. The intercluster voids can be filled by various cations such as alkali (Li, Na, K, Rb or Cs), alkaline-earth (Ba) or transition metals (Ag, In, Fe, Ti or Cu) with a strongly disordered character (Figure 1). Additional inserted cations (Ag or Cu) contribute to both tuning the *p*-type electronic properties and lowering the lattice thermal conductivity down to extremely low values on the order of 0.3 – 0.5 W m<sup>-1</sup> K<sup>-1</sup> at high temperatures (Figure 2) in several compounds such as Ag<sub>x</sub>Mo<sub>9</sub>Se<sub>11</sub>, Ag<sub>2</sub>Ti<sub>2</sub>Mo<sub>9</sub>Se<sub>11</sub>, Ag<sub>3</sub>RbMo<sub>9</sub>Se<sub>11</sub> or Ag<sub>3</sub>In<sub>2</sub>Mo<sub>15</sub>Se<sub>19</sub> [5-8]. With these values being similar to those achieved in the best-performing *p*-type Zintl phases, improving the power factor of quaternary molybdenum chalcogenides through a careful selection of inserted cations and band-structure-engineering tools (resonant levels, band convergence...) offers interesting prospects to design rare-earth-free compounds with thermoelectric performance rivalling the best thermoelectric materials operating above 900°C.



### Current and Future Challenges

The key advantages of these phases – chemical richness and flexibility, high melting points, inherently poor thermal conductors – are counterbalanced by several drawbacks that need to be addressed in future works. A first difficulty is related to the complex synthesis route required to produce phase-pure samples, which usually involves high-temperature solid-state reactions of powdered, mixed binary or ternary precursors followed by ion-exchange reactions to insert alkali or alkaline-earth elements. This complexity in the synthesis process contrasts with more direct, time-efficient techniques typically employed such as powder metallurgy or high-energy ball-milling. Whether some of these cluster materials can be obtained in high yield by such techniques remain to be investigated. A second challenge to address is tied to their lower thermoelectric performance with respect to optimized Zintl phases, with maximum  $ZT$  values remaining limited to 0.7 at 800 K [5-8] due to their moderate power factors. Being inherently  $p$ -type metals, inserting cations drives the electronic properties towards a highly-doped semiconducting state. However, the hole concentrations achieved remain too high which, combined with the multiband character of transport, contributes to lower the thermopower values. Further adjustment of the hole concentration through aliovalent substitutions or insertions will be important to make them competitive with Zintl phases. Although rare examples of  $n$ -type Mo cluster compounds have been reported [10], the fundamental question of  $n$ -type dopability remains another issue that will require more thorough investigations. In addition to these materials-related issues, their integration into thermoelectric legs will also face challenges. While most of these materials are relatively immune against sublimation up to the sintering temperature (1000 – 1200°C), they remain sensitive to oxidizing atmospheres, as the vast majority of thermoelectric materials. Efforts to determine their aging behaviour in such environments and in contact with other types of materials used in thermoelectric generators will be worthwhile to fully assess their potential for power generation applications.

### Advances in Science and Technology to Meet Challenges

Overcoming the above-mentioned challenges will be facilitated by the recent progress realized in the synthesis of complex thermoelectric materials and their integration into devices. High-energy ball milling may be employed to synthesize various precursors prior to a second annealing step of mixed powders. Alternatively, efforts should also be devoted to replace this second, time-consuming step by a direct ball-milling reaction. A successful synthesis of these cluster compounds by this technique would speed up the identification of novel phases with potentially superior thermoelectric properties, thereby contributing to address the second challenge related to their still moderate  $ZT$  values. Deploying the arsenal of band-structure-engineering tools will be an interesting line of research to pursue in parallel, which will require electronic band structure and transport property calculations as a theoretical guide. An inherent difficulty of such calculations is the proper modelling of the cationic disorder that characterizes these compounds. Recent efforts towards this goal have shown a good agreement between the thermopower values computed and the experimental data. Further calculations will allow for a full screening of the rich landscape of possible chemical compositions, offering valuable insights into the most judicious dopants and cations to be investigated. Detailed characterizations of the thermal stability of these materials under oxidizing atmospheres and under vacuum should be performed using state-of-the-art techniques. This will enable to determine the temperature range over which these materials are thermally stable with respect to mass loss and oxidation. Finally, first attempts to fabricate thermoelectric legs would be worthwhile to identify the main issues to be solved for the development of  $p$ -type, and possibly  $n$ -type, legs. This might require the identification of diffusion barriers and braze to minimize the electrical contact resistance and the thermomechanical stresses undergone under operating conditions. In this regard, determining the mechanical properties of these materials will be necessary.

### Concluding Remarks

With the remarkable ability for crystalline materials to poorly conduct heat and high melting points, multinary molybdenum cluster chalcogenides offer an interesting playground to design and optimize novel phases for thermoelectric applications at very high temperatures. Despite the growing number of studies devoted to these materials, the surface of the vast landscape of chemical compositions has only been barely scratched. Further manipulating the types of clusters and cations inserted may open up new avenues for achieving improved  $ZT$  values. Solving issues identified herein will pave the way to the development of rare-earth free, highly efficient Mo cluster compounds that can be integrated in thermoelectric generators for both space and industry-related applications.

### Acknowledgements

The authors acknowledge the financial support of the French Agence Nationale de la Recherche (ANR), through the program Energy Challenge for Secure, Clean and Efficient Energy (Challenge 2, 2015, project MASSCOTE, ANR-15-CE05-0027).

### References

- [1] S. R. Brown, S. M. Kauzlarich, F. Gascoin and G. J. Snyder, "Yb<sub>14</sub>MnSb<sub>11</sub>: New High Efficiency Thermoelectric Material for Power Generation", *Chem. Mater.*, vol. 18, 1873–1877, March 2006.
- [2] A. F. May, J.-P. Fleurial and G. J. Snyder, "Thermoelectric performance of lanthanum telluride produced via mechanical alloying", *Phys. Rev. B*, vol. 78, pp. 125205-1–125205-12, Sept. 2008.
- [3] D. Cheikh, B. E. Hogan, T. Vo, P. Von Allmen, K. Lee, D. M. Sniadak, A. Zevalkink, B. S. Dunn, J.-P. Fleurial and S. K. Bux, "Praseodymium Telluride: A High-Temperature, High-ZT Thermoelectric Material", *Joule*, vol. 2, pp. 698-709, April 2018.
- [4] C. B. Vinning and J.-P. Fleurial, "Silicon-Germanium: An Overview of Recent Development", AIP Press, pp. 87–120, 1993.
- [5] T. Zhou, B. Lenoir, M. Colin, A. Dauscher, R. Al Rahal Al Orabi, P. Gougeon, M. Potel and E. Guilmeau, "Promising thermoelectric properties in Ag<sub>x</sub>Mo<sub>9</sub>Se<sub>11</sub> compounds (3.4 ≤ x ≤ 3.9)", *Appl. Phys. Lett.*, vol. 98, pp. 162106-1–162106-3, April 2011.
- [6] R. Al Rahal Al Orabi, P. Gougeon, P. Gall, B. Fontaine, R. Gautier, M. Colin, C. Candolfi, A. Dauscher, J. Hejtmanek, B. Malaman and B. Lenoir, "X-ray Characterization, Electronic Band Structure, and Thermoelectric Properties of the Cluster Compound Ag<sub>2</sub>Tl<sub>2</sub>Mo<sub>9</sub>Se<sub>11</sub>", *Inorg. Chem.*, vol. 53, pp. 11699-11709, Oct. 2014.
- [7] P. Gougeon, P. Gall, O. Merdrignac-Conanec, L. Aranda, A. Dauscher, C. Candolfi and B. Lenoir, "Synthesis, Crystal Structure, and Transport Properties of the Hexagonal Mo<sub>9</sub> Cluster Compound Ag<sub>3</sub>RbMo<sub>9</sub>Se<sub>11</sub>", *Inorg. Chem.*, vol. 56, pp. 9684-9692, Aug. 2017.
- [8] P. Gougeon, P. Gall, R. Al Rahal Al Orabi, B. Fontaine, R. Gautier, M. Potel, T. Zhou, B. Lenoir, M. Colin, C. Candolfi and A. Dauscher, "Synthesis, Crystal and Electronic Structures, and Thermoelectric Properties of the Novel Cluster Compound Ag<sub>3</sub>In<sub>2</sub>Mo<sub>15</sub>Se<sub>19</sub>", *Chem. Mater.*, vol. 24, pp. 2899-2908, July 2012.
- [9] T. Caillat, J.-P. Fleurial and G. J. Snyder, "Potential of Chevrel Phases to Thermoelectric Applications", *Solid State Sci.*, vol. 1, no. 7-8, pp. 535–544, 1999.
- [10] P. Gougeon, P. Gall, S. Migot, J. Ghanbaja, M. Hervieu, P. Levinsky, J. Hejtmanek, A. Dauscher, B. Malaman, B. Lenoir and C. Candolfi, "Ti<sub>0.6</sub>Mo<sub>3</sub>S<sub>5</sub>, an original large tunnel-like molybdenum sulfide with Mo zigzag chains and disordered Tl cations", *Mater. Adv.*, vol. 2, pp. 6020-6030, Aug. 2021.

## 5.12 Organic Thermoelectrics

Deepak Venkateshvaran<sup>1</sup> and Bernd Kaestner<sup>2</sup>

<sup>1</sup>Cavendish Laboratory, University of Cambridge, JJ Thomson Avenue, Cambridge, CB3 0HE, United Kingdom. <https://orcid.org/0000-0002-7099-7323>

<sup>2</sup>Physikalisch-Technische Bundesanstalt (PTB), Berlin, Germany, Abbestrasse 2-12, 10587, Berlin, Germany. <https://orcid.org/0000-0002-6575-6621>

### Status

Organic semiconductors are relevant for applications in thermoelectrics owing to their low thermal conductivities ( $\kappa$ ), relatively large and tuneable Seebeck coefficients ( $S$ ) and their ability to conduct charge carriers with reasonably high electrical conductivities ( $\sigma$ ). Since the thermoelectric figure of merit is defined as  $ZT = \left(\frac{S^2\sigma}{\kappa}\right)T$ , an organic semiconductor having  $\kappa = 0.3 \text{ W m}^{-1} \text{ K}^{-1}$  and a power factor  $S^2\sigma \sim 10^{-3} \text{ W m}^{-1} \text{ K}^{-2}$  should effortlessly demonstrate the benchmark figure in thermoelectrics of  $ZT \sim 1$  at 300 K. [1] Experimental evidence shows that such values of the thermal conductivity and the power factor lie within the parameter space accessible by organic semiconductors, justifying their search in the effort to maximise  $ZT$ .

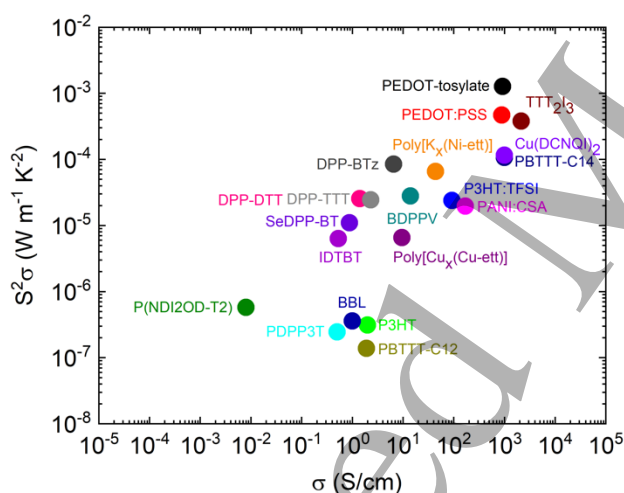


Figure 5.12.1 Thermoelectric power factor vs electrical conductivity in organic semiconductors

An organic semiconductor's low thermal conductivity arises from the intrinsic nature of van der Waal's bonding and molecular vibration-induced phonon scattering. Their large Seebeck coefficients (i.e., several times  $\frac{k_B}{e}$ ) are a consequence of configurational entropy, and their electrical conductivities spur from rapid hopping of charge carriers along the polymer backbone, along the inter-molecular  $\pi$ - $\pi$  stacking direction, or along both simultaneously. The hopping rates are influenced by intra-molecular torsion as well as disorder in the manner molecules pack within the solid state. A picture that connects both molecular conformation and structural properties with the thermoelectric transport coefficients is starting to evolve. [2] Such an interdependence demands comprehensive investigation and validation through the design of new organic molecules. Figure 5.12.1 shows the power factors of a selection of organic semiconductors as a function of their conductivity. [3], [4] The heuristic trend is clear; An increasing electrical conductivity gives rise to an increasing power factor.

1  
2  
3  
4 By modulating the carrier density,  $n$ , over three orders of magnitude from  $10^{18}$  to  $10^{21}$   $\text{cm}^{-3}$ , the Seebeck  
5 coefficient of an organic semiconductor decreases from 100s of  $\mu\text{V}/\text{K}$  to 10s  $\mu\text{V}/\text{K}$ . Its electrical  
6 conductivity increases by several orders of magnitude over the same range. The boost in the power factor  
7 got by increasing the electrical conductivity in these soft electronic systems is known to outweigh the  
8 accompanying reduction in the Seebeck coefficient. For this reason, the last few years have focused on  
9 charge carrier doping as a route to increase the power factor, and thus  $ZT$  of organic semiconductors.

### 11 12 **Current and Future Challenges**

13 1. An understanding of the transport coefficients  $\kappa$ ,  $S$  and  $\sigma$ , and their influence on the power factor  
14 continues to rapidly develop. Empirical trends such as  $S \propto \sigma^{-\frac{1}{4}}$  and  $S^2\sigma \propto \sigma^{\frac{1}{2}}$  have been found, but a  
15 foundational description of why these scaling laws arise is still lacking. [5] In addition, although polaronic  
16 transport theories at high charge carrier densities are known to explain the behaviour of the Seebeck  
17 coefficient and the power factor in the 'near-degenerate' transport regime, more experimental evidence  
18 is necessary to validate their use. In general,  $S$  decreases with increasing  $n$  and  $\sigma$  is proportional to both  
19  $n$  and the carrier mobility  $\mu$ . Thus, increasing  $\mu$  beyond its current benchmark of  $1 \text{ cm}^2/\text{Vs}$  is another  
20 prospective route to increasing the overall power factor. [6] Progress in this direction has been sluggish.

21  
22  
23  
24 2. Efficient doping techniques that guarantee increases in the charge density of organic semiconductors  
25 are currently possible only through the incorporation of additional dopant molecules within the lattice.  
26 This can cause changes to the rigidity of molecular packing. [2], [1] In other words, the original organic  
27 system needs to gradually distort to be able to show improved thermoelectric performance. In so doing,  
28 the pristine properties of the original semiconductor are not preserved.

29  
30  
31 3. Very high carrier densities upon doping instil 'metallic transport' properties in organic semiconductors.  
32 This causes its thermal transport to sport a strong electronic contribution in addition to its lattice  
33 contribution. Although intermediate doping densities under controlled conditions can preserve a low  
34 thermal conductivity, such is not the case for very high electrical conductivities. [7] The simultaneous  
35 increase in the electrical and thermal transport coefficients in the organic semiconductor imposes a limit  
36 on the maximum achievable  $ZT$ . The common belief that organic semiconductors can embody a 'phonon-  
37 glass electron-crystal' necessary for high performance thermoelectrics is thus invalidated at very high  
38 carrier densities. [1] One workaround in overcoming the intrinsic limits to  $ZT$  within organic systems is to  
39 actualise 'phonon stack electron tunnel composites' using selective interfaces. [6] In such composites,  
40 conductive carbon nanotubes are incorporated within the matrix of organic semiconductors to ensure  
41 that charge carriers preserve high mobility pathways through carbon nanotubes. Phonons on the other  
42 hand continue to be scattered, ensuring reduced thermal conductivities. [8]

43  
44  
45 4. There is also a lack of stable, high-performance, n-type organic thermoelectric materials beyond the  
46 fullerenes, which makes impedance-matched all-organic thermoelectric generators very complex to  
47 realise.

48  
49  
50 5. Evolving the optimum properties for thermoelectric conversion within single component organic films,  
51 without the incorporation of additional dopant molecules or without building carbon-based composites,  
52 remains a challenge. One way to preserve the compositional purity of organic semiconductors for science  
53 and applications of heat to voltage conversion is to augment ongoing research (that focuses majorly on  
54  $ZT$  optimisation) with novel devices and measurement techniques that use the efficient heat flow within  
55 molecular films under IR vibrational resonance. [9] Doing so unravels the nature of thermal transport

1  
2  
3 within molecular systems and evolves new applications of organic polymers in ultrafast bolometers and  
4 nanoscale heat switches.  
5

### 6 **Advances in Science and Technology to Meet Challenges**

7 To probe the scattering characteristics of electrons and phonons within composite micro- and nanoscale  
8 organic polymer matrices, as well as within semicrystalline polymer films containing grain boundaries,  
9 advanced metrology tools need to be developed. Performing measurements on composite materials is a  
10 challenge because of the sample complexity and the requirement for doing measurements with very high  
11 spatial, temporal, and energy resolution. Complex device geometries such as organic-inorganic multilayer  
12 structures can make use of multi-modal analytic tools like Infrared Scanning Nearfield Optical Microscopy  
13 (IR-SNOM), which when employed within the spectral region containing molecular fingerprints, permits  
14 chemical and crystallinity characterization. [9] IR-SNOM also makes contactless electrical characterisation  
15 possible over a limited conductivity range. Despite having a wavelength range in micrometres, its spatial  
16 resolution is not sacrificed since it is governed by the tip geometry. Hence, such a multi-modal tool can  
17 be used in understanding the role of grains and domain boundaries within thin films for thermoelectrics.  
18 It also allows one to characterize time-resolved degradation phenomena that are expected to start at the  
19 grain boundaries simultaneously with their influence on electronic transport.  
20  
21  
22

23 For accurately mapping the temperature distribution in organic semiconductors, techniques such as  
24 Scanning Thermal Microscopy (SThM), Time Domain Thermoreflectance or Frequency Domain  
25 Thermoreflectance can be used. Thermoreflectance makes use of the change in the reflectance of the  
26 surface upon heating to derive the thermal properties. The probe in SThM is sensitive to local  
27 temperatures, and therefore acts like a nano-scale thermometer. SThM measures the local thermal  
28 conductivity with an uncertainty of 20% for low thermal conductivity materials at room temperature. The  
29 spatial resolution can be down to a few tens of nanometres. Thermoelectric characterization using raster-  
30 scanned lasers also have sub-wavelength, nanometre-scale resolution, as demonstrated using nearfield  
31 enhancement of metallized scanning probes. [10] The above techniques make possible an evaluation of  
32 the thermoelectric transport coefficients within single ordered domains, without the drawbacks  
33 presented by domain boundaries in polycrystalline films.  
34  
35  
36

### 37 **Concluding Remarks**

38  $ZT = 1$  is yet to be demonstrated in the field of organic thermoelectrics. Despite tremendous progress  
39 at characterising various macromolecular systems over the last decade, several roadblocks continue to  
40 prevail. These roadblocks are linked to factors such as dopant stability, doping efficiency, control of  
41 microstructure and molecular conformation, a limit on the achievable charge carrier mobility, a lack of  
42 sufficient competitive n-type organic materials, a difficulty in describing transport within disordered  
43 systems having an abundance of domain boundaries, and the absence of strategies which decouple  $\sigma$   
44 from  $\kappa$  at large carrier densities. Consistent and precise measurements of thermoelectric transport  
45 coefficients at the nanoscale and molecular scale are only starting to be pursued. Such techniques might  
46 ultimately yield the clarity required to build a framework to understand and describe the fundamental  
47 limits on thermoelectric efficiency using organic semiconductors and organic semiconductor-based  
48 hybrids.  
49  
50

### 51 **Acknowledgements**

52 D. Venkateshvaran acknowledges the Royal Society for funding in the form of a Royal Society University  
53 Research Fellowship (Royal Society Reference No. URF/R1/201590).  
54  
55  
56  
57  
58  
59  
60



## References

- [1] J. Liu, B. van der Zee, R. Alessandri, S. Sami, J. Dong, M. I. Nugraha, A. J. Barker, S. Rousseva, L. Qiu, X. Qiu, N. Klasen, R. C. Chiechi, D. Baran, M. Caironi, T. D. Anthopolous, G. Portale, R. W. A. Havenith and S. J. Marrink, "N-type organic thermoelectrics: demonstration of  $ZT > 0.3$ ," *Nature Communications*, vol. 11, p. 5694, 2020.
- [2] A. Abutaha, P. Kumar, E. Yildirim, W. Shi, S.-W. Yang, G. Wu and K. Hippalgaonkar, "Correlating charge and thermoelectric transport to paracrystallinity in conducting polymers," *Nature Communications*, vol. 11, p. 1737, 2020.
- [3] K. Broch, D. Venkateshvaran, V. Lemauryer, Y. Olivier, D. Beljonne, M. Zelazny, I. Nasrallah, D. J. Harkin, M. Statz, R. Di Pietro, A. J. Kronemeijer and H. Siringhaus, "Measurements of Ambipolar Seebeck Coefficients in High-Mobility Diketopyrrolopyrrole Donor–Acceptor Copolymers," *Adv. Electron. Mater.*, vol. 3, p. 1700225, 2017.
- [4] M. Lindorf, K. A. Mazzio, J. Pflaum, K. Nielsch, W. Brütting and M. Albrecht, "Organic-based thermoelectrics," *Journal of Materials Chemistry A*, vol. 8, p. 7495, 2020.
- [5] B. Russ, A. Glauddell, J. J. Urban, M. L. Chabynyc and R. A. Segalman, "Organic thermoelectric materials for energy harvesting and temperature control," *Nature Reviews Materials*, vol. 1, p. 16050, 2016.
- [6] M. Campoy-Quiles, "Will organic thermoelectrics get hot?," *Phil. Trans. R. Soc. A*, vol. 377, p. 20180352, 2019.
- [7] O. Zapata-Arteaga, A. Perevedentsev, S. Marina, J. Martin, J. S. Reparaz and M. Campoy-Quiles, "Reduction of the Lattice Thermal Conductivity of Polymer Semiconductors by Molecular Doping," *ACS Energy Letters*, vol. 5, no. 9, pp. 2972–2978, 2020.
- [8] P. A. Finn, C. Asker, K. Wan, E. Bilotti, O. Fenwick and C. B. Nielsen, "Thermoelectric Materials: Current Status and Future Challenges," *Frontiers in Electronic Materials*, vol. 1, p. 677845, 2021.
- [9] G. Ulrich, E. Pfitzner, A. Hoehl, J.-W. Liao, O. Zadvorna, G. Schweicher, H. Siringhaus, J. Heberle, B. Kästner, J. Wunderlich and D. Venkateshvaran, "Thermoelectric nanospectroscopy for the imaging of molecular fingerprints," *Nanophotonics*, vol. 9, no. 14, p. 4347–4354, 2020.
- [10] T. Janda et. al., "Magneto-Seebeck microscopy of domain switching in collinear antiferromagnet CuMnAs," *Phys. Rev. Materials*, vol. 4, p. 094413, 2020.

## 5.13 Two-dimensional (2D) materials for thermoelectric applications

Yunshan Zhao<sup>1</sup> and Gang Zhang<sup>2</sup>

<sup>1</sup>NNU-SULI Thermal Energy Research Center (NSTER) and Center for Quantum Transport and Thermal Energy Science (CQTES), School of Physics and Technology, Nanjing Normal University, Nanjing 210023, China

<sup>2</sup>Institute of High Performance Computing, A\*STAR, Singapore

### Status

Although the commercial bulk TE materials were well developed around 1960s, the research interest in low dimensional TE traces back to 1990s, where the effect of quantum-confinement was proposed to modulate the TE coefficients in a nearly independent way [1]. Among the low dimensional materials for TE, the family of two-dimensional (2D) materials is one of the largest and latest groups, which becomes the subject of intense study in last decade.

1  
2  
3 In contrast with the traditional bulk TE materials, 2D materials represent a discretized electron density of  
4 states (DOS) due to the quantum size effect [1], which is beneficial for an enhanced Seebeck coefficient  
5 [2,3]. In bulk forms, the charge carriers are normally introduced during the process of materials growth,  
6 while for 2D materials, the carrier concentrations could be easily tuned by intercalating ions or an electric  
7 gating. Meanwhile, the layered 2D can be exfoliated into few layers, with a dimension close to the mean  
8 free paths of phonons, therefore, the electrical conductivity or thermal conductivity could be tuned  
9 individually. Moreover, the bandgap of 2D is easily tuned by the strategy of 'thickness engineering'. All of  
10 these advantages of 2D materials are beneficial for a high  $ZT$  [2,3].  
11  
12  
13

### 14 **Current and Future Challenges**

15 With the advancement of nano-fabrications and nano-characterizations, a series of TE devices based on  
16 2D materials have been developed and investigated, showing outstanding TE energy conversion potential,  
17 such as  $\text{TiS}_2$  with a  $ZT$  value 0.2 [4] at 300K, which is nearly comparable to that of bulk TE forms at room  
18 temperature. While for even higher temperature regime that bulk TE materials typically outperform, there  
19 is lacking experimental data related to the 2D TE performance.  
20

21 Currently, strategies of exploring 2D TE are dominated by theoretical calculations and simulations. By  
22 constructing a monolayer lattice structure,  $S$ ,  $\sigma$  and  $\kappa$  can be obtained through atomistic simulations, and  
23 the optimized  $ZT$  is achieved, like  $\text{TiS}_2$  [5] and BP [6] with  $ZT$  values around 1 and 1.5, respectively, as  
24 shown in Figure 1. Compared to the theoretical high  $ZT$  under a much high carrier concentration, the  
25 current experimental treatments like top- or back-gate are insufficient to achieve a high charge  
26 concentration in the system, thus the optimization of  $ZT$  in 2D materials is far from being satisfactory for  
27 potential applications. Some experimental approaches like thickness engineering, tunability of carrier  
28 scattering mechanisms and defects engineering [7,8] are proposed, while the tunability of TE conversion  
29 efficiency is limited.  
30

31 Moreover, there is lacking study for the measurement of each  $ZT$  parameter, especially for the evaluation  
32 of power factor. A high  $ZT$  value and thus improved heat-to-electricity energy conversion efficiency is the  
33 key challenge for 2D TE materials in the current and future study. Since the TE performance of 2D  
34 materials is based on field-effect transistor (FET) devices, a better electrical ohmic contact is desirable to  
35 extract the intrinsic transport property of the measured materials. On the other hand, considering the  
36 sensitivity to environment and super tiny scale of each 2D TE device, integration of 2D TE units is another  
37 key consideration for their practical use. Further advances on 2D TE should be focused on the design of  
38 new materials and new contacts to achieve optimal TE properties. Physically, the phonon and electron  
39 transport mechanisms in 2D should be clarified as well to further manage their contributions in  $ZT$ .  
40  
41  
42  
43  
44  
45  
46  
47  
48  
49  
50  
51  
52  
53  
54  
55  
56  
57  
58  
59  
60

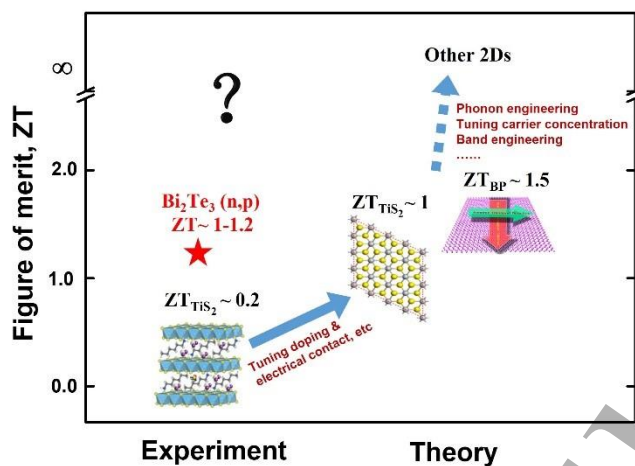


Figure 1. The trend of  $ZT$  based on experimental characterization and theoretical calculation. The  $ZT$  value of  $TiS_2$  is 0.2 (experiment) [4] and 1 (theory) [5]. The  $ZT$  for black phosphorus (BP) by calculation is 1.5 [6]. The data of bulk  $Bi_2Te_3$  is shown for comparison, with  $ZT$  ranging from  $\sim 1$  (n doping) to  $\sim 1.2$  (p doping) [9]. All the data are extracted at room temperature. Further improvements of 2D  $ZT$  would be focused on strategies like phonon engineering, band engineering and tuning the carrier concentration, etc.

### Advances in Science and Technology to Meet Challenges

Following graphene, numerous of 2D materials with unique transport properties are discovered. The 2D family and the subsequent in-plane and out-of-plane heterostructures provide a new platform to explore the TE performance. Among them, 2D semiconductors with a tunable bandgap and high electron/hole mobilities have shown superior TE property [2,3], which even disgraces the TE performance of bulk forms in the low temperature range. These 2D semiconductors with rich physical properties would be further explored for TE applications. Meanwhile, more interesting 2D semiconductor materials and their complex heterostructures should be fabricated and further designed for TE application.

As for the huge family of 2D semiconductors, it is challenging to conduct measurement for  $ZT$  value of each sample and the high-throughput machine learning (ML) techniques should be developed to search for the appropriate 2D with a high  $ZT$  [10]. ML, well known for its data-analysis capability, provides an efficient and convenient tool to discover the appropriate TE candidate before conducting experimental measurement. By evaluating each parameter in  $ZT$ , ML accelerates the exploration of the TE properties based on 2D materials by linking its various unique characteristics. On the other hand, the current theoretical and modelling tools should be developed as well to better simulate the TE transport properties and thus advance the TE performances.

Moreover, advanced nano-fabrication technologies during sample growth and the subsequent TE device fabrication based on 2D materials should be considered carefully. As for the characterization of TE properties of 2D, the standard commercialized techniques should be developed, which is still lacking and needs more attentions for future study. Different from that of bulk TE materials, both the quality of substrate and the environment would significantly affect the TE performance of 2D materials. 2D materials with a super-high crystalline supported on a clean substrate (normally treated by a dielectric  $h$ -BN) is necessary for TE measurement. For the device level applications, the factors of electrical shock, electrical contact and moisture, etc, are the main considerations for integrated TE devices based on 2D semiconductors. These strategies for modifying 2D  $ZT$  have been shown in Figure 1.

### Concluding Remarks

To conclude, we briefly introduce the current status of 2D materials for TE applications, together with the current challenges and advancement in science and technology required. Although numerous 2D materials have been designed and fabricated, the attempt of using them for TE application is scarce, and this research field is still in its infancy, which definitely requires further research effort. The 2D materials with high  $ZT$  under low carrier concentration are quite potential in TE energy conversion. In experiments, the advanced nano-technologies toward 2D TE devices like achieving better electrical contact and high carrier doping, etc, would be developed, which are beneficial for TE performance optimization. Meanwhile, with the advent of 2D library, more 2D semiconductors appropriate for TE applications should be filtered and selected with the help of high-throughput machine learning studies.

### Acknowledgements

YSZ is supported by the National Natural Science Foundation of China (No. 12204244), Natural Science Foundation of Jiangsu Province (Grant No. BK20210556) and Jiangsu Specially-Appointed Professor Program. GZ is supported in part by RIE2020 Advanced Manufacturing and Engineering (AME) Programmatic (A1898b0043) and A\*STAR Aerospace Programme (M2115a0092).

### References

- [1] Hicks, L.; Dresselhaus, M. S. Effect of quantum-well structures on the thermoelectric figure of merit [J]. *Physical Review B* 1993, 47, (19), 12727.
- [2] Zhao Y, Cai Y, Zhang L, et al. Thermal transport in 2D semiconductors—considerations for device applications[J]. *Advanced Functional Materials*, 2020, 30(8): 1903929.
- [3] Wu J, Chen Y, Wu J, et al. Perspectives on thermoelectricity in layered and 2D materials[J]. *Advanced Electronic Materials*, 2018, 4(12): 1800248.
- [4] Wan C, Gu X, Dang F, et al. Flexible n-type thermoelectric materials by organic intercalation of layered transition metal dichalcogenide  $TiS_2$ [J]. *Nature materials*, 2015, 14(6): 622-627.
- [5] Li G, Yao K, Gao G. Strain-induced enhancement of thermoelectric performance of  $TiS_2$  monolayer based on first-principles phonon and electron band structures[J]. *Nanotechnology*, 2017, 29(1): 015204.
- [6] Ouyang Y, Zhang Z, Li D, et al. Emerging theory, materials, and screening methods: new opportunities for promoting thermoelectric performance[J]. *Annalen der Physik*, 2019, 531(4): 1800437.
- [7] Zhao Y, Yu P, Zhang G, et al. Low-Symmetry  $PdSe_2$  for High Performance Thermoelectric Applications[J]. *Advanced Functional Materials*, 2020, 30(52): 2004896.
- [8] Suh J, Yu K M, Fu D, et al. Simultaneous enhancement of electrical conductivity and thermopower of  $Bi_2Te_3$  by multifunctionality of native defects[J]. *Advanced materials*, 2015, 27(24): 3681-3686.
- [9] Chen S, Ren Z. Recent progress of half-Heusler for moderate temperature thermoelectric applications[J]. *Materials today*, 2013, 16(10): 387-395.
- [10] Wang T, Zhang C, Snoussi H, et al. Machine learning approaches for thermoelectric materials research[J]. *Advanced Functional Materials*, 2020, 30(5): 1906041.

## 5.14 Carbon nanotubes for thermoelectric energy harvesting

Yoshiyuki Nonoguchi

Faculty of Materials Science and Engineering, Kyoto Institute of Technology, Kyoto 606-8585, Japan

### Status

The thermoelectric properties of carbon nanotubes (CNT) are of interest in both the fundamental researches of physical properties, and the development of advanced power generators.[1] Particularly, single-walled carbon nanotubes (SWCNTs) show unique thermoelectric properties compared to conventional thermoelectric materials. Due to their chemically stable structures, SWCNTs are recognized as a platform for studying low-dimension-derived thermoelectric transport.[2] Additionally, due to their mechanical stability, SWCNT-based materials are candidates for the components of flexible thermoelectric power generators.[3] SWCNTs are seamless cylinders made from graphene sheets, and their electronic structures vary depending on the chiral (rolling) angles of graphene. Dependent on the periodic condition, SWCNTs possess semiconducting and metallic electronic structures. Rather than single nanotubes, due to their limited scaling, most studies deal with sheets made from SWCNT networks. In this context, secondary structures such as orientation and inter-tube contacts are highly dominant for thermoelectric properties, along with primary structures (e.g. electronic type and bandgap (diameter), crystallinity).

So far, tremendous efforts have been made for seeking excellent thermoelectric properties of CNT-based materials. A growing body of evidence suggests that the films composed of enriched semiconducting SWCNTs show superior thermoelectric properties upon viable chemical doping, compared to metal-enriched SWCNT networks.[4] The state-of-the-art work reported the dimensionless figure of merit as high as 0.12 around room temperature, for sorted semiconducting SWCNTs made by the Hipco method.[5] Multi-walled carbon nanotubes (MWCNTs) exhibit advantages for the preparation of structured materials. For example, their yarns and webs can be prepared by the direct spinning of MWCNT products in chemical vapor deposition synthesis,[6] where these materials are robust, and show excellent thermoelectric power factor exceeding  $2000 \text{ mW m}^{-1} \text{ K}^{-2}$ . For the elucidation of physical properties, various emerging chemical processes had yet to be developed, including chemical and electrochemical doping. For optimizing thermoelectric properties, heavy doping to SWCNTs are highly demanded along with the improvement of anti-oxidation in the doped state, particularly n-type SWCNTs. In this context, various approaches to stable n-type doping were reported. Simple electron transfer, hydride transfer, and also supramolecular complexation were examined for this purpose.[7], [8] All these efforts would contribute to the further development of practical power generators as well as the exploration of emerging physical properties.

### Current and Future Challenges

This field based on CNT has showed rapid evolution in the past 15 years, leading to the generation of new physics idea, chemical treatments, and emergent applications in energy harvesting. Despite such progress, structure-property relationship in their thermoelectrics has yet to be explored. Methods of increasing the efficiency of thermoelectric conversion are extremely paradoxical. Usually, there is a trade-off between electrical conductivity and the Seebeck coefficient, from which the optimal power factor must be found. In the case of carbon nanotubes, controlling their inherently huge thermal conductivity is also a challenge.

The understanding of physical and chemical aspects in the thermoelectric properties of SWCNTs should be brought by preparing single-phase materials while the sorting of uniform, high-quality SWCNTs is still under investigation. SWCNTs usually show significant inhomogeneity in their forms (Fig. 1). As-synthesized

carbon nanotubes vary in their diameter and chiral angle (called “chirality”), and these physical variations result in significant changes in their electronic/thermoelectric transport. Controlling the degree of structural perfection and defect density (crystallinity) is crucial for determining the electronic structures and their corresponding transport. Additionally, the thermoelectric properties of the SWCNT assembly are of interest for most applications. In this case, the length of SWCNTs could limit the transport properties (i.e. electrical and thermal conductivity), and the morphology of SWCNT networks might play an important role.[5] The morphology includes the degree of nanotube bundles and entanglement. The thermoelectric properties of aligned SWCNT thin films showed isotropic Seebeck coefficient and anisotropic electrical and thermal conductivity. It is still difficult to independently control each structure, where procedures for the sophisticated sorting and the morphological control of SWCNTs without degradation have yet to be explored. In this context, there still remain many requirements for thermoelectric applications with CNTs, including the controlled growth, the postsynthesis sorting and morphological control, and the characterization techniques.

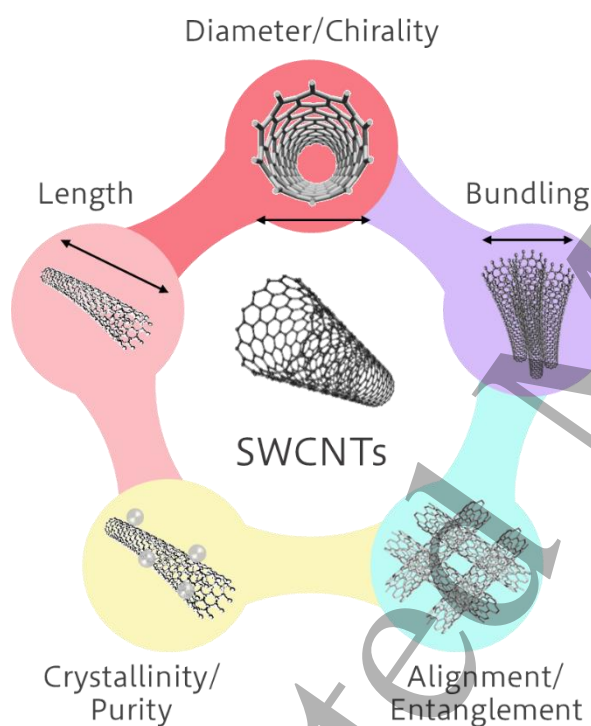


Figure 1. Possible key parameters for the determination of thermoelectric transport in SWCNT films.

### Advances in Science and Technology to Meet Challenges

#### 1. Theoretical approaches

Keeping pace with structural sorting, it is necessary to clarify desirable materials design at an individual SWCNT and SWCNT networks levels. Theoretical knowledge is becoming increasingly important, including calculations on phonons and lattices, calculations on heat transfer, and theoretical depictions of various correlations such as linear response theory, as well as calculations on electronic states and band structures.[9]



## 2. Composite science

Various approaches for high-performance thermoelectric composites with CNTs have been proposed, where thermoelectricity enhancement effects originating from inhomogeneous materials are proposed. For more details, see Section 5.15.

## 3. Power generator design

Most thermoelectric generators are composed of the series circuit of p-type and n-type components (Fig. 2). Their conventional geometry enables power generation in 1) cross-plane and 2) in-plane directions.[10] Due to the shape of nanotubes, it is easy to fabricate their cast film, non-woven sheets, and composite materials where CNTs are oriented two-dimensionally. These sheets show excellent mechanical flexibility, which can be readily applied for the development of in-plane type thermoelectric generators (Fig. 2(b)). Additionally, flexibility in the fabrication of SWCNTs might expand the module design; for example, SWCNTs and MWCNTs can be fabricated into flexible yarns (strings), where the knitting of a fabric is an emerging procedure for the fabrication of thermoelectric generators (Fig. 2(c)).[6] The optimal structures for thermoelectric generators would rely on the applications and should further be investigated.

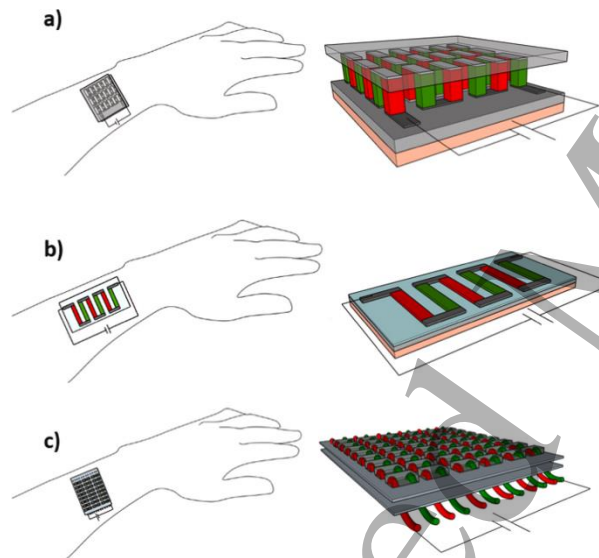


Fig. 2. Schematics of different configurations of thermocouples in wearable TEGs: a) ingot-shaped; b) film-shaped; and c) yarn-shaped. Reproduced with permission.[10] Copyright 2021, Elsevier Ltd..

### Concluding Remarks

The study of thermoelectric conversion with CNTs are still providing new science including physics, thermal engineering, and chemistry, as well as applications in flexible power generators. Regarding the former, in other words, new thermoelectric conversion mechanisms and effects may be discovered by exploring complex fields. In the latter, the price of SWCNTs has dropped significantly over the past two decades due to the realization of mass production, and large-area sheets and longer wire rods are available. This may lead to the development of a completely new type of thermoelectric device. In recent years, environmental power generation through thermoelectric conversion has been attracting attention toward the realization of IoT and physical cyber systems. CNTs, which show relatively low environmental impact, are expected to be used as a realistic thermoelectric material for this purpose.

## Acknowledgements

The author thanks financial supports including JSPS KAKENHI grant number 19H02536, JST PRESTO grant number JPMJPR16R6, JST CREST grant number JPMJCR21Q1, and MEXT Leading Initiative for Excellent Young Researchers (LEADER).

## References

- [1] J. L. Blackburn, A. J. Ferguson, C. Cho, and J. C. Grunlan, "Carbon-Nanotube-Based Thermoelectric Materials and Devices," *Adv. Mater.*, vol. 30, no. 11, p. 1704386, Mar. 2018, doi: 10.1002/ADMA.201704386.
- [2] Y. Ichinose *et al.*, "Solving the Thermoelectric Trade-Off Problem with Metallic Carbon Nanotubes," *Nano Lett.*, vol. 19, no. 10, pp. 7370–7376, Oct. 2019, doi: 10.1021/acs.nanolett.9b03022.
- [3] Y. Nonoguchi *et al.*, "Systematic conversion of single walled carbon nanotubes into n-type thermoelectric materials by molecular dopants," *Sci. Rep.*, vol. 3, p. 3344, 2013, doi: 10.1038/srep03344.
- [4] Y. Nakai *et al.*, "Giant Seebeck coefficient in semiconducting single-wall carbon nanotube film," *Appl. Phys. Express*, vol. 7, no. 2, p. 025103, Feb. 2014, doi: 10.7567/APEX.7.025103.
- [5] B. A. Macleod *et al.*, "Large n- and p-type thermoelectric power factors from doped semiconducting single-walled carbon nanotube thin films," *Energy Environ. Sci.*, vol. 10, no. 10, pp. 2168–2179, Oct. 2017, doi: 10.1039/c7ee01130j.
- [6] J. Choi *et al.*, "Flexible and Robust Thermoelectric Generators Based on All-Carbon Nanotube Yarn without Metal Electrodes," *ACS Nano*, vol. 11, no. 8, pp. 7608–7614, Aug. 2017, doi: 10.1021/acs.nano.7b01771.
- [7] Y. Nakashima, N. Nakashima, and T. Fujigaya, "Development of air-stable n-type single-walled carbon nanotubes by doping with 2-(2-methoxyphenyl)-1,3-dimethyl-2,3-dihydro-1H-benzo[d]imidazole and their thermoelectric properties," *Synth. Met.*, vol. 225, pp. 76–80, Mar. 2017, doi: 10.1016/J.SYNTHMET.2016.11.042.
- [8] Y. Nonoguchi *et al.*, "Simple Salt-Coordinated n-Type Nanocarbon Materials Stable in Air," *Adv. Funct. Mater.*, vol. 26, no. 18, pp. 3021–3028, 2016, doi: 10.1002/adfm.201600179.
- [9] T. Yamamoto and H. Fukuyama, "Possible High Thermoelectric Power in Semiconducting Carbon Nanotubes ~A Case Study of Doped One-Dimensional Semiconductors~, " *J. Phys. Soc. Japan*, vol. 87, no. 2, p. 024707, Jan. 2018, doi: 10.7566/JPSJ.87.024707.
- [10] Z. Soleimani, S. Zoras, B. Ceranic, Y. Cui, and S. Shahzad, "A comprehensive review on the output voltage/power of wearable thermoelectric generators concerning their geometry and thermoelectric materials," *Nano Energy*, vol. 89, p. 106325, Nov. 2021, doi: 10.1016/J.NANOEN.2021.106325.

## 5.15 Polymer-carbon composites for thermoelectric energy harvesting

Bob C. Schroeder<sup>1</sup> and Emiliano Bilotti<sup>2</sup>

<sup>1</sup> Department of Chemistry, University College London, 20 Gordon Street, London WC1H 0AJ, UK

<sup>2</sup> Department of Aeronautics, Imperial College London, Exhibition Road, London SW7 2AZ, UK

### Status

Low dimensional materials, such as fullerenes (0D), carbon nanotubes (1D) and graphene (2D), have long been considered for thermoelectric applications as interesting materials to increase the figure of merit ZT. In particular, low dimensionality has been shown to increase the boundary scattering of phonons

1  
2  
3 without significantly increasing electron scattering and to allow for manipulating the density of states near  
4 the Fermi energy level.[1]

5 Despite these theoretical advantages of carbon allotropes, their high thermal conductivities ( $>2000 \text{ W}\cdot\text{m}^{-1}\cdot\text{K}^{-1}$  for CNT and graphene) and often poor processing characteristics limit their application in  
6 thermoelectrics. To overcome these drawbacks, carbon nanomaterials can be combined with a polymer  
7 matrix (either electrically insulating or conjugated) into polymer nanocomposites.[2] The introduction of  
8 a polymer allows to reduce the aforementioned high thermal conductivity, due to phonon scattering over  
9 a polymer allows to reduce the aforementioned high thermal conductivity, due to phonon scattering over  
10 the extended interfacial area without compromising the electrical conductivity for percolated  
11 nanoparticle networks. Moreover, several authors have reported an even improved thermoelectric  
12 thermopower due to the phenomenon of energy filtering; unique interfaces, with controlled interfacial  
13 energy barriers, can act as an energy filter that allows high-energy charge carriers to preferentially cross  
14 the energy barrier at the interface, while deterring low-energy charge carriers.[3]

15 The formation of carbon-polymer composites however is not only advantageous to tune the  
16 thermoelectric properties, but also to modulate the mechanical properties. The often-poor solubility and  
17 brittle nature of carbon allotropes makes it a challenge to process them into continuous large area thin  
18 films and, even more, into thicker thermoelectric elements and generators, a prerequisite for efficient  
19 thermal energy recovery. By blending and dispersing the carbon nanomaterials with a polymer, the  
20 processing is facilitated, and the resulting composites display enhanced mechanical properties,[4] which  
21 is of particular interest for applications requiring conformal, tough and flexible thermoelectric  
22 generators.

23  
24  
25  
26 Over the past decades, tremendous advances have been made in understanding and optimising the  
27 unique thermoelectric properties of carbon nanomaterials, yet more efforts are needed to explore their  
28 full potential in thermoelectric generators. The further development of carbon-polymer composites offers  
29 the opportunity to unite the promising thermoelectric properties of carbon allotropes with the distinctive  
30 mechanical and thermal characteristics of polymers in the quest to develop high-performing  
31 thermoelectric composites.

### 32 33 34 **Current and Future Challenges**

35 While the electrical conductivity values presented in the scientific literature are often high, simultaneously  
36 suppressing the intrinsically high thermal conductivity of carbon nanomaterials, remains difficult.  
37 Moreover, the Seebeck coefficients of carbon-composites are still significantly lower than for the best  
38 performing inorganic thermoelectric materials despite the promising theoretical values predicted.[5]  
39 Furthermore, carbon-polymer nanocomposites are anisotropic materials with orders of magnitude higher  
40 electrical and thermal conductivities in plane, than the corresponding out-of-plane (normal direction)  
41 values.[6] Anisotropy however is both an opportunity and a challenge for thermoelectric generators, yet  
42 only one of several aspects to consider.

43  
44  
45 The chemical composition of both the carbon allotrope and polymer must be controlled to achieve  
46 consistent thermoelectric properties. While it is technically possible to separate and purify carbon  
47 nanotubes to a very high degree, considering different chiralities, diameters and lengths, this remains a  
48 challenge for graphene; in particular for chemically modified graphene, such as reduced graphene oxide,  
49 where batch to batch variations can be severe. Similarly the polymer composition depends on the  
50 synthetic pathway, particularly if the composite is formed via in-situ polymerisation, in which case  
51 monomers are directly polymerised on the carbon allotrope surface [7] or grown with the help of bacteria  
52 around the carbon nanomaterial (Figure 1).[8]

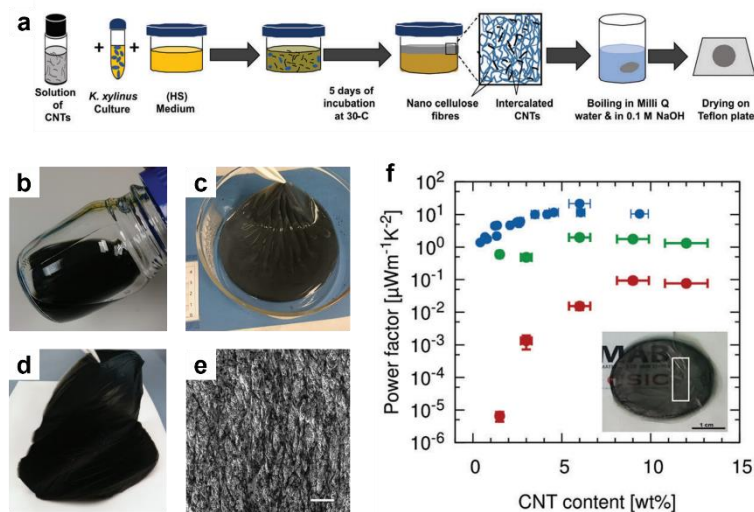


**Figure 1:** (a) Scheme for the preparation of carbon nanotubes (CNT) embedded in bacterial grown nanocellulose (BC). (b) Homogenously dispersed CNTs in bacterial culture medium. (c) Large CNT/BC composite film (diameter = 11 cm) in water after incubation and (d) dried. (e) Scanning electron microscope image of the CNT/BC composite (scale bar = 1 mm). (f) power factor versus CNT loading for different types of CNTs (CoMoCAT (red), Supergrowth (green) and eDIPS (blue)) CNTs. Adapted from Ref. [8] with permission from the Royal Society of Chemistry.

Flexibility and mechanical robustness are other desirable features often reported and emphasised. Flexible thin films under bending are relatively simple to achieve, whereas tensile deformations remain a challenge. The best performing materials used (e.g. PEDOT:PSS and CNT networks) are brittle and will only withstand little tensile strain before breakage. The use of mechanically robust polymer matrices hosting functional nanofillers has been demonstrated to be a very efficient strategy to achieve flexibility and stretchability as well as improved processability.[9]

Recently, it was demonstrated that the electrical conductivity and thermopower of semiconducting single-wall carbon nanotube networks tend to increase with temperature, whereas the thermal conductivity decreases.[10] These findings indicate an opportunity of maximising the thermoelectric efficiency at temperatures above ambient. The challenge remaining however is the limited availability of appropriate dopants to boost electrical conductivity. The dopants must not only be stable under ambient conditions, which is particularly difficult to achieve for n-type dopants, but also resistant to prolonged exposure to elevated temperatures, both with regards to chemical decomposition and morphological instabilities.

### Advances in Science and Technology to Meet Challenges

Carbon-polymer nanocomposites have demonstrated their potential for thermoelectric power generation, yet significant challenges remain and will require a concerted and multidisciplinary effort to promote key scientific and technological advances.

Ease of processability is one of the features often brought forward in favour of organic electronics, yet this is not necessarily true, particularly if bulk thermoelectrics are the target. Numerous techniques have been developed to process carbon-polymer composites, from simple mixing to liquid-phase exfoliation to more advanced layer-by-layer deposition, achieving a thermoelectric power factor of up to  $1825 \mu\text{W m}^{-1} \text{K}^{-2}$ . [11] A true commercial breakthrough in bulk organic thermoelectric materials and carbon-polymer composites would come from finding a way to process the materials via continuous melt extrusion or injection moulding without compromising the thermoelectric properties.



Optimising the often-contrasting physical properties in carbon-polymer composites is possible only by finely controlling structure at different hierarchical length-scales, from nano to macro. As such the dispersion and orientation of long carbon nanotubes or large graphene sheets is of paramount importance, together with the precise control of the conductive percolated (electrical and thermal) networks and the polymer/nanofiller interface. Moreover, the above will be ideally achieved utilising processing routes that are compatible with large-scale production, of both thin films and bulk components.

Another often overlooked factor is the thermoelectric module design and fabrication, which so far has been inspired by the established designs used in commercial inorganic thermoelectric devices. These device structures require millimetre to centimetre thick bulk material to maintain sufficient temperature gradients. This approach however is unsuitable for many organic materials currently processed into thin films and difficult to translate into thicker bulk processing without negatively altering the thermoelectric properties. Novel device architectures fabrication methods will be needed to ideally convert 2D printed arrays of thin-film composite legs into 3D module architectures (Figure 2).

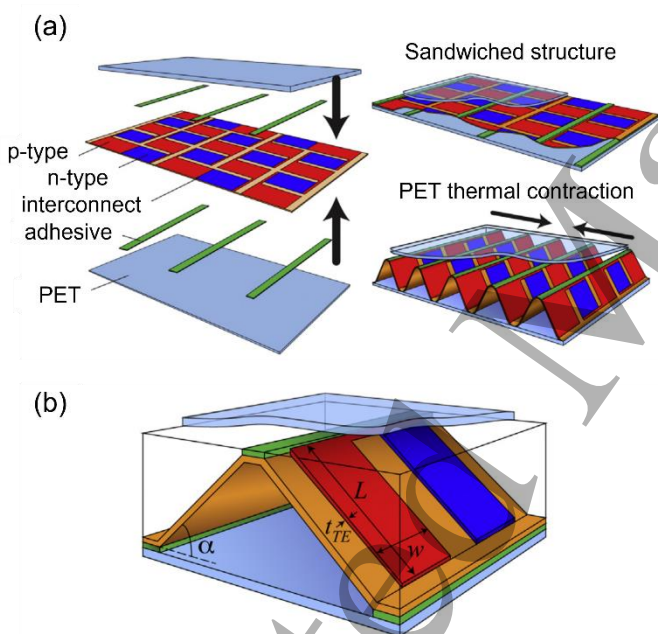


**Figure 2:** (a) Schematic illustration of the fabrication process of a 3D thermoelectric module from a 2D printed array using heat-shrink PET. (b) Simplified geometric model of final thermoelectric generator module with thermoelectric leg dimensions describing the thermoelectric layer thickness ( $t_{TE}$ ), length ( $L$ ), width ( $w$ ), and stacking angle ( $\alpha$ ). Adapted from Ref. [12] with permission.

### Concluding Remarks

Carbon-polymer composites have demonstrated their potential for thermoelectric applications. While they are currently unsuitable for large scale energy generation due to the prohibitively high costs of the carbon nanomaterials, they hold great promise for self-powered and wearable sensors. Numerous researchers have demonstrated the mechanical flexibility of composite materials and incorporated the materials into wearable thermoelectric generators by exploring new module geometries and more sustainable and biocompatible materials (*e.g.* gelatine, cellulose). In order for carbon-polymer composites to successfully power wearable electronic devices however, it is paramount to develop new and bespoke electronic components (*e.g.* energy storage, wireless communication), able to operate at lower power

and, at the same time, be lightweight, compact and flexible. Once these technological challenges are overcome, polymer-carbon composites can showcase their full potential and spearhead the development of self-powered wearable electronics.

### Acknowledgements

BCS acknowledges the UK Research and Innovation Future Leaders Fellowship (grant No: MR/S031952/1). EB would like to acknowledge the Innovate UK Smart Grant project KiriTEG (project No: 51868).

### References

- [1] M. S. Dresselhaus *et al.*, "New Directions for Low-Dimensional Thermoelectric Materials," *Advanced Materials*, vol. 19, no. 8, pp. 1043-1053, 2007, doi: <https://doi.org/10.1002/adma.200600527>.
- [2] Y. Zhang, Q. Zhang, and G. Chen, "Carbon and carbon composites for thermoelectric applications," *Carbon Energy*, vol. 2, pp. 408-436, 2020, doi: <https://doi.org/10.1002/cey2.68>.
- [3] C. Meng, C. Liu, and S. Fan, "A Promising Approach to Enhanced Thermoelectric Properties Using Carbon Nanotube Networks," *Advanced Materials*, vol. 22, no. 4, pp. 535-539, 2010, doi: <https://doi.org/10.1002/adma.200902221>.
- [4] Z. Li *et al.*, "Mechanically Robust and Flexible Films of Ionic Liquid-Modulated Polymer Thermoelectric Composites," *Advanced Functional Materials*, vol. 31, no. 42, p. 2104836, 2021, doi: <https://doi.org/10.1002/adfm.202104836>.
- [5] N. T. Hung, A. R. T. Nugraha, E. H. Hasdeo, M. S. Dresselhaus, and R. Saito, "Diameter dependence of thermoelectric power of semiconducting carbon nanotubes," *Physical Review B*, vol. 92, no. 16, p. 165426, 10/21/ 2015, doi: 10.1103/PhysRevB.92.165426.
- [6] C.-K. Mai *et al.*, "Anisotropic Thermal Transport in Thermoelectric Composites of Conjugated Polyelectrolytes/Single-Walled Carbon Nanotubes," *Macromolecules*, vol. 49, no. 13, pp. 4957-4963, 2016/07/12 2016, doi: 10.1021/acs.macromol.6b00546.
- [7] Q. Wang, Q. Yao, J. Chang, and L. Chen, "Enhanced thermoelectric properties of CNT/PANI composite nanofibers by highly orienting the arrangement of polymer chains," *Journal of Materials Chemistry*, 10.1039/C2JM32750C vol. 22, no. 34, pp. 17612-17618, 2012, doi: 10.1039/C2JM32750C.
- [8] D. Abol-Fotouh *et al.*, "Farming thermoelectric paper," *Energy & Environmental Science*, 10.1039/C8EE03112F vol. 12, no. 2, pp. 716-726, 2019, doi: 10.1039/C8EE03112F.
- [9] K. Wan *et al.*, "Highly stretchable and sensitive self-powered sensors based on the N-Type thermoelectric effect of polyurethane/Nax(Ni-ett)n/graphene oxide composites," *Composites Communications*, vol. 28, p. 100952, 2021/12/01/ 2021, doi: <https://doi.org/10.1016/j.coco.2021.100952>.
- [10] J. L. Blackburn, A. J. Ferguson, C. Cho, and J. C. Grunlan, "Carbon-Nanotube-Based Thermoelectric Materials and Devices," *Advanced Materials*, vol. 30, no. 11, p. 1704386, 2018, doi: <https://doi.org/10.1002/adma.201704386>.
- [11] C. Cho *et al.*, "Completely Organic Multilayer Thin Film with Thermoelectric Power Factor Rivaling Inorganic Tellurides," *Advanced Materials*, <https://doi.org/10.1002/adma.201405738> vol. 27, no. 19, pp. 2996-3001, 2015/05/01 2015, doi: <https://doi.org/10.1002/adma.201405738>.
- [12] T. Sun, J. L. Peavey, M. David Shelby, S. Ferguson, and B. T. O'Connor, "Heat shrink formation of a corrugated thin film thermoelectric generator," *Energy Conversion and Management*, vol. 103, pp. 674-680, 2015/10/01/ 2015, doi: <https://doi.org/10.1016/j.enconman.2015.07.016>.



## 5.16 Hybrid Organic – Inorganic Thermoelectrics

Akanksha K. Menon<sup>1</sup> and Jeffrey J. Urban<sup>2</sup>

<sup>1</sup>George W. Woodruff School of Mechanical Engineering, Georgia Institute of Technology, Atlanta, GA 30332, USA.

<sup>2</sup>The Molecular Foundry, Lawrence Berkeley National Laboratory, Berkeley, CA 94720, USA.

### Status

All thermoelectric materials enable the direct conversion of thermal energy into electrical energy via the Seebeck effect. There are, however, different classes of thermoelectric materials covered in this issue and elsewhere - the choice of which thermoelectric to pursue is driven by the end use (*i.e.*, the temperature of heat available). Given that heat is a (by)product of any non-isentropic “real-world” process, it represents a natural resource existing from just a few degrees above room temperature all the way to high-temperature processes. Historically, thermoelectrics research has largely focused on inorganic materials for power generation using higher-temperature sources, but about 10-15 years ago a strong interest began to develop in organic and hybrid thermoelectrics. This was driven to some extent by academic interest in the new physics being exhibited by these materials, as well as their inherently low thermal conductivity and/or decoupled electronic and thermal transport [1]. Compared to single-phase inorganic and organic thermoelectric materials, hybrids promise “the best of both worlds” and are comprised of inorganic nanostructures chemically conjoined with organic materials to form something fundamentally new. The main appeal of hybrids is that interfacial effects enable tuning the thermoelectric properties beyond what is otherwise attainable with single-phase materials or even composite mixtures. For example, PEDOT:PSS with Tellurium (Te) nanowires has been shown to overcome the conventional  $S - \sigma - k$  tradeoffs prevalent in both inorganic and organic thermoelectrics to achieve  $zT$  values as high as 0.4 at room temperature [2].

In addition to the interesting physics, hybrid materials retain the solution processability of their organic constituents for low-temperature energy harvesting (<150°C), thereby enabling new application spaces – wearable electronics, remote sensing, interactive displays, functional textiles, and biomedical devices. For these use cases, we argue that optimizing device efficiency is less important as these applications typically only require a low power density ( $\sim$ mW/cm<sup>2</sup>) for operation. Instead, the focus should be on developing lightweight and flexible devices with high reliability and minimal maintenance [3]. This also changes the equation in terms of what constitutes viability for these materials – rather than chasing a high material  $zT$  (as a proxy for efficiency), a fit-for-purpose techno-economic analysis or  $\$/W$  metric that includes scalability and stability considerations may be more appropriate [4]. In this roadmap, we outline the opportunity space for hybrid thermoelectrics and project the anticipated material and system-level breakthroughs needed to render them competitive with their inorganic and organic counterparts, as shown in Figure 1.

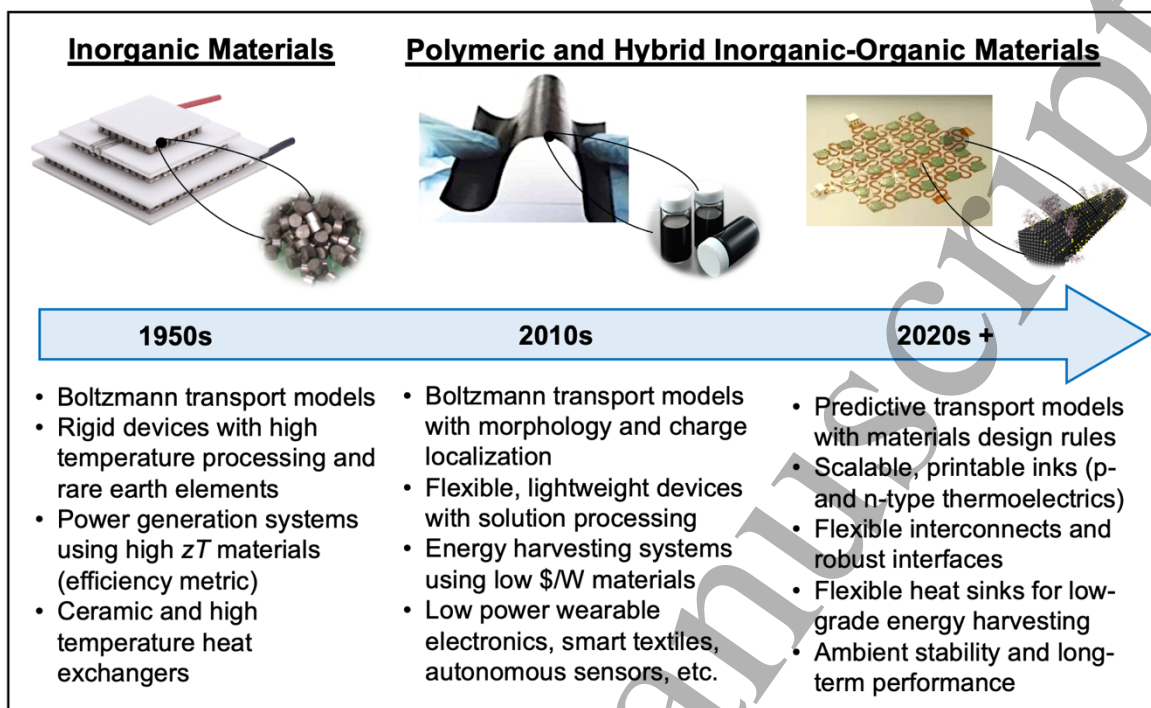


**Figure 1.** Evolution of thermoelectric materials and applications from high-temperature inorganic devices to flexible energy harvesters that leverage organic materials for the internet of things.

### Current and Future Challenges

One central challenge with hybrid thermoelectrics is understanding the non-linear interactions that occur between the two phases at the interface. Effective medium models (*e.g.*, Bergman-Levy) do not apply, and hybrid material performance can exceed that of either pure component even without any extrinsic doping. To explain these results, mechanisms such as energy filtering due to the different work functions of Te and PEDOT:PSS have been incorrectly posited since there are no methods to directly probe the interface. Recent work on single nanowire hybrids has revealed that it is the interfacial interactions at the nanoscale that are at play, leading to self-assembly or templating of the organic phase along the crystalline inorganic nanowire [2]. This however is a purely morphological effect dependent on nanowire diameter rather than true hybrid behavior, as there is no change in the electronic structure or scattering mechanisms. Thus, synthesis routes that can harness effects like energy filtering to enable new materials with vastly improved properties remains a challenge.

The other enduring challenge is that the structure and bonding of standard organic elements (C, H, N, O) has resulted in primarily p-type hybrids with a high thermoelectric performance. In theory, hybrids can be potent owing to seamless introduction of new electronic states via an inexhaustible library of inorganic materials to generate unforeseen n-type materials that retain the flexibility of organic thermoelectrics. For example, the Seebeck coefficient of Te nanowires can be tuned via interfacial charge transfer (*i.e.*, resonant doping) to achieve an n-type hybrid material. However, design of materials beyond Te is yet to be practically realized.

At the device level, the overall stability of these materials to oxidation, thermal cycling, and mechanical strain has not been thoroughly studied. There is thus considerable opportunity to take advantage of the ability to lithographically work with hybrid materials to create incredibly robust structures mimicking

those in nature by using hard/soft concepts and hierarchical design principles such as negative Gaussian curvature and tensegrity [5, 6].

One of the elements favoring hybrid materials is their processability and manufacturability using pre-existing infrastructure developed for other stretchable electronics. However, this advantage brings with it several important research questions that are yet to be adequately solved: the role of processing when applying the material in a given form factor to a device for energy harvesting can result in properties that are very different from the hybrid single nanowire or thin film form, then there are real needs for flexible interconnects that enable the materials to retain their function over multiple bending or strain cycles, and there is also a need for flexible heat exchangers. While there has been some recent work in this space [7, 8], there is significant room for improvement and innovation.

### Advances in Science and Technology to Meet Challenges

Currently, hybrid thermoelectrics are at the research stage, with some development through industrial partnerships and small startups. Long-term it will be important to understand if extant materials are maximizing their potential, or if we are limited by current materials science, syntheses, and manufacturing principles. For example, there is no thermoelectric equivalent of the Shockley-Quieser evaluation for soft thermoelectrics and it is unclear exactly how good they can become (*e.g.*, nothing physically prevents a  $zT$  of infinity). Charge transport models can set some bounds on these materials, but only recently has there been reconciliation of vastly different physical models (*e.g.*, hopping- to metal-like transport) using a generalized charge transport model and the semi-localized transport (SLoT) model [9, 10]. However, these models are predicated on insight from temperature-dependent measurements to infer the energetic landscape, as a result of which they cannot be predictive and have limited utility.

For hybrid organic-inorganic thermoelectric devices, the clear target is cost-effective harvesting of low-grade thermal energy for low-power electronics ( $\text{mW}/\text{cm}^2$ ). Therefore, the motivation is no longer chasing high- $zT$  materials but is instead oriented towards making the entire device robust, reliable, and capable of being manufactured in arbitrary geometries at scale. This will require a paradigm shift from the status quo (*i.e.*, synthesizing novel organic materials/dopants and characterizing them in an inert environment) to thinking in terms of integrating the material in a device. Here, processing and scale-up parameters will need to focus on consistency (both batch-batch and at scale), along with minimizing the adverse impact of any binders/additives necessary for fabricating large-area devices, and measuring thermoelectric performance in the direction in which the device experiences a temperature gradient.

Other prominent technological challenges are flexible heat exchangers to partner with the flexible thermoelectrics and enable the most efficient use of the small thermal resources available. This area has seen little interest, but it is a substantial need as traditional ceramic heat exchangers for high temperature semiconductor thermoelectrics will not be viable. It is also strongly recommended that thermoelectric devices be tested for months and not days (like in most academic papers) and under various environmental conditions.

### Concluding Remarks

Research in hybrid thermoelectrics is, in many ways, still in its infancy. Despite having limited time and investment relative to traditional inorganic semiconductor thermoelectrics, this field has made several landmark discoveries (both in terms of the physics and material performance) and demonstrated accelerated development on an annual basis. However, to realize the promise of what has been achieved thus far, directed investments into fundamental aspects of materials science, the charge and thermal transport physics of these materials, and translational innovations into the processing and

1  
2  
3 implementation of these 'soft thermoelectrics' are desperately needed. Flexible and stable n- and p-type  
4 hybrid thermoelectrics that can be woven together into arbitrary geometries can be impactful to a future  
5 where distributed low-power electronics and sensors will play a prominent role.  
6

### 7 **Acknowledgements**

8 Work at the Molecular Foundry was supported by the Office of Science, Office of Basic Energy Sciences,  
9 of the U.S. Department of Energy under Contract No. DE-AC02-05CH11231.  
10  
11

### 12 **References**

- 13 [1] J. J. Urban, A. K. Menon, Z. Tian, A. Jain, and K. Hippalgaonkar, "New horizons in thermoelectric  
14 materials: Correlated electrons, organic transport, machine learning, and more," *Journal of Applied*  
15 *Physics*, vol. 125, no. 18, p. 180902, 2019/05/14 2019, doi: 10.1063/1.5092525.  
16 [2] L. Yang *et al.*, "Decoupling electron and phonon transport in single-nanowire hybrid materials for  
17 high-performance thermoelectrics," *Science Advances*, vol. 7, no. 20, p. eabe6000, doi:  
18 10.1126/sciadv.abe6000.  
19 [3] E. W. Zaia, M. P. Gordon, P. Yuan, and J. J. Urban, "Progress and Perspective: Soft Thermoelectric  
20 Materials for Wearable and Internet-of-Things Applications," *Advanced Electronic Materials*,  
21 <https://doi.org/10.1002/aelm.201800823> vol. 5, no. 11, p. 1800823, 2019/11/01 2019, doi:  
22 <https://doi.org/10.1002/aelm.201800823>.  
23 [4] S. K. Yee, S. LeBlanc, K. E. Goodson, and C. Dames, "\$ per W metrics for thermoelectric power  
24 generation: beyond ZT," *Energy & Environmental Science*, 10.1039/C3EE41504J vol. 6, no. 9, pp.  
25 2561-2571, 2013, doi: 10.1039/C3EE41504J.  
26 [5] H. Lee *et al.*, "3D-printed programmable tensegrity for soft robotics," *Science Robotics*, vol. 5, no. 45,  
27 p. eaay9024, 2020/08/26 2020, doi: 10.1126/scirobotics.aay9024.  
28 [6] M. Sajadi Seyed *et al.*, "Damage-tolerant 3D-printed ceramics via conformal coating," *Science*  
29 *Advances*, vol. 7, no. 28, p. eabc5028, doi: 10.1126/sciadv.abc5028.  
30 [7] J. Choi, C. Dun, C. Forsythe, M. P. Gordon, and J. J. Urban, "Lightweight wearable thermoelectric  
31 cooler with rationally designed flexible heatsink consisting of phase-change  
32 material/graphite/silicone elastomer," *Journal of Materials Chemistry A*, 10.1039/D1TA01911B vol.  
33 9, no. 28, pp. 15696-15703, 2021, doi: 10.1039/D1TA01911B.  
34 [8] H. M. Elmoughni, A. K. Menon, R. M. W. Wolfe, and S. K. Yee, "A Textile-Integrated Polymer  
35 Thermoelectric Generator for Body Heat Harvesting," *Advanced Materials Technologies*,  
36 <https://doi.org/10.1002/admt.201800708> vol. 4, no. 7, p. 1800708, 2019/07/01 2019, doi:  
37 <https://doi.org/10.1002/admt.201800708>.  
38 [9] S. D. Kang and G. J. Snyder, "Charge-transport model for conducting polymers," *Nature Materials*,  
39 vol. 16, no. 2, pp. 252-257, 2017/02/01 2017, doi: 10.1038/nmat4784.  
40 [10] S. A. Gregory *et al.*, "Quantifying charge carrier localization in chemically doped semiconducting  
41 polymers," *Nature Materials*, vol. 20, no. 10, pp. 1414-1421, 2021/10/01 2021, doi: 10.1038/s41563-  
42 021-01008-0.  
43  
44  
45  
46  
47  
48  
49  
50  
51  
52  
53  
54  
55  
56  
57  
58  
59  
60

## 5.17 Halide perovskites for thermoelectric energy harvesting

Oliver Fenwick<sup>1</sup> and Ceyla Asker<sup>1</sup>

<sup>1</sup> School of Engineering & Materials Science, Queen Mary University of London, Mile End Road, London E1 4NS, United Kingdom.

### Status

The reason for low uptake of thermoelectric technology lies in the combination of device efficiency and low elemental abundance, cost and often toxicity of the materials from which current TEGs are made. A new generation of thermoelectric materials is needed, which addresses some or all of these issues. Halide perovskites are materials that have promise to address more than three or more of these challenges simultaneously. Halide perovskites are crystalline semiconductors with an  $ABX_3$  stoichiometry and can be fully inorganic or organic-inorganic hybrids. The B-site is a metal cation (e.g.  $Pb^{2+}$ ,  $Sn^{2+}$ ), the X-site a halide anion and the A-site can be an organic or inorganic cation (e.g.  $Cs^+$ ,  $CH_3NH_3^+$ ,  $CH_5N_2^+$ ) (**Figure 1**). They have been widely studied as absorbers in solar cells and can be processed by low-cost methods from solution or by mechanochemical synthesis and low temperature sintering. A wide range of elements can be used on the A-, B- and X-sites which can be abundant and (when Pb is avoided) non-toxic.

Thermoelectric figure of merit,  $zT$ , values of  $MABl_3$  (MA = methylammonium, B =  $Pb^{2+}$  or  $Sn^{2+}$ ) are predicted to be between 1 and 2.[2] The mixed halide version,  $CsPb(I_{1-x}Br_x)_3$ , is predicted to have  $zT = 1.7$ ,[3] whilst the low-dimensional  $Cs_3Cu_2I_5$  perovskite derivative is predicted to have  $zT = 2.6$  at 600 K (**Figure 2**).[4] This therefore puts the predicted thermoelectric performance of halide perovskites alongside the state-of-the-art in the low to mid temperature range and offers the possibility of high-performance sustainable thermoelectric materials.

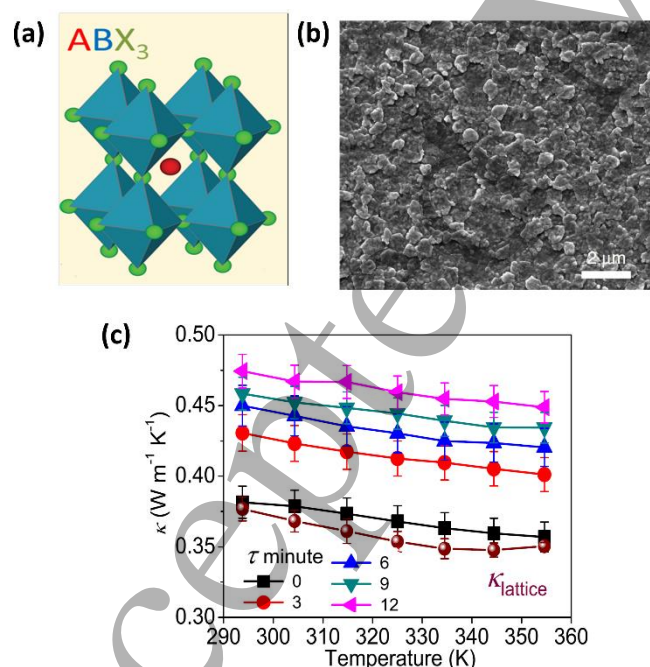


**Figure 1** (a) The location of A-, B- and X-sites in the perovskite structure. (b) Morphology of a  $CsSnI_3$  thin film. (c) Thermal conductivity,  $\kappa$ , of  $CsSnI_{3-x}Cl_x$ , where the oxidation time is given by  $\tau$  and  $\kappa_{lattice}$  is the derived lattice thermal conductivity. Reproduced under CC BY 4.0 license from [5] and [4].



### Current and Future Challenges

Despite high predicted thermoelectric performance in halide perovskites, experimental results have only shown low to modest thermoelectric figure of merit,  $zT$ . Understanding this discrepancy is key to developing the field. On the positive side, halide perovskites have been identified as “phonon glass electron crystals” where there is a role of the A-site cation in phonon scattering, resulting in thermal conductivities that are in (or close to) the ultralow regime, which is defined as  $<0.5 \text{ W}\cdot\text{m}^{-1}\text{K}^{-1}$ . Charge mobilities in these materials are known to be quite reasonable, in the range of 10s to 100s  $\text{cm}^2\text{V}^{-1}\text{s}^{-1}$  [5] and Seebeck coefficients are commonly  $>100 \mu\text{V}/\text{K}$ , depending on doping level.

Nonetheless, electrical conductivities of halide perovskites in their intrinsic state are low. Extrinsic doping, self-doping, off-stoichiometry doping and charge transfer doping have been applied experimentally to improve the electrical conductivities and the overall  $zT$  value. The greatest success in terms of figure of merit has been in the Sn-perovskites, where the oxidation of  $\text{Sn}^{2+}$  to  $\text{Sn}^{4+}$  provides a route to self-doping.  $zT$  values of  $\text{CsSnI}_3$  have been reported in several studies, with a  $zT$  of 0.11 achieved at 320 K [6]. However, since oxidation is the source of charge carriers, stability of Sn-perovskites is a potential issue. Self-doping of  $\text{CsSnI}_{3-x}\text{Cl}_x$  has achieved hole-doping concentrations of  $10^{18} - 10^{19} \text{ cm}^{-3}$  and  $zT$  of 0.14 at 345 K, where Cl-dopants enhanced the stability as well as acting as a sacrificial source of free charges.[7] The highest  $zT$  value of 0.19 (at room temperature) was achieved with charge transfer doping of thin films using the molecular dopant F4TCNQ.[8]

Doping of more stable (non-Sn-containing) perovskite systems for thermoelectrics has been achieved, but the low doping efficiency[9] results in low electrical conductivities and low  $zT$ . The main current challenge is therefore to improve doping efficiencies in this class of materials where doping is a challenge due to ionic compensation of point defects in addition to an electronic structure that is tolerant of defects.

### Advances in Science and Technology to Meet Challenges

The potential for halide perovskites as sustainable high  $zT$  thermoelectric materials has therefore been demonstrated computationally and only partly realised experimentally. These authors believe that the principle 6 challenges to realise high thermoelectric performance in halide perovskites are:

1. *To understand electrical doping better in these materials.* They have been developed mostly as solar cell absorbers, where a low density of free charges is advantageous, and there has still been relatively little work on ways to achieve doping densities  $>10^{18} \text{ cm}^{-3}$ .
2. *To balance conductivity and stability.* Currently, the best halide perovskite thermoelectric materials are Sn-based, which are among the least atmospherically stable of the material class. Methods to achieve similar doping densities in more stable halide perovskites will be needed.
3. *Computational materials discovery.* Currently, relatively few of the 1000s of possible halide perovskites have been explored, and this is experimentally time-consuming. Computational approaches to explore the materials space for the best candidates and the best doping strategies is much needed.
4. *Exploring lower dimensional analogues.* Halide perovskites have low-dimensional counterparts which comprise metal halide clusters separated by organic or inorganic cations (**Figure 2**). These halide perovskite derivatives have shown potential for further reduced thermal conductivity and even higher Seebeck coefficients.
5. *Balancing cost and scalability.* Halide perovskites have been developed as thin film (sub- $\mu\text{m}$ ) materials in photovoltaic devices. Thermoelectric generators would typically require millimetre thicknesses (i.e. bulk material). Avoiding costly or toxic elements in the composition is therefore important, as well as considering solid-state synthesis approaches to avoid solvent cost and solvent waste.

6. *Incorporating them into prototype thermoelectric generators.* Many processes can occur in TEGs that are not captured by a  $zT$  measurement of the material in isolation. These may include electrode reactions that may require passivation by organic interlayers and careful choice of electrode material. There may be contact resistances, ionic migration and Joule heating effects to name a few. On the other hand the processability of these materials may enable innovative device geometries that are not possible with conventional ceramic thermoelectric generators.

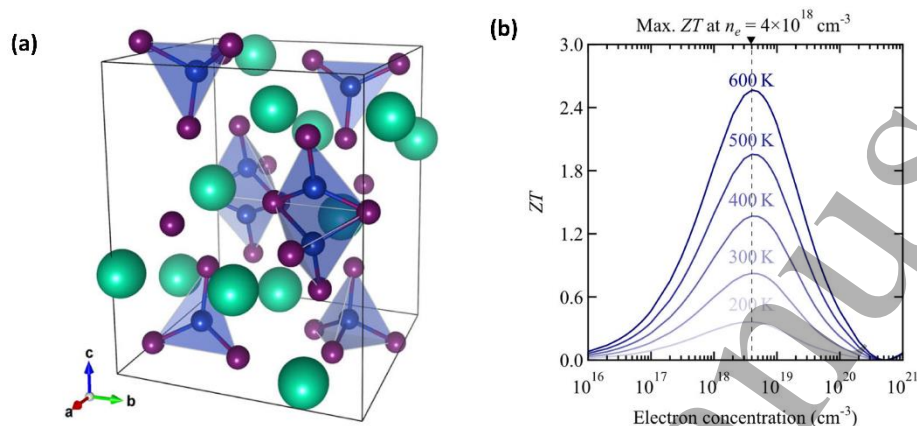


**Figure 2 (a)** Structure of zero-dimensional  $\text{Cs}_3\text{Cu}_2\text{I}_5$ , where  $\text{Cs}^+$  is in green,  $\text{Cu}^+$  in blue and  $\text{I}^-$  in purple. **(b)** Thermoelectric figure of merit computationally predicted for  $\text{Cs}_3\text{Cu}_2\text{I}_5$  as a function of charge carrier concentration. Reproduced under CC BY 4.0 license from [4].

### Concluding Remarks

Halide perovskite materials are well known in the research community and increasingly to industry through their development in high-efficiency single- and multi-junction solar cells. Whilst they remain underexplored for thermoelectrics, interest is certainly increasing. This is perhaps unsurprising due to their intrinsically low thermal conductivity that is comparable to polymers, decent charge mobility and large Seebeck coefficients. Experimental reports of  $zT > 0.1$  and computational predictions of  $zT > 2$  have given researchers some confidence. If the challenge of doping to achieve charge carrier densities  $> 10^{18} \text{ cm}^{-3}$  can be achieved in a wider range of halide perovskite materials, then we would expect to see much higher  $zT$  values in the future and perhaps halide perovskite TEGs operating with high power conversion efficiencies.

### Acknowledgements

OF is funded by a Royal Society University Research Fellowship [UF140372 and URF/R/201013].

### References

- [1] "Waste Heat Recovery System Market Size, Share & Trends Analysis Report By Application (Preheating, Power & Steam Generation), By End User (Petroleum Refinery, Power, Metal Production), And Segment Forecasts, 2020–2027," *Grand View Research*, 2020.
- [2] Y. He and G. Galli, "Perovskites for Solar Thermoelectric Applications: A First Principle Study of  $\text{CH}_3\text{NH}_3\text{Al}_3$  ( $A = \text{Pb}$  and  $\text{Sn}$ )," *Chemistry of Materials*, vol. 26, no. 18, pp. 5394-5400, 2014.
- [3] L. Yan, M. Wang, C. Zhai, L. Zhao, and S. Lin, "Symmetry Breaking Induced Anisotropic Carrier Transport and Remarkable Thermoelectric Performance in Mixed Halide Perovskites  $\text{CsPb}(\text{I}_{1-x}\text{Br}_x)_3$ ," *ACS Applied Materials & Interfaces*, vol. 12, no. 36, pp. 40453-40464, 2020.

- [4] Y.-K. Jung, I. T. Han, Y. C. Kim, and A. Walsh, "Prediction of high thermoelectric performance in the low-dimensional metal halide  $\text{Cs}_3\text{Cu}_2\text{I}_5$ ," *npj Computational Materials*, vol. 7, no. 1, p. 51, 2021.
- [5] L. M. Herz, "Charge-Carrier Mobilities in Metal Halide Perovskites: Fundamental Mechanisms and Limits," *ACS Energy Letters*, vol. 2, no. 7, pp. 1539-1548, 2017.
- [6] W. Lee, H. Li, A. B. Wong, D. Zhang, M. Lai, Y. Yu, Q. Kong, E. Lin, J. J. Urban, J. C. Grossman, and P. Yang, "Ultralow thermal conductivity in all-inorganic halide perovskites," *Proceedings of the National Academy of Sciences*, vol. 114, no. 33, p. 8693, 2017.
- [7] T. Liu, X. Zhao, J. Li, Z. Liu, F. Liscio, S. Milita, B. C. Schroeder, and O. Fenwick, "Enhanced control of self-doping in halide perovskites for improved thermoelectric performance," *Nature Communications*, vol. 10, no. 1, p. 5750, 2019.
- [8] L. Zheng, T. Zhu, Y. Li, H. Wu, C. Yi, J. Zhu, and X. Gong, "Enhanced thermoelectric performance of F4-TCNQ doped  $\text{FASnI}_3$  thin films," *Journal of Materials Chemistry A*, vol. 8, no. 47, pp. 25431-25442, 2020.
- [9] W. Tang, J. Zhang, S. Ratnasingham, F. Liscio, K. Chen, T. Liu, K. Wan, E. S. Galindez, E. Bilotti, M. Reece, M. Baxendale, S. Milita, M. A. McLachlan, L. Su, and O. Fenwick, "Substitutional doping of hybrid organic-inorganic perovskite crystals for thermoelectrics," *Journal of Materials Chemistry A*, vol. 8, no. 27, pp. 13594-13599, 2020.

## 5.18 Metal Organic Frameworks for Thermoelectric Energy Conversion Applications

A. Alec Talin

Sandia National Laboratories, Livermore, CA 94551

### Status

Metal organic frameworks (MOFs) are extended, crystalline compounds consisting of metal ions interconnected by organic ligands, forming scaffolding-like structures that are sometimes referred to as "molecular tinker toys".[1] These porous coordination polymers have attracted considerable attention for traditional applications of microporous materials, such as gas storage and separation. More recently, the discovery that certain MOFs conduct electrons by virtue of the electronic coupling within their structures or by interactions with guest molecules (Guest@MOF) that facilitate charge delocalization and hopping, has sparked interest in using MOFs in TE applications.[2] The interest in MOFs, and coordination polymers more broadly, is motivated by the practical need for TE materials that are low cost, non-toxic, are mechanically flexible, and can conform over complex shapes. A potential advantage of MOFs and Guest@MOF materials compared to organic polymers is their synthetic and structural versatility.[1] Specifically, the choice of metal, ligand, and guest molecule enables tuning of the electronic transport, and therefore promote high charge mobility because of the long-range crystalline order inherent in these materials while maintaining low thermal conductivity. In this section, we briefly review the recent advances in development of MOFs, Guest@MOFs and coordination polymers for TE applications and discuss how the Seebeck coefficient, electrical conductivity and the thermal conductivity could be tuned to further optimize their TE performance.

Table 1. Thermoelectric properties of selected MOF, Guest@MOF, coordination polymer and organic polymer materials.

Material	S ( $\mu\text{V/K}$ )	$\sigma$ (S/cm)	$\kappa$ (W/mK)	PF ( $\mu\text{W/mK}^2$ )	ZT	Ref.
$\text{Ni}_3(\text{HITP})_2$	-11.9	58.8	0.2	0.83	$1.2 \times 10^{-3}$	[3]
CNT@ZIF-67	55.6	825.7	4.1	255.6	0.02	[4]
TCNQ@ $\text{Cu}_3(\text{BTC})_2$	375	$4.5 \times 10^{-3}$	0.25	0.06	$10^{-4}$	[5]
Cu-BHT	-21	2000	1.99	88	0.013	[6]
PEDOT:PSS	76	$9 \times 10^5$	0.24	480	0.42	[7]

### Current and Future Challenges

Irrespective of the material type, the efficiency of a TE device is determined by the ZT figure of merit,  $ZT = S^2 \sigma T / \kappa$ , where S is the Seebeck coefficient,  $\sigma$  is the electronic conductivity, T is temperature, and  $\kappa$  is the thermal conductivity.[2] Because the parameters are interdependent, finding materials with  $ZT \gg 1$  has been a major challenge for developing practical TE systems. The Seebeck coefficient, or thermopower, is the voltage difference that arises when a temperature gradient exists across a slab of material[2]. Its sign indicates the majority carrier, positive for hole conductors and negative for electron conductors, and its magnitude ranges from a few  $\mu\text{V/K}$ , typically for metals, to over 1 mV/K, observed in lightly doped semiconductors. S values for several p-type and n-type MOFs and non-porous coordination polymers are included in Table 1.

The second factor that is needed to realize TE systems with high efficiency is low thermal conductivity. Indeed, MOFs exhibit a low thermal conductivity, typically  $\sim 0.2$  W/mK, which is  $\sim 10 \times$  lower compared to  $\text{Bi}_2\text{Te}_3$  (see Table X for a few representative examples). The low  $\kappa$  for MOFs is consistent with their weak bonding (metal-ligand coordination bonds are generally weaker compared to covalent bonds), complex atomic structures, and high anharmonicity, which decrease the amount of energy carried per vibrational mode, the phonon propagation speed and the phonon mean-free path.

The electronic conductivity is the third factor that determines ZT. In general, high electronic conductivity is observed in solids with strong electronic coupling between neighboring atoms leading to large band dispersion and delocalization of carriers across many lattice sites[1]. Most MOFs, on the other hand, have little or no band dispersion due to low atomic density and strong localization of the electron wave function characteristic of Werner-type coordination complexes. Because electronic conductivity is key to so many potential applications (e.g. electronics, sensors, energy conversion and storage), designing electronically conducting frameworks has been a major research thrust in the MOF community.[1] In general, electronic conduction mechanisms in MOFs can be classified as either intrinsic or guest induced (see Figure 1). Examples of intrinsically conducting MOFs include  $\text{Ni}_3(\text{HITP})_2$  and  $\text{Cu}_3(\text{HHTP})_2$ , examples of guest induced conductivity include TCNQ@ $\text{Cu}_3(\text{BTC})_2$  [2] and CNT@ZIF-67[4], and an example of a conducting non-porous coordination polymer is Cu-BHT.[6] Note that while adsorption of guest molecules or nanostructures can dramatically boost electronic conductivity, it can also increase the thermal conductivity by increasing phonon modes and depending on the guest-host interaction, the framework rigidity (see Table 1).

### Advances in Science and Technology to Meet Challenges

Although the 2D MOF  $\text{Ni}_3(\text{HITP})_2$  has a relatively high electrical conductivity (compared to other MOFs) of  $\sim 60$  S/cm and a very low thermal conductivity of  $\sim 0.2$  W/mK, exhibits a very low ZT of  $\sim 10^{-3}$ , well below the typical values of  $ZT \sim 1$  for inorganic TE materials. This is in part due to this framework's relatively low Seebeck coefficient of  $-11.9$   $\mu\text{V/K}$  and an electrical conductivity that is considerably lower compared to

values observed for inorganic and organic polymer TE materials. The nanocrystalline character of the  $\text{Ni}_3(\text{HITP})_2$  used in ref. [3] likely contributed to the lower value of the electrical conductivity. Indeed, Wu et al. reported electron mobility as high as  $\sim 50 \text{ cm}^2/\text{Vs}$  for field-gated  $\text{Ni}_3(\text{HITP})_2$  thin films fabricated using an alternative route based on liquid-air interface method, resulting in much better crystalline quality[8]. This mobility is well above the values typically observed for hopping conduction associated with small polaron formation and indicates substantial delocalization of the electron wave function[1]. The fact that much higher charge mobilities of  $>200 \text{ cm}^2/\text{Vs}$  have been reported for single crystals 2D MOF such as  $\text{Fe}_3(\text{THT})_2(\text{NH}_4)_3$  [9] suggests that there is ample opportunity to improve TE characteristics using 2D conducting MOFs. It is also worth noting that while Sun et al. reported a negative Seebeck coefficient for  $\text{Ni}_3(\text{HITP})_2$ , the transfer characteristics observed by Wu et al. for nominally the same material suggest that this framework is ambipolar (i.e. can conduct both electrons and holes), which is encouraging for developing practical TE conversion systems where elements with majority electron and hole carriers are necessary.

To achieve MOF TEs with  $ZT > 1$  will require both increases in the electronic conductivity and the Seebeck coefficient. Since  $S \propto \frac{dn(E)_{E=E_F}}{dE}$  where  $n(E)_{E=E_F}$  is the density of states at the Fermi level, materials with higher  $S$  typically result in lower electronic conductivities due to fewer carriers at the Fermi level[2]. In traditional TEs like  $\text{Bi}_2\text{Te}_3$  and its alloys, low bandgap and high doping concentrations enable a compromise to optimize  $S$  and  $\sigma$ . Recent demonstrations of continuously tunable bandgap of 0.3 – 0.8 eV in the binary alloy system  $(\text{M}_x\text{M}')_{3-x}(\text{HITP})_2$  ( $\text{M}, \text{M}' = \text{Cu}, \text{Ni}, \text{Co}$ ) suggests that such an approach could also work with MOFs[10].

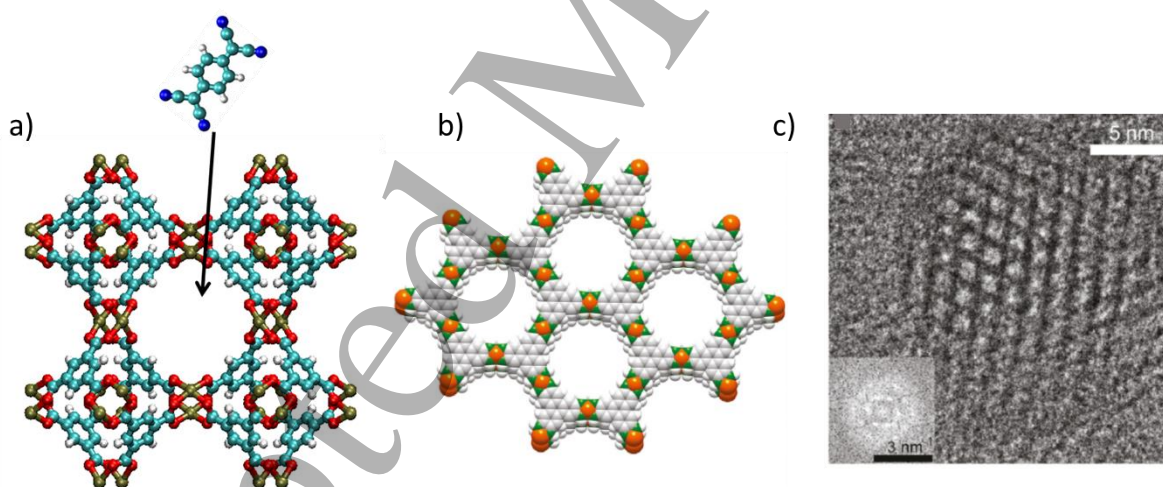


Figure 1. Tetracyanoquinodimethane (TCNQ) above a  $\text{Cu}_3(\text{BTC})_2$  with arrow pointing to the pore. Color code: white, H; blue, N; cyan, C; red, O; ochre (light brown), Cu. Reprinted with permission from Reference 2. © Springer Nature. b) A portion of the crystal structure of  $\text{Ni}_3(\text{HITP})_2$  showing multiple stacked 2D layers. Orange, green, gray, and white spheres represent Ni, N, C, and H atoms, respectively. c) TEM micrographs of  $\text{Ni}_3(\text{HITP})_2$  nanoparticles viewed along the pores. Reprinted with permission from Reference 3 © Elsevier

### Concluding Remarks

In summary, MOFs offer tremendous opportunity to tune the electronic structure, electronic transport and thermal conductivity via their composition, bonding character and three-dimensional assembly (including structural porosity). Thus, MOFs are excellent candidate materials both for fundamental



exploration of TE phenomena as well as for discovery of novel TEs that combine high performance with low cost, low toxicity and mechanical flexibility.

### Acknowledgements

The work at Sandia National Laboratories was supported by the Laboratory-Directed Research and Development (LDRD) Programs. Sandia National Laboratories is a multimission laboratory managed and operated by National Technology and Engineering Solutions of Sandia, LLC, a wholly owned subsidiary of Honeywell International Inc., for the U.S. Department of Energy's National Nuclear Security Administration under contract DE-NA-0003525. This paper describes objective technical results and analysis. Any subjective views or opinions that might be expressed in the paper do not necessarily represent the views of the U.S. Department of Energy or the United States Government.

### References

- [1] I. Stassen, N. C. Burtch, A. A. Talin, P. Falcaro, M. D. Allendorf, and R. Ameloot, "An updated roadmap for the integration of metal-organic frameworks with electronic devices and chemical sensors," *Chemical Society Reviews*, vol. 46, no. 11, pp. 3185-3241, Jun 2017, doi: 10.1039/c7cs00122c.
- [2] A. A. Talin, R. E. Jones, and P. E. Hopkins, "Metal-organic frameworks for thermoelectric energy-conversion applications," *Mrs Bulletin*, vol. 41, no. 11, pp. 877-882, Nov 2016, doi: 10.1557/mrs.2016.242.
- [3] L. Sun *et al.*, "A Microporous and Naturally Nanostructured Thermoelectric Metal-Organic Framework with Ultralow Thermal Conductivity," *Joule*, vol. 1, no. 1, pp. 168-177, 2017/09/06/2017, doi: <https://doi.org/10.1016/j.joule.2017.07.018>.
- [4] Y. F. Xue *et al.*, "Boosting thermoelectric performance by in situ growth of metal organic framework on carbon nanotube and subsequent annealing," *Carbon*, vol. 157, pp. 324-329, Feb 2020, doi: 10.1016/j.carbon.2019.10.049.
- [5] K. J. Erickson *et al.*, "Thin Film Thermoelectric Metal-Organic Framework with High Seebeck Coefficient and Low Thermal Conductivity," (in English), *Advanced Materials*, Article vol. 27, no. 22, pp. 3453-3459, Jun 2015, doi: 10.1002/adma.201501078.
- [6] R. Tsuchikawa *et al.*, "Unique Thermoelectric Properties Induced by Intrinsic Nanostructuring in a Polycrystalline Thin-Film Two-Dimensional Metal-Organic Framework, Copper Benzenehexathiol," *physica status solidi (a)*, vol. 217, no. 23, p. 2000437, 2020, doi: <https://doi.org/10.1002/pssa.202000437>.
- [7] G. H. Kim, L. Shao, K. Zhang, and K. P. Pipe, "Engineered doping of organic semiconductors for enhanced thermoelectric efficiency," *Nature Materials*, vol. 12, no. 8, pp. 719-723, Aug 2013, doi: 10.1038/nmat3635.
- [8] G. D. Wu, J. H. Huang, Y. Zang, J. He, and G. Xu, "Porous Field-Effect Transistors Based on a Semiconductive Metal-Organic Framework," *Journal of the American Chemical Society*, vol. 139, no. 4, pp. 1360-1363, Feb 2017, doi: 10.1021/jacs.6b08511.
- [9] R. Dong *et al.*, "High-mobility band-like charge transport in a semiconducting two-dimensional metal-organic framework," *Nature Materials*, vol. 17, no. 11, pp. 1027-1032, 2018/11/01 2018, doi: 10.1038/s41563-018-0189-z.
- [10] T. Chen *et al.*, "Continuous Electrical Conductivity Variation in M3(Hexamino-triphenylene)2 (M = Co, Ni, Cu) MOF Alloys," *Journal of the American Chemical Society*, vol. 142, no. 28, pp. 12367-12373, 2020/07/15 2020, doi: 10.1021/jacs.0c04458.

## 6. Materials for Radiofrequency Energy Harvesting

### 6.1 Introduction to Materials for Electromagnetic Energy Harvesting

Thomas D. Anthopoulos

King Abdullah University of Science and Technology (KAUST), KAUST Solar Center (KSC), Thuwal 23955-6900, Saudi Arabia

#### Status

Electromagnetic signals in the radio frequency (RF) range are ubiquitous and originate from various sources, including wireless networks, broadcast transmission antennas, mobile base stations and mobile phones, Wi-Fi signals, and dedicated RF base stations, among others. Harvesting the energy of such signals has recently emerged as a promising method for powering electronic devices wirelessly including distributed sensor networks and more broadly the rapidly expanding internet of things (IoT) device ecosystem. In 2022 alone, the total number of connected IoT devices grew by 18% to 14.4 billion and is predicted to reach 27 billion globally by 2025 [1]. Each physical 'Thing' (sensor node, etc) is identifiable within the IoT ecosystem and can exchange information wirelessly. Powering this rapidly increasing number of devices is now recognised as a major techno-economic challenge with no obvious solution in sight. This is precisely where RF wireless energy harvester (RF-WEH) technologies offer a promising alternative to conventional batteries by enabling the autonomy required by the IoT nodes. Moreover, RF-WEHs can be operated 24 hours indoors and outdoors and supply enough energy for the periodical operation of IoT devices.

The prospect of energy-autonomous operation of distributed IoT devices has also highlighted RF-WEH technologies as a more sustainable and greener option that promises to reduce the environmental impact associated with the manufacturing, maintenance, and disposal of conventional electrochemical batteries. The environmental impact of emerging electronic technologies is now becoming a major concern since the continuously increasing availability of electronics has fuelled the generation of electronic waste (e-waste), making it the fastest-growing waste stream globally [2]. Thus, developing technologies that can help address this timely issue has become a strategic priority for the electronic industry.

A typical wireless RF energy harvesting system consists of several components the most critical of which is the rectenna, as it determines the RF to direct current (DC) conversion efficiency (**Fig. 6.1a**). The rectenna comprises an antenna which is responsible for capturing the RF signal and a rectifier circuit that converts it into DC, which is then used to power the load (sensor, microcontroller, etc.). An impedance-matching network is often used to connect the antenna with the rectifier circuit, ensuring optimal transfer of the captured RF power. The most critical component within the RF-to-DC unit is the diode element that rectifies the electromagnetic signal collected by the antenna [3]. Along with the required high-frequency response, a critical parameter that describes the ability of a diode to rectify an electrical signal is the short circuit current responsivity (in A/W). The latter can be calculated directly from the second-order derivative of the experimentally measured current-voltage  $I(V)$  characteristic and is broadly used to quantify and compare the performance of the various rectifier technologies.

1  
2  
3 Traditionally, Schottky diodes have dominated the application landscape, but other technologies have  
4 been demonstrated, including backward tunnel (Esaki) diodes, tunnel diodes, and spin diodes [4]. The use  
5 of metal-oxide-semiconductor (MOS) transistors as the rectifying element has also been explored  
6 extensively in complementary MOS (CMOS) circuitry as well as in several other transistor technologies [5-  
7 10]. Although simpler to integrate, the intrinsic characteristics of conventional transistors often result in  
8 inferior rectification compared to the corresponding Schottky diode technologies [11]. To maximize the  
9 RF-to-DC power conversion efficiency (PCE) of the RF-WEH, the impedance matching network connecting  
10 the antenna and the load circuit needs to be carefully designed to avoid signal reflection back to the  
11 environment. Additional circuit elements, such as a voltage multiplier and a power management module,  
12 are also required to increase the output voltage of the rectenna so it can drive the load module and charge  
13 the energy storage unit, often consisting of a battery or a capacitor. The efficiency of each block  
14 determines the overall PCE of the RF-WEH; therefore, all elements are equally important to achieve  
15 optimal performance [12].  
16  
17  
18

19 Despite the exploding interest in RF WEHs, numerous challenges still need addressing before the  
20 technology can be fully embraced commercially. One such challenge is the limited RF power in the  
21 ambient environment (**Fig. 6.1b**). The steady progress in developing low-power circuitry and the  
22 continuously increasing abundance of RF signals have partially helped alleviate this issue. Another  
23 challenge relates to the system's physical shape and size. As the size of the IoT node continues to reduce,  
24 its integral components also need to be miniaturized and integrated cost-efficiently. The silicon industry  
25 has responded to this challenge by developing manufacturing processes that enable the integration of the  
26 load circuitry with the RF components, such as the antenna, to deliver system-on-chip (SoC) solutions [13].  
27 In parallel, research on new materials for substrates, dielectrics, semiconductors, and conductors has  
28 propelled these emerging technologies to the forefront of research in emerging RF-WEH technologies [14-  
29 18]. The rapid pace of recent progress shows that harvesting ambient RF energy could offer unique  
30 solutions and lead to truly enabling technologies for the IoT device ecosystem of the future.  
31  
32  
33

34 This section discusses recent progress in RF energy harvesting technologies with a primary focus on  
35 emerging materials and their integration into devices and systems for IoT applications. Caironi *et al.*  
36 (section 6.2) and Georgiadou (section 6.3), discuss the prospects of organic and metal oxide  
37 semiconductors in RF rectifying devices processed via scalable manufacturing techniques. Peng *et al.*,  
38 (section 6.4) and Lemme *et al.*, (section 6.5) summarise recent advances in RF rectennas based on low-  
39 dimensional materials, such as carbon nanotubes (CNT) and two-dimensional (2D) materials and highlight  
40 the need for appropriate modelling tools. Finally, Wagih and Beeby (section 6.6) underline the importance  
41 of emerging conductors for the development of RF antennas, the critical role of material-induced losses,  
42 and the importance of new rectenna designs.  
43  
44  
45  
46  
47  
48  
49  
50  
51  
52  
53  
54  
55  
56  
57  
58  
59  
60

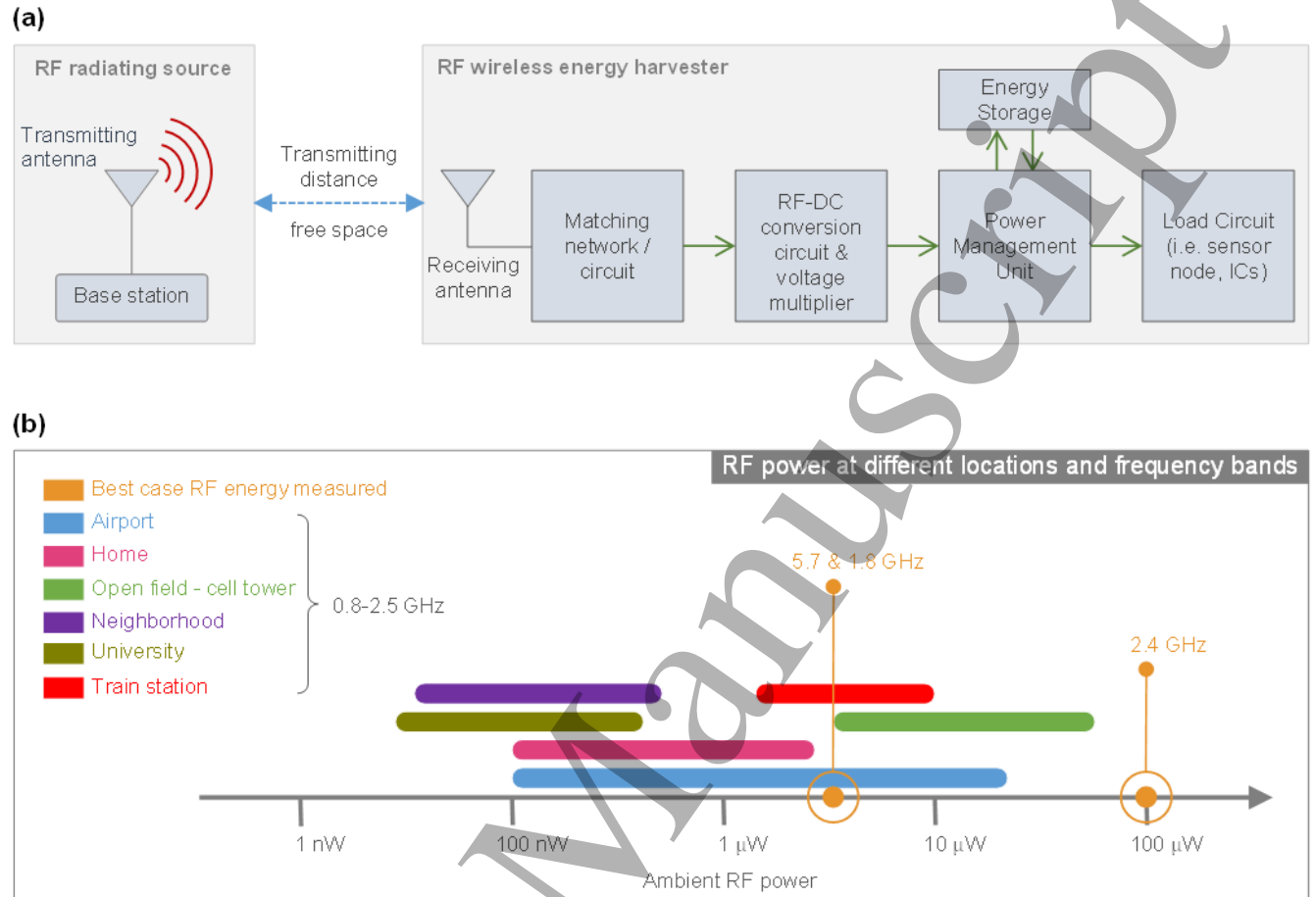


Figure 6.1 a) Schematic of an RF energy harvesting system comprising an antenna, a matching circuit, a rectifier, a voltage multiplier, a power management unit, an energy storage unit, and a load. The RF energy harvester captures the RF signal transmitted by a radiating source and convert it to useful electrical power. b) Measured ambient RF power at various locations in the Calgary areas in Canada, including a mix of rural/urban, public/private locations across different frequency bands for cell phones (824-960 MHz, 1710-2170 MHz), and unlicensed industrial, scientific and medical devices (2.4-2.5 GHz, 5.150-5.875 GHz). The power ranges highlighted in (b) represent the minimum and maximum values measured experimentally at the various locations, as reported by Kwan and Fapojuwo [19].

## References

1. IoT Analytics Research. (2022). Global IoT Market Forecast. <https://iot-analytics.com/number-connected-iot-devices/>
2. <https://www.statista.com/topics/3409/electronic-waste-worldwide/#dossierKeyfigures>
3. James Semple *et al* 2017 *Semicond. Sci. Technol.* **32** 123002
4. S. Hemour and K. Wu, "Radio-Frequency Rectifier for Electromagnetic Energy Harvesting: Development Path and Future Outlook," in *Proceedings of the IEEE*, vol. 102, no. 11, pp. 1667-1691, Nov. 2014, doi: 10.1109/JPROC.2014.2358691.
5. J. Yi, W. Ki and C. Tsui, "Analysis and Design Strategy of UHF Micro-Power CMOS Rectifiers for Micro-Sensor and RFID Applications," in *IEEE Transactions on Circuits and Systems I: Regular Papers*, vol. 54, no. 1, pp. 153-166, Jan. 2007, doi: 10.1109/TCSI.2006.887974.
6. *Appl. Phys. Lett.* **98**, 162102 (2011); <https://doi.org/10.1063/1.3579529>

- 1
  - 2
  - 3
  - 4
  - 5
  - 6
  - 7
  - 8
  - 9
  - 10
  - 11
  - 12
  - 13
  - 14
  - 15
  - 16
  - 17
  - 18
  - 19
  - 20
  - 21
  - 22
  - 23
  - 24
  - 25
  - 26
  - 27
  - 28
  - 29
  - 30
  - 31
  - 32
  - 33
  - 34
  - 35
  - 36
  - 37
  - 38
  - 39
  - 40
  - 41
  - 42
  - 43
  - 44
  - 45
  - 46
  - 47
  - 48
  - 49
  - 50
  - 51
  - 52
  - 53
  - 54
  - 55
  - 56
  - 57
  - 58
  - 59
  - 60
7. E. Cantatore *et al.*, "A 13.56-MHz RFID System Based on Organic Transponders," in *IEEE Journal of Solid-State Circuits*, vol. 42, no. 1, pp. 84-92, Jan. 2007, doi: 10.1109/JSSC.2006.886556.
8. Appl. Phys. Lett. **88**, 123502 (2006); <https://doi.org/10.1063/1.2186384>
9. K. Myny, S. Steudel, S. Smout, P. Vicca, F. Furthner, B. van der Putten, A.K. Tripathi, G.H. Gelinck, J. Genoe, W. Dehaene, P. Heremans. Organic RFID transponder chip with data rate compatible with electronic product coding. *Organic Electronics*, Volume 11, Issue 7, 2010. Pages 1176-1179
10. Franklin, Aaron D. Nanomaterials in transistors: From high-performance to thin-film applications. 2015. Science. aab2750. Vol 349 pp6249. doi:10.1126/science.aab2750
11. H. Dai, Y. Lu, M. -K. Law, Sai-Weng Sin, U. Seng-Pan and R. P. Martins, "A review and design of the on-chip rectifiers for RF energy harvesting," *2015 IEEE International Wireless Symposium (IWS 2015)*, 2015, pp. 1-4, doi: 10.1109/IEEE-IWS.2015.7164642.
12. S. Hemour and K. Wu, "Radio-Frequency Rectifier for Electromagnetic Energy Harvesting: Development Path and Future Outlook," in *Proceedings of the IEEE*, vol. 102, no. 11, pp. 1667-1691, Nov. 2014, doi: 10.1109/JPROC.2014.2358691.
13. Z.N. Chen et al. (eds.), Handbook of Antenna Technologies. DOI **10.1007/978-981-4560-44-3\_56**.
14. *ACS Appl. Electron. Mater.* 2021, 3, 9, 3747–3753
15. C. -Y. Fan, M. -D. Wei, B. Uzlu, Z. Wang, D. Neumaier and R. Negra, "Fully Integrated 2.4-GHz Flexible Rectifier Using Chemical-Vapor-Deposition Graphene MMIC Process," in *IEEE Transactions on Electron Devices*, vol. 68, no. 3, pp. 1326-1333, March 2021, doi: 10.1109/TED.2021.3049756.
16. Xu Zhang, Jesús Grajal, Marisa López-Vallejo, Elaine McVay, Tomás Palacios. Opportunities and Challenges of Ambient Radio-Frequency Energy Harvesting. *Joule*, Volume 4, Issue 6, 2020. Pages 1148-1152
17. Georgiadou, D.G., Semple, J., Sagade, A.A. *et al.* 100 GHz zinc oxide Schottky diodes processed from solution on a wafer scale. *Nat Electron* **3**, 718–725 (2020). <https://doi.org/10.1038/s41928-020-00484-7>
18. [Chan-mo Kang, Jessica Wade, Sumin Yun, Jaehoon Lim, Hyunduck Cho, Jeongkyun Roh, Hyunkoo Lee, Sangwook Nam, Donal D. C. Bradley, Ji-Seon Kim, Changhee Lee](#). Organic Electronics: 1 GHz Pentacene Diode Rectifiers Enabled by Controlled Film Deposition on SAM-Treated Au Anodes (*Adv. Electron. Mater.* 2/2016).
19. J. C. Kwan and A. O. Fapojuwo, "Measurement and Analysis of Available Ambient Radio Frequency Energy for Wireless Energy Harvesting," *2016 IEEE 84th Vehicular Technology Conference (VTC-Fall)*, 2016, pp. 1-6, doi: 10.1109/VTCFall.2016.7881084.



## 6.2 Organic semiconductors for radiofrequency rectifying devices

Tommaso Losi<sup>1</sup>, Fabrizio Viola<sup>1</sup> and Mario Caironi<sup>1</sup>

<sup>1</sup>Center for Nano Science and Technology@PoliMi, Istituto Italiano di Tecnologia, Via Pascoli, 70/3, 20133 Milano

### Status

One of the most exploited methods to wirelessly power *smart objects* for IoT without the use of batteries is the coupling with radio-frequency (RF) waves incoming from a transmitter. Such waves resonate with a suitably designed antenna, following which a rectifying electronic device performs the AC-DC field rectification, as required to operate the load (sensors, circuits etc.). Target frequencies span from the High-Frequency (HF) – from 3 to 30 MHz – to the Ultra-High Frequency (UHF) – from 300 MHz to 3 GHz – depending on the final application. UHF is suited for *far-field* powering and communication protocols (with a read range up to 100 m) typically employed for security, while HF allows *near-field*, cm-range, communication and powering. In this scenario, different semiconductor technologies and scalable manufacturing processes have been investigated with the goal of ensure cost-effective fabrication of RF rectifiers, capable to be integrated with everyday objects at viable costs. Organic semiconductors are one of the most promising technologies to achieve such goal, since they can be deposited through cheap, low-waste and energy efficient techniques, such as printing [1]. Furthermore, organic materials do not need high temperature processing, thus being compatible with flexible substrates [1]. In the last decade, a lot of efforts has been devoted to the improvement of organic semiconductors performance, achieving the *operational frequency* in the HF regime when integrated in rectifiers. The latter are typically based on two-terminal devices, such as organic diodes, or three-terminal ones, such as organic field-effect transistors (OFETs) connected in trans-diode mode. Thanks to the development of scalable fabrication processes for device footprint reduction and for the deposition of high quality organic semiconducting layers with outstanding charge transport properties, supported by metal-semiconductors interface engineering to reduce contact resistance effects, operational frequency of both OFETs and organic diodes increased in the recent past: several demonstrations are available in the tens of MHz range [2], [3], with the record value so far of 160 MHz for the OFETs [4], and 14 GHz for the organic diodes [5]. Such progresses renewed the interest in this field towards the adoption of organic rectifiers for a plethora of applications, such as remote healthcare and distributed sensing, which require a technology integrating wireless-powered and large-area electronics with RF-communication capabilities.

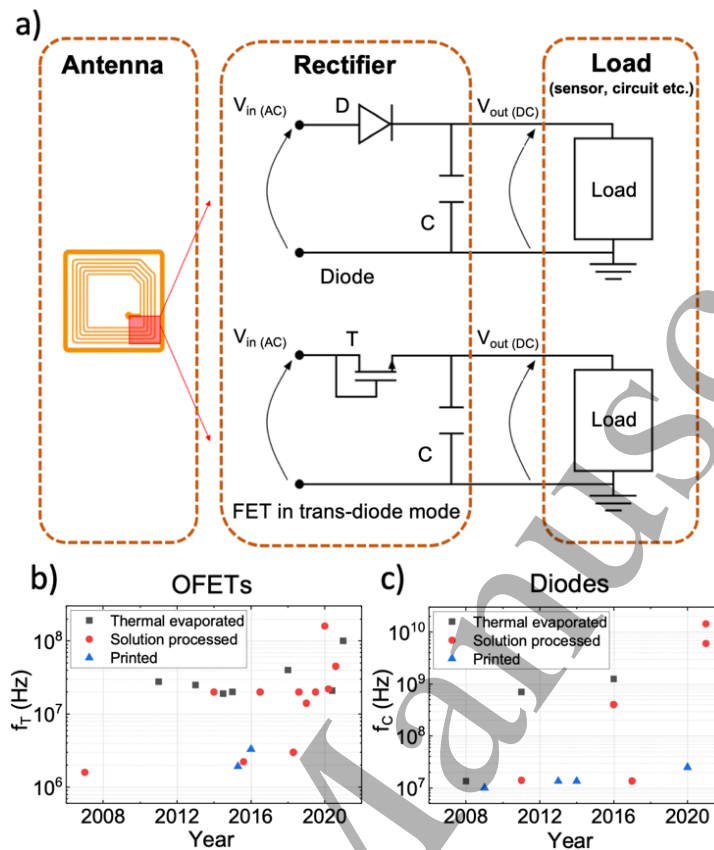


**Figure 1:** a) Schematic of an RF harvester employing a diode or OFET based rectifier circuit. b) Comparison graph of the maximum operational frequency (transition frequency,  $f_T$ ) of organic OFETs. c) Comparison graph of the maximum operational frequency (cut-off frequency,  $f_c$ ) of organic diodes.

### Current and Future Challenges

Despite recent improvements in operational frequency of organic rectifiers, there are still several limitations which prevent the unlocking of their full potential, especially for UHF operation. Refined RF design of optimized rectifiers for efficient energy harvesting typically requires the use of transistors, while a diode-only technology poses limits in this sense. Therefore a technology enabling both diodes and transistors is preferable, with the additional advantage of allowing integration of electronic circuits with the same process. On the one side, current high-frequency organic diodes for which a multi-GHz cut-off frequency ( $f_c$ ) was demonstrated [5], are based on ad-hoc two-terminal Schottky diode architectures. However, there are still major technological limitations (such as limited-throughput and scalability, as well as limited compatibility with large-area production), which do not allow the massive adoption of the reported multi-GHz cut-off frequency diodes. On the other, owing to a higher complexity, the achievement of high speed operation has proven more difficult for OFETs. One of the main reasons that has limited the achievement of UHF operation for OFETs so far, is inefficient charge injection or, in other words, a too high *width-normalized contact resistance* ( $R_c W$ ) [6], rather than a low *charge carrier mobility*  $\mu$  that is now comparable with that of low-temperature metal oxides ( $\sim 10 \text{ cm}^2/\text{Vs}$ ). As a matter of fact,

only few works report  $R_C W$  values  $< 100 \Omega\text{cm}$ , which are order of magnitudes higher compared to other thin-film technologies [6]. The detrimental effect of contact resistance becomes critical when high mobility semiconductors are employed in downscaled OFETs structures. However, the combination of high mobility semiconductors and downscaling is crucial for (i) the reduction of the *capacitive parasitism* related to the gate-to-source and gate-to-drain geometrical overlap ( $C_g$ ), and for (ii) maximize *channel transconductance* ( $g_m$ ), thus improving transition frequency according to:

$$f_T = g_m/2\pi C_g = \mu_{eff}(V_g - V_T)/2\pi L_c(L_c + 2L_{ov})$$

where  $\mu_{eff}$  is the *effective carrier mobility*, while  $L_c$  and  $L_{ov}$  are *channel* and *overlap length*. Another important limit is related to heat generation (or *self-heating*) during OFETs high-frequency operation. For example, typical planar test-bed OFETs with micron-scale  $L_c$ , sustaining a current per unit width  $> 1 \text{ mA/mm}$  and voltages in the range of few tens of volts, need to dissipate efficiently a power density in the range of  $10\text{-}100 \text{ W/mm}^2$ . The *low thermal conductivity* of common flexible substrates and dielectrics does not allow it and irreversible thermal breakdowns take place. Reduction of driving voltages is by itself a challenge for  $f_T$  values at UHF, considering also that enhanced areal capacitances inevitably increase parasitism. Such thermal dissipation limit was evidenced also in vertical OFETs architectures, characterized by low voltages but much higher current densities, precluding continuous operation [7].

### Advances in Science and Technology to Meet Challenges

As for UHF organic diodes, processes and architecture that can be exploited also for three-terminal transistors have the potential to enable monolithic integration of UHF circuitry. To this extent, recently proposed adhesion lithography nano-gaps [5], which were exploited to demonstrate coplanar organic diodes with  $f_c$  of 14 GHz, may offer an interesting platform also for nano-gap based organic transistors. At the same time, current developments in RF vertical organic transistors [8], should in principle offer excellent RF diodes. Yet, UHF operation has to be demonstrated in both cases, with necessary developments in charge injection and electrostatic control of nano-channels through a gate. Controlled multilayer methods, derived from vertical trench-based microfabrication techniques, have rarely been attempted with organics [DOI: 10.1109/TNANO.2020.2994640] and appear currently out of reach, yet might offer inspiration for future breakthroughs.

Concerning planar OFETs, charge injection issues are prevalent in limiting  $f_T$ , irrespectively of the technology adopted. The use of *self-assembling monolayers* (SAMs) on source and drain contacts, such as thiols, to reduce charge carrier injection barrier by energy levels matching and improved semiconductor morphology at the contacts, has been consistently adopted for more than 20 years [6]. Without doubt, this strategy sustained so far the improvement of AC characteristics of OFETs based on the adoption of more performing semiconductors in terms of mobility (e.g. dif-TES-ADT and DPh-DNTT for vacuum while IDT-BT, P(NDI2OD-T2) and DPPT-TT for solution based approaches). Yet, to benefit from even higher mobility materials (e.g. C<sub>9</sub>-DNBDT, C<sub>8</sub>-BTBT and organic blends between small molecules and insulating/semiconducting polymers such PS, PMMA and IDT-BT), alternative schemes are necessary to definitely overcome contact limitations. To this end, stable and controlled electronic doping strategies, to

allow engineering of *charge carrier density profiles* in organic semiconductors, are still largely missing. It is therefore important to further develop doping strategies, and in particular to achieve spatially controlled p- and n-type doping, so that charge carrier density can be controlled locally, e.g. at source and drain electrodes only, in order to achieve ohmic contacts while preserving current on-off ratio. The latter is particularly challenging owing to dopants diffusivity, which may change over time the doping profile.

Since contact resistance strongly depends on the local electric field at the electrode, in absence of local doping it is possible to mitigate its effect by exploiting high capacitance dielectrics [9]. High capacitances are also needed to reduce operating voltages, necessary for low power consumption. To this end, since low frequency relaxations make high- $k$  organic dielectrics not viable, one efficient strategy may be represented by *pinhole-free ultra-thin dielectric layers*, robust enough against leakage currents and low voltage breakdowns [10]. The increased channel capacitance inherently produces a corresponding increase in capacitive parasitism, with an overall net decrease of  $f_T$  if more efficient device architectures for parasitism management are not adopted, compatibly scalable manufacturing. Self-alignment techniques are therefore highly desired. For instance, *self-aligned gate techniques*, whose compatibility with printing methods has been already demonstrated in the past [11], combined with local doping at contacts, appears to be a required advancement.

For what concerns the self-heating effect of OFETs, a further solution, along with reduce voltage operation, is the development of *flexible substrates with enhanced thermal conductivity ( $k_T$ )*, such as plastic composites, or the introduction of heat dissipation layers [12].

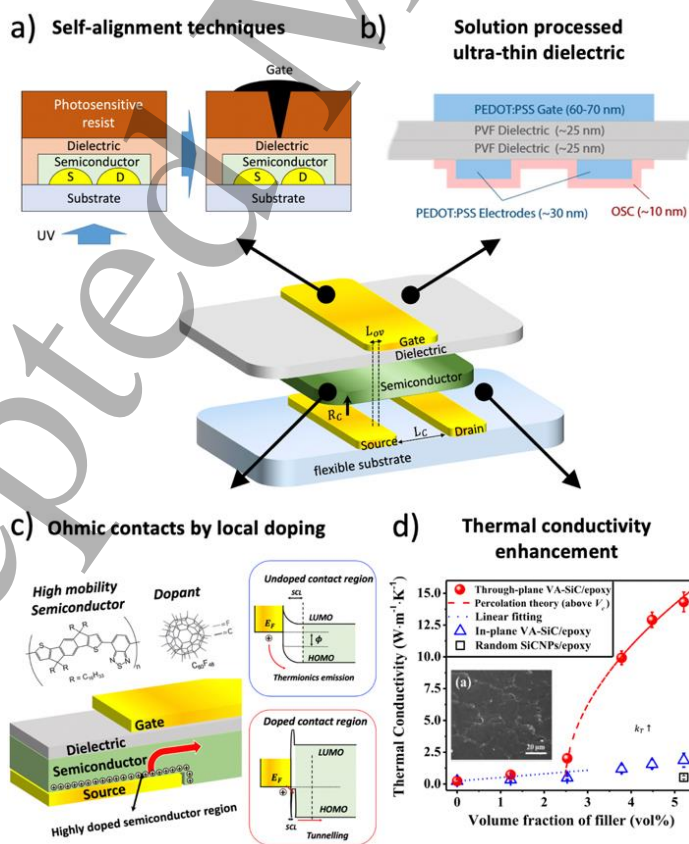


**Figure 2.** Summary of possible strategies to overcome current limitations for organic transistors used as rectifying devices: a) employment of self-aligned gate techniques, for parasitism reduction; b) employment of ultra-thin dielectrics to lower voltages (Adapted with permission from [10]. Copyright 2021, Springer Nature); c) capability of spatially control charge carrier density profiles in semiconductors with doping; d) the use of flexible substrates with enhanced thermal conductivity (Adapted with permission from [12]. Copyright 2020, American Chemical Society).

## Concluding Remarks

Organic semiconductors are undoubtedly one of the most promising candidates for the development of RF rectifiers for IoT applications. They are particularly indicated when large area, high-throughput manufacturing, and easiness of integration with everyday objects are required. Moreover, they can offer many advantages (such as flexibility, energy efficient solution processability, low-cost, bio-compatibility, recyclability), including the possibility of realizing complementary devices, with accessible schemes to monolithic circuit integration, distinguishing traits with respect to other emerging technologies. Yet, prospective downscaled manufacturing schemes should face real scenarios, with available fabrication facilities largely offering lithographic processes, and high-resolution mass scale printing facilities not yet deployed. Therefore, further scientific and technological advancements, required to tackle present drawbacks, should be contextualized in plausible manufacturing approaches to make this technology ready for commercialization towards a plethora of applications such as remote healthcare, distributed sensing, among others.

## References

- [1] Y. Chu, C. Qian, P. Chahal, and C. Cao, "Printed Diodes: Materials Processing, Fabrication, and Applications," *Adv. Sci.*, vol. 6, no. 6, 2019.
- [2] F. A. Viola *et al.*, "A 13.56 MHz Rectifier Based on Fully Inkjet Printed Organic Diodes," *Adv. Mater.*, vol. 32, no. 33, pp. 1–7, 2020.
- [3] A. Yamamura *et al.*, "High-Speed Organic Single-Crystal Transistor Responding to Very High Frequency Band," *Adv. Funct. Mater.*, vol. 30, no. 11, 2020.
- [4] A. Perinot, M. Giorgio, V. Mattoli, D. Natali, and M. Caironi, "Organic Electronics Picks Up the Pace: Mask-Less, Solution Processed Organic Transistors Operating at 160 MHz," *Adv. Sci.*, vol. 8, no. 4, pp. 1–6, 2021.
- [5] K. Loganathan *et al.*, "14 GHz Schottky Diodes Using a p-Doped Organic Polymer," *Adv. Mater.*, vol. 34, no. 22, 2022.
- [6] J. W. Borchert, R. T. Weitz, S. Ludwigs, and H. Klauk, "A Critical Outlook for the Pursuit of Lower Contact Resistance in Organic Transistors," *Adv. Mater.*, vol. 34, no. 2, 2022.
- [7] M. P. Klinger, A. Fischer, H. Kleemann, and K. Leo, "Non-Linear Self-Heating in Organic Transistors Reaching High Power Densities," *Sci. Rep.*, vol. 8, no. 1, pp. 1–9, 2018.
- [8] B. Kheradmand-Boroujeni, M. P. Klinger, A. Fischer, H. Kleemann, K. Leo, and F. Ellinger, "A Pulse-Biasing Small-Signal Measurement Technique Enabling 40 MHz Operation of Vertical Organic



- Transistors,” *Sci. Rep.*, vol. 8, no. 1, pp. 1–9, 2018.
- [9] J. W. Borchert *et al.*, “Small contact resistance and high-frequency operation of flexible low-voltage inverted coplanar organic transistors,” *Nat. Commun.*, vol. 10, no. 1, pp. 1–11, 2019.
- [10] F. A. Viola *et al.*, “A sub-150-nanometre-thick and ultraconformable solution-processed all-organic transistor,” *Nat. Commun.*, vol. 12, no. 1, p. 5842, 2021.
- [11] Y. Y. Noh, N. Zhao, M. Caironi, and H. Sirringhaus, “Downscaling of self-aligned, all-printed polymer thin-film transistors,” *Nat. Nanotechnol.*, vol. 2, no. 12, pp. 784–789, 2007.
- [12] M. C. Vu *et al.*, “High Thermal Conductivity Enhancement of Polymer Composites with Vertically Aligned Silicon Carbide Sheet Scaffolds,” *ACS Appl. Mater. Interfaces*, vol. 12, no. 20, pp. 23388–23398, May 2020.

### 6.3 Metal-oxide semiconductors for radiofrequency rectifying devices

Dimitra G. Georgiadou

Electronics and Computer Science, University of Southampton, Highfield Campus, Southampton SO17 1BJ, United Kingdom

#### Status

Metal oxide semiconductors are excellent candidates to replace Si and III–V compound semiconductors, such as gallium arsenide (GaAs), in wireless energy harvesting applications. They are characterised by good electrical properties, high optical transparency and compatibility with conventional semiconductor processes, e.g., photolithography. Metal oxide thin films can be deposited either via vacuum-based processes, such as sputtering, thermal evaporation, pulsed laser deposition (PLD) and atomic layer deposition (ALD) or solution-based methods (e.g., spin-coating, spray-coating, blade-coating, screen and inkjet printing), rendering processing on large-area flexible substrates possible. The potential to tune their optoelectronic properties through structural modification during deposition and their non-toxic nature render them ideal candidates to harvest wireless energy and power the IoT ecosystem or be implemented in novel wearable devices.

In their simpler binary form, they comprise a metal cation (i.e., Zn, In, Cu) and an oxide anion, while ternary, such as Indium Zinc Oxide (IZO), and quaternary metal oxides, such as Indium Gallium Zinc Oxide (IGZO), may also be formed. The latter oxides constitute amorphous semiconductors and are beneficial to the binary, usually polycrystalline ones, as they can be processed at lower temperatures and achieve greater film uniformity and higher device performance due to the lack of grain boundaries. Ultra-high mobilities over  $100 \text{ cm}^2/\text{V}\cdot\text{s}$  have been obtained with amorphous oxide-based thin film transistors (TFT) [1].

From all metal oxides, IGZO is probably the most technologically mature material due to its wide implementation in the display industry. The Hosono group demonstrated in 2004 that high mobility IGZO films could be deposited with PLD at room temperature on flexible substrates [2]. Almost a decade later Schottky diodes based on RF-sputtered IGZO with rectification ratios  $>10^8$ , barrier heights of 0.85 eV and ideality factors close to unity were implemented by Chasin *et al.* in a single-stage rectifier reaching 1.1 GHz frequencies [3]. The diodes were then integrated in energy harvesters comprising antenna, optimised impedance matching network and double half-wave rectifier with cut-off frequency of 3 GHz that could output  $>1 \text{ V}_{\text{dc}}$  when placed 2 m away from the transmitter antenna [4]. Recently, record intrinsic cutoff

frequencies >100 GHz and extrinsic cutoff frequencies of 42 GHz were demonstrated with Schottky diodes based on solution-processed ZnO [5] and IGZO [6], respectively, using a coplanar 10-nm gap asymmetric electrode structure.

### Current and Future Challenges

To increase the RF performance of Schottky diodes, junction resistance ( $R_j$ ) and capacitance ( $C_j$ ) need to be minimised at the same time. Increasing the mobility of metal oxide semiconductors is one way to reduce  $R_j$  and boost forward current. A thin layer of the oxide contributes also to resistance drop, although at the expense of lower rectification ratio and increased capacitance, limiting thus the frequency response.

Another issue with most metal oxides is the defects present in their structure, such as oxygen vacancies ( $V_O$ ) formed during deposition or exposure to ambient air. The donor levels associated with  $V_O$  can lower the diode breakdown voltage and increase the leakage current.

The selection of suitable metal contacts and engineering the metal/semiconductor interface, both play a decisive role in the formation of ohmic or Schottky contacts. For instance, a polycrystalline top metal, exposing different facets to the semiconductor, may create inhomogeneities in the Schottky barrier height, whereas deposition of thin-film oxide semiconductors via sputtering often produces local variations in the oxide's electron affinity and the density of interface states [7]. On the other hand, certain metals can induce electrical doping of the oxide film. As an example, when Mo was used as bottom electrode in vertical diodes, where a zinc tin oxide film was produced from precursor inks, a low-doped Zn-Sn-Mo-O intermediate layer was formed. This has been found to form a rectifying junction, resulting in high voltage output  $V_{out} \approx 5$  V when brought close to an RFID reader, while  $V_{out}/V_{in}$  exceeding 80% at <40 mm of distance was obtained [8].

The contact resistance challenge has been traditionally addressed by applying thermal annealing, oxygen plasma and UV-ozone to treat the Pt or Pd Schottky contacts with IGZO, as it ensures better stoichiometry at the interface. Lately, applying a hydrogen plasma treatment to the surface of an IGZO-based varactor to reach cutoff frequencies of 30 GHz was also demonstrated [9]. It was proposed that hydrogen passivates native defects in amorphous IGZO and increases the electron density, resulting in an ultra-low contact resistance of  $1.33 \times 10^{-6} \Omega \cdot \text{cm}^2$  when Mo was used as the top metal. These concepts, however, have to be verified also for other metals and/or metal oxides.

Finally, from a purely material perspective, the future scarcity of some of the elements comprising the metal oxides should be taken into account, as the supply of Indium, Gallium and Zinc is uncertain in the longer term, while Tin is considered to be a conflict mineral.

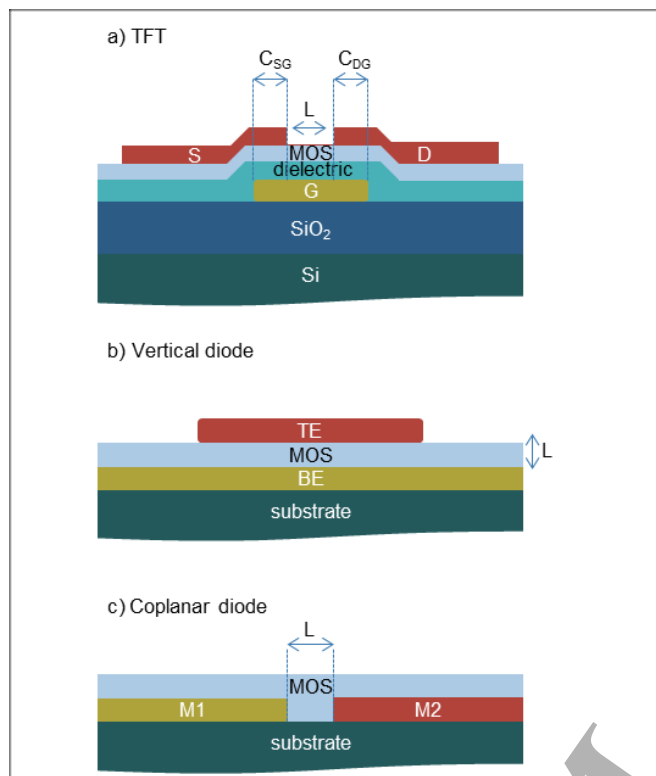


**Figure 1.** Examples of different device structures employed in high frequency diodes and geometrical considerations: a) thin film transistor, b) vertical diode, c) coplanar diode. The cutoff frequency (or transit frequency in TFTs) has an inverse relation to the carrier transit length,  $L$ , which is some micrometers in TFTs (the channel length), around 50-100 nm in vertical diodes (the film thickness) and 10-20 nm in coplanar nanogap diodes (the nanogap length). S is source; D is drain; G is gate;  $C_{GS}$  is source-gate parasitic capacitance;  $C_{DS}$  is drain-gate parasitic capacitance; MOS is metal oxide semiconductor; BE is bottom electrode; TE is top electrode; M1 is metal 1 and M2 is metal 2.

### Advances in Science and Technology to Meet Challenges

Despite recent advances, there is still a lot of room for improvement to overcome the current challenges of metal oxide RF energy harvesting devices and enable operation at 5G and 6G frequencies.

The quest to increase the rectifier performance in terms of operational frequency and power output demands ingenious geometry optimisation in both TFTs and diodes structures. In TFTs, one approach is to minimise as much as possible the parasitic capacitance at the overlapping area between gate and source/drain by self-aligning the gate (Figure 1a). First attempts towards this direction have resulted in maximum transit frequency ( $f_T$ ) and oscillation frequency ( $f_{max}$ ) beyond 1.1 and 3.1 GHz, respectively - the current record performance for IGZO-based TFTs [10]. In Schottky diodes, coplanar nanogap separated asymmetric electrodes (Figure 1c), fabricated with a large area, high throughput nanopatterning technique, named adhesion lithography, constitute a promising recent development. Indeed, energy-harvesting circuits based on solution-processed ZnO and Al-doped ZnO films deposited on such 10 nm gap Al-Au coplanar electrodes showed intrinsic cutoff frequencies above 100 GHz and delivered output voltages of 600 mV and 260 mV at 2.45 GHz and 10 GHz for 8 dBm input, respectively [5]. However, the efficiency of these RF energy harvesters is still quite low, and their breakdown voltage is limiting the applications, thus more elaborate design of the electrodes is needed to minimise the transmission losses. It is noteworthy

that, although there are several reports in the literature for such vertical nanotrench fabrication methods, there is no demonstration of those nanostructures in rectifier circuits, as they are significant challenges in creating asymmetric electrode structures, which are needed to obtain rectification in diodes. For this reason, they have been traditionally applied in biosensing applications (<https://doi.org/10.1016/j.bios.2022.114486>) or in photonics (<https://doi.org/10.1021/nl1012085>). There is, thus, ample room for further investigations in the field of nanotechnology, specifically targeting RF energy harvesting.

Moreover, from a manufacturing standpoint, it is important to increase the fabrication yield on flexible (e.g. plastic) substrates, as well as the monolithic patterning of the antenna and the rectifier on the same substrate, something which will be paramount in the field of flexible RF electronics. In this regard, substituting the annealing step of the metal oxide film by xenon flash lamp photonic sintering to protect the temperature sensitive substrates from prolonged exposure to high thermal budget processes has proven to be instrumental in obtaining solution-processed IGZO rectifiers operating at 47 GHz and can be applied more broadly in the fabrication of metal oxide films on flexible substrates [6].

Finally, the electronic devices still show insufficient durability to extreme physical deformation. To employ them in fully flexible applications, it is imperative to develop devices that can endure further mechanical stress.

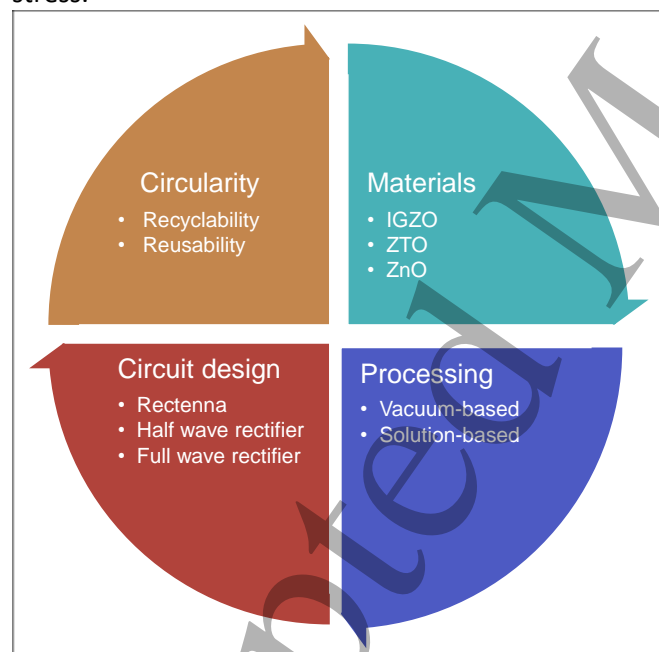


**Figure 2.** The four pillars that drive progress in the metal oxide semiconductor based wireless energy harvesters: high mobility materials, low-cost processing at large areas, ingenious circuit design to fit the application's requirements and compliance with circularity aspects.

### Concluding Remarks

Significant strides have been already made to develop efficient low-cost wireless energy harvesting systems to be deployed in the ever-growing IoT, especially in urban and industrial environments (Figure 2). The development of ultra-high mobility metal oxide semiconductors, motivated by the next generation display industry, was achieved by controlling their chemical composition and applying diligent doping

strategies. Although vacuum-based processes are well-established in the complementary metal oxide semiconductor (CMOS) manufacturing and enable high-quality uniform films, solution-processing is a low-cost alternative, compatible with flexible and printable devices. The interplay between high frequency and maximum efficiency imposes meticulous design of the ensuing rectifier topology to tune the performance according to the requirements of the targeted applications. Finally, the potential to recycle or reuse the metals and metal oxides of the energy harvesting system will be critical in the following years, as we move towards a circular economy fostering more sustainable electronic technologies [11].

## Acknowledgements

D.G.G. acknowledges support from the UKRI Future Leaders Fellowship Grant (MR/V024442/1).

## References

- [1] J. Y. Choi and S. Y. Lee, "Comprehensive review on the development of high mobility in oxide thin film transistors," *Journal of the Korean Physical Society*, vol. 71, no. 9, pp. 516-527, 2017/11/01 2017, doi: 10.3938/jkps.71.516.
- [2] K. Nomura, H. Ohta, A. Takagi, T. Kamiya, M. Hirano, and H. Hosono, "Room-temperature fabrication of transparent flexible thin-film transistors using amorphous oxide semiconductors," *Nature*, vol. 432, no. 7016, pp. 488-492, Nov 25 2004, doi: 10.1038/nature03090.
- [3] A. Chasin, M. Nag, A. Bhoelokam, K. Myny, S. Steudel, S. Schols, J. Genoe, G. Gielen, and P. Heremans, "Gigahertz Operation of a-IGZO Schottky Diodes," *IEEE Trans. Electron Devices*, vol. 60, no. 10, pp. 3407-3412, 2013, doi: 10.1109/TED.2013.2275250.
- [4] A. Chasin, V. Volskiy, M. Libois, K. Myny, M. Nag, M. Rockele, G. A. E. Vandenbosch, J. Genoe, G. Gielen, and P. Heremans, "An Integrated a-IGZO UHF Energy Harvester for Passive RFID Tags," *IEEE Trans. Electron Devices*, vol. 61, no. 9, pp. 3289-3295, Sep 2014, doi: 10.1109/ted.2014.2340462.
- [5] D. G. Georgiadou, J. Semple, A. A. Sagade, H. Forstén, P. Rantakari, Y.-H. Lin, F. Alkhalil, A. Seitkhan, K. Loganathan, H. Faber, and T. D. Anthopoulos, "100 GHz zinc oxide Schottky diodes processed from solution on a wafer scale," *Nature Electronics*, vol. 3, no. 11, pp. 718-725, 2020/11/01 2020, doi: 10.1038/s41928-020-00484-7.
- [6] K. Loganathan, H. Faber, E. Yengel, A. Seitkhan, A. Bakytbekov, E. Yarali, B. Adilbekova, A. AlBatati, Y. Lin, Z. Felemban, S. Yang, W. Li, D. G. Georgiadou, A. Shamim, E. Lidorikis, and T. D. Anthopoulos, "Rapid and up-scalable manufacturing of gigahertz nanogap diodes," *Nature Communications*, vol. 13, no. 1, p. 3260, 2022/06/07 2022, doi: 10.1038/s41467-022-30876-6.
- [7] J. Wilson, J. Zhang, Y. Li, Y. Wang, Q. Xin, and A. Song, "Influence of interface inhomogeneities in thin-film Schottky diodes," *Appl. Phys. Lett.*, vol. 111, no. 21, p. 213503, 2017, doi: 10.1063/1.5004247.
- [8] Y. Son and R. L. Peterson, "Exploiting In Situ Redox and Diffusion of Molybdenum to Enable Thin-Film Circuitry for Low-Cost Wireless Energy Harvesting," *Adv. Funct. Mater.*, vol. 29, no. 5, p. 1806002, 2019, doi: <https://doi.org/10.1002/adfm.201806002>.
- [9] H. Park, J. Yun, S. Park, I.-s. Ahn, G. Shin, S. Seong, H.-J. Song, and Y. Chung, "Enhancing the Contact between a-IGZO and Metal by Hydrogen Plasma Treatment for a High-Speed Varactor (>30 GHz)," *ACS Applied Electronic Materials*, vol. 4, no. 4, pp. 1769-1775, 2022/04/26 2022, doi: 10.1021/acsaelm.2c00028.
- [10] C. Tückmantel, U. Kalita, T. Haeger, M. Theisen, U. Pfeiffer, and T. Riedl, "Amorphous Indium-Gallium-Zinc-Oxide TFTs Patterned by Self-Aligned Photolithography Overcoming the GHz Threshold," *IEEE Electron Device Letters*, vol. 41, no. 12, pp. 1786-1789, 2020, doi: 10.1109/LED.2020.3029956.



- [11] S. Li, Y. Liu, Y. Che, J. Song, Y. Shu, J. He, B. Xu, and B. Yang, "Recycling of Spent Indium–Gallium–Zinc Oxide Based on Molten Salt Electrolysis," *ACS Sustainable Chemistry & Engineering*, vol. 8, no. 43, pp. 16296-16303, 2020/11/02 2020, doi: 10.1021/acssuschemeng.0c05986.

## 6.4 Carbon nanotubes for radiofrequency rectifying devices

Li Ding<sup>1</sup> and Lian-Mao Peng<sup>1,2</sup>

<sup>1</sup> Key Laboratory for the Physics and Chemistry of Nanodevices and Center for Carbon-based Electronics, School of Electronics, Peking University, Beijing 100871, China.

<sup>2</sup> Academy for Advanced Interdisciplinary Studies, Peking University, Beijing 100871, China.

### Status

Carbon nanotubes (CNTs) can be derived from graphene by rolling up along a chiral vector  $C_h(n, m)$  which decides electrical properties such as excellent carrier mobility, saturation velocity and quasi-one-dimensional structure with small diameter leading to large current driving capability and high-speed performance for radio-frequency (RF) energy harvesting. Early rectifying devices built by CNTs based diodes were fabricated on single CNTs by asymmetric contacts between Al or Ti (Schottky) and Au or Pt (Ohmic) [1]-[3] with cut-off frequency up to 6-18 GHz which were typically characterized with rectified signal (with frequency range from 7 to 18 GHz, a radiated power input of -8 to 9 dBm, and a 0.25 V bias) of 3.5 to 100 nA. But these approaches were limited severely by the use of individual semiconducting CNTs in the device channel, and more importantly the use of non-perfect contacts which inevitably leads to the formation of Schottky barrier which reduces the injection efficiency of electrons into the conducting CNT channel and thus results in large series resistance of over several hundreds of K $\Omega$  to more than 1 M $\Omega$ . Some other types of CNTs based diodes were also reported, for example those based on half chemically doped channel [4] and heterojunction built with other nanomaterials [5]. However, the performance of these diodes is typically poor and these diodes are thus not suitable for RF rectifying devices.

The first high performance CNT rectifying barrier-free bipolar diode using individual semiconducting single-walled CNTs in the channel was reported in 2008 [6], where barrier-free and thus highly efficient carrier injection was realized by using Sc contact for n-region and Pd contact for p-region. Recent progress on aligned high purity and density CNTs arrays by Peking University [7-8] further remarkably improved CNT based RF rectifying devices with cut-off frequency of over 500 GHz, series resistance of down to 32 $\Omega$  and large DC output of over 350 mV by rectifying 50 GHz signals. Figure 1 summaries progresses on CNT materials and device fabrication. It is worth noting, however, that the results achieved so far are still far from theoretical prediction, and it is expected that with further advances on CNT materials and process, faster and more efficient CNTs rectifying devices will be soon developed.

	Material	$f_c$ (GHz)	$R_s(\Omega)$	$C_j(F)$	Rectified signal (V or A)	Rectification ratio	Year	Ref
1	Single-CNT	3100 (540) with 100 (4) CNTs, calculated	160K	N/A	N/A	$\sim 10^3$	2005	[1]
2	CVD grown CNTs	> 18 GHz, extrapolated $\sim 400$ GHz, calculated	420K	$\sim 10^{-18}F$	100 nA @ 7 GHz & 0.25 V ( $P_m = 9$ dBm); 3.5 nA @ 18 GHz & 0.25 V ( $P_m = -8$ dBm)	$\sim 10^2$	2008	[2]
3	CVD grown single-CNT on Quartz	$\sim 6$ GHz, extrapolated $\sim 200$ GHz, calculated	1.38 M	$\sim 100$ aF	23 nA/mW @ 10 GHz & 1.5 V	$\sim 10^3$	2011	[3]
4	Random oriented CNTs	N/A	N/A	N/A	1.8 V @ 10 MHz & 3 V	$> 10^3$	2011	[4]
5	Single-CNT	N/A	N/A	N/A	N/A	24	2021	[5]
6	Random oriented/aligned CNTs	from 170 to over 500 GHz	$< 32\Omega$	$C_{total} < 100fF$	350mV @ 50GHz & 1.5 V ( $P_m = -2$ dBm)	N/A	2022	Unpublished

Figure 1. Representative works on CNTs based RF rectifying devices, with such key performance parameters as cut-off frequency, series resistance and junction capacitance.

### Current and Future Challenges

RF energy harvesting technologies demand excellent performance on conversion efficiency, insertion loss (series resistance  $R_s$ ) and bandwidth (high-speed). CNTs possess excellent electrical properties such as ultrathin bodies that resulting in excellent electrostatic properties and leading to high conversion efficiency, high current-carrying capability (low series resistance) derived from the ballistic nature of transport and high carrier mobility and saturation velocity with ultrasmall intrinsic capacitance for high-speed and have been regarded as promising materials for RF energy harvesting. However, based on reported results in Figure 1, there remains large space for further performance improvement, and numerous challenges need to be solved to realize the complete potential of CNT RF harvesting technology. These include: (1) Material challenges. Wafer-scale high-quality aligned semiconducting CNTs arrays are required for RF energy harvesting with density of 200-300 CNTs/ $\mu m$  (over 300 CNTs/ $\mu m$  would suffer severe tube-tube shielding and crosstalk inducing performance degradation), mobility of more than  $2500 \text{ cm}^2 \text{ V}^{-1} \text{ s}^{-1}$  and a saturation velocity of up to  $3.5 \times 10^7 \text{ cm s}^{-1}$ . Additional material challenge is to develop methods for decoupling polymer residues from solution processed CNTs arrays while not introducing additional damages to the otherwise perfect CNT structure. (2) Device structure and process. For improving current carrying capability and lowering series resistance, the rectifying device channel length should be scaled down to less than one micron or even 100 nm to maximize quantum efficiency. In principle metal parasitic resistance could be reduced by adopting specially designed device structures, such as T-shape contact. The fabrication of extremely scaled CNT diodes with T-shape contact remains challenging for the commonly used planar fabrication approach, and more innovative approaches/architectures should be developed/adopted. (3) Circuits consideration. Energy harvesting applications require more than just rectifying devices (diodes). In addition to the regular half/full wave bridge rectifier, voltage multiplier for boosting output and filtering circuits are also required. However, these important circuits have not been demonstrated for CNT RF harvesting technology. Additional challenges include improvements on the uniformity of the tube-to-tube pitch, direction, and diameter of CNTs on a larger scale (such as on an 8-inch wafer).

### Advances in Science and Technology to Meet Challenges

For material challenges, it is very important to design/select proper polymer molecules warping around CNTs for sorting and alignment procedure. Selection of polymer with fewer alkyl chains and decreased

1  
2  
3 dispersion cycles would reduce scattering along the CNTs in the channel and improve CNT quality, leading  
4 to better mobility and saturation velocity. Degradable polymer would help for decoupling polymer from  
5 CNTs arrays with dedicated post treatment approach. Density of CNTs array could be improved by  
6 selection a pair of solution and polymer with stronger bonding force during self-alignment procedure.  
7 Further, cheaper and larger scale processes are needed for preparing better CNT materials for energy  
8 harvesting devices, i.e., monolayers or multilayers high-purity and high-density semiconducting CNTs with  
9 narrower diameter distribution, lower defect density and better-quality interfaces with both metallic  
10 contacts and high-k dielectric for better control and utilization of wasted RF power in air. For device  
11 structure and fabrication, parasitic effects derived from channel length scaling and the adoption of T-  
12 shape contact should be further reduced by, e.g. adopting innovative 3D integrated architecture [9]. For  
13 example, the two thick metal contacts of a diode could be fabricated separately into two adjacent layers  
14 to lower the parasitic effect of the conventional planar devices. Also, Inkjet technique may be utilized for  
15 low-cost fabrication of CNT devices. For circuits, due to the low power nature of harvested RF energy,  
16 extremely low-power processing and communication devices are required. To this end, CNT Dirac source  
17 devices technology [10], which demonstrated almost half of power consumption compared with that of  
18 14 nm node silicon devices, could be utilized for carbon nanotube RF rectifying devices. In principle, CNTs  
19 also have the advantages of being able to provide digital, radiofrequency and transducer components so  
20 that CNTs based energy harvesting modules could be integrated into more powerful systems by System-  
21 on-Chip (SoC) compatible processes with planar or even 3D architecture. It is worth noting that relevant  
22 advances on RF rectifying technologies are of multidisciplinary nature and could also be utilized in a range  
23 of important emerging applications, including wireless sensor networks (WSNs), Internet-of-Things (IoT),  
24 machine-to-machine (M2M) communications, smart skins/cities, medical monitoring and wearable  
25 electronics.  
26  
27  
28  
29  
30  
31  
32  
33  
34  
35  
36  
37  
38  
39  
40  
41  
42  
43  
44  
45  
46  
47  
48  
49  
50  
51  
52  
53  
54  
55  
56  
57  
58  
59  
60

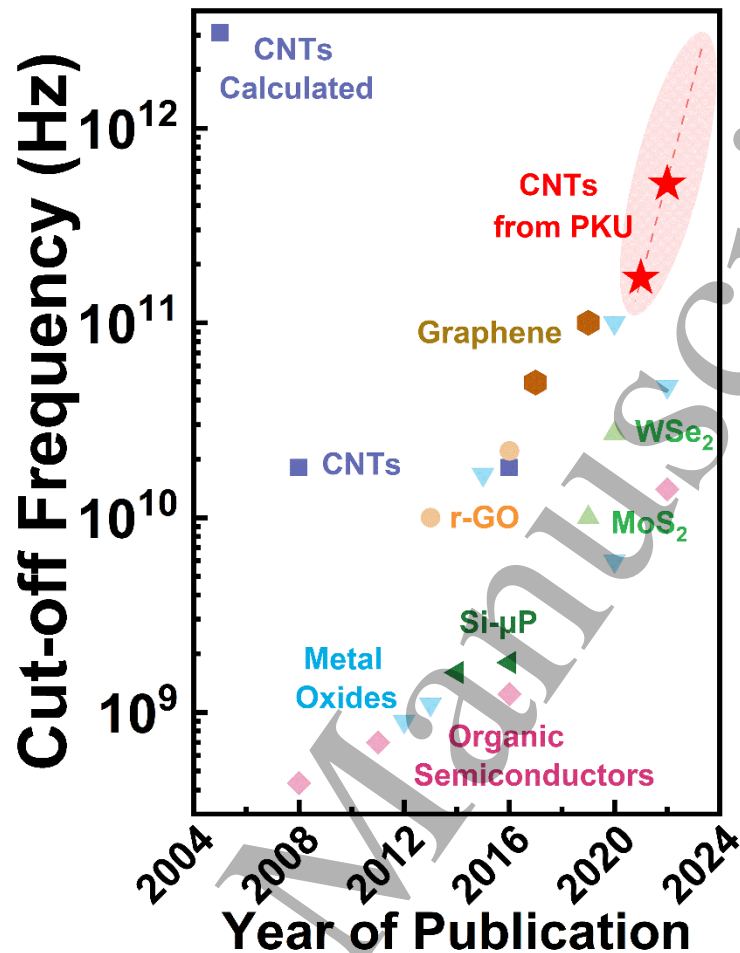


Figure 2. Benchmarking of the cut-off frequency of state-of-the-art rectifying devices based on CNTs and other materials, including metal oxides, two-dimensional materials, silicon particles and organic semiconductors.

### Concluding Remarks

While early work has demonstrated that CNT based rectifying devices are promising in providing necessary modules for constructing highly efficient energy harvesting systems, numerous challenges need to be solved before the technology could be deployed into commercial products. It is expected that milestone performance progress on CNTs based rectifying devices with low-cost and cut-off frequency surpassing 1 THz as shown in Figure 2, will be accomplished in the near future with advances in science and technology including cheaper and larger scale material preparation processes and utilization of innovative 3D integrated architecture with Dirac source devices technology for carbon nanotube RF energy harvesting. Furthermore, the integration of CNT RF rectifying devices, high-performance digital CMOS ICs and ultrasensitive sensors in 3D SoC architecture will not only provide energy harvesting function, but also more active and powerful chips for a range of important emerging applications, including 5G/6G, IoT and smart skins/cities.

### Acknowledgements

This work is supported in part by the National Science Foundation of China (Grant Nos. 62171004 and 61888102) and in part by National Key Research and Development Program under Grant 2022YFB4401602.

## References

- [1] H. M. Manohara, E. W. Wong, E. Schlecht, B. D. Hunt, and P. H. Siegel, "Carbon Nanotube Schottky Diodes Using Ti-Schottky and Pt-Ohmic Contacts for High Frequency Applications," *Nano Letters*, vol. 5, no. 7, pp. 1469–1474, May 2005, doi: 10.1021/nl050829h.
- [2] E. Cobas and M. S. Fuhrer, "Microwave rectification by a carbon nanotube Schottky diode," *Applied Physics Letters*, vol. 93, no. 4, p. 043120, Jul. 2008, doi: 10.1063/1.2939095.
- [3] E. D. Cobas, S. M. Anlage, and M. S. Fuhrer, "Single Carbon Nanotube Schottky Diode Microwave Rectifiers," *IEEE Transactions on Microwave Theory and Techniques*, vol. 59, no. 10, pp. 2726–2732, Oct. 2011, doi: 10.1109/tmtt.2011.2164548.
- [4] C. Biswas, S. Y. Lee, T. H. Ly, A. Ghosh, Q. N. Dang, and Y. H. Lee, "Chemically Doped Random Network Carbon Nanotube p-n Junction Diode for Rectifier," *ACS Nano*, vol. 5, no. 12, pp. 9817–9823, Nov. 2011, doi: 10.1021/nn203391h.
- [5] Y. Feng, H. Li, T. Inoue, S. Chiashi, S. V. Rotkin, R. Xiang, and S. Maruyama, "One-Dimensional van der Waals Heterojunction Diode," *ACS Nano*, vol. 15, no. 3, pp. 5600–5609, Mar. 2021, doi: 10.1021/acsnano.1c00657.
- [6] S. Wang, Z. Zhang, L. Ding, X. Liang, J. Shen, H. Xu, Q. Chen, R. Cui, Y. Li, and L.-M. Peng, "A Doping-Free Carbon Nanotube CMOS Inverter-Based Bipolar Diode and Ambipolar Transistor," *Advanced Materials*, vol. 20, no. 17, pp. 3258–3262, Sep. 2008, doi: 10.1002/adma.200703210.
- [7] L. Liu, J. Han, L. Xu, J. Zhou, C. Zhao, S. Ding, H. Shi, M. Xiao, L. Ding, Z. Ma, C. Jin, Z. Zhang, and L.-M. Peng, "Aligned, high-density semiconducting carbon nanotube arrays for high-performance electronics," *Science*, vol. 368, no. 6493, pp. 850–856, May 2020, doi: 10.1126/science.aba5980.
- [8] H. Shi, L. Ding, D. Zhong, J. Han, L. Liu, L. Xu, P. Sun, H. Wang, J. Zhou, L. Fang, Z. Zhang, and L.-M. Peng, "Radiofrequency transistors based on aligned carbon nanotube arrays," *Nature Electronics*, vol. 4, no. 6, pp. 405–415, Jun. 2021, doi: 10.1038/s41928-021-00594-w.
- [9] M. M. Shulaker, G. Hills, R. S. Park, R. T. Howe, K. Saraswat, H.-S. P. Wong, and S. Mitra, "Three-dimensional integration of nanotechnologies for computing and data storage on a single chip," *Nature*, vol. 547, no. 7661, pp. 74–78, Jul. 2017, doi: 10.1038/nature22994.
- [10] C. Qiu, F. Liu, L. Xu, B. Deng, M. Xiao, J. Si, L. Lin, Z. Zhang, J. Wang, H. Guo, H. Peng, and L.-M. Peng, "Dirac-source field-effect transistors as energy-efficient, high-performance electronic switches," *Science*, vol. 361, no. 6400, pp. 387–392, Jun. 2018, doi: 10.1126/science.aap9195.

## 6.5 2D Materials for radiofrequency energy harvesting

Zhenxing Wang<sup>1</sup>, Muh-Dey Wei<sup>2</sup>, Renato Negra<sup>2</sup>, Max C. Lemme<sup>1,3</sup>

<sup>1</sup>AMO GmbH, Otto-Blumenthal-Str. 25, 52074 Aachen, Germany;

<sup>2</sup>Chair of High Frequency Electronics, RWTH Aachen University, Kopernikusstr. 16, 52074 Aachen, Germany

<sup>3</sup>Chair of Electronic Devices, RWTH Aachen University, Otto-Blumenthal-Str. 2, 52074 Aachen, Germany

### Status

2D materials, such as graphene and transition metal dichalcogenides (TMDCs), are considered for semiconductor technology applications due to their extraordinary electrical, optical, thermal and mechanical properties [1]. Specifically for the application in energy harvesting there are different approaches such as photovoltaic cells, thermoelectric energy harvesting, piezoelectric energy harvesting, rectifying antenna (rectenna-)based RF energy harvesting [2]. Here, we will focus on the rectenna-based approach, since the rest have been discussed in detail in [2].

A rectenna is typically composed of a nonlinear device like a diode and an antenna to harvest energy from electromagnetic radiation. The antenna receives an electromagnetic wave in free space, which is then converted to a DC voltage by the nonlinear device. There are many advantages in using 2D materials such as graphene or TMDCs for such energy harvesting systems. Firstly, the high mobility of graphene is crucial to enable operation at THz frequencies or even optical frequency [3]. Secondly, graphene can be used to realize antennas with smaller dimensions compared to metals, which is relevant for the high-density integration of such systems [4]. In addition, the Fermi energy in graphene can be controlled by an electric field, which enables the tunability of the antenna oscillation frequency [4]. Last but not least, the high mechanical strength and flexibility of 2D materials, combined with a thin-film technology that allows processing them on arbitrary substrates, largely expands the application field of graphene diodes and antennas for wearable electronics compared to canonical semiconductor devices.

For example, a flexible rectenna system has been realized for Wi-Fi band wireless energy harvesting based on MoS<sub>2</sub> material. The core of this device is a Schottky diode based on a MoS<sub>2</sub> phase heterojunction, which operates up to 12 GHz, covering most of the unlicensed industrial, scientific and medical radio bands, including the bands for Wi-Fi. [5] At higher frequencies, graphene has been utilized for energy harvesting at frequencies up to 170 GHz, employing metal-insulator-graphene (MIG) diodes, [6] and up to 28 THz based on geometrical graphene diodes. [7]

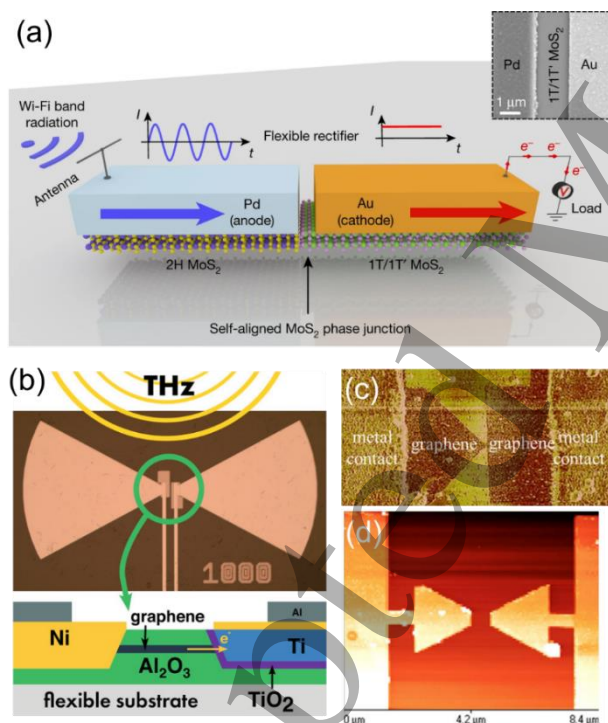


**Figure 1.** 2D materials-based energy harvesters for electromagnetic radiation. (a) MoS<sub>2</sub>-based heterojunction for energy harvesting at Wi-Fi frequencies. Permission of Reprint [5]. (b) Metal-insulator-graphene diode-based rectenna for energy harvesting up to 170 GHz. Permission of Reprint [6]. (c) (d) Graphene geometrical diode-based rectennas for energy harvesting at 28 THz. AFM image of the diode (c) and the antenna (d). Permission of Reprint [7].

### Current and Future Challenges

Several key challenges currently prevent the application of RF energy harvesting with 2D materials. Firstly, the operation frequency of the rectenna system is limited by the  $RC$  time constant, where  $R$  is the series resistance of the rectenna, and  $C$  is the parasitic capacitance. The sheet resistance of 2D materials



is typically much higher compared to bulk materials [8]. In addition, the electric contacts to 2D materials also contribute considerably to the total resistance due to the van-der-Waals bonds between the metals and the 2D materials [8]. These two components of  $R$  limit the operation frequency of the system. When it comes to the parasitic capacitance,  $C$ , 2D materials have a clear advantage over other materials. For example, in the MIG diode configuration shown in Figure 1b, the parasitic capacitance can be largely reduced due to the 1-dimensional junction. In a geometrical diode like shown in Figure 1c, the parasitic capacitance is largely reduced since there is no dielectric involved in the operation of such diodes, although the resistance is a limiting factor due to the small dimension of the junction. These aspects must be considered when designing a rectenna for high frequency operation.

Secondly, the efficiency of the energy harvesting is limited by several factors. These include, but are not limited to, the absorption efficiency of the antenna, the impedance matching between the antenna and the diode and the power consumption of the electronic circuits that manage the power between the energy harvesting unit and the functional unit, e.g. the communication circuits.

Thirdly, the 2D material growth needs to be scaled up and become manufacturable, i.e the quality, repeatability and reliability of the process technology must meet semiconductor industry standards. This is a prerequisite for 2D energy harvesting systems to achieve the desired functionality, because semiconductor technology provides a mature platform, especially in terms of electronics [8]. Although this aspect can be considered an engineering issue, it is still rather challenging and will require substantial resources.

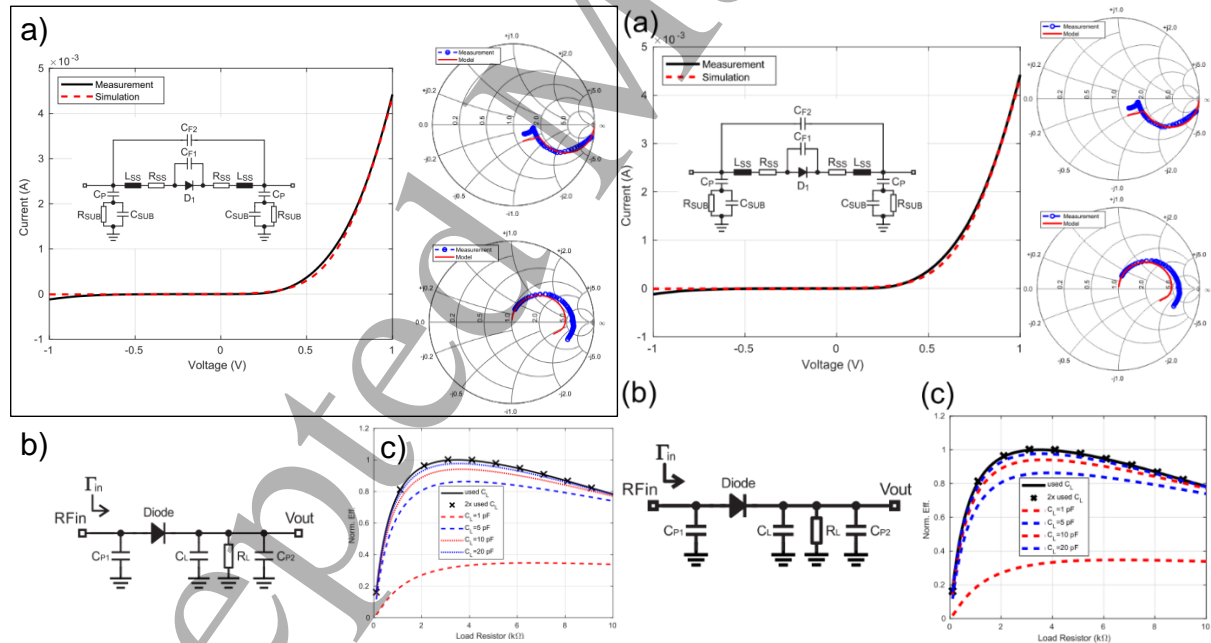


**Figure 2.** (a) Large-signal model for a metal-insulator-graphene diode and corresponding Smith charts. (b) Schematic of a fully integrated rectifier on a flexible polyimide substrate. (c) Design optimisation based on the model. Permission of Reprint [10]

### Advances in Science and Technology to Meet Challenges

This section describes further research and development required to meet the current challenges.

Firstly, the quality of the 2D materials grown by scalable methods such as chemical vapour deposition or epitaxy needs to be further improved to realize the lowest possible sheet resistance. Here, the availability

of large-scale material is a significant point to address high-volume production. The material should be ideally single-crystalline material over entire wafers to enable ballistic transport at room temperature, which is especially relevant for the geometrical graphene diodes shown in Figures 1c and 1d. MIG diodes may have lower quality requirements and may tolerate uniform polycrystalline material with relatively high room temperature mobility. Similarly, a scalable approach is needed to provide low contact resistances between the metals and the 2D materials, a challenge that has recently seen promising progress. [9] These efforts will lead to increasing the operation frequency of 2D rectennas.

Secondly, to design and optimize the input matching networks as well as the output load networks for rectifiers, a precise large-signal RF/microwave model is necessary [10] (Figure 2a). A fully integrated rectifier with a suitable load impedance ( $C_L$  and  $R_L$ ) is as critical as the input matching network (Figure 2b). Such a model can then be used to optimize the load versus efficiency (Figure 2c). This example indicates that an accurate large-signal model is essential to obtain high efficiency. Once, such a value chain is implemented, full integration is needed to realize rectifier arrays to boost output energy.

Lastly, device and circuit fabrication have to be scaled up to enable the integration into existing semiconductor platforms. Currently, the 2D Experimental Pilot Line (2D-EPL), a project funded by the European Commission, focusses efforts on solving issues with relevant process steps, such as 2D layer growth and transfer, electrical contacts, active area patterning, passivation and process chemistry. If successful, this endeavour can pave the way towards reliable semiconductor manufacturing of 2D materials and circuits.

### Concluding Remarks

2D materials are promising candidates for energy harvesting devices, especially for wearable systems due to their mechanical flexibility. In this section we focused on rectennas for electromagnetic radiation harvesting. Graphene-based devices, in particular, have been shown to rectify signals up to THz frequencies. However, minimizing parasitic RC components will be required to maximize the efficiency of the energy harvesting systems. Wafer-scale fabrication in existing semiconductor platforms is a serious engineering problem but probably not a basic scientific roadblock. There are ample examples in literature that indicate that a technology based on 2D materials can play a unique role for future (wearable) electronic systems.

### Acknowledgements

The authors acknowledge funding from the European Union's Horizon 2020 research and innovation programme under grant agreements No. 101006963 (GreEnergy), 952792 (2D-EPL), 881603 (Graphene Flagship Core 3), 863337 (WiPLASH), and funding from the German Research Foundation (DFG) under project No. 391996624 (HiPeDi), 407080863 (MOSTFLEX), 273177991 (GLECS2).

### References

- [1] M.C. Lemme, D. Akinwande, C. Huyghebaert, C. Stampfer, "2D Materials for Future Heterogeneous Electronics", *Nature Communications*, 13, 1392, 2022.
- [2] M. H. Lee, and W. Wu, "2D Materials for Wearable Energy Harvesting", *Adv. Mater. Technol.*, 2101623, 2022.
- [3] Z. Wang, A. Hemmetter, B. Uzlu, M. Saeed, A. Hamed, S. Kataria, R. Negra, D. Neumaier, and M. C. Lemme. "Graphene in 2D/3D Heterostructure Diodes for High Performance Electronics and Optoelectronics", *Adv. Electron. Mater.*, 7, 2001210, 2021.
- [4] S. Abadal, R. Guirado, H. Taghvaei, A. Jain, E. Pereira de Santana, P. Haring Bolívar, M. Saeed, R. Negra, Z. Wang, K.-T. Wang, M. C. Lemme, J. Klein, M. Zapater, A. Levisse, D. Atienza, D. Rossi, F. Conti, M. Dazzi,

1  
2  
3 G. Karunaratne, I. Boybat, and A. Sebastian, "Graphene-based Wireless Agile Interconnects for Massive  
4 Heterogeneous Multi-chip Processors", arXiv:2011.04107.

5 [5] X. Zhang, J. Grajal, J. L. Vazquez-Roy, U. Radhakrishna, X. Wang, W. Chern, L. Zhou, Y. Lin, P.-C. Shen,  
6 X. Ji, X. Ling, A. Zubair, Y. Zhang, H. Wang, M. Dubey, J. Kong, M. Dresselhaus, and T. Palacios, "Two-  
7 dimensional MoS<sub>2</sub>-enabled flexible rectenna for Wi-Fi-band wireless energy harvesting", *Nature*, 566, 368,  
8 2019.

9 [6] A. Hemmetter, X. Yang, Z. Wang, M. Otto, B. Uzlu, M. Andree, U. Pfeiffer, A. Vorobiev, J. Stake, M. C.  
10 Lemme, and D. Neumaier, "Terahertz Rectennas on Flexible Substrates Based on One-Dimensional Metal-  
11 Insulator-Graphene Diodes", *ACS Appl. Electron. Mater.*, 3, 3747, 2021.

12 [7] Z. Zhu, S. Joshi, S. Grover, and G. Moddel, "Graphene geometric diodes for terahertz rectennas", *J.*  
13 *Phys. D: Appl. Phys.*, 46 185101, 2013.

14 [8] D. Neumaier, S. Pindl, M, C. Lemme, "Integrating graphene into semiconductor fabrication lines", *Nat.*  
15 *Mater.*, 18, 525, 2019.

16 [9] P.-C. Shen et al., "Ultralow contact resistance between semimetal and monolayer semiconductors,"  
17 *Nature*, 593, 7858, 2021.

18 [10] C. -Y. Fan, M. -D. Wei, B. Uzlu, Z. Wang, D. Neumaier, and R. Negra, "Fully Integrated 2.4-GHz Flexible  
19 Rectifier Using Chemical-Vapor-Deposition Graphene MMIC Process", *IEEE Trans. Electron Devices*, 68,  
20 1326, 2021.

## 21 22 23 24 25 26 **6.6 Materials for rectennas and radiofrequency energy harvesters**

27 Mahmoud Wagih<sup>1, 2</sup> and Steve Beeby<sup>2</sup>

28 <sup>1</sup>James Watt School of Engineering, University of Glasgow, Glasgow G12 8QQ, UK

29 <sup>2</sup>School of Electronics and Computer Science, University of Southampton, Southampton SO17 1BJ, UK

### 30 31 **Status**

32 Rectennas were first conceived in the 1960s for powering Unmanned Aerial Vehicles (UAVs), with over  
33 100 W being received by a UAV rectenna array over five metres indicating that microwave power beaming  
34 can enable battery-less systems. Given the importance of mass in UAVs and in applications in microwave  
35 solar power beaming envisaged later, the first material challenge was realizing lightweight rectenna arrays  
36 that minimised the vehicle's payload [1]. The research then moved to mmWave frequencies to enable  
37 antenna miniaturization in both terrestrial and space, given the shorter wavelength which enables more  
38 directional antennas [2].

39  
40  
41 Nowadays, there is renewed interest in rectennas following the rise of energy harvesting as a method of  
42 powering the growing IoT. Rectennas can recycle ambient RF emissions from cellular networks [3], as well  
43 as receive microwatt-level power 'packets' in RF-powered networks. Rectennas are distinguishable from  
44 energy harvesters requiring smart materials such as piezoelectric and thermoelectric harvesters;  
45 rectennas only rely on conductors, for the antenna, and semiconductors, for the rectifiers; both are found  
46 in most electronic systems. With advances in "large-area electronics" including flexible, printed, and  
47 textile-based conductors, rectennas can be utilized in new application domains, where other energy  
48 harvesters might be impractical or inappropriate. From an RF design perspective, this imposes new  
49 challenges, where cost and size are the major constraints, implying a potential trade-off between optimal  
50 RF performance and material choice.

51  
52  
53  
54  
55  
56  
57  
58  
59  
60

### Current and Future Challenges

For rectennas to replace, or augment, batteries, their power harvesting (converting radiation to guided waves) and power conversion (from RF to DC) efficiencies need to be improved. This has been the main research challenge in the context of RF energy harvesting [3] and is often limited by conductive and dielectric material losses. Therefore, passive RF components, such as a rectenna's matching network and antennas, are often implemented on low-loss materials. Additional challenges arise from the electromagnetic medium surrounding the rectennas, where rectennas cannot be considered in isolation of the materials in their environment. Antennas are affected, for example, by operating near high-permittivity or lossy (low-resistivity) materials including biological tissue [4], moisture absorbing materials, or reflective surroundings.

The traditional route of implementing rectennas on low-loss materials can compromise other requirements. The key electrical and mechanical requirements, which represent ongoing research challenges can be summarized as:

1. Rectenna conductors maintaining a low sheet resistance, at RF, to reduce conductive losses in the antenna and any rectifier impedance matching network.
2. The rectenna being limited to geometrical features which can be resolved using low-cost and scalable fabrication processes such as additive manufacturing.
3. Fabrication processes enabling the integration of packaged or unpackaged devices, e.g. Schottky diodes or monolithic CMOS ICs, for different rectifier topologies.
4. The conductors, and any encapsulating dielectrics, exhibiting suitable mechanical properties for applications such as flexible, wearable, implantable, or spaceborne rectennas.
5. Ultimately, the rectennas must be able to maintain their RF performance in their deployment environment, for example without the antennas detuning or suffering from absorption.

### Advances in Science and Technology to Meet Challenges

Rectennas have been successfully demonstrated across the breadth of IoT applications utilising flexible conductors, textiles, Laser-induced Graphene (LiG), biodegradable metals (Mg), and ultra-thin liquid metals, as shown in Figure 1. Transitioning to such materials, which often have sub-optimal RF properties, cannot be simply achieved by copying existing rectenna designs.



1  
2  
3 Figure 1. The evolution of large-area rectennas: (a) the earliest metal/air light-weight rectenna [1] (CC-BY); (b)  
4 flexible beamforming mmWave "5G" rectenna on LCP [5] (CC-BY); broadband copper-on-textile wearable mmWave  
5 rectenna [6]; (d) fully-textile information and power transfer rectenna [8] (CC-BY); (e) LiG rectenna on rubber [9]  
6 (©Elsevier, reprinted with permission); (f) bioresorbable Mg rectenna [10]; (g) stretchable and tissue-adhesive liquid  
7 metal resonator [4] (©John Wiley And Sons, reprinted with permission).  
8

9  
10 Material-induced losses can be minimized through effective rectenna design. For example, by designing  
11 the antennas to directly match a rectifier or IC's input impedance, a separate matching network stage can  
12 be eliminated reducing the additional insertion losses in planar transmission lines or lumped components  
13 [7, 8]. This antenna-circuit co-design approach has enabled a pervasive technology such as RFID; RFID tags  
14 are a rectenna with the rectifier monolithically integrated within the IC. Recently, rectennas were  
15 integrated within the aperture of communication antennas, enabling miniaturized systems that can  
16 simultaneously receive power and information without compromising the RF performance of either the  
17 communication or energy harvesting [8]. Effective RF and mechanical co-design has also be used to  
18 improve the resilience of rectennas. For example, a meandered structure can negate the effects of strain  
19 on the performance of a LiG-on-rubber rectenna [9]. The use of liquid metals and other highly deformable  
20 ultra-thin materials could enable rectennas to be utilized in implants and other challenging environments  
21 [4].  
22  
23

24 As low-cost IoT rectennas move towards the mmWave "beyond 5G" spectrum (>24 GHz), new designs  
25 have evolved to overcome material and channel losses [2]. For instance, beamforming rectenna arrays  
26 can be used to achieve wide angular coverage and high gain [5], whereas broadband antennas  
27 miniaturized-radiator could be used to overcome dielectric losses on lossy or biodegradable substrates  
28 including textiles and paper [6]. Metamaterials and quasi-wireless transmission lines are expected to play  
29 a role in "engineering" the environment surrounding rectennas, enabling higher efficiency than near-  
30 omnidirectional radiation [11].  
31  
32

### 33 **Concluding Remarks**

34 Rectennas can be, and have been, realized using virtually any conductive material, making them a strong  
35 candidate for most power-autonomous systems. Future rectennas will be realized using hybrid integration  
36 of different platforms such as large-area passive circuits, monolithic ICs, and novel semiconductors.  
37 Optimal rectenna design for overcoming material losses is expected to be an ongoing research challenge,  
38 as new biodegradable, flexible, and large-area electronic devices are developed.  
39  
40

### 41 **Acknowledgements**

42 M. Wagih was supported by the UK Royal Academy of Engineering and the Office of the Chief Science  
43 Adviser for National Security under the UK Intelligence Community Post-Doctoral Research Fellowship  
44 programme. S. Beeby was supported by the UK Royal Academy of Engineering under the Chairs in  
45 Emerging Technologies scheme.  
46

### 47 **References**

- 48 1. Christopher T. Rodenbeck, Paul I. Jaffe, Bernd H. Strassner II, Paul E. Hausgen, James O.  
49 McSpadden, Hooman Kazemi, Naoki Shinohara, Brian B. Tierney, Christopher B. DePuma and  
50 Amanda P. Self "Microwave and Millimeter Wave Power Beaming," in *IEEE Journal of Microwaves*,  
51 vol. 1, no. 1, pp. 229-259, Jan. 2021, doi: 10.1109/JMW.2020.3033992.
- 52 2. M. Wagih, A. S. Weddell and S. Beeby, "Millimeter-Wave Power Harvesting: A Review," in *IEEE*  
53 *Open Journal of Antennas and Propagation*, vol. 1, pp. 560-578, 2020, doi:  
54 10.1109/OJAP.2020.3028220.  
55  
56  
57  
58  
59  
60

3. X. Gu, S. Hemour and K. Wu, "Far-Field Wireless Power Harvesting: Nonlinear Modeling, Rectenna Design, and Emerging Applications," in *Proceedings of the IEEE*, vol. 110, no. 1, pp. 56-73, Jan. 2022, doi: 10.1109/JPROC.2021.3127930.
4. Yamagishi, K., Zhou, W., Ching, T., Huang, S. Y., Hashimoto, M., Ultra-Deformable and Tissue-Adhesive Liquid Metal Antennas with High Wireless Powering Efficiency. *Adv. Mater.* 2021, 33, 2008062. <https://doi.org/10.1002/adma.202008062>
5. Eid, A., Hester, J.G.D., and Tentzeris, M.M. "5G as a wireless power grid," *Scientific Reports* 11, 636 (2021). Doi: 10.1038/s41598-020-79500-x
6. M. Wagih, G. S. Hilton, A. S. Weddell and S. Beeby, "Broadband Millimeter-Wave Textile-Based Flexible Rectenna for Wearable Energy Harvesting," in *IEEE Transactions on Microwave Theory and Techniques*, vol. 68, no. 11, pp. 4960-4972, Nov. 2020, doi: 10.1109/TMTT.2020.3018735.
7. M. Wagih, A. S. Weddell and S. Beeby, "Rectennas for Radio-Frequency Energy Harvesting and Wireless Power Transfer: A Review of Antenna Design [Antenna Applications Corner]," in *IEEE Antennas and Propagation Magazine*, vol. 62, no. 5, pp. 95-107, Oct. 2020, doi: 10.1109/MAP.2020.3012872.
8. M. Wagih, G. S. Hilton, A. S. Weddell and S. Beeby, "Dual-Polarized Wearable Antenna/Rectenna for Full-Duplex and MIMO Simultaneous Wireless Information and Power Transfer (SWIPT)," in *IEEE Open Journal of Antennas and Propagation*, vol. 2, pp. 844-857, 2021, doi: 10.1109/OJAP.2021.3098939.
9. Jia Zhu, Zhihui Hu, Chaoyun Song, Ning Yi, Zhaozheng Yu, Zhendong Liu, Shangbin Liu, Mengjun Wang, Michael Gregory Dexheimer, Jian Yang and Huanyu Cheng, "Stretchable wideband dipole antennas and rectennas for RF energy harvesting," in *Materials Today Physics*, Vol. 18, 2021, doi: 10.1016/j.mtphys.2021.100377.
10. Hwang, S.-W., et al. "Materials for Bioresorbable Radio Frequency Electronics." *Adv. Mater.*, Vol. 25, pp. 3526-3531, 2013, doi: 10.1002/adma.201300920
11. Tian, X., Lee, P.M., Tan, Y.J. *et al.* Wireless body sensor networks based on metamaterial textiles. *Nat Electron* 2, 243–251 (2019). <https://doi.org/10.1038/s41928-019-0257-7>



## 7 Sustainability Considerations on Energy Harvesting Materials Research

T. Ibn-Mohammed,<sup>1</sup> K.B. Mustapha<sup>2</sup> and A.P. Joshi<sup>1</sup>

<sup>1</sup>Warwick Manufacturing Group (WVG), The University of Warwick, Coventry, CV4 7AL, UK

<sup>2</sup>Departments of Mechanical, Materials and Manufacturing Engineering, University of Nottingham (Malaysia Campus), Semenyih 43500, Selangor, Malaysia

### The significance of sustainability in energy harvesting materials research

Remote wireless sensor network (WSN), untethered devices associated with the internet of things (IoT), self-powered wearable gadgets, and a host of other high-performance low-power microelectronics are central to the progress of connected cars, smart homes, smart factories, futuristic smart cities, large-scale embedded automation, and monitoring of critical infrastructure in dangerous/harsh/isolated environment. A crucial factor to consider for the operation of these devices is the power requirement. A cornerstone of the current source of power for most of these devices comprises various kinds of batteries, which may be in the form of either: (i) a primary battery, which is non-rechargeable and inherently beset by environmentally disastrous disposal problems; or (ii) a secondary battery which is rechargeable but plagued by cumbersome dismounting, recharging, and mounting routine. No doubt, several notable revolutionary signs of progress have been reported about battery technology in recent years [1].

Despite this, as we inch closer to the possibility of a “Trillion Sensor Universe” and the prediction of a spike in uptake of IoT-connected devices reaching tens of billions by 2023, valid concerns have been expressed about the cost and reliability of batteries. Besides, with the projected increase in sensors and IoT-connected devices, the cumulative public health and sustainability issues around the production, disposal, and recharging of zillions of batteries to power these devices have rightly ignited interest in scavenging low-profile, wasted energy through energy harvesting devices. Matured technologies in this regard include photovoltaic and wind energy harvester systems, both of which have received a preponderant of attention due to their higher power densities for macroscale power generations. However, waves of significant development in recent years have enabled the growth of low-amplitude power harvesting schemes [2]. Broadly, this includes: (i) harvesting of thermal gradients with thermoelectric generators; (ii) kinetic harvesting from mechanical movement through piezoelectric/triboelectric/magnetolectric effects; and (iii) harvesting of ambient radio/electromagnetic wave/acoustic energy, among others.

Collectively, the above-mentioned energy harvesting systems have been recognized as essential to the achievement of the Sustainable Development Goal (Goal 7: “Ensure access to affordable, reliable, sustainable and modern energy for all”). Fundamentally, the practical implementation of the energy harvesting scheme is tightly bound to rigorous materials research, regardless of the conversion technology category. Correspondingly, a huge volume of work has been dedicated to the investigation of the functional performance of the attendant materials [3]. For instance, high performing photovoltaic solar cells, thermoelectric materials with high electrical conductivity and Seebeck coefficient and low thermal conductivity, kinetic and thermal energy harvesting materials. On the other hand, as these devices move from laboratory-based proof-of-concept to actual applications, the sustainability of materials, which has been much so far overlooked, must be pursued.

### LCA case studies of energy harvesting materials technologies.

In this section, four life cycle assessment (LCA) example case studies that have identified environmental sustainability hotspots in energy harvesting materials technologies including perovskite solar cells

(photovoltaics), piezoelectric, triboelectric, and thermoelectric are discussed. LCA is a computational technique for assessing the potential environmental impacts associated with a product across its entire supply chain and it involves four main steps including (i) goal and scope definition, (ii) inventory analysis, (iii) lifecycle impact assessment, and (iv) interpretation [4]. It is science-based, but not free from subjective judgement, covering a broad spectrum of environmental impacts to avoid burden shift from one aspect to another. Figure 1 provides a system boundary illustration for the comparative lifecycle analysis of non-oxide vs. oxide-based thermoelectric modules.

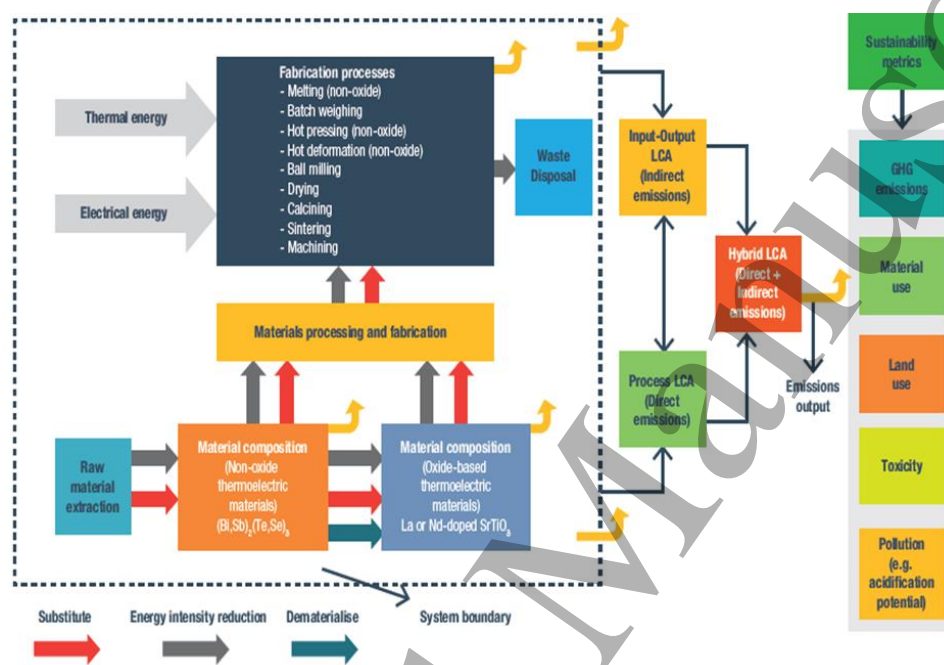


Figure 1: System boundary defined for the LCA of two thermoelectric modules.

Several types of novel solar photovoltaic materials including organic, dye sensitized, colloidal quantum dot, and perovskite solar cells (PSCs) have emerged in recent years and have been touted to be economically and environmentally viable option to traditional silicon-based technology. To verify this assertion, several comparative LCA studies have been conducted. Gong et al. presented the environmental impacts of two PSC types across sixteen impact categories in comparison to other photovoltaic types concluding that not only the PSC demonstrated environmental edge, but they also possess ultra-low energy payback period [5]. This reduced energy payback period is attributed to a reduction in the energy intensive processes required for PSC manufacturing due to the elimination of silicon and rare earth element processing. Nonetheless, the use of gold in the material architecture of PSC caused significant environmental impact due to the enormous energy required for its production from its ore. In the context of ambient energy harvesting for IoT applications, more LCA work is required.

Due to its toxicity, global policy initiatives and legislation, such as the Waste Electrical and Electronic Equipment (WEEE) and Restriction of Hazardous Substance (RoHS), have called for the prohibition of lead in piezoelectric materials. This has reinvigorated the race to develop lead-free alternatives based on potassium sodium niobate (KNN) and sodium bismuth titanate (NBT) for lead zirconate titanate (PZT). To ascertain the environmental benefits of lead-free alternatives over lead-based ones, Ibn-Mohammed et al. adopted LCA to establish the fact that KNN is environmentally worse than PZT with respect to climate

change and eco-toxicity due to the presence of the niobium pentoxide whose mining and milling, through hydro- and pyro-metallurgical processing, for refining niobium has substantial adverse impacts across numerous environmental indicators [6]. The same authors in another paper [7] highlighted that the lower energy consumed by NBT during synthesis yielded a lower overall environmental profile, based on primary energy consumption and toxicological impact, in comparison to PZT and KNN, Figure 2. Nonetheless, the authors noted that bismuth and its oxide constitute by-product of lead smelting, and when NBT is compared with PZT, it was shown that across several key indicators, bismuth oxide has higher environmental impact compared to lead oxide, because of the additional processing and refining steps which pose extra challenges in metallurgical recovery.

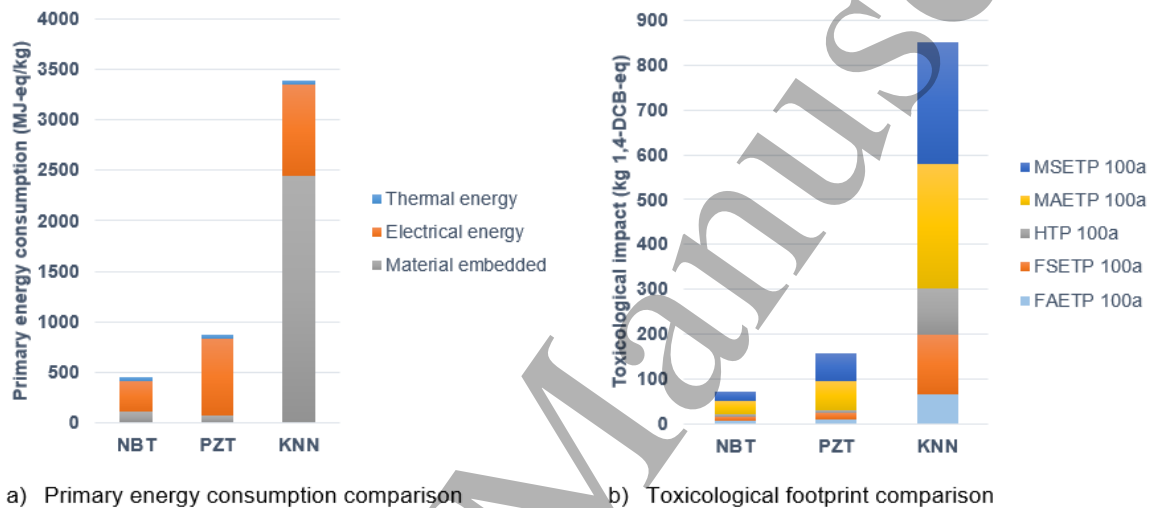


Figure 2: Comparative environmental profile of PZT vs KNN and NBT piezoelectric functional ceramics.

Triboelectric nanogenerators (TEGs) offer the potential to generate energy in self-powered devices at low cost but their environmental impact was unknown until Ahmed et al conducted the LCA and techno-economic analysis of two TENG modules [8]. Module A, a thin-film-based micro-grating TENG, with its electrode arrays arranged linearly generates enough energy to power standard electronics and Module B, which uses a planar structure based on electrodes generating periodically charged triboelectric potential, yielding energy from water and air flow and bodily movement. Their results reveal that compared to Module B, Module A presents a better environmental profile, lower production costs, lower CO<sub>2</sub> emissions and shorter energy payback period (EPBP). Module B's higher environmental impact is due to its higher content of acrylic in its structure and higher electrical energy requirements during fabrication. Acrylic can however be recycled or reused at the end-of-life stage releasing no toxic gases during combustion, thus improving its overall profile. Nonetheless, when compared with emerging solar PV materials technologies, TENG modules offer better environmental profile and shorter EPBP, although Module B is marginally higher than that of a PV technology based on perovskite structured methyl ammonium lead iodide. Future works on TENG pertains to lifetime and efficiency improvements rather than the identification of cheaper materials and manufacturing processes. Although EPBP was employed as a figure of merit in this analysis, this may not be the best for ambient energy harvesting applications. This is because the embodied energy (i.e., the emissions across the entire value chains) of ambient energy harvesters can be potentially high. As such, a better figure of merit would be the net environmental gain, which is a function of how the embodied energy compares with the operational energy saved over their lifetime as well as the energy that would otherwise be required if, for instance, batteries were employed as the power source. This

aspect, however, has yet to be assessed in a systematic way, which demands further investigations across the various energy harvesting technologies.

Thermoelectric materials constitute the main element of thermoelectric generators, enabling the conversion of waste heat into electricity. Due to the presence of heavy metals and rare-earth elements in the constituent materials, attention has been paid to their toxicity, with less work focusing on their supply-chain environmental profile. However, Soleimani et al. conducted a comparative lifecycle impacts of inorganic, organic and hybrid thermoelectric materials at their production stage, across multiple environmental indicators namely resource consumption, emission, waste, primary energy demand, and global warming potential [9]. The authors concluded that the inorganic type yielded significantly higher environmental impacts in comparison to the other two due to the energy-intensive nature of their manufacturing processes.  $\text{Bi}_2\text{Te}_3$  was identified as the only inorganic exception whose environmental impact was the lowest compared to all the thermoelectric materials studied. For organic and hybrid types, issues pertaining to raw material supply risks was identified as the main sustainability issue.

### **Challenges and outlook in assessing sustainability of energy harvesting materials**

Charting the path toward sustainability of energy harvesting materials is not straightforward. One reason for this is due to the diversity of components such as transducers, power management and energy storage making up the harvesters. To underscore this, in grappling with the challenge of sustainability of energy harvesting materials, a major challenge is a difficulty in synthesizing materials that are simultaneously efficient for maximum energy conversion and environmentally benign [10]. In cases where such materials are needed, the sustainability of the manufacturing route is not guaranteed. Nonetheless, concerns about the “health” of our planet necessitate an evaluation of the environmental profile of energy harvesting materials and technologies at the design or pilot stage before expensive investments and resources are committed. Such evaluations, when conducted in a manner that anticipates foreseeable deleterious consequences whilst identifying opportunities for improvement and mitigation strategies, can aid the communication of key findings to materials developers and policymakers.

### **References**

- [1] M. Titirici, “Sustainable Batteries—Quo Vadis?,” *Advanced Energy Materials*, vol. 11, no. 10, p. 2003700, Mar. 2021, doi: 10.1002/aenm.202003700.
- [2] H. Akinaga, “Recent advances and future prospects in energy harvesting technologies,” *Japanese Journal of Applied Physics*, vol. 59, no. 11, p. 110201, Nov. 2020, doi: 10.35848/1347-4065/abbfa0.
- [3] K. Calautit, D. S. N. M. Nasir, and B. R. Hughes, “Low power energy harvesting systems: State of the art and future challenges,” *Renewable and Sustainable Energy Reviews*, vol. 147, p. 111230, Sep. 2021, doi: 10.1016/j.rser.2021.111230.
- [4] S. Hellweg and L. Milà i Canals, “Emerging approaches, challenges and opportunities in life cycle assessment,” *Science (1979)*, vol. 344, no. 6188, pp. 1109–1113, Jun. 2014, doi: 10.1126/science.1248361.
- [5] J. Gong, S. B. Darling, and F. You, “Perovskite photovoltaics: life-cycle assessment of energy and environmental impacts,” *Energy & Environmental Science*, vol. 8, no. 7, pp. 1953–1968, 2015, doi: 10.1039/C5EE00615E.
- [6] T. Ibn-Mohammed *et al.*, “Integrated hybrid life cycle assessment and supply chain environmental profile evaluations of lead-based (lead zirconate titanate) versus lead-free (potassium

1  
2  
3 sodium niobate) piezoelectric ceramics,” *Energy & Environmental Science*, vol. 9, no. 11, pp. 3495–3520,  
4 2016, doi: 10.1039/C6EE02429G.  
5

6 [7] T. Ibn-Mohammed *et al.*, “Life cycle assessment and environmental profile evaluation of lead-  
7 free piezoelectrics in comparison with lead zirconate titanate,” *J Eur Ceram Soc*, vol. 38, no. 15, pp.  
8 4922–4938, Dec. 2018, doi: 10.1016/j.jeurceramsoc.2018.06.044.  
9

10 [8] A. Ahmed *et al.*, “Environmental life cycle assessment and techno-economic analysis of  
11 triboelectric nanogenerators,” *Energy & Environmental Science*, vol. 10, no. 3, pp. 653–671, 2017, doi:  
12 10.1039/C7EE00158D.  
13

14 [9] Z. Soleimani, S. Zoras, B. Ceranic, S. Shahzad, and Y. Cui, “The cradle to gate life-cycle  
15 assessment of thermoelectric materials: A comparison of inorganic, organic and hybrid types,”  
16 *Sustainable Energy Technologies and Assessments*, vol. 44, p. 101073, Apr. 2021, doi:  
17 10.1016/j.seta.2021.101073.  
18

19 [10] T. Mori and S. Priya, “Materials for energy harvesting: At the forefront of a new wave,” *MRS*  
20 *Bulletin*, vol. 43, no. 3, pp. 176–180, Mar. 2018, doi: 10.1557/mrs.2018.32.  
21  
22  
23  
24  
25  
26  
27  
28  
29  
30  
31  
32  
33  
34  
35  
36  
37  
38  
39  
40  
41  
42  
43  
44  
45  
46  
47  
48  
49  
50  
51  
52  
53  
54  
55  
56  
57  
58  
59  
60

1  
2  
3  
4  
5  
6  
7  
8  
9  
10  
11  
12  
13  
14  
15  
16  
17  
18  
19  
20  
21  
22  
23  
24  
25  
26  
27  
28  
29  
30  
31  
32  
33  
34  
35  
36  
37  
38  
39  
40  
41  
42  
43  
44  
45  
46  
47  
48  
49  
50  
51  
52  
53  
54  
55  
56  
57  
58  
59  
60

Accepted Manuscript